TECHNISCHE UNIVERSITÄT MÜNCHEN

Lehrstuhl für Ernährungsmedizin

Novel effects of n-3 LC-PUFA on adipose tissue and liver in diet-induced obesity in mice

Tobias Ludwig

Vollständiger Abdruck der von der Fakultät Wissenschaftszentrum Weihenstephan für Ernährung, Landnutzung und Umwelt der Technischen Universität München zur Erlangung des akademischen Grades eines

Doktors der Naturwissenschaften

genehmigten Dissertation.

Vorsitzender: Univ.-Prof. Dr. M. Klingenspor

Prüfer der Dissertation:

1. Univ.-Prof. Dr. J. J. Hauner
2. Univ.-Prof. Dr. H. Daniel

Die Dissertation wurde am 29.03.2012 bei der Technischen Universität München eingereicht und durch die Fakultät Wissenschaftszentrum Weihenstephan für Ernährung, Landnutzung und Umwelt am 4.06.2012 angenommen.

Table of Contents

Zusammenfassung

Das Auftreten von Adipositas und damit einhergehenden Erkrankungen wie Bluthochdruck, kardiovaskulären Erkrankungen, Typ 2 Diabetes und Krebs steigen stark an. Die Entwicklung einer Adipositas ist gekoppelt an eine ungewöhnliche und pathologische Veränderung der Fettgewebsmorphologie und Sekretion, die zu Hyperlipidämie, ektopischer Fetteinlagerung, Entzündungserscheinungen und Insulinresistenz führen kann. Das mesenteriale Fettgewebe befindet sich an der Schnittstelle intestinaler Nährstoffaufnahme und steht über die Portalvene in engem Kontakt mit der Leber, womit eine besondere Rolle bei der Krankheitsentstehung naheliegt. Ausgehend von seiner Rolle in intestinalen Erkrankungen und der anatomischen Besonderheit mesenterialer Lymphknoten, wurde insbesondere das mesenteriale Fettgewebe mit der Entstehung einer Insulinresistenz in Verbindung gebracht. Die Auswirkungen einer erhöhten Zufuhr von langkettigen, mehrfach-ungesättigten omega-3 Fettsäuren (n-3 LC-PUFA) in Hochfettdiäten auf die Genexpression und Funktion des mesenterialen Fettgewebes im Vergleich zum murinen epididymalen Fettdepot sind kaum beschrieben. Tierversuche haben gezeigt, dass n-3 LC-PUFA anti-adipöse und anti-inflammatorische Effekte hervorrufen können, aber gerade ihre Auswirkungen auf Entzündungsprozesse im Fettgewebe bleiben unschlüssig.

In der vorliegenden Arbeit wurde in einer Fütterungsstudie in C57BL/6J Mäusen eine Hochfettdiät mit n-3 LC-PUFA (HF/n-3; 48 en% Fett inklusive 4.8 % Eikosapentaen- und Dokosahexaensäure) mit einer isokalorischen Hochfettdiät (HF) und einer Niedrigfettdiät (Kontrolle, C) verglichen, um die Auswirkungen auf 1. Körper- und Organgewichte, Insulinwerte, hepatische Genexpression und Lipide, 2. die Morphologie sowie Gen- und Proteinexpression des mesenterialen (MAT) und epididymalen (EAT) Fettgewebes und 3. Metabolitwerte in Leber, Plasma, mesenterischem und epididymalem Fettgewebe zu charakterisieren.

Mäuse, die mit HF/n-3 gefüttert wurden, waren signifikant weniger adipös im Vergleich zu HF-gefütterten Tieren und zeigten

1. ein verringertes Körper- und durch NMR Spektroskopie bestimmtes Fettgewebsgewicht sowie eine reduzierte Leptin-Genexpression in der RT-qPCR und kleinere Adipozytengrößen in morphometrisch ausgewerteten Fettgewebsschnitten; außerdem eine durch RT-qPCR bestimmte unveränderte Fettgewebs-Genexpression metabolisch aktiver Enzyme aber erhöhte Ucp1 mRNA-Mengen in braunem Fettgewebe,
2. verbesserte Insulin-Werte im ELISA ohne einen Effekt auf die durch intraperitoneale Verabreichung von Glukose bestimmte Blut-Glukose-Toleranz,

3. verringerte Werte unveresterter Fettsäuren im Blutplasma und hepatischer Triacylglycerine (TAG) nach biochemischer Analyse und Oil Red O-Färbung von Gewebeschnitten der Leber und Genexpression von Lipogenese-Enzymen (Scd1, Acacα) einhergehend mit erhöhten mRNA-Werten für das peroxisomale Enzym Acox1 aber nicht für die mitochondriale β-oxidation, reguliert durch Cpt1α.

Überraschenderweise zeigte die Analyse des viszeralen Fettgewebes mit Hilfe von RT-qPCR und Western blot

1. eine erhöhte Genexpression von Immunzell-Markermolekülen (Itgax, Mrc1) sowohl in mesenterischem als auch epididymalem Fett,
2. gleichzeitige Erhöhungen der Genexpression pro- und anti-inflammatorischer Moleküle (OPN, Tnf-α, Mcp-1, Il10) in HF/n-3 Mäusen begleitet von
3. stärkeren Veränderungen im epididymalen Fett als im mesenterischen Fett. Dieser Effekt war jedoch nicht systemisch, da sowohl im ELISA gemessenes Plasma Serum Amyloid A als auch die Genexpression von Adhäsions- und Angiogenesemolekülen im Dünndarm sowie Marker für T-Zell-Aktivierung in der Milz durch HF/n-3 im Vergleich zur HF negativ reguliert wurden. Die Analyse von Metaboliten wie Phospho- und Sphingolipiden, Acyl-Carnitinen, biogenen Aminen und Aminosäuren im Fett, Plasma und der Leber sowie von n-3 LC-PUFA Metaboliten in der Leber durch massenspektrometrische Methoden zeigte große durch die HF/n-3 hervorgerufene Veränderungen in Übereinstimmung mit den gefütterten Diäten sowie die Bildung von Molekülen, die direkt an Auflösungsprozessen bei Entzündungen beteiligt sind.

Die Ergebnisse dieser Arbeit zeigen, dass n-3 LC-PUFA eine mäßige aber signifikante Verringerung der Adipositas in Mäusen aufgrund verringerter Fettmasse und Adipozytengröße hervorgerufen haben. Da die Expression der im Fettgewebe untersuchten Gene nicht verschieden reguliert war, ist es unwahrscheinlich, dass n-3 LC-PUFA hier nennenswerte metabolische Effekte hervorrufen, was allerdings im Gegensatz zu anderen Studien steht. Insulin-, TAG-Werte und hepatische Genexpression deuten an, dass die Leber eine wichtige Rolle in lipolytischen Stoffwechselprozessen spielt, die zu den beobachteten Veränderungen geführt haben, was in Übereinstimmung mit der vorhandenen Literatur steht. Allerdings weist auch die hier untersuchte erhöhte Ucp1 Genexpression im braunen Fett auf einen durch n-3 LC-PUFA-induzierten Energieverbrauch durch biochemische Thermogenese hin.

Die Verwendung von n-3 LC-PUFA in HF/n-3 erbrachte erwartete anti-inflammatorische Effekte. Allerdings kam es zu einem neuartigen, noch nicht beschriebenen fettgewebsspezifischen Anstieg von sowohl pro- als auch anti-inflammatorischer

Genexpression im mesenterialem und epididymalen Fett. Dieser könnte möglicherweise von n-3 LC-PUFA-spezifischen Effekten in Verbindung mit der Art der Studie oder der Menge und Zusammensetzung der Fettkomponente abhängig sein, was auf die erhöhte Palmsäureaufnahme oder eine unzureichende Vitamin E-Versorgung zurückzuführen sein kann. Inflammatorische Effekte im MAT könnten durch das Vorhandensein von Lymphknoten reduziert worden sein, was auf eine Interaktion zwischen Adipozyten und Lymphozyten hindeutet, die eine Verringerung der Immunzellaktivierung im Vergleich mit EAT zur Folge hat.

Zusammenfassend zeigt diese Arbeit zusätzlich zu der anti-inflammatorischen Rolle von n-3 LC-PUFA auch immunmodulierende wie pro-inflammatorische Effekte, die zur Auflösung von Entzündungsprozessen führen können. Sie legt damit die Grundlage für eine weitergehende Untersuchung spezifischer molekularer Effekte von Hochfettdiäten angereichert mit n-3 LC-PUFA im Fettgewebe auf zellulärer Ebene.

Summary

Obesity and its associated diseases like hypertension, cardiovascular disease, type 2 diabetes and cancer show an increasing prevalence in humans. The development of obesity is tightly connected to an abnormal and pathological development of adipose tissue morphology and secretory function contributing to hyperlipidemia, ectopic lipid deposition, inflammation and insulin resistance. Mesenteric adipose tissue is located at the interface of intestinal nutrient uptake, drained by the portal circulation, and the liver, and may thus play a decisive role in disease progression. Especially, mesenteric adipose tissue is supposed to play an important role as inferred from its relevance in intestinal inflammatory diseases and the harboring of lymph nodes. While it has been implicated in the development of insulin resistance, specific effects of high fat diets with elevated levels of omega-3 long-chain polyunsaturated fatty acids (n-3 LC-PUFA) on gene expression and function of mesenteric adipose tissue in comparison to the rodent epididymal adipose tissue have only poorly been described. Animal studies have shown that n-3 LC-PUFA induced anti-obesogenic and anti-inflammatory changes. However, in particular their effects on adipose tissue inflammation remain inconclusive.

In this study, a feeding trial in C57BL/6J mice was performed using a high fat diet enriched with n-3 LC-PUFA (HF/n-3; 48 en% fat including 4.8 % eicosapentaenoic and docosahexaenoic acid) in comparison with an isocaloric standard high fat diet (HF) and a low fat diet (control, C) to characterize effects on 1) body composition, fasting insulin levels, hepatic gene expression and lipid levels, 2) mesenteric (MAT) and epididymal adipose tissue (EAT) morphology, gene expression and protein expression, and 3) on metabolite levels in liver, plasma, mesenteric and epididymal adipose tissue.

Mice fed HF/n-3 exhibited a significant anti-obesogenic effect compared with high fat-fed animals showing

1) decreased body mass and adipose tissue depot mass revealed by NMR spectroscopy paralleled by reduced leptin gene expression in RT-qPCR and decreased adipocyte sizes as determined by morphometric histological analysis as well as unchanged metabolic adipose tissue gene expression, but increased Ucp1 mRNA levels in brown adipose tissue by RT-qPCR,

2) improved plasma insulin levels determined by ELISA but with no apparent effect on blood glucose tolerance after an intraperitoneal glucose injection,

3) decreased plasma non-esterified fatty acids and hepatic triacylglycerol (TAG) concentrations in plasma determined biochemically and by Oil Red O-staining of liver tissue sections, and diminished hepatic lipogenic gene expression (Scd1, Acacα) paralleled by increased enzyme mRNA levels for peroxisomal Acox1 but not mitochondrial β-oxidation, e.g. Cpt1α.

Surprisingly, RT-qPCR and Western blot analysis of visceral adipose tissue revealed

1) an increased gene expression of immune cell markers (Itgax, Mrc1) in both mesenteric and epididymal adipose tissue,

2) parallel increases of pro- and anti-inflammatory molecule gene expression (OPN, Tnf-α, Mcp-1, Il10) in mice on HF/n-3 with

3) effects more pronounced in epididymal than in mesenteric adipose tissue. However, this effect was not systemic, since plasma serum amyloid A levels measured by ELISA as well as gene expression of adhesion and angiogenesis molecules in small intestine and markers of T cell activation in spleen were negatively regulated by n-3 LC-PUFA-enriched high fat diet in comparison with the high fat diet. Metabolite analysis of phospholipids, sphingolipids, acyl-carnitines, biogenic amines, amino acids in adipose tissue, plasma and liver as well as n-3 LC-PUFA metabolite analysis in liver using mass spectrometry revealed marked changes induced by HF/n-3 diet indicating molecular compliance to the study design and the formation of molecules involved in the resolution of inflammation.

The data indicate that n-3 LC-PUFA induced a moderate but significant anti-obesity effect in mice due to decreased fat mass development and adipocyte sizes in adipose tissue. Because expression of the genes investigated in adipose tissue was not differentially regulated, it is unlikely that n-3 LC-PUFA exert relevant metabolic effects here, which is in contrast to other studies. Insulin levels, TAG levels, and hepatic gene expression indicate that the liver might play an important lipolytic role in the induced changes, which is in agreement with current literature. However, increased gene expression of Ucp1 in brown adipose tissue points to n-3 LC-PUFA-induced energy expenditure via non-shivering thermogenesis.

Overall n-3 LC-PUFA in HF/n-3 showed the expected observed anti-inflammatory effects. However, a novel adipose tissue-specific increase of both pro- and anti-inflammatory gene expression in whole mesenteric as well as in epididymal adipose tissue, that has not yet been described, was discovered. This may depend on n-3 LC-PUFA-specific effects in association with the study design, fat content and composition, e.g. due to increased palmitate intake or insufficient vitamin E levels. Inflammatory effects in MAT might have been reduced by the presence of lymph nodes indicating adipocyte-lymphocyte interactions

decreasing immune cell activation in comparison with EAT.

In conclusion, this study shows that in addition to the anti-inflammatory effects, actions of n-3 LC-PUFA are immunomodulatory, also involving pro-inflammatory molecules, and contributing to the resolution of inflammation. This warrants further research of the specific molecular effects of n-3 LC-PUFA high fat diet in adipose tissue on a cellular level.

1 Introduction

1.1 The obesity pandemic

Obesity is the worldwide most frequent and strongly increasing nutritionally caused disease (WHO, 2000). Worldwide an estimated 1.46 billion adults and 10 % of the global children population have a body mass index above 25 kg / m^2 and are thus classified as overweight or obese (Lobstein et al., 2004; Finucane et al., 2011). Estimates of the OECD show that in 2009 51.4 % of the German population were considered overweight or obese, an increase of almost 4 % in the past decade (OECD, 2011). According to the World Health Statistics Report 2011, non-communicable diseases – a range of chronic diseases including cardiovascular diseases, diabetes, cancer and chronic respiratory disease caused by factors like diet, physical inactivity, tobacco and alcohol overconsumption – lead to 36 million deaths worldwide (i.e. 63 % of all deaths) and affect both developed and developing countries (Lancet, 2011; WHO, 2011). The importance and need for action has recently been acknowledged by a UN summit on non-communicable diseases.

The rise of obesity-related diseases will also cost governments an expected 30 trillion U.S. dollars in the next 20 years (Lancet, 2011). And as governments are recognizing the urgency, biomedical research is increasingly important to study dietary behavior, physical activity, psychological drivers, genetic influences (Rutter, 2011) and molecular causes of obesity.

In biomedical research, obesity is regarded as a characteristic of metabolic syndrome, a cluster of pathologies also including hypertension, dyslipidemia, insulin resistance and impaired glucose tolerance (Koehler et al., 2007), and colon cancer (Calle et al., 2003; Hauner, 2005). Besides genetic models of obesity (Mathes et al., 2011), animal and especially rodent models are frequently applied to study molecular causes of metabolic syndrome (Varga et al., 2009) by diet-induced obesity (Buettner et al., 2007).

Obesity causes a massive increase of adipose tissue but also an infiltration of macrophages, T and B lymphocytes in the adipose tissue. Some studies also point to an involvement of adipose tissue in the pathophysiology of inflammatory intestinal and mesenteric diseases, e.g. Crohn's Disease (Schaffler et al., 2005).

1.2 Adipose tissue and adipokines

Adipose tissue is made up mostly of adipocytes and pre-adipocyes, but also of fibroblasts, immune cells, connective tissue, vascular, lymphatic and neural tissue. It has long been regarded simply as an energy storage organ. But since the discovery that adipsin (Cook et

al., 1987), TNF-α (Hotamisligil et al., 1993) and leptin (Zhang et al., 1994) are secreted by adipocytes, it has become accepted that adipose tissue is secreting protein factors, namely adipokines, with autocrine, paracrine and endocrine effects. Today, more than 100 factors are synthesized and secreted by adipocytes (Hauner, 2005). Generally, the adipokines can influence energy metabolism as well as neurendocrine and immune functions (Lord et al., 1998; Tilg and Moschen, 2006).

The major storage form of lipids in adipocytes are triacylglycerols (TAG). In general, fatty acids are taken up by the small intestine and packed into, for example, chylomicron-TAG reaching the adipose tissue via the lymphatic system. Lipoprotein lipase, an enzyme in the extracellular matrix of adipose tissue and skeletal muscle, actively cleaves fatty acids bound in chylomicrons to enter the adipocyte for re-esterification into TAG or the muscle for oxidation (Frayn, 2010). *De novo* lipogenesis in adipose tissue only contributes to about 20 % of lipid turnover in human adipocytes (Strawford et al., 2004) and may be even downregulated as adipocytes expand (Roberts et al., 2009). Experiments in rats suggest that during obesity adipocytes massively increase in size (hypertrophy) prior to an increase in their cell numbers (hyperplasia; Faust et al., 1978). However, especially the rate of hyperplasia seems to be dependent on genetics as a comparison of two mouse strains showed (Jo et al., 2009).

The release of fat from adipose tissue storage, i.e. lipolysis, is enzyme-mediated and involves adipose triglyceride lipase and hormone-sensitive lipase. Fatty acids are set free as non-esterified fatty acids bound to albumin (Frayn, 2010) and thus made available for other tissues for oxidation. Endogenous fatty acid oxidation in adipocytes is rather low in normally fed animals and only amounts up to 0.2 % whereas the majority is used for release or re-esterification (Wang et al., 2003).

1.2.1 Adipose tissue depots

Adipose tissue depots can be divided into brown (BAT) and white adipose tissue (WAT) depots. WAT is further differentiated into subcutaneous (scWAT) and visceral adipose tissue (vWAT) depots (Cinti, 2005). scWAT is superficial to abdominal and back muscles (Wajchenberg, 2000) and in mouse includes posterior (dorsolumbar, inguinal, gluteal) and anterior depots (axillary, interscapular, cervical). vWAT is located surrounding the inner organs of the thorax (mediastinic), abdomen and pelvis (omental, mesenteric, perirenal, retroperitoneal, parametrial, periovaric, epididymal, perivesical). Brown adipocytes of BAT can be found interspersed in many of the aforementioned depots, but the most prominent depot in mice is in the interscapular region (Figure 1).

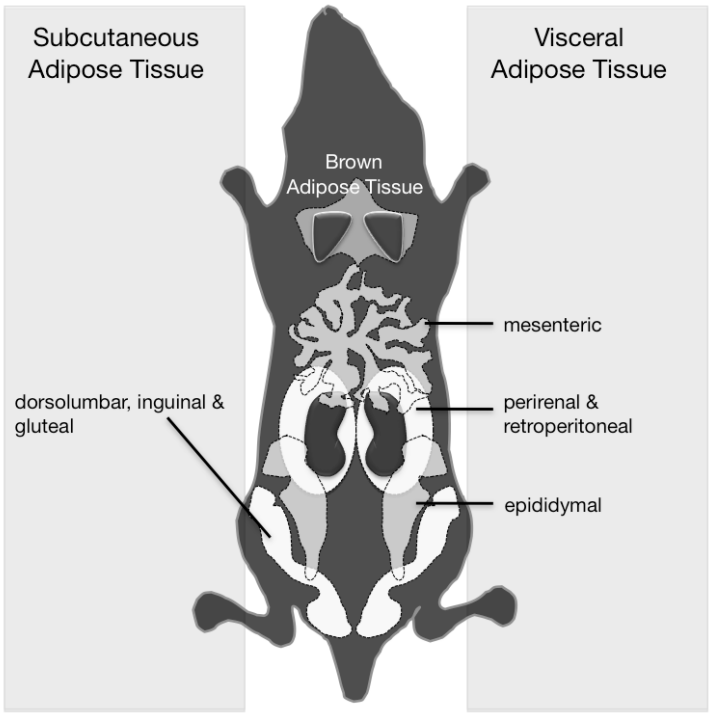

Figure 1: Selected adipose tissue depots in the mouse. Adipose tissue depots can be differentiated into brown adipose tissue (BAT) and white adipose tissue (WAT). The BAT shown here is the interscapular depot in the neck region of the animal. WAT further segregates into subcutaneous (scWAT) and visceral depots (vWAT). Here, only the posterior scWAT is shown with dorsolumbar, inguinal and gluteal fat depots. The vWAT depots include the intra-abdominal mesenteric adipose tissue attached to the abdominal back wall and the small intestine, the perirenal and retroperitoneal depot surrounding the kidneys and the epididymal vWAT depot attached to the epididymis of male mice (adapted from Cinti, 2005).

Subcutaneous and visceral adipose tissues not only differ by location but are also distinct in structure and function. scWAT contains smaller adipocytes whereas visceral adipocytes are larger in diameter (Sackmann-Sala et al., 2012) and are more vascularized and innvervated (Ibrahim, 2009). They show differences in gene expression (Perrini et al., 2008) and secretory profile (Ibrahim, 2009), which also depend on size (Skurk et al., 2007). Visceral adipocytes are more metabolically active. For example, visceral adipocytes have higher lipolytic activity than subcutaneous ones (Arner, 1995; Nielsen et al., 2004). In contrast, subcutaneous adipocytes have been shown to be more important for insulin sensitivity as the rate of insulin-stimulated glucose uptake is lower compared with visceral adipocytes (Abate et al., 1995; Perrini et al., 2008). Recently, it has been proposed that hypertrophy of visceral adipocytes might be responsible for the dyslipidemic conditions seen in obesity, whereas hypertrophic subcutaneous adipocytes might be indicative of an insulin-resistant state (Hoffstedt et al., 2010).

In contrast, BAT might act anti-obesogenic by burning excess energy through non-shivering thermogenesis (Smith and Horwitz, 1969), i.e. respiratory uncoupling, a process mediated by expression of uncoupling protein 1 (Ucp1). Studies in obese rodents show that Ucp1

gene expression is increased (Fromme and Klingenspor, 2010).

1.2.2 Mesenteric adipose tissue

Already in 1947 Vague noted that different adipose tissue depots might contribute differently to obesity and related complications (Vague, 1947). Later studies established that there is a correlation of intra-abdominal visceral adipose tissue (mesenteric and omental depots) with disturbed lipid metabolism and manifestation of insulin resistance (Fujioka et al., 1987; Despres et al., 1989). Only mesenteric and omental fat directly drain into the portal vein and the liver (Matsuzawa et al., 1995), which is unique compared to other visceral fat depots, i.e. epididymal and retroperitoneal fat, commonly used in the study of obesity. During digestion and nutrient uptake by the small intestinal mucosa, nutrients reach the portal vascular system via mesenteric vessels but also the circulation via the lymphatic system (thoracic duct). After nutrient uptake these vessels have the highest blood flow rate (West et al., 1989).

Both omentum and mesentery are peritoneal structures in humans and mice. The omentum lines the greater curvature of the stomach (Wilkosz et al., 2005) whereas the mesentery connects the small intestine to the abdominal back wall (Figure 2). Both are made up of adipose tissue, vascular and lymphatic tissue, immune cell-enriched mesenteric lymph nodes or omental “milky spots” (Platell et al., 2000), connective tissue and neuronal tissue. Compared with mesenteric adipose tissue, however, the “omental fat band” connecting the distal spleen and the duodenal lobe of the pancreas (Carlow et al., 2009) is rather small in mice.

Mesenteric fat has not only been connected with the development of obesity and metabolic syndrome, but also with Crohn’s Disease and colitis (Schaffler et al., 2005; Peyrin-Biroulet et al., 2007; Batra et al., 2010), by the secretion of pro-inflammatory adipocytokines like TNF-α and MCP-1 (Schaffler et al., 2005). It has been proposed that the pathogenic role of mesenteric fat in obesity-related pathologies might be caused by impaired gut barrier function (Li et al., 2008). Until now only few studies show the critical importance of mesenteric adipose tissue, for example, in the development of insulin resistance (Catalano et al., 2010).

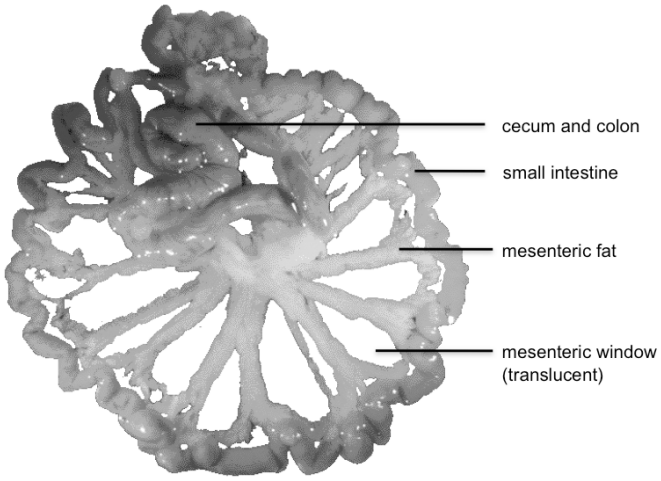

Figure 2: The mesentery.
Shown is an expanded mouse mesentery with attached intestinal tissue. The mesentery is connecting the small intestine (jejunum and ileum) with the abdominal back wall. The mesentery consists of mesenteric vessels lined by adipose tissue in a ray-like fashion. These are connected by translucent membranous "mesenteric windows".

Due to the strong vascularization and the localization of mesenteric lymph nodes (MLN) / immune cells, a special function of mesenteric fat in comparison with other depots can be assumed. Moreover, there even seem to be intra-depot-specific functions of the mesenteric fat located near a MLN (perinodal) and those adipocytes further away in experimental colitis (de Oliveira et al., 2009). Perinodal adipose tissue was more insulin sensitive whereas the distal adipose tissue displayed insulin resistance and severe macrophage infiltration. Furthermore, it could be shown that an increase in mesenteric fat mass in obese mice leads to a reduction of local lymph nodes by programmed cell death of immune cells (Kim et al., 2008). Studies comparing the fatty acid composition of perinodal adipose tissue and nodal immune cells show a positive correlation and established the view of adipocytes influencing immune cell metabolism and function (Pond and Mattacks, 2003; Pond, 2005; Knight, 2008). This function might have evolutionary origins as studies of the Drosophila fat body show a conglomerate of mammalian homologues for hepatocytes, adipocytes and lymphocytes (Hotamisligil, 2006).
Yet the role of mesenteric adipose tissue, the cellular and molecular changes it is undergoing during the course of obesity in contrast to intestinal diseases, and its relation to other adipose tissue depots were not well investigated at the beginning of the study.

1.2.2.1 Adipose tissue inflammation and insulin resistance

Adipose tissue is strongly increased in obesity and is involved in the development of inflammatory conditions and insulin resistance by the secretion of pro-inflammatory adipokines (cytokines and chemokines), non-esterified fatty acids (NEFA), glycerol, and hormones like leptin or adiponectin (Hauner, 2005; Kahn et al., 2006; Guilherme et al., 2008).

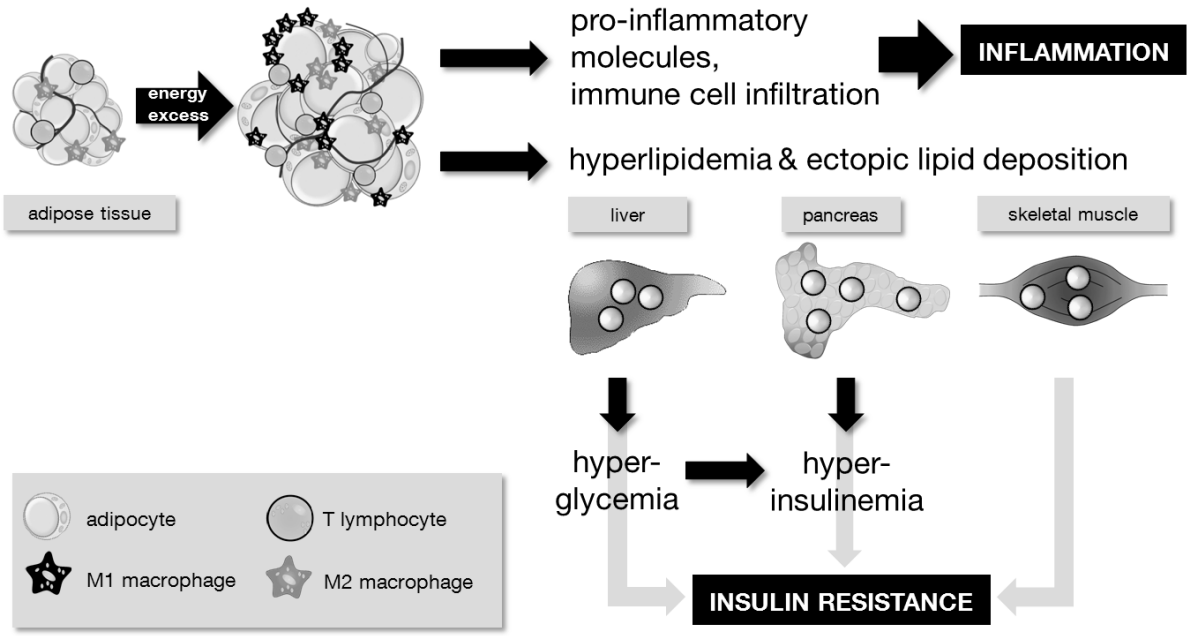

Figure 3: Adipose tissue inflammation and insulin resistance. In times of dietary energy excess and low energy expenditure, adipocytes store energy as triacylglycerols and enlarge in size (hypertrophy). As vascularization lags behind adipocyte growth, adipocytes might not be sufficiently supplied with oxygen. Adipocytes increasingly secrete pro-inflammatory molecules attracting immune cells, e.g. T lymphocytes and macrophages. Pro-inflammatory macrophages increase in number leading to a chronic state of inflammation in adipose tissue. Metabolic activity is increased in visceral adipocytes and non-esterified fatty acids (NEFA) released. Fat will be ectopically stored in liver, pancreas, and muscle. Hepatic glucose output is increased leading to hyperglycemia and compensation by increased insulin production in the pancreas. Eventually, liver, muscle and adipose tissue will become insensitive to insulin stimulation, i.e. insulin resistant.

In obesity, adipocytes can store high amounts of lipids and enlarge up to 140-180 µm in diameter (Iozzo, 2009). Blood flow is decreased in obesity (Frayn et al., 2003) and the lack of sufficient and timely angiogenesis leads to hypoxic conditions (Trayhurn et al., 2008) that favor pro-inflammatory conditions (Rausch et al., 2008). This might explain that the increase of adipose tissue mass is characterized by a striking infiltration of immune cells like B cells (Winer et al., 2011), CD4-positive T lymphocytes (Kintscher et al., 2008), CD8-positive, cytotoxic T lymphocytes (Rausch et al., 2008; Nishimura et al., 2009) observed in parallel with or contributing to macrophage infiltration. On the other hand, adipose tissue of obese mice has reduced numbers of regulatory CD4-Foxp3-positive T lymphocytes compared with lean mice (Feuerer et al., 2009). Additionally, dendritic cells and natural killer cells might be involved in this process, but have not been characterized much yet (Lolmede et al., 2011).

Macrophages have been the immune cell type first described in the context of adipose tissue inflammation (Weisberg et al., 2003) and numerically make up the highest proportion of immune cells infiltrating adipose tissue (Chawla et al., 2011). The adipokine monocyte chemoattractant protein-1 (MCP-1 / Ccl2) has been shown to be critical for macrophage infiltration into mesenteric adipose tissue (Yu et al., 2006). However, due to redundancy, it

might not prevent macrophage infiltration and adipose tissue inflammation as a targeted knock-out of the MCP-1 receptor CCR2 shows (Chen et al., 2005).

Other factors might have the same effect. One of these is the pro-inflammatory molecule osteopontin that is abundantly released by T lymphocytes (Weber and Cantor, 1996) as well as macrophages (Singh et al., 1990) and probably also contributes to a concerted infiltration of these cell types. It is critical for adipose tissue macrophage infiltration and the development of insulin resistance in diet-induced obesity (Nomiyama et al., 2007).
It is assumed that obesity drives the differentiation of two macrophage subsets with contrasting characteristics in adipose tissue, namely pro-inflammatory F4/80-CD11c-positive M1 macrophages and anti-inflammatory F4/80-CD206-positive M2 macrophages (Lumeng et al., 2007; Fujisaka et al., 2009). These studies suggest that there might be a "switch" of resident adipose tissue macrophages from a M2 to a M1 phenotype and additional recruitment of macrophages to the site of inflammation.

Probably coinciding with adipose tissue immune cell infiltration and inflammation is the decreasing responsiveness of tissues to insulin (Figure 3). Insulin resistance is a pre-requisite for the development of type 2 diabetes and often a co-morbidity of obesity (Kahn et al., 2006).
For a long time the prevailing view was that increased circulating NEFA lead to insulin resistance (Randle et al., 1963). This view has been recently challenged by Keith Frayn's group who showed that only acutely elevated NEFA levels might be responsible for insulin resistance. However, obesity is not necessarily causing elevated NEFA levels in plasma (Karpe et al., 2011). Moreover, the reason for insulin resistance during long-term lipid excess arises from ectopic lipid deposition (Yki-Jarvinen, 2002). When adipocytes in the obese organism reach their storage capacity limit, the excess lipid may be stored in other organs like liver, pancreas, skeletal muscle, and heart (Iozzo, 2009). Indeed, high fat diet-induced insulin resistance in a transgenic mouse model first starts in liver and then progressing to adipose tissue (Kleemann et al., 2010). The reason for this might be the anatomical neighborhood of both tissues connected by the portal system (Kim et al., 2003; Kahn et al., 2006). Several molecular mechanisms are involved in liver, for example, that inhibit the transmission of the insulin signal by the insulin receptor (Kumashiro et al., 2011) leading to increased glucose output. Resulting hyperglycemia is counteracted by enhanced β-cell mass and function (Kahn et al., 2006) leading to the typically observed hyperinsulinemia. Eventually, as type 2 diabetes develops, β-cell function cannot compensate for the decreased insulin sensitivity and is compromised.

One of these mechanisms in the rise of insulin resistance relates back to adipose tissue infiltration of immune cells and involves the effects pro-inflammatory mediators (Donath and Shoelson, 2011). Thus, obesity as a state of chronic lipid overload and adipose tissue inflammation may lead to the progression of insulin resistance and type 2 diabetes.

1.3 High fat diet-induced obesity

Apart from the use of genetic models (Robinson et al., 2000; Chen and Wang, 2005) in the study of obesity and symptoms of metabolic syndrome like insulin resistance and adipose tissue inflammation, high fat (HF) diet-induced obesity in rodents is commonly applied (Buettner et al., 2006; Wang and Liao, 2012). Fat is the most energy dense macronutrient (37 kJ / g; cf. carbohydrates and proteins: 17 kJ / g; FAO, 2002), and in humans and virtually all animal models investigated, HF feeding is positively correlated with an increase in body fat mass (West and York, 1998). Initially, this is likely to be caused by overconsumption (hyperphagia) and failure of anorexigenic mechanisms in the central nervous system (Tian et al., 2004; Clegg et al., 2005) but may be transient and substituted by other mechanisms like lowered physical activity or a decrease in basal metabolic rate (West and York, 1998).

There is no standardized HF diet for modeling HF diet-induced obesity. Hence, fat contents range from 20 % to more than 60 % of either animal fat – typically, lard, beef tallow or fish oil –, plant oils or mixtures (Buettner et al., 2007). Apart from fat quantity (de Wit et al., 2011), type of fat (Storlien et al., 2000; Buettner et al., 2006), and palatability (Kinney and Antill, 1996) study design components like feeding duration (acute vs. chronic treatment; Newberry et al., 2008; Yoshioka et al., 2008), food access (*ad libitum* vs. restricted; Alexenko et al., 2007) and physical activity levels (Bradley et al., 2008) can influence the study outcome. Furthermore, characteristics of the animal model like age, gender (Lemonnier, 1972) and genetic background (Gallou-Kabani et al., 2007; Svenson et al., 2007) determine the observed effects. It has even been shown that the genetically identical inbred mouse strain C57BL/6J shows different responses in body mass to HF diet-induced obesity, which implies an interaction between the diet and genes (Burcelin et al., 2002; Koza et al., 2006).

Due to this high variability, it is critically important to clearly define the composition of the diet, the characteristics of the study and to thoroughly analyze metabolic effects to allow for comparison with other studies of HF diet-induced obesity.

1.4 Long chain polyunsaturated fatty acids

1.4.1 Chemistry

As mentioned above, the effect of excess lipid intake depends on the type of fat for HF diet and its fatty acid composition. Fatty acids are carboxylic acids that are characterized by variable carbon chain lengths and the number of carbon double bonds, i.e. the degree of saturation (Figure 4).

In the sum formula *x:y* indicates the length of the fatty acyl chain with *x* carbon atoms containing *y* double bonds. In addition, n-3 or n-6 indicates the position of a double bond closest to the last carbon (n or ω / omega). Generally, saturated fatty acids (x:0) have been associated with the appearance of obesity and insulin resistance whereas monounsaturated and long chain polyunsaturated fatty acids (LC-PUFA) are beneficial (Storlien et al., 2000; Buettner et al., 2006). Moreover, LC-PUFA with a double bond in the n-6 position are known to have contrasting effects compared with n-3 LC-PUFAs (Schmitz and Ecker, 2008).
Arachidonic acid (ARA, 20:4n-6), eicosapentaenoic acid (EPA, 20:5n-3), and docosahexaenoic acid (DHA, 22:6n-3) are the most prominent LC-PUFA that can be synthesized in mammals from the essential linoleic acid (LA, 18:2n-6) and α-linolenic acid (ALA, 18:3n-3) but with very low conversion rates (Gerster, 1998; Wallis et al., 2002; Burdge, 2004). LA and ALA are abundant in plant oils whereas EPA and DHA are mainly found in fatty fish enriched from feeding on marine microbes (Martin, 1986; Damude and Kinney, 2008).

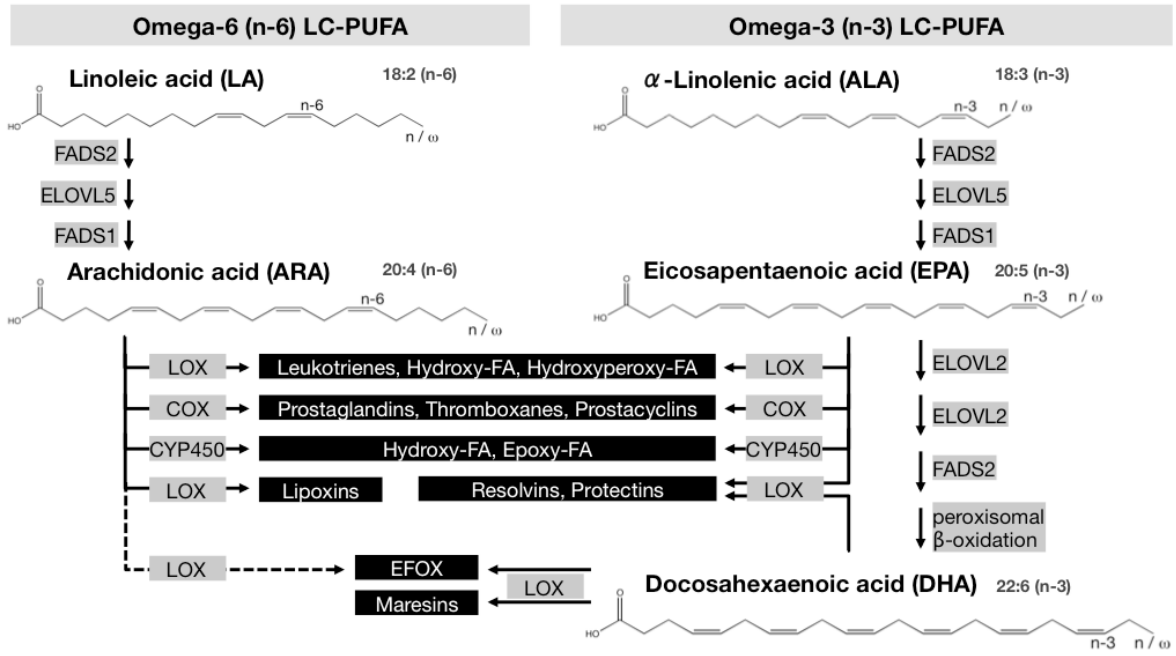

Figure 4: Lipid mediators generated from long chain polyunsaturated fatty acids (LC-PUFA). LC-PUFA can be divided into two groups depending on the closest position of a *cis*-double bond relative from the last carbon atom (n- or ω-C-atom) – the n-6 and n-3 LC-PUFA. Linoleic acid (LA, 18:2n-6) and α-linolenic acid (ALA, 18:3n-3) are essential fatty acids and are precursors for arachidonic acid (ARA, 20:4n-6) and eicosapentaenoic acid (EPA, 20:5n-3), respectively. These C-20 fatty acids are precursor molecule for eicosanoids, enzymatically generated lipid mediators with often contrary actions depending on the molecule of origin. They are involved in the modulation of inflammation. Both ARA and EPA can be further elongated and desaturated, for example from EPA to docosahexaenoic acid (DHA, 20:6n-3) that also serves as precursor to certain anti-inflammatory and pro-resolution lipid mediators. *x:y* indicates the length of the fatty acid with *x* carbons containing *y* double bonds. n-3, n-6 indicates the position of a double bond closest to the last carbon (n or ω / omega). Grey-shaded molecules are enzymes. COX, cyclooxygenase; CYP450, cytochrome P450; EFOX, electrophilic oxo-derivative; ELOVL, elongation of very long chain fatty acids protein (elongase); FA, fatty acid; FADS, fatty acid desaturase; LOX, lipoxygenase.

1.4.2 Mechanisms of action

While n-3 LC-PUFA are generally reported as beneficial, the effect on diseases like cardiovascular disease (GISSI-Investigators, 1999; Hooper et al., 2004), colon cancer (Engeset et al., 2007; Hall et al., 2008), inflammatory diseases (Goldberg and Katz, 2007; Hartweg et al., 2008) and neurological disease (Calon and Cole, 2007; Montgomery and Richardson, 2008) often shows conflicting results and depends on parameters like type of study, health / disease status, and dose of n-3 LC-PUFA administered. A reason for this are the different functions n-3 LC-PUFA can exert on cellular processes.

1.4.2.1 Cell membranes

In spite of low n-3 LC-PUFA synthesis, EPA and DHA are vital for cellular function and relatively abundant. For example, DHA constitutes up to 50 % of fatty acids in cell membrane phospholipids in the retina and 40 % in the brain (Kurlak and Stephenson, 1999; Singh, 2005).

In biological membranes, LC-PUFA can unfold their biological activities by various mechanisms. Fatty acyl chains of LC-PUFA with carbon double bonds in *cis*-configuration are kinked, take up more space and hence, increase membrane fluidity (Else and Hulbert, 2003). In the vascular system this might have effects on blood flow rate, for example (Ernst, 1989). They might affect membrane signaling processes and T lymphocyte activation by displacing proteins from lipid rafts (Stulnig et al., 2001) or the acylation of proteins (Muszbek and Laposata, 1993).

1.4.2.2 Lipid mediators

LC-PUFA themselves can act as signaling molecules by the formation of eicosanoids (derived from EPA and ARA) and other oxidized adducts (Figure 4). The eicosanoids include lipoxins, leukotrienes, and hydroxy / hydroxyperoxy fatty acids that are synthesized by lipoxygenases as well as prostaglandins, prostacyclins and thromboxanes generated by the enzyme cyclooxygenase (Calder, 2008). Here, the ARA- and EPA-derived mediators have antagonizing functions. Generally, the n-3 eicosanoids act anti-thrombotic, vasorelaxant, hypotensive and anti-inflammatory whereas n-6 eicosanoids counteract these effects (Calder, 2004). These apparently separated functions are, however, sometimes minimal and blurred by exceptions like the ARA-derived, anti-inflammatory lipoxin B_4 (Serhan et al., 2008).

In the past decade, new n-3 LC-PUFA-derived bioactive molecules, namely resolvins, protectins and maresins, with powerful anti-inflammatory and pro-resolution properties have been described (Serhan et al., 2008; Serhan et al., 2009). Recently, epoxy / hydroxy

eicosanoids generated by cytochrome P450 enzymes *in vitro* (Arnold et al., 2010) and electrophilic oxo-derivates (EFOX) of DHA and docosapentaenoic acid (DPA, C22:5n-6; Groeger et al., 2010) have increased the broad spectrum of LC-PUFA metabolites even more.

A general concern that is raised with the use of LC-PUFA is their susceptibility to auto- and photo-oxidation (Choe and Min, 2006). If not harmful this could at least explain the absence of effects in some studies, but data on n-3 LC-PUFA per-oxidation are inconsistent (Nenseter and Drevon, 1996). In contrast, neuroprostanes, a molecule class generated by the per-oxidation of DHA, have been shown to have anti-inflammatory effects by inhibition of nuclear factor κB (NF-κB) activation *in vitro* (Musiek et al., 2008). Furthermore, LC-PUFA might also act as anti-oxidants (Richard et al., 2008), and per-oxidation has been observed as low with an adequate intake of anti-oxidative vitamin E (Saito and Kubo, 2003).

1.4.2.3 Regulation of gene expression

Another aspect of LC-PUFA metabolic effects is the regulation of gene expression by transcription factor binding. Peroxisome proliferator-activated receptors (PPAR) α, γ and δ can be directly bound and activated by EPA, DHA or their derivatives (Forman et al., 1997; Kliewer et al., 1997) and indirectly mediate intestinal barrier function gene expression (de Vogel-van den Bosch et al., 2008a) but also mRNA synthesis of genes related to adipogenesis, lipid metabolism and inflammation in adipose tissue (Flachs et al., 2009). By modulation of liver X receptor α / β, hepatic nuclear factor-4 α, and sterol regulatory element binding protein 1 / 2, LC-PUFA can influence hepatic carbohydrate, fatty acid, triacylglycerol, cholesterol and bile acid metabolism (Jump, 2002). Additionally, binding to retinoid X receptor by DHA and ARA has been shown to influence gene expression (de Urquiza et al., 2000; Lengqvist et al., 2004).

A metabolome-directed approach can address overall changes in LC-PUFA-derived molecules and has been extensively exploited for the characterization of obesity and high fat diet-induced changes (Koves et al., 2008; Mihalik et al., 2010). Data on n-3 LC-PUFA-induced changes have so far mostly described effects in plasma (Lankinen et al., 2009; Kus et al., 2011), but could partially show improved metabolic effects by differential effects on acylcarnitine levels (Kus et al., 2011) and downregulation of proinflammatory ceramides, diacylglycerols and lysophosphatidylcholines (Lankinen et al., 2009). However, n-3 LC-PUFA changes in organs are scarce. Given the effects of n-3 LC-PUFA on phospholipid

composition, eicosanoid production and regulation of metabolism gene expression in adipose tissue and liver, it would be interesting to characterize these tissues more closely.

1.4.2.4 Effects on obesity

Data on the reduction of adiposity by n-3 LC-PUFA in humans are scarce and not clear (Buckley and Howe, 2009).

In animals the majority of literature indicates anti-obesity effects (Ruzickova et al., 2004; Mori et al., 2007). The observed anti-obesity and hypolipidemic effects of n-3 LC-PUFA probably result from a multitude of molecular mechanisms. They involve the differential regulation of adipocyte differentiation and metabolic gene expression via transcription factors (Madsen et al., 2005; Ailhaud et al., 2008) and might improve adipose tissue (Puglisi et al., 2011) and hepatic lipid storage (Jelenik et al., 2010).

Additionally, as different fatty acids may have variable substrate properties, n-3 LC-PUFA can also influence enzyme activities directly. For example, EPA is rarely esterified to cholesterol and diacylglyerol (Rustan et al., 1988a; Rustan et al., 1988b). Furthermore, n-3 LC-PUFA increase peroxisomal fatty acid oxidation (Rustan et al., 1992) and enhance lipoprotein lipase activity (Park and Harris, 2003). It is shown that plasma triacylglycerol (TAG) and non-esterified fatty acid (NEFA) levels are decreased also postprandially (Rustan et al., 1998).

A question not yet answered is if and how n-3 LC-PUFA can modulate respiratory uncoupling via uncoupling protein 1 (Ucp1) and thus lead to decreased adiposity via non-shivering thermogenesis (Flachs et al., 2009). Evidence from a high fat study with n-3 LC-PUFA indicates that Ucp1 gene expression might be exclusively regulated by these fatty acids (Sadurskis et al., 1995). It might also be possible that n-3 LC-PUFA lead to a redistribution of lipids with an improvement of lipid homeostasis but no overall effects on body mass (Rokling-Andersen et al., 2009).

1.4.2.5 Effects on inflammation

LC-PUFA are important mediators of inflammation. The most convincing reports on the anti-inflammatory properties of n-3 LC-PUFA come from atherosclerosis research (Tziomalos et al., 2007; Siddiqui et al., 2009) and rheumatoid arthritis whereas their role in other inflammatory diseases remains speculative (Calder, 2006; Fritsche, 2006). Moreover, an adverse role of n-3 LC-PUFA in inflammatory bowel disease has also been reported repeatedly and might be due to immunosuppressive function and thus increased susceptibility to infection (Woodworth et al., 2010).

As reviewed earlier, eicosanoids of the n-6 and n-3 series have potent pro- and anti-inflammatory effects, respectively (Calder, 2006). Furthermore, n-3 LC-PUFA directly inhibit activity of NF-κB (Zhao et al., 2004) or via toll-like receptors (Lee et al., 2003) and thereby indirectly attenuate expression of pro-inflammatory molecules including cytokines, chemokines, adhesion molecules and enzymes (Ghosh and Karin, 2002; Schmitz and Ecker, 2008). Interaction of n-3 LC-PUFA with specific receptor molecules, as shown by the stimulation of G protein-coupled receptor 120 (GPR120) also have anti-inflammatory effects (Oh et al., 2010).

Studies with intestinal epithelial cells as well as endothelial cells show that n-3 LC-PUFA can improve barrier function of these cellular structures by lowering permeability (Horie et al., 1998) and increase cell-cell contacts by increased generation of contact molecules (Jiang et al., 1998). This could inhibit the transfer of bacteria across the intestinal mucosa and the extravasation of inflammatory cells from the vessels into surrounding tissues with an indirect anti-inflammatory effect (Khalfoun et al., 1996).

Another proof of the immunomodulatory functions of fatty acids comes from studies investigating the role of perinodal adipose tissue in lymph node activation (Pond, 2005). It was shown that perinodal adipocytes have an elevated LC-PUFA content that either stimulate or suppress immune cell activation depending on the supply of n-6 or n-3 LC-PUFA, respectively.

On the other hand, n-3 LC-PUFA can also activate the immune system, induce TNF-α secretion by macrophages (Petursdottir et al., 2002), and lead to an increased spleen size probably by immune cell proliferation (Blok et al., 1996a).

When interpreting effects of LC-PUFA on inflammation, one has to take into account that different results observed might depend on the model organism and cell type studied (Blok et al., 1996b), on the dose of n-3 LC-PUFA (Yaqoob, 2010), on insufficient power of study subjects but also on genotypic polymorphisms especially in humans (Fritsche, 2006).

1.4.2.6 Effects on insulin resistance

A recent meta-analysis of human studies has come to the conclusion that there is no statistically significant effect of n-3 LC-PUFA on glycemic control and fasting insulin (Hartweg et al., 2008).

The administration of high fat diets is causing an impaired glucose disposal in glucose-sensitive tissues ultimately leading to insulin resistance in mice (Buettner et al., 2006). Positive effects on glucose tolerance by n-3 LC-PUFA in animals are not consistent in literature, but positive effects on insulin secretion are described (Winzell et al., 2006; Neschen et al., 2007; Fedor and Kelley, 2009). This might be due to an improvement of lipid

metabolism and inflammatory parameters described above, but outcomes vary according to assessment method (Martin de Santa Olalla et al., 2009) and type of study.

1.4.2.7 n-6 and n-3 LC-PUFA balance

The most important aspects that have to be considered when administering n-3 LC-PUFA are the balance with n-6 LC-PUFA and their absolute dose. Modern Western diets show a ratio of n-6 : n-3 LC-PUFA of around 10–25 : 1 (Simopoulos, 2011). This is largely due to the recommendation and increased use of n-6 LC-PUFA-rich vegetable oils in human nutrition in the second half of the 20th century but varies with the type of vegetable oil used. During the evolution of humans this ratio was balanced 1 : 1 (Simopoulos, 2011). Especially, since it has been shown that n-6 LC-PUFA also act anti-inflammatory (Pischon et al., 2003), a debate has started on what is more important: ratio or amounts (Deckelbaum, 2010).

Today recommendations for dietary intake in humans vary between 200-500 mg EPA + DHA per day equivalent to two portions fatty fish per week (Singer, 2010) and about 15 g linoleic acid according to the American Heart Association (Harris, 2010). These are mainly based on findings from studies investigating cardiovascular disease. As shown above, however, LC-PUFA have implications in various other disease settings where the difficulty of establishing dietary recommendations persists. Even EPA and DHA have specific effects on the cellular mechanisms that might affect the study outcome (Gorjao et al., 2009).
Due to metabolic differences, it is even more difficult to draw conclusions from animal studies. Usually, these apply excessive ratios, e.g. n-6 : n-3 of 201 : 1 (Huber et al., 2007), and huge concentrations of EPA + DHA, e.g. 10 % of dietary energy intake. Often data are not provided or impossible to extract because essential information on food intake, macronutrient and fatty acid composition are lacking. This further complicates comparability of LC-PUFA supply to the human situation.

1.5 Summary

Literature and statistical data indicate that obesity with its co-morbidities is a strongly increasing disease. It is tightly connected to an abnormal and pathological development of adipose tissue morphology and secretory function affecting also other organs.
Especially visceral adipose tissue as the fat depot surrounding the inner organs has come into focus of high fat diet-induced obesity research, since it is anatomically situated at the interface of intestinal nutrient uptake, drained by the portal circulation, and the liver. Especially, mesenteric adipose tissue is supposed to play an important role as inferred from its relevance in intestinal inflammatory diseases and the harboring of lymph nodes. While it

has been implicated in the development of insulin resistance, not much is known about specific effects of high fat diets with elevated levels of n-3 LC-PUFA on gene expression and function of mesenteric adipose tissue in comparison to the extensively studied but uniquely rodent epididymal adipose tissue.

n-3 LC-PUFA were shown to act anti-obesogenic in rodents and hypotriglyceridemic in rodents and humans, the anti-inflammatory potential, however, is strongly dependent on the study conditions. Literature on high-fat diet induced obesity with an n-3 LC-PUFA intervention is complex and due to the lack of dietary standards in studies hardly comparable.

Thus, it would be worthwhile to investigate the molecular effects of n-3 LC-PUFA in a broad tissue context but also with a focus on mesenteric adipose tissue in comparison to epididymal adipose tissue. It is interesting to explore how these fat depots differentially behave regarding the anti-obesogenic and anti-inflammatory effects of n-3 LC-PUFA.

2 Aim of the Study

Obesity shows an increasing prevalence in humans and is the cause of many associated metabolic disorders like hypertension, cardiovascular disease, type 2 diabetes and cancer. During obesity, adipose tissue as an active metabolic organ plays a major role as it expands to increase storage capabilities and is contributing to the observed complications by causing hyperlipidemia, ectopic lipid deposition, inflammation and insulin resistance. A common model to study the etiology of obesity is the diet-induced obesity mouse model.

The aim of this work was to show that in male wild-type C57BL/6J mice high fat diets cause adipose tissue expansion, ectopic lipid deposition, inflammation and insulin resistance. To counteract these pathological characteristics, omega-3 long chain polyunsaturated fatty acids (n-3 LC-PUFA) were used. These have been shown to act hypolipidemic and beneficial in many disease settings, but their role in obesity and inflammation is less clear.
In this thesis, the analysis focused on intra-abdominal mesenteric adipose tissue, a fat depot that has been implicated in intestinal diseases and the development of insulin resistance. It has also a high potential to be involved also in obesity-related metabolic and inflammatory processes due to its location at the interface between intestinal nutrient uptake and portal drainage to the liver and circulation. However, in mice it has only been poorly addressed how this fat depot behaves in relation to the more extensively studied epididymal fat when a high fat diet with elevated amounts of n-3 LC-PUFA is applied. Additionally, effects of n-3 LC-PUFA were to be investigated in liver, which is active in lipid metabolism and is positively affected by n-3 LC-PUFA treatment as shown by other studies.

Therefore, the aims pursued in this study were to

1) establish high fat diets without and with enrichment of n-3 LC-PUFA eicosapentaenoic acid (EPA) and docosahexaenoic acid (DHA) in C57BL/6J mice in comparison with a low fat (control) diet and analyze suggested anti-obesity effects initiated by n-3 LC-PUFA during chronic high fat feeding with a focus on adipose tissue and liver.
2) demonstrate whether a high fat diet enriched with n-3 LC-PUFA EPA / DHA can improve glucose and lipid metabolism by measurement of glucose tolerance with an intraperitoneal glucose tolerance test, insulin levels with ELISA, lipid levels in plasma and ectopic lipid deposition in liver, and gene and protein expression in liver and adipose tissue with RT-qPCR and Western blot, respectively.

3) characterize the modulation of the adipose tissue inflammation through high fat diet enriched with n-3 LC-PUFA EPA / DHA focusing on the differential effects on gene expression in intra-abdominal mesenteric adipose tissue and the frequently used epididymal adipose tissue by RT-qPCR and histological analysis.

4) describe overall effects of n-3 LC-PUFA focusing on lipid metabolite levels in liver, plasma and adipose tissue and the levels of n-3 LC-PUFA metabolites in liver.

3 Methods

3.1 Mice

Six-week-old male C57BL/6J mice were obtained from Charles River Laboratories and single-housed under controlled, specific pathogen-free (SPF) conditions at constant temperature (22 °C) and humidity (55 %) with a 12 h light / dark cycle with *ad libitum* access to food and water in the SPF animal facility at Technische Universität München (TUM) in Freising-Weihenstephan. Mice were kept in type II long, individually ventilated cages (IVC) with wood shavings as cage enrichment (TECNIPLAST® Green Line IVC Sealsafe PLUS, surface area: 540 cm^2).

It was also necessary to single-house the mice for the measurement of food intake and excretion of feces. Even though the Society of Laboratory Animal Science (Gesellschaft für Versuchstierkunde, GV-SOLAS) does not recommend to single-house social animals like mice, it is not regarded as isolation stress to separate male mice (GV-SOLAS: „Tiergerechte Haltung: Labormäuse“, Part 5). Visual contact to conspecifics was realized by using transparent cages.

3.2 Study design

Upon arrival, mice were adapted on a control diet (Ssniff Spezialdiäten GmbH; cat. no. S5745-E720 [C]) for two weeks and body mass monitored. At the age of eight weeks mice were randomly assigned to two cohorts. One cohort was fed for six weeks and the other for twelve weeks.

Each cohort was divided into three dietary groups (n=12 mice per group): the formerly used control diet with 13 en% fat (C), high fat diet with 48 en% fat (HF) and high fat diet enriched with an n-3 LC-PUFA concentrate (EPAX 1050-TG, kindly provided by Goerlich Pharma International) with 48 en% fat (HF/n-3). For more detailed information on diets, cf. 4.2; Table 1.

During the trial body mass was measured weekly, food was exchanged two times a week to limit lipid autoxidation and peroxidation (Gardner, 1989). Body composition (i.e. fat mass and lean mass) was measured every other week with nuclear magnetic resonance spectroscopy (cf. 3.6). Food intake (accounting for spillage) and feces production were measured every two weeks over the period of one week.

At the end of the feeding period, animals were euthanized in the postprandial state by carbon dioxide and cervical dislocation. Death was confirmed by reflex test at the hind paw and by subsequent blood withdrawal from the *Vena cava inferior* and plasma stored in heparinized and EDTA-coated tubes (Sarstedt). Organs were immediately removed,

weighed on a precision balance and snap-frozen in liquid nitrogen and stored at –80 °C for optimal RNA and protein quality preservation. For analysis adipose tissue depots (mesenteric, epididymal, inguinal, interscapular brown), liver, spleen and small intestinal mucosa were sampled.

All procedures applied throughout this study were conducted according to the German guidelines for animal care and approved by the district Oberbayern ethics committee.

3.3 Diets

For more detailed information on the diets, see the Results section under 4.2. All diets were purified experimental diets that were served as pellets. They had been manufactured by Ssniff Spezialdiäten GmbH (cat. no. S5745-E720 [C], S5745-E722 [HF], S5745-E725 [HF/n-3]), sterilized with 25 kGy γ-radiation by Isotron Deutschland and stored in the dark at either –20 °C (long-term) or 4 °C (short-term).

Diet composition (cf. 4.2; Table 1) was constant among diets for the following ingredients (values given in w / w): 24 % casein, 5.6 % maltodextrin, 5 % sucrose, 5 % cellulose, 1.2 % vitamins, 6 % minerals. Fat and starch content were the only variables: Control diet (C) – 5 % soybean oil and 47.8 % corn starch; high fat diet (HF) – 5 % soybean oil, 20 % palm oil and 27.8 % corn starch; high fat/n-3 diet (HF/n-3) – 5 % soybean oil, 11.25 % palm oil, 8.75 % EPAX 1050 TG and 27.8 % corn starch. All diets were fortified with 0.015 % butylhydroxytoluene (BHT) and 0.018 % α-tocopherol acetate to limit lipid oxidation.

3.4 Sterol analysis and fatty acid composition

Cholesterol in the diets was determined with a colorimetric test according to the manufacturer's instructions (Boehringer Mannheim / Roche Diagnostics) at the TUM Bioanalytik.

Cholesterol and phytosterol contents were determined in animal fats, fish oil, and plant oils (performed by T. Lubinus, Food Technology Unit, TUM). First, sample size was determined by the expected sterol content and 50 µl internal standards added (cholesterol for phytosterol quantification, stigmasterol for cholesterol quantification). The sample was saponified with ethanolic KOH at 70 °C for 50 min. Subsequently, samples were derivatized with a trimethylsilyl (TMS) group at 80 °C for 20 min and resuspended in a n-hexane / methyl-tert-butyl ether mixture. 1 µl of underivatized or TMS-derivatized sample was analyzed by Agilent 6890N gas chromatography with flame ionization detector (GC-FID). Alternatively, 1.1 µl TMS-derivatized samples were injected into a Trace GC UltraTM coupled to a Trace DSQ mass spectrometer (GC-MS; Thermo Finnigan). Analysis was

performed with ChemStation Software vA.09.03 (GC-FID), Xcalibur Software v1.4 SR1 (GC-MS; Thermo Finnigan) and Excel (Microsoft).

To guarantee stability of fatty acids, fats from food were extracted, fatty acids derivatized with tri-methylsulfoniumhydroxide (TMSH) and analyzed by gas chromatography (TUM Bioanalytik; Bligh and Dyer, 1959; Hallermayer, 1976).

3.5 Body mass, feces collection and food and energy intake

Mice were placed into fresh cages with fresh bedding, food and water every week. At the same time body mass was measured. Mice were placed into an open plastic beaker on a mini scale (Sartorius), and mass was recorded. Afterwards, approximately 100 g of food was put into the food rack inserted in the cage. It had been portioned by the provider (Ssniff Spezialdiäten) to avoid long storage of open food bags and was kept in the dark at –20 °C (long-term) or 4 °C (short-term) before use. After equilibration to room temperature, the exact food portion mass supplied per cage was recorded.

Fresh food was provided twice a week: first, when cages were changed – usually at the beginning of the week (Monday / Tuesday) and second, at the end of the week (Friday).

Feces was collected from used cages, mass in g recorded and dried for three days at 60 °C. It was further used for bomb calorimetry (cf. 3.7).

Food intake in g was determined after one week by subtraction of left-over food from the recorded mass of fresh food. To account for food spillage, the mass difference between fresh and used cages (without mouse, food and feces) was determined. Urine mass was not taken into account, since it might have partially evaporated in the ventilated cages over the week. Energy intake was determined by multiplication of food intake in g with gross energy obtained by bomb calorimetry.

3.6 Nuclear magnetic resonance (NMR) spectroscopy

Body composition, i.e. fat mass and lean mass, of mice was determined every other week for twelve weeks using a “Minispec” mq 7.5 whole animal body composition NMR analyzer with Bruker Minispec plus and OPUS v5.5 software (Bruker BioSpin). To yield optimal results, movement of mice had to be limited by a polycarbonate restrainer. It was colored red to observe the mouse. The restrainer with the mouse was placed horizontally into the device and measurement was executed at an ambient temperature of 37 °C in the NMR spectrometer for three minutes. Afterwards values were recorded in g and mice placed back into their cages. Before data acquisition the NMR analyzer was calibrated with dissected adipose tissue and lean muscle.

3.7 Bomb calorimetry

Gross energy of food and feces was determined with a Parr® 6300 Calorimeter (Parr Instrument Co.). To prepare samples for measurement, they were homogenized with a TissueLyser II (Qiagen/Retsch) and powder then pressed as pills of approximately 1 g. The pill was weighed and then placed into the calorimeter connected to an ignition thread. Energy in MJ / kg was determined by the software with the exact pill mass provided.

3.8 Indirect calorimetry

During the trial four animals per group from both the HF and HF/n-3 group were analyzed for energy consumption over four consecutive days. They were placed into fresh cages with bedding (Ehret, cage type I, surface area of 200 cm^2) in a climate simulation station (22 °C; Feutron). Cages were sealed to specifically measure oxygen consumption and carbon dioxide exhalation (TSE Systems Calorimetry module "CaloSys"), but animals had *ad libitum* access to food and water and visual contact to other mice.

Daily energy expenditure (DEE) per animal per day was calculated providing the respiratory quotient (RQ) and the volume of oxygen consumed per minute (VO_2) modified from Heldmaier's formula: DEE = (16 + 5.3 x RQ) x VO_2 (Heldmaier, 1975).

3.9 Locomotor activity

To determine the influence of the diets on locomotor activity, animals were put into specific open cages for twelve days (Ehret, type III cage, surface area of 825 cm^2). Animals had *ad libitum* access to food and water, the surface was covered with bedding. Mice had olfactory and acoustic contact to each other. A frame surrounding the cage measured locomotor activity of the animals automatically with the help of light beams (TSE Systems Drinking & Feeding Monitor module "ActiMot"). Central ambulatory and fine as well as peripheral ambulatory and fine movements were counted by numbers of breaking the light beams and summed up per animal and hour. Then the mean ± standard error was calculated and plotted for every dietary group over the experimental period for every hour.

Food and water intake as well as activity were recorded with the TSE Labmaster v2.1.5 software (TSE Systems).

3.10 Intraperitoneal glucose tolerance test (ipGTT)

A glucose tolerance test serves as an indirect measure of systemic glucose tolerance and as an indicator of insulin resistance (Kahn et al., 2006; Andrikopoulos et al., 2008). For the

assessment of glucose tolerance after 4, 6 and 12 weeks of feeding, mice were fasted for six hours (8 a.m. to 2 p.m.). After six hours, basal blood glucose levels were determined with a handheld glucometer (“FreeStyle Lite”, Abbott). Blood was retrieved by amputation of the tail tip (< 2 mm). 2 g / kg body mass of a sterile 20 % glucose solution (B. Braun Melsungen) were injected intraperitoneally. Blood glucose levels were measured after 15, 30, 60 and 120 min. Afterwards, mice were moved back to their home cages with *ad libitum* access to food and water.

3.11 Blood collection

Blood collection from the live animal was necessary for determination of insulin levels during the trial. Recommendations of GV-SOLAS were obeyed: ca. 6–7 % of a mouse’s body mass is blood. Of this a maximum of 10 % of the blood volume may be taken once with a recovery time of at least two weeks (e.g. 170 µl blood may be withdrawn once from a 25 g mouse).

Mice were fasted for 5 hours (8 a.m. to 1 p.m.). Mice were fixed in a restrainer to retrieve blood from the hanging tail. To facilitate blood withdrawal, the tail vein was dilated by massaging and infrared light radiation. A horizontal incision was made with a sterile scalpel distally in the lower third end of the tail to collect blood (≤ 50 µl) in EDTA-coated tubes (Sarstedt). The bleeding was then stopped with autoclaved paper and the mouse placed back into its cage.

Blood for the determination of plasma non-esterified fatty acids, metabolites (Biocrates platform) and osteopontin levels was collected with a 0.5 ml syringe (Terumo Europe) after killing the animal from the *Vena cava inferior* and collected in Heparin- or EDTA-coated tubes (Sarstedt).

Full blood was incubated at room temperature for 10 min and for 30 min on ice before separation of plasma and erythrocytes by centrifugation at 3000 x g for 10 min. Plasma was aliquoted and frozen at –80 °C until further use.

3.12 RNA and protein isolation

To obtain homogenous tissue samples, tissues were separately ground in frozen state with liquid nitrogen and stored at –80 °C. Aliquots of the tissue powder were homogenized in Qiazol® lysis reagent (Qiagen) or radioimmunoprecipitation assay (RIPA) buffer (recipe cf. 3.25.1) for RNA or protein extraction, respectively.

mRNA or total RNA (including small RNAs) was extracted with chloroform and purified with mRNeasy® mini kit or the miRNeasy® mini kit (Qiagen) according to the manufacturer’s

instructions, respectively. To avoid DNA contamination, on-column DNase I (Qiagen) digestion was performed. The RNA concentration of the eluate was determined with NanoDrop ND-1000 UV-Vis spectrophotometer (Peqlab) and quality confirmed with the RNA 6000 Nano kit on an Agilent 2100 Bioanalyzer (Agilent Technologies) according to the manufacturer's instructions. Samples compared were matched for RNA integrity number (RIN), which was always above a value of five. RNA was used in PCR and RT-qPCR assays (cf. 3.15; 3.16).

For protein extractions homogenates were kept in cold RIPA buffer with added proteinase and phosphatase inhibitors (Sigma & Roche) and centrifuged with 2000 x g at 4 °C for 2 min to remove cell debris. Protein concentration of extracts was then determined by bicinchoninic acid (BCA) method (Smith et al., 1985; Pierce / Thermo Scientific) in a 96-well plate with a bovine serum albumin (BSA) standard at 562 nm in a UV-Vis spectrophotometer (Tecan). Extracts were then diluted with SDS-PAGE sample buffer and stored at –20 °C until use in SDS-PAGE (3.17).

3.13 Primer design and primer testing

For differential gene expression analysis, oligonucleotides, herein called primers, were either commercially available as QuantiTect® primer assays (Qiagen) or custom-designed primer pairs, i.e. forward and reverse primers, selected according to strict criteria (cf. 9.1, page 163 for primer details).

Before starting primer design, Mouse Genome Informatics (www.informatics.jax.org) and Ensembl genome browser (www.ensembl.org) databases were checked for alternative transcript variants. "GeneInfo Identifier" (GI) and coding sequence were retrieved from the website of the National Center of Biotechnology Information (NCBI, www.ncbi.nlm.nih.gov/nuccore) and the gene of interest checked for alternative gene names. If needed, an alignment with NCBI Basic Local Alignment Search Tool (BLAST) was performed. The obtained GI was used to open NCBI Sequence Viewer (www.ncbi.nlm.nih.gov/projects/sviewer) where areas of primer annealing were chosen and primers automatically designed with NCBI Primer-BLAST software (www.ncbi.nlm.nih.gov/tools/primer-blast). In Primer-BLAST primer characteristics were specified: an amplicon size of 100–150 bp, maximum melting temperature (T_m) difference of 1 °C, exon-exon spanning primer with minimum intron size of at least 300 bp. A suitable primer was picked and further analyzed with OligoCalc (www.basic.northwestern.edu/biotools/oligocalc.html). Primers should be between 18–25 bp long with a G-C base pair content of 40–70 % and a T_m (salt-adjusted) of 60–64 °C and T_m (nearest neighbor) of 56–58 °C. At the 3'-end, thymidine-nucleotides, mismatches of

primer and target template, and runs of three or more guanosine- or cytosine-nucleotides were avoided. Furthermore, primer pairs were checked for self-complimentarity and "blasted" with BLAST to exclude annealing to non-specific target sequences. Next, primer sequences were checked for heterodimer formation by IDT OligoAnalyzer (http://eu.idtdna.com/analyzer/applications/oligoanalyzer). Finally, the sequences were checked for target specificity with University of California, Santa Cruz (UCSC) *in silico* PCR (http://genome.ucsc.edu).

Primers were synthesized commercially by metabion international AG. Specificity and specific annealing temperature were then tested in PCR and RT-qPCR and verified with agarose gel electrophoresis (cf. 3.14).

3.14 Agarose gel electrophoresis

Agarose gel electrophoresis was performed to verify molecular sizes of PCR-products and to evaluate primer specificity. A 2 % agarose gel (Peqlab) in Tris / borate / EDTA (TBE) buffer was cast in a suitable chamber (Biometra). Ethidium bromide (Roth) was added to the agarose-TBE solution to allow for visualization under UV-light (Intas) by intercalation into nucleic acids. Samples were diluted with Orange G dye (Sigma) 5:1 before they were applied to the gel. For reference a 50-bp ladder (Fermentas) was used.

3.15 Gene expression analysis

Expression of specific target genes was evaluated with real-time quantitative PCR (RT-qPCR). For each sample, 10 ng of extracted RNA were used per reaction using the QuantiTect® quantitative, real-time one-step RT-PCR kit (Qiagen) following the supplier's protocol. Primer design was executed according to specific selection criteria (cf. 3.13) to guarantee for primer specificity. Alternatively, commercially available primers were used from Qiagen. RT-qPCR was performed using SYBR Green I dye and a realplex^4 Mastercycler epgradient S (Eppendorf). The following thermal cycling conditions were used: 30 min at 50 °C (cDNA synthesis), 15 min at 95 °C (RT enzyme inactivation) followed by 40 cycles at 95 °C for 15 s, 60 °C (55 °C for Qiagen primers) for 30 s and 72 °C for 30 s. The PCR was concluded with a melting curve analysis of the PCR product (1.75 °C / min). C_q-values were retrieved from the realplex 2.0 software (Eppendorf) and analyzed according to the $\Delta\Delta C_q$-method (Livak and Schmittgen, 2001) using β-actin (Actb), glyceraldehydephosphate dehydrogenase (Gapdh) and hypoxanthine-guanine-phosphoribosyltransferase 1 (Hprt1), cyclophilin B (Cph) and heat shock protein 90 α (cytosolic), class B member 1 (Hsp90αb1) as the invariant controls to normalize the data.

For all groups, data were expressed as mean ± standard error relative to control samples. As RT-qPCR assay controls non-template assays and –RT assays were included for every primer used. Target specificity was checked for by melting curve analysis and agarose gel electrophoresis. Additionally, primer PCR efficiency was determined with LinRegPCR v12.16 (J.M. Ruijter, Academic Medical Center) using the raw fluorescence data from RT-qPCR (Appendix Table 7).

3.16 RT-qPCR Arrays

Pathway-specific "RT^2 Profiler™ RT-qPCR arrays" (SABiosciences / Qiagen) were purchased for "T and B cell activation" and "Endothelial cell biology" (Cat. no. PAMM-053 and PAMM-015) and RT-qPCR was performed according to the supplier's instructions. Specific primers for targets, housekeeping genes and controls were already supplied lyophilized in a 96-well plate. One plate was used per dietary group. An equal amount of RNA from four animals per dietary group was pooled, and 1 µg of pooled RNA was reverse transcribed according to the manufacturer's instructions. Along with a RT-qPCR master mix containing SYBR Green I, the newly synthesized cDNA was added to the 96-well plate and the RT-qPCR was performed according to instructions. For analysis, baseline was set automatically but the threshold was set to 400 units of fluorescence (same for all analyses). C_q-values were normalized with the given housekeepers (Actb, Hprt1, Gapdh, Hsp90αb) and fold changes calculated with a web-based analysis tool provided by the manufacturer (http://pcrdataanalysis.sabiosciences.com/) according to $\Delta\Delta C_q$-method (Livak and Schmittgen, 2001).

3.17 SDS-PAGE and Western blot

Protein expression was analyzed in mesenteric adipose tissue and liver. Sodium dodecyl sulphate polyacrylamide gel electrophoresis (SDS-PAGE) was performed using 40 µg protein per sample and prestained PageRuler® (Fermentas) as a protein standard ladder on a 10–12.5 % Tris-glycine separating gel. Subsequently, proteins were blotted on to a nitrocellulose membrane (Whatman) using semi-dry blotting (Biometra). The membrane was washed with TBS and blocked with 2 % ECL AdvanceTM blocking reagent (GE Healthcare). After washing with TBS + Tween-20 (TBS-T), membranes were incubated with primary antibody at 4 °C over night in TBS-T + 2 % ECL Advance™ blocking reagent. Detection with a secondary antibody was performed using the Odyssey Infrared Detection system (LI-COR Biosciences). Protein expression was normalized to ACTB (Cell Signalling) protein

expression and quantified using the Odyssey software v3.0 (LI-COR Biosciences). A list of antibodies can be found in the materials sections (cf. 9.2).

3.18 Chemical analysis

To determine hepatic triacylglycerol (TAG) content, livers were ground in frozen state with liquid nitrogen and dissolved in 0.9 % NaCl. TAG was extracted as follows: homogenates were incubated with 0.5 M ethanolic KOH (30 min, 71 °C), 0.15 M Magnesium sulphate was added and, after centrifugation with 13000 x g for 10 min, TAG concentrations were determined using a commercial enzymatic colorimetric kit following the manufacturer's instructions (Triglycerides liquicolor^{mono}, Human) at 500 nm on a UV-Vis spectrophotometer (Amersham / GE Healthcare).

TAG values were normalized to the protein content of the samples as determined by the Bradford assay with Coomassie® Brilliant Blue G-250 dye at 595 nm according to the manufacturer's instructions (Bradford, 1976; BioRad).

For measurement of non-esterified fatty acids (NEFA) in plasma samples were processed and analyzed with the NEFA-HR(2) kit (WAKO) according to the manufacturer's protocol.

3.19 Para-formaldehyde fixed and paraffin-embedded tissue sections

For histological analysis, liver and white adipose tissue were fixed in 4 % para-formaldehyde over night, washed in phosphate-buffered saline twice and then kept in 70 % ethanol for one week before tissues were dehydrated in ethanol and xylene of different concentrations with a TP1020 Tissue Processor (Leica) and embedded in pre-warmed Paraplast® paraffin (Carl Roth) at 60 °C on a Mikrom AP280-1/2/3 automatic embedding station (Microm / Thermo Fisher Scientific).

3.20 Oil Red O-staining of histological cryo-sections

For Oil Red O-staining of triacylglycerol (TAG) content in liver, fresh tissue was embedded in TissueTek O.C.T. (Sakura Finetek) freezing medium and cut in 10 µm sections with a Cryo-Star HM 560 MV microtome (Microm/Thermo Fisher). Sections were briefly fixed in 10 % formalin and washed with water and isopropanol. Staining and counterstaining was performed with freshly prepared Oil Red O-solution and hematoxylin (Roth), respectively. After mounting in aqueous medium (Merck), sections were photographed under a Leica DMI 4000B Microscope with Leica CTR 4000 light source (Leica) at 200-fold magnification.

3.21 Measurement of adipocyte cross-sectional area

Para-formaldehyde fixed and paraffin-embedded ventral subcutaneous inguinal, mesenteric and epididymal white adipose tissue was cut in 6 µm sections with a microtome HM 355 S (Mikrom / Thermo Fisher Scientific) and stained with hematoxylin and eosin in a Leica ST5020 integrated workstation (Leica). Micrographs were taken using a Leica DMI 4000B Microscope with Leica CTR 4000 light source (Leica) at 200-fold magnification and Leica Application Suite v3.7 software (Leica). Cell cross-sectional area was determined for three animals per group and five representative areas per sample. Individual cell cross-sectional area was measured with ImageJ software (National Institutes of Health) and calculation and analysis was performed with Excel 2010 (Microsoft) and Prism 5 (GraphPad). At least 200 cells per animal and tissue were measured.

3.22 ELISA

Fasting plasma insulin was determined with a commercially available Ultra Sensitive Mouse Insulin ELISA Kit (Crystal Chem., Inc.) using 5 µl EDTA-stabilized plasma per sample. Homeostatic model assessment of insulin resistance (HOMA-IR; Matthews et al., 1985) was calculated as follows: fasting glucose (mmol l^{-1}) x fasting insulin (mU l^{-1}) / 22.5. Insulin concentrations were converted to units using the molecular mass of Insulin A + B peptides (5791 Da) and the factor 6.945 according to the SI Unit Conversion Calculator of the Society Biomedical Diabetes Research (www.soc.bdr.org).

Osteopontin (OPN) plasma levels were determined using the commercially available Quantikine® Mouse Osteopontin Immunoassay kit (R&D systems) with 10 µl heparin-stabilized plasma per sample in a 1:100 or 1:200 dilution.

Serum amyloid A (SAA) plasma levels were determined using a commercially available ELISA kit and following the supplier's instructions (Cat. no. E-90SAA, ICL, Portland, USA).

3.23 Metabolite measurements

Lipid mediators in livers were measured in liver samples in collaboration and according to standard procedures (Gomolka et al., 2010; performed by K.H. Weylandt / M. Rothe, Lipidomix).

Measurement of amino acids, biogenic amines, acyl-carnitines, phosphatidyl cholines, lyso-phosphatidyl cholines and sphingolipids in plasma, liver, mesenteric and epididymal white adipose tissue of mice were performed according to Biocrates standard operating procedures for plasma (Römisch-Margl et al., 2012) with an Absolute IDQ™ Kit p180 (Biocrates) at Molecular Nutrition Unit, TUM, performed by A. Haag.

To obtain a homogenous tissue sample, tissues were ground in frozen state with liquid nitrogen. Tissue powder was dissolved in 300 µl ice-cold methanol on ice to denature proteins and extract metabolites followed by incubation at 4 °C for 10 min. After centrifugation, the supernatant was then transferred into a new reaction vial and 10 µl internal standard (amino acids and biogenic amines) added. Methanol was evaporated at room temperature und 1 mbar pressure in a vacuum centrifuge (SpeedVac SPDIIIV, Thermo Savant). For extraction, the dried pellet was dissolved in 5 % (v / v) phenylisothiocyanate according to weight of tissue sample and 20 µl were added to a Biocrates 96-well microfilter plate. This plate contained also quality controls like blanks for PBS and phosphate buffer controls as well as internal standards in seven concentrations for biogenic amines and amino acids. Furthermore, test plasma was added spiked in three different concentrations. Derivatization was performed by shaking and stopped by drying the samples in the plate. Microfilters were eluted with 300 µl methanol and shaking for 30 min into a 96-deep well plate. Samples were then diluted 1:30 for flow injection analysis (FIA) or 1:10 for liquid chromatography (LC). For lipid analysis, FIA coupled with mass spectrometry (AB SCIEX, QTRAP5500) was performed whereas biogenic amines and amino acids were detected with liquid chromatography (LC) and mass spectrometry. Peak control for LC was performed with Analyst software v1.5.1 (AB SCIEX), data were analyzed with MetIQ software v1.2.2 (Biocrates).

To visualize metabolic changes in the MS profiles of different body compartments, cluster and variance analysis was combined with the TIGR MeV software v4.6.0 (J. Craig Venter Institute) whereby the variance of each metabolite was separately tested via Fisher tests and Bonferroni adjustment between three groups of samples. Clustering was based on Euclidean distance and average linkage. Metabolite data matrices were standardized via a z-transformation and data normalized to initial tissue mass used.

3.24 Statistical analysis

All data are expressed as means ± standard error of the means (SEM). Statistical analyses were performed using Prism 5 (GraphPad). Differences were considered statistically significant with * $p<0.05$, ** $p<0.01$, *** $p<0.001$ in figures or indicated by letters a or b when compared to control group or high fat group, respectively ($p<0.05$). One-way ANOVA was used to detect differences between dietary groups with Tukey post-test to identify significant differences. For body mass development and glucose tolerance tests, Two-way ANOVA was used with Bonferroni post-test to identify statistically significant differences between dietary groups.

Correlation analysis between gene expression and mass or between masses was performed using the Pearson test.
Analysis of co-variance (ANCOVA) was performed using a combination of linear regression and ANOVA according to Packard et al. (Packard and Boardman, 1999).

3.25 Buffer recipes

3.25.1 Protein isolation and SDS-PAGE

Radio-immunoprecipitation assay (RIPA) buffer

0.05 M Tris / HCl, pH 8
0.15 M NaCl
0.001 M EDTA, pH 8
0.2 % SDS
1 % NP-40
0.25 % Na-Deoxycholate
in H_2O, to pH 7.4

5 x sample buffer ("Laemmli buffer")

1.875 g Tris / HCl
2.5 g SDS
12.5 g (14 ml) glycerol
2.5 ml 1 M DTT, 1 M
500 µl 250 mM EDTA
+ H_2O ad 50 ml, to pH 6.8
+ ≈1 mg bromophenolblue

Stacking gel stock (5 %) for 1 gel

1.17 ml H_2O
0.5 ml 0.5 M Tris / HCl, pH 6.8
20 µl 10 % SDS
0.33 ml 30 % Acrylamide / Bis-acrylamide
2 µl TEMED
15 µl 10 % (w / v) APS, 10 % (w/v)
+ ≈1 mg bromophenolblue

10 x (glycine) running buffer

250 mM Tris / HCl
2 M glycine
1 % (w / v)
+ H_2O, to pH 8.3

Separating gel buffer

1.5 M Tris / HCl
+ H_2O, to pH 8.8

3.25.2 Western blot

Anode 1 buffer

0.3 M Tris

200 ml methanol

+ H_2O ad 1 l

Anode 2 buffer

25 mM Tris

200 ml methanol

+ H_2O ad 1 l

Cathode buffer

25 mM Tris

40 mM aminocaproic acid

200 ml methanol

+ H_2O ad 1 l

10 x tris-buffered saline (TBS)

200 mM Tris

1.37 M NaCl

+ H_2O ad 1 l, to pH 7.6

1 x TBS + Tween-20® (TBS-T)

100 ml 10 x TBS

0.1 % Tween-20®

+ H_2O ad 1 l

3.25.3 Agarose gel electrophoresis

10 x Tris / borate / EDTA (TBE) buffer

500 ml H_2O

54 g Tris

27.5 g boric acid

20 ml 5 M EDTA, pH 8

+ H_2O ad 1 l, to pH 8

50 x Tris / acetate / EDTA (TAE) buffer

500 ml H_2O

242 g Tris

57.1 ml 100 % acetic acid

100 ml 5 M EDTA, pH 8

+ H_2O ad 1 l, to pH 8

4 Results

4.1 Study Design

The study of diet-induced obesity in animals involves some critical aspects that have to be determined and clearly defined because they influence the outcome. The study design is dependent on:

1) the characteristics of the model organism and statistical power based on the primary outcome investigated,

2) the housing conditions and characteristics of the applied diets, and

3) the time period of the study.

Furthermore, experiments to answer the research question, will require:

1) measurements and physiological tests during the study (live animal) and

2) time point dependent organ sampling and analysis (dead animal).

This work was based on an intervention study design comparing three diets (Figure 5). Male wild-type C57BL/6J mice were kept at standard specific pathogen-free conditions. They were singly housed and introduced to the experiment with 8 weeks of age after an adaptation phase of 2 weeks. The animals (n=28 per group) were randomly assigned to be fed one of three diets, namely a control diet (C), a high fat diet (HF) and a high fat diet enriched with n-3 LC-PUFA eicosapentaenoic (EPA) and docosahexaenoic acid (DHA; HF/n-3). To analyze effects of time, twelve mice per group were fed for 6 or 12 weeks (with 4 additional mice) in each dietary group before termination of the experiment.

During the study the following measurements and physiological tests were performed with live animals:

1) body mass was monitored weekly,

2) body compositon was analyzed every other week,

3) food intake over the course of one week was measured 8 times,

4) feces of one week was collected 8 times,

5) glucose tolerance tests were performed after 4, 6, and 12 weeks of feeding,

6) blood was withdrawn after 4, 6, and 12 weeks of feeding.

Experiments were finished after 6 or 12 weeks of feeding with tissue dissection and sampling for analysis of gene and protein expression and histological analysis.

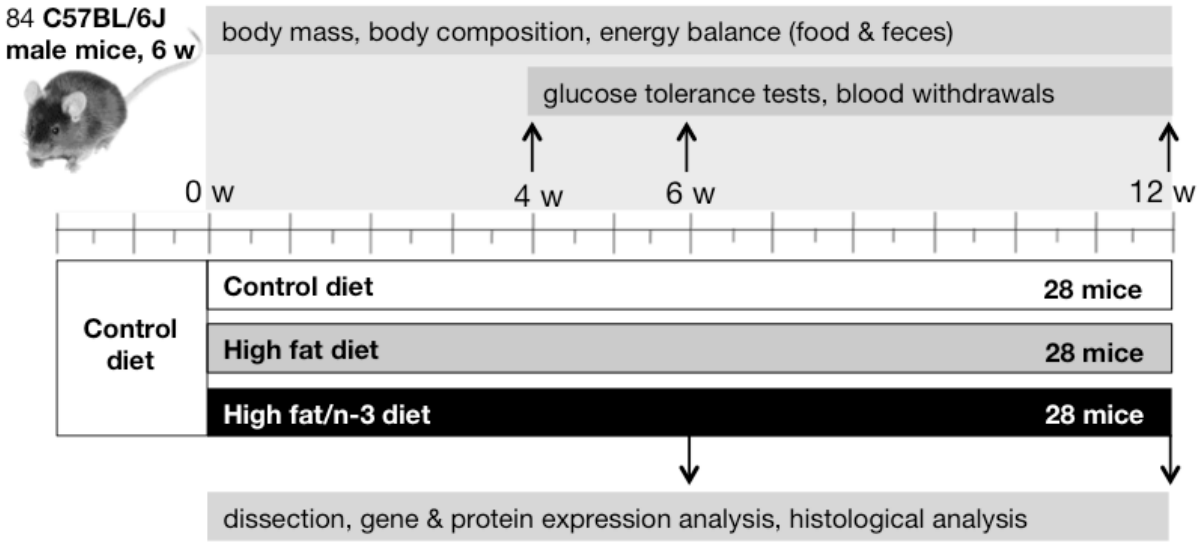

Figure 5: Study design. 84 male C57BL/6J mice aged 6 weeks were adapted on control diet for 2 weeks. Mice were then randomly assigned to three groups fed different diets. 28 mice remained on control diet, 28 mice were switched to a high fat diet and the remaining 28 mice to a high fat diet enriched in n-3 LC-PUFA eicosapentaenoic (EPA) and docosahexaenoic acid (DHA). Body mass was measured weekly, body composition, food intake, and feces production were determined every other week. At week 4, 6, and 12, mice were fasted for blood withdrawal and glucose tolerance tests. Mice were sacrificed after 6 or 12 weeks for dissection and organ sampling for gene and protein expression as well for histological analysis.

4.2 Diet composition

High fat diet-induced obesity is a common model in the study of obesity and its associated pathologies (Buettner et al., 2006; Wang and Liao, 2012). Since there is no standard high fat diet, the characteristics of the diet need to be clearly defined and ingredients carefully analyzed to allow for comparability with other studies when generating an obese, hyperlipidemic, and insulin resistant phenotype (Buettner et al., 2007).

The experimental diets applied in this study were newly designed for studies of diet-induced obesity in the mouse model under specific-pathogen-free conditions. Emphasis was put on the specification of the fat component as the only variable to guarantee as much comparability of dietary groups as possible.

The applied diets (Table 1) were three purified experimental diets, manufactured by Ssniff Spezialdiäten GmbH (Soest, Germany) as pellets of 10 mm diameter made from powdered components or oils at 25–30 °C and sterilized with 25 kGy / min (Isotron Deutschland, Allershausen, Germany). They included a low-fat, herein called “control” diet (C), a high fat diet (HF) and a high fat diet enriched with n-3 LC-PUFA EPA / DHA (HF/n-3).

4.3 Macronutrient and micronutrient composition

Macronutrient and micronutrient composition were provided by the manufacturer (Table 1). All diets contained the essential macronutrients (fat, carbohydrates, protein), vitamins, minerals as well as anti-oxidants. Lipid and starch content were the only nutrients that varied among the different diets.

For the protein fraction, 24 % (w / w) were from non-hydrolyzed casein in all three diets. The carbohydrate component consisted of 5.6 % (w / w) maltodextrin, 5.0 % (w / w) sucrose and 5.0 % (w / w) cellulose in fixed amounts for each diet. As an exception, corn starch was added in variable amounts depending on the diet [C, 47.49 % (w / w); HF and HF/n-3, 27.79 % (w / w)] for reasons of energy balance.

The quantity and composition of fat varied with every diet. In the low fat control diet, lipids were only 5 % (w / w) and solely from soybean oil. This fraction of soybean oil was included in all three diets. In the HF diets the fat quantity was increased to 25 % (w / w) by addition of 20 % (w / w) palm oil. To increase the content of n-3 LC-PUFA without changing any other ingredient, 8.75 % (w / w) of palm oil were exchanged by an n-3 LC-PUFA-rich concentrate from fish oil (EPAX 1050 TG; kindly provided by Goerlich Pharma International GmbH, Edling, Germany) in the HF/n-3 diet.

To guarantee stability of the diets during storage, handling and feeding, the diets were enriched with 0.015 % (w / w) anti-oxidant butylhydroxytoluene (BHT) and 0.018 % (w / w) dl-α-tocopheryl acetate.

Additionally, a vitamin mix including vitamins A, D_3, E, K_3, C, B_1, B_2, B_6, B_{12}, Ca-D-pantothenic acid, niacin, folic acid, biotin and inositol (personal communication with A. Schuhmacher, Ssniff Spezialdiäten GmbH) was added. Since these diets had to be sterilized for their usage in the SPF animal facility, the amount of the vitamin mix was increased by 20 % to 12 g / kg [1.2 % (w / w)]. Other minerals and ingredients specified were L-cystine [6 % (w / w)], minerals & trace elements [6 % (w / w)], and choline chloride [0.2 % (w / w)].

Table 1: Composition of diets. Shown are w / w or energy% (en%) macronutrients and other ingredients in different diets. C, control diet; HF, high fat diet; HF/n-3, high fat diet enriched with n-3 LC-PUFA EPA / DHA. Nutrient composition was kept constant across different diets except for corn starch and fat components. Gross energy was determined by bomb calorimetry (n=3). Index letter a indicates significant difference compared with control group ($p<0.0001$).

Nutrient	Diet		
	C	HF	HF/n-3
Lipids (w / w %)			
Soybean oil	5.00	5.00	5.00
Palm oil	-	20.00	11.25
EPAX 1050 TG (DHA / EPA)	-	-	8.75
Cholesterol	0.013	0.038	0.021
Carbohydrates (w / w %)			
Corn starch	47.79	27.79	27.79
Maltodextrin	5.60	5.60	5.60
Sucrose	5.00	5.00	5.00
Cellulose	5.00	5.00	5.00
Protein (w / w %)			
Caseine	24.00	24.00	24.00
Antioxidants (w / w %)			
Butylhydroxytoluene	0.015	0.015	0.015
dl-α-tocopheryl acetate	0.018	0.018	0.018
Others (w / w %)			
L-cystine	0.20	0.20	0.20
Vitamins	1.20	1.20	1.20
Minerals & trace elements	6.00	6.00	6.00
Choline-chloride	0.20	0.20	0.20
Gross energy (MJ / kg)	16.61± 0.04	21.16 ± 0.08a	20.92 ± 0.37a
Fat (en%)	13.00	48.00	48.00
Carbohydrates (en%)	64.00	34.00	34.00
Protein (en%)	23.00	18.00	18.00

4.4 Sterol content

Cholesterol and phytosterols may have effects on lipid metabolism and intestinal uptake that may influence the research aim and possibly counter-act n-3 LC-PUFA-mediated effects (Stangl et al., 1994; Calpe-Berdiel et al., 2009) even though phytosterols are usually excreted (von Bergmann et al., 2005). Compared with other studies, the diets used here can be considered almost cholesterol-free (Nishina et al., 1990; Stangl et al., 1994; Lichtman et al., 1999; Maxwell et al., 2003; Ringseis and Eder, 2004).

To get an overview of the sterol content of different fat sources, cholesterol and phytosterol content were determined in animal fats (beef tallow, lard, n-3 LC-PUFA concentrate EPAX 4050 TG from fish) and plant oils (soybean oil, palm oil) by GC-FID / GC-MS (Table 2). The results showed that the animal fats only contain cholesterol with the highest amount in lard (101.0 mg / 100 g), but also the fish oil contained 75.3 mg / 100 g, which was almost 75 % of the lard value. In contrast, cholesterol was lacking in the pure plant oils, but they contained phytosterols with sitosterol as the most abundant sterol. Compared with palm oil (58.7 mg / 100 g sterols), soybean oil contained 6 to 7 times more phytosterols, respectively. This was mainly due to higher sitosterol contents (soybean oil, 169.5 mg / 100 g).

Additionally, cholesterol content was determined in the diets (Table 1). Surprisingly, cholesterol was detected in all three diets. Even though in the isolated soybean oil and palm oil no cholesterol was detectable, it was found in the control and the HF diet. However, measured cholesterol levels were lower than 0.04 % in the diets.

In summary, even though the control and HF diet only contained plant-derived fats that should not contain cholesterol, but only phytosterols, cholesterol was present in these diets. Fish oil also contained cholesterol in comparable levels to other animal fats.

Table 2: Quantitative analysis of identified sterols and total sterol content in different fat types. (T. Lubinus, Food Technology Unit, TUM).

fat type	sterol (mg / 100 g)		total sterol content (mg / 100 g)
beef tallow	cholesterol	48.2	48.2
lard	cholesterol	101.0	101.0
EPAX 4050 TG	cholesterol	75.3	75.3
soybean oil	campesterol	55.2	298.0
	stigmasterol	56.4	
	sitosterol	169.5	
	lanosterol	8.7	
	sitostanol	8.3	
palm oil	campesterol	12.9	58.7
	stigmasterol	7.5	
	sitosterol	38.3	

4.5 Fatty acid composition

Because effects of changes in fat quality in a high fat diet were the focus of this work, it was of critical importance to specify the fatty acid composition of the fats and diets.

Fatty acid composition of soybean and palm oil (Table 3, Table 4) was determined by gas chromatography-FID/MS whereas EPAX 1050 TG composition was provided by the manufacturer (EPAX, 2012).

In soybean oil more than 90 % of fatty acids were from the n-6 PUFA linoleic acid (53.37 %), the monounsaturated oleic acid (23.06 %), the saturated palmitic acid (11.01 %) and n-3 PUFA α-linolenic acid (5.97 %). Thus, more than half of total fatty acids were PUFA with a ratio of n-6 : n-3 PUFA of 8.97 : 1. Only about 15 % of fatty acids were saturated fatty acids.

In contrast, in palm oil more than 95 % of fatty acids were from the saturated palmitic acid (42.47 %), the monounsaturated oleic acid (39.21 %), the n-6 PUFA linoleic acid (9.90 %), and the saturated stearic acid (4.30 %). Here, the content of PUFA was only 10 % (n-6 : n-3 PUFA of 70.71 : 1) whereas about 50 % of total fatty acids were saturated species.

The composition table of the EPAX 1050 TG concentrate did not specify every individual fatty acid, but provided information about groups (Table 4). 70–75 % of fatty acids were n-3 LC-PUFA eicosapentaenoic acid (EPA) and docosahexaenoic acid (DHA) whereas saturated species did not even amount to 10 %.

Table 3: Fatty acid pattern of soybean and palm oil as determined by gas chromatography-FID / MS. X:n indicates the length of the fatty acid with x carbons containing n double bonds. ratio n-6 / n-3, ratio of omega-6 to omega-3 PUFA.

fatty acid species			mass %	
			soybean oil	palm oil
Lauric acid	12:0		-	0.25
Myristic acid	14:0		0.12	1.09
Pentadecanoic acid	15:0		-	0.05
Palmitic acid	16:0		11.01	42.37
Palmitoleic acid	16:1		0.11	0.17
Heptadecanoic acid	17:0		0.09	0.10
Heptadecenoic acid	17:1		0.05	-
Stearic acid	18:0		2.97	4.30
Elaidic acid	18:1		-	0.07
Oleic acid	18:1		23.06	39.21
cis-Vaccenic acid	18:1		1.65	0.69
Linoleic acid	18:2	n-6	53.37	9.90
Linolenic acid	18:3	n-3	5.97	0.14
Arachidic acid	20:0		0.31	0.36
Eicosenoic acid	20:1		0.22	0.15
Behenic acid	22:0		0.43	0.08
Lignoceric acid	24:0		0.15	0.07
ratio n-6 / n-3			8.97	70.71

Table 4: Composition of EPAX 1050 TG n-3 LC-PUFA concentrate. EPA, eicosapentaenoic acid; DHA, docosahexaenoic acid; TAG or TG, triacylglycerol; FA, fatty acid; SFA, saturated fatty acids; MUFA, monounsaturated fatty acid; LC-PUFA, long chain polyunsaturated fatty acids (adapted from EPAX, 2012).

ingredient	amount (% or mg / g)		
EPA C20:5 (%)	max. 17	min. 150 mg / g as TAG	min. 150 mg / g as FA
DHA C22:6 (%)	min. 50	min. 430 mg / g as TAG	min. 400 mg / g as FA
n-3 LC-PUFA total (%)	70-75	min. 600 mg / g as TAG	
SFA (%)		3-8	
MUFA (%)		8-15	
PUFA (%)		74-81	
Calories (kJ / g)		38	
Carbohydrates (%)		-	
Protein (%)		-	
Sodium (%)		-	
Mixed tocopherols (mg / g)		2.8-4.5	
DHA / EPA		2.94	

As these data only represented the analysis of isolated oils but did not account for the fatty acid composition of a composite diet (e.g. for HF/n-3 with a mixture of soybean oil, palm oil and EPAX 1050 TG), fat was additionally extracted from manufactured diets and analyzed as above (Table 5).

As expected, the fatty acid composition of the control diet was similar to the isolated analysis of soybean oil with a deviation of less than 10 %. The HF diet contained almost balanced amounts of the saturated palmitic acid (36.70 %) and the monounsaturated oleic acid (35.81 %); saturated species constituted 42.66 %. About one fifth of total fatty acids were n-6 PUFA linoleic acid (18.07 %), but only 1.34 % of n-3 PUFA α-linolenic acid. Compared with palm oil alone (Table 3), the ratio of n-6 : n-3 PUFA of 13.50 : 1 was about fivefold lower.

The HF/n-3 diet showed the broadest pattern of fatty acids including many n-6 and n-3 PUFA species. The n-3 LC-PUFA DHA (15.05 %), EPA (4.05 %) – in a ratio of 3.72 : 1 –, and α-linolenic acid (1.40 %) constituted more than 20 % of total fatty acids. This was almost balanced by about 18 % n-6 PUFA with linoleic acid (16 %) as the predominant species and minute amounts of n-6 LC-PUFA arachidonic acid (0.9 %), which was not detectable in the other diets. This balance was reflected in a ratio of n-6 : n-3 PUFA of 0.84 : 1.

Compared with the high fat diet, saturated fatty acids with high amounts of palmitic acid (23.91 %) were decreased by 13 % to 30 % of total fatty acids. Oleic acid made up another 26.08 % of total fatty acids.

In summary, all three diets showed high amounts of saturated palmitic and monounsaturated oleic acid especially in the HF diets. In contrast, the essential PUFA

linoleic acid and α-linolenic acid showed high variability relative to total fatty acids when comparing control diet with HF diets. The n-3 LC-PUFA DHA and EPA were only detectable in the HF/n-3 diet, but constituted 20 % of total fatty acids.

Table 5: Fatty acid pattern of diets as determined by gas chromatography-FID / MS. X:n indicates the length of the fatty acid with x carbons containing n double bonds. C, control diet; HF, high fat diet; HF/n-3, high fat diet enriched with n-3 LC-PUFA EPA / DHA; SFA, saturated fatty acids; MUFA, monounsaturated fatty acids; ratio n-6 / n-3, ratio of omega-6 / omega-3 PUFA.

fatty acid species			mass %		
			C	HF	HF/n-3
Lauric acid	12:0		0.07	0.13	0.09
Myristic acid	14:0		0.30	0.88	0.66
Pentadecanoic acid	15:0		0.04	0.05	0.07
Palmitic acid	16:0		11.37	36.70	23.91
Palmitoleic acid	16:1		0.12	0.15	0.30
Heptadecanoic acid	17:0		0.09	0.10	0.18
Heptadecenoic acid	17:1		0.05		0.07
Stearic acid	18:0		3.60	4.18	4.00
Elaidic acid	18:1		0.08	0.14	0.07
Oleic acid	18:1		23.47	35.81	26.08
cis-Vaccenic acid	18:1		1.53	0.87	1.11
18:2 Isomer	18:2		0.38	0.20	0.14
Linoleic acid	18:2	n-6	50.85	18.07	16.00
γ-Linolenic acid	18:3	n-6			0.12
Conjugated Linoleic acid (CLA)	18:2		0.11		
18:3 Isomer	18:3		0.39	0.09	0.10
Linolenic acid	18:3	n-3	5.16	1.34	1.40
Stearidonic acid	18:4	n-3			0.16
Arachidic acid	20:0		0.35	0.38	0.48
Eicosenoic acid	20:1		0.22	0.15	0.83
Eicosadienoic acid	20:2	n-6			0.21
Heneicosanoic acid	21:0				0.04
Eicosatrienoic acid	20:3, 8c, 11c, 14c	n-6			0.09
Eicosatrienoic acid	20:3, 11c, 14c, 17c	n-3			0.14
Arachidonic acid	20:4	n-6			0.90
Eicosapentaenoic acid (EPA)	20:5	n-3			4.05
Behenic acid	22:0		0.48	0.16	0.27
Cetoleic acid	22:1		0.11		0.11
Erucic acid	22:1				0.12
Docosatetraenoic acid	22:4	n-6			0.11
Docosapentaenoic acid	22:5	n-6			0.77
Docosapentaenoic acid (DPA)	22:5	n-3			0.88
Docosahexaenoic acid (DHA)	22:6	n-3			15.05
Tricosanoic acid	23:0		0.04		
Lignoceric acid	24:0		0.17	0.09	0.13
Nervonic acid	24:1		0.36		0.36
SFA			16.55	42.66	29.83
MUFA			25.95	37.14	29.05
PUFA			56.90	19.70	40.12
n-3 PUFA			5.16	1.34	21.68
n-6 PUFA			50.85	18.07	18.19
ratio n-6 / n-3			9.85	13.50	0.84

4.6 Food energy and energy balance

Gross energy was determined by bomb calorimetry and was significantly different between control (16.61 ± 0.04 MJ / kg) and HF diet but isocaloric among HF diets (HF, 21.16 ± 0.08 MJ / kg; HF/n-3, 21.92 ± 0.37 MJ / kg; Table 1).

About 10 en% (= % energy) in the control and 48 en% in both high fat diets were from fat. Thus, fat was the macronutrient providing about half and thus most of the energy in the HF and HF/n-3 diets.

To assure that diet-induced obesity and an expected amelioration by n-3 LC-PUFA intervention was not caused by differences in food intake, weekly food consumption was measured for a total of eight weeks throughout the study. To allow assumptions on energy assimilation, feces mass and energy were determined additionally.

Weekly food intake was not different between groups (C, 22.01 ± 0.43 g; HF, 20.89 ± 0.31 g; HF/n-3, 22.21 ± 0.38 g; $p=0.0542$, Figure 6A). Since gross food energy was significantly different between control and HF diets but isocaloric among HF diets, weekly energy intake displayed the same pattern (C, 365.51 ± 7.11 kJ; HF, 442.05 ± 6.57 kJ; HF/n-3, 464.53 ± 8.02 kJ; $p<0.0001$; Figure 6B).

Furthermore, weekly energy excretion as the product of weekly feces output mass and feces energy was not different between control (30.45 ± 0.60 kJ) and HF group (33.08 ± 1.30 kJ) but the difference between HF and HF/n-3 group (29.02 ± 0.65 kJ; $p=0.0172$; Figure 6C) was about 13 %. The difference between the energy intake and energy output constitutes the assimilated energy. Energy output here does not include, however, the energy excreted by urine, but only by feces. Assimilation efficiency is the expression of assimilated energy relative to total energy intake (Figure 6D) and was significantly different between all dietary groups (C, 91.54 ± 0.24 %; HF, 92.53 ± 0.23 %; HF/n-3, 93.69 ± 0.11 %; $p<0.0001$).

In summary, animals did not consume different amounts of food, but energy intake was significantly higher in HF and HF/n-3 animals. Mice fed HF/n-3 excreted significantly less energy compared with HF animals. In turn, assimilation efficiency was highest in HF/n-3-fed mice.

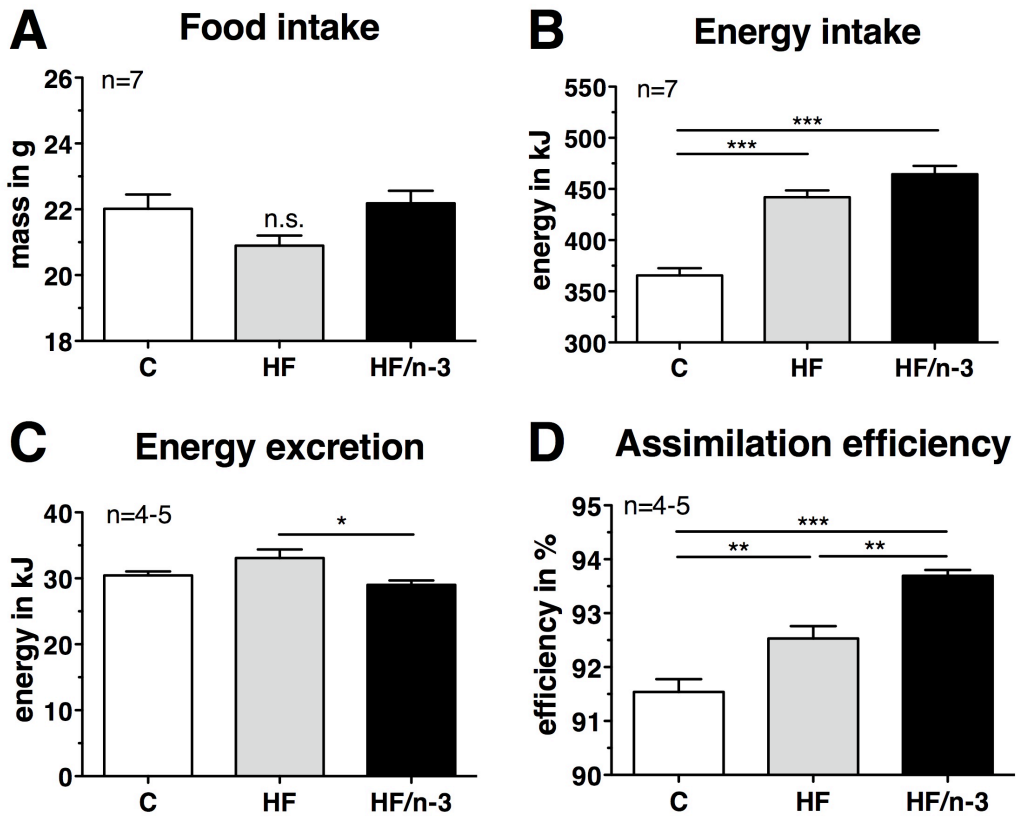

Figure 6: Energy balance in mice. Shown are the average values for weekly food intake (A), weekly energy intake (B), weekly fecal energy excretion (C) and assimilation efficiency (D). Energy intake was calculated with the provided gross energy of food (Table 1). All data are represented as means ± standard error. Statistical analysis was performed using One-Way ANOVA and Tukey post-test. Asterisks indicate significant differences compared with control or between groups as indicated. * $p<0.05$; ** $p<0.01$; *** $p<0.001$; n.s., not significant.

4.7 Fatty acid and EPA / DHA intakes

With the information of food intake (Figure 6) and the amount of dietary fat (Table 1) and fatty acid composition (Table 5) provided, it was possible to calculate the daily absolute amounts of fatty acids taken in by mice per day.

EPA = daily food intake [g / d] * fraction of fat in diet [%] * fraction of EPA in fat [%]

EPA = (22.23 / 7) [g / d] * 25 [%] * 4.05 [%] = 3.18 [g / d] * 0.25 * 0.0405 = 0.032 [g / d]

EPA = 32 mg / d.

DHA = daily food intake [g / d] * fraction of fat in diet [%] * fraction of EPA in fat [%]

DHA = (22.23 / 7) [g / d] * 25 [%] * 15.05 [%] = 3.18 [g / d] * 0.25 * 0.1505 = 0.120 [g / d]

DHA = 120 mg / d.

For later comparison this calculation was also performed for a study by Ruzickova et al. (Ruzickova et al., 2004). With the information of food intake (high fat diet "cHF", 65 kJ / day; n-3 LC-PUFA-rich diet "cHF-F2", 60 kJ / day), the energy density of the food (22.8 kJ / g), the amount of fat in the diets [35.2 % (w / w)], and the amount of EPA / DHA in fat (3.3 % / 29.2 %) provided, it was possible to calculate the daily absolute amounts of EPA and DHA consumed by mice in this study.

Daily food intake = energy intake (kJ / d) / food energy density (kJ / g)
Daily food intake = (60 kJ / day) / (22.8 kJ / g) = 2.63 g / d

EPA = daily food intake (g / d) * fraction of fat in diet (%) * fraction of EPA in fat (%)
EPA = 2.63 g / d * 35.2 % * 3.3 % = 2.63 g / d * 0.352 * 0.033 = 0.031 g / d
EPA = 31 mg / d.
DHA = daily food intake (g / d) * fraction of fat in diet (%) * fraction of EPA in fat (%)
DHA = 2.63 g / d * 35.2 % * 29.2 % = 2.63 g / d * 0.352 * 0.292 = 0.270 g / d
DHA = 270 mg / d.

Similarly, high fat diets from this study and Ruzickova's study were compared by intake of absolute amounts of selected fatty acids (Figure 7). An estimation of absolute fatty acid intake for control diets was not possible due to lack of data for respective control group in the reference study (Ruzickova et al., 2004).
The comparison to the HF diet applied in this thesis work (Figure 7A) demonstrated that mice fed cHF consumed less than half the amount of palmitic acid C16:0 (cHF, 113 mg; HF, 274 mg) but almost twice as much oleic acid C18:1 (cHF, 510 mg; HF, 267 mg). For palmitic acid this pattern was also observed when comparing the fish oil diets HF/n-3 and cHF-F2 (cHF-F2, 91 mg; HF/n-3, 190 mg), but not for oleic acid anymore (cHF-F2, 240 mg; HF/n-3, 207 mg; Figure 7B). Compared to these fatty acids, LC-PUFA intake was small with the exception of DHA with a difference of 150 mg in intake between both studies (cHF-F2, 270 mg; HF/n-3, 120 mg).

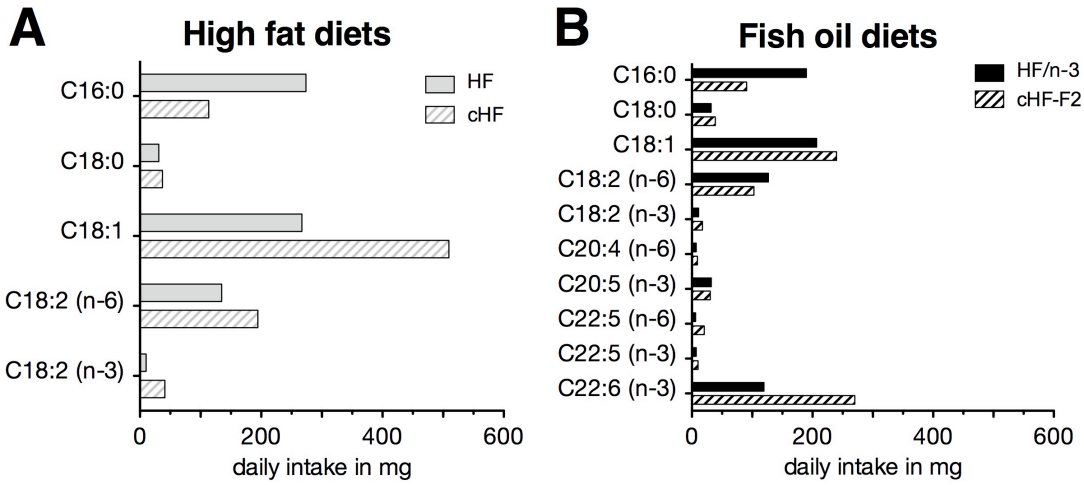

Figure 7: Absolute daily intakes of fatty acids in high fat diets. Shown are the absolute daily intakes of selected fatty acids in high fat diets (HF and cHF, **A**) and fish oil high fat diets (HF/n-3 and cHF-F2, **B**) from this study (HF and HF/n-3) and a study by Ruzickova and co-workers (cHF and cHF-F2; Ruzickova et al., 2004). Amounts in mg were calculated with the information of food intake and fat and fatty acid composition of diets in both studies. Cx:n indicates the length of the fatty acid with x carbons containing n double bonds, trivial names are given in Table 5.

Another way of displaying n-3 LC-PUFA intake that is frequently used in human studies is the calculation of energy% n-3 LC-PUFA provided. According to the Food and Nutrition Board of the U.S. National Academy of Sciences, Institute of Medicine the Acceptable Macronutrient Distribution Range (AMDR), i.e. “the range of intake for a particular energy source that is associated with reduced risk of chronic disease while providing intakes of essential nutrients”, for n-3 LC-PUFA is 0.6-1.2 en% (U.S. National Academy of Sciences / NAS, 2005) and 0.7 to 0.9 en% in Germany (German Nutrition Society / DGE, 2006).

From the data provided in this thesis the absolute amount of n-3 LC-PUFA taken in per day can be calculated (Figure 6, Table 1, Table 5):

n-3 LC-PUFA = daily food intake [g / d] * fat in diet [%] * n-3 LC-PUFA in fat [%]

n-3 LC-PUFA = (22.23 / 7) [g / d] * 25 [%] * 21.68 [%] = 3.18 [g / d] * 0.25 * 0.2168 = 0.1724 [g / d]

n-3 LC-PUFA = 172 mg / d.

Assuming that fat contains 37.67 kJ / g (= 9 kcal / g), the relative daily energy consumption from n-3 LC-PUFA is:

n-3 LC-PUFA = (daily n-3 LC-PUFA intake [g / d] * fat energy [kJ / g]) / daily intake [kJ / d]

n-3 LC-PUFA = (0.1724 [g / d] * 37.67 [kJ / g]) / (439.70 / 7) [kJ / d]

n-3 LC-PUFA = 6.49 [kJ / d] / 62.81 [kJ / d] = 0.1034

n-3 LC-PUFA = 10.3 en%

For the study of Ruzickova et al. (Ruzickova et al., 2004) the approach is equivalent:
n-3 LC-PUFA = daily food intake [g / d] * fat in diet [%] * n-3 LC-PUFA in fat [%]
n-3 LC-PUFA = 2.63 [g / d] * 35.2 [%] * 36.1 [%] = 2.63 [g / d] * 0.352 * 0.361 = 0.3342 [g / d]
n-3 LC-PUFA = 334 mg / d.
n-3 LC-PUFA = (daily n-3 LC-PUFA intake [g / d] * fat energy [kJ / g]) / daily intake [kJ / d]
n-3 LC-PUFA = (0.3342 [g / d] * 37.67 [kJ / g]) / 60 [kJ / d]
n-3 LC-PUFA = 12.59[kJ / d] / 60 [kJ / d] = 0.2098
n-3 LC-PUFA = 21.0 en%

To compare intakes of EPA and DHA from this study (152 mg / d) with recommendations for humans (0.5 g / d according to the International Society for the Study of Fatty Acids and Lipids / ISSFAL, 2004), intakes can be scaled to body mass. Assuming an average body mass of 35 g for mice and 70 kg for humans, the following difference is estimated:

Mouse: 152 mg / d / 0.035 kg = 4343 mg / d per kg body mass
Human: 500 mg / d / 70 kg = 7 mg / d per kg body mass

Thus, mice took in the 620-fold amount of EPA and DHA compared with recommendations for humans per kg body mass. This calculation would apply if metabolic data from mice could be isometrically extrapolated to the human situation and vice versa. The researcher Max Kleiber was the first to note that metabolic rate is inversely related to body size and proposed an equation that accounts for these differences (allometric scaling; Kleiber, 1932, 1961).

Metabolic rate P_{met} [kcal / d] = 70 * body mass M_b [kg]$^{0.75}$. Entering the same body masses as above, gives:
Mouse: P_{met} [kcal / d] = 70 * 0.035 [kg]$^{0.75}$ = 5.66 [kcal / d]
Human: P_{met} [kcal / d] = 70 * 70 [kg]$^{0.75}$ = 1694.03 [kcal / d]

Thus, there is roughly a 300-fold difference in metabolic rate between mice and humans. Taking this difference in metabolic rate into account, mice in this study have taken in about twice (620 / 300) as much EPA and DHA compared with current recommendations for humans per day.

4.8 Locomotor activity and indirect calorimetry

Because Western diets tend to negatively affect physical activity and energy metabolism and thus lead to an obese phenotype (Bjursell et al., 2008) that can be counteracted by n-3 LC-PUFA (Rustan et al., 1993; Sato et al., 2010), the effect of n-3 LC-PUFA EPA / DHA in a HF diet on locomotor activity and energy consumption was investigated in a group of mice.

When animals (n=4) of the HF and HF/n-3 groups were placed into a climate simulation station at 22 °C for four days after 8 weeks of feeding, both groups of animals showed a repeating pattern of the respiratory quotient peaking at the beginning of the dark phase and reaching a low at the beginning of the light phase (Figure 8A-C). Apparently, this state of equilibrium was not reached before 48 hours, also indicated by food intake which was not different between groups after this time point anymore (data not shown).

HF/n-3 mice had a slightly elevated respiratory quotient (RQ) during the first half of the dark phase (Figure 8A). This was confirmed by an analysis of average RQ during the dark phases (Figure 8B), but failed to show a significant elevation of energy consumption in HF/n-3 animals (RQ in dark phase 3: HF, 0.735 ± 0.01; HF/n-3, 0.750 ± 0.01; RQ in dark phase 4: HF, 0.728 ± 0.01; HF/n-3, 0.743 ± 0.01). Similarly, there was no change in daily energy expenditure (Figure 8C).

For the measurement of locomotor activity (Figure 8D-F) mice were observed for 12 consecutive days after 12 weeks of feeding on the three experimental diets. The average locomotor activity per day and group showed highly elevated counts for control-fed mice during the early light phase (6–9 h) and the first half of the dark phase (19–1 h) compared with the HF groups (Figure 8D).

Interestingly, mice of all dietary groups showed a sharp increase of activity shortly before the end of the nocturnal dark phase (5 h). Slightly differing levels of physical activity in the HF groups could only be observed in the morning phase (7–11 h; activity of HF>HF/n-3) and in the early dark phase (18–22 h, activity of HF<HF/n-3).

These tendencies were also visible when analyzing the cumulated locomotor activity over the whole light (Figure 8E) and dark phase (Figure 8F). Both HF groups showed a significant reduction of physical activity compared with control animals, but a significant change between HF and HF/n-3 mice could not be observed.

Taken together, control mice showed significantly elevated locomotor activity compared with HF and HF/n-3 animals. The dietary treatment with n-3 LC-PUFA, however, neither significantly increased physical activity nor elevated energy consumption in these mice compared with HF animals.

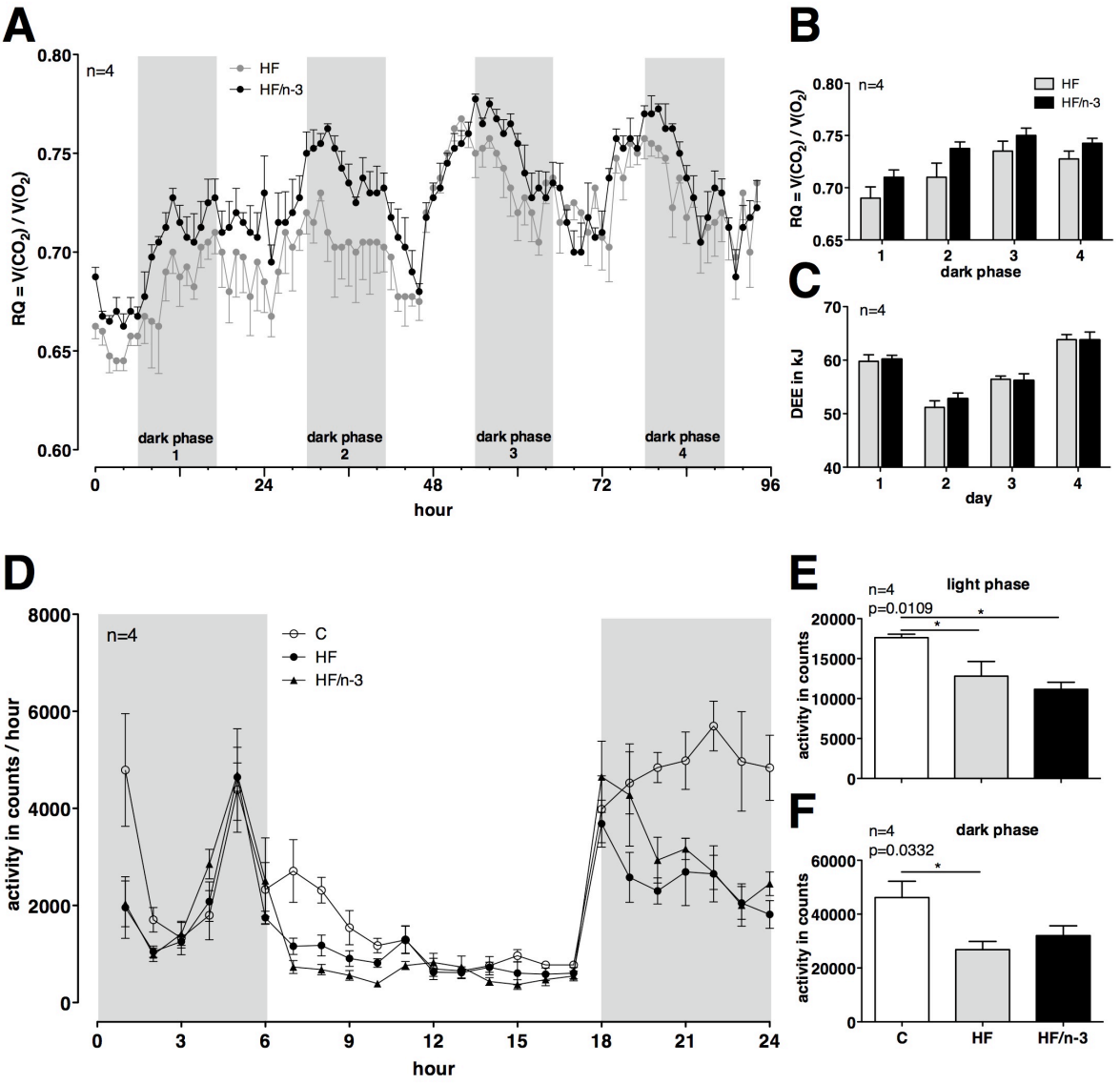

Figure 8: Energy consumption (indirect calorimetry) and locomotor activity. After 8 weeks of feeding on high fat (HF) or high fat diet enriched with n-3 LC-PUFA EPA / DHA (HF/n-3) animals were analyzed for energy consumption over four consecutive days. Respiratory quotient (RQ) per group per hour was plotted with grey-shaded areas showing the dark phase (**A**). RQ per group was analyzed for every dark phase (**B**). Mean daily energy expenditure (DEE) per group was plotted per day (**C**). Activity was determined after 12 weeks of feeding for 2 weeks on C, control diet; HF, high fat diet; HF/n-3, high fat diet enriched with n-3 LC-PUFA EPA / DHA. Shown are activity per group per hour with the dark phase as grey-shaded area (**D**), and cumulated activity during light (**E**) and dark phase (**F**). All data are means ± standard error. Statistical analysis was performed using Two-ANOVA and Bonferroni post-test for indirect calorimetry analysis and One-Way ANOVA and Tukey post-test for cumulated activity analysis. Asterisks indicate significant differences compared with control or between groups as indicated. * $p<0.05$; ** $p<0.01$; ** $p<0.0001$. BM, body mass; VCO_2 / VO_2, carbon dioxide exhalation / oxygen consumption.

4.9 Body mass and composition

HF diet-induced obesity induces an increase in adipose tissue mass that affects body mass, but also other organs like the liver, which might be a target of ectopic lipid deposition whereas n-3 LC-PUFA counteract these effects (Ruzickova et al., 2004; Mori et al., 2007). Table 6 summarizes the data to be described in more detail below.

4.9.1 Body mass

Body mass was determined weekly and weight gain also used as a measure of animal wellbeing and compliance to the study. Initial body mass was at a total average of 21.88 ± 0.16 g and not significantly different in any of the experimental groups to be studied for 6 or 12 weeks (Table 6). After 6 weeks animals in the HF groups had gained significantly more body mass compared with control animals (C, 28.68 ± 0.76 g; HF, 34.42 ± 0.95 g; HF/n-3, 32.52 ± 0.72 g), but a significant reduction of body mass by HF/n-3 diet compared with HF diet was only apparent after 12 weeks (HF, 40.83 ± 1.27 g; HF/n-3, 36.81 ± 0.89 g; Table 6). Only animals in the HF groups were significantly heavier after 12 weeks compared with animals fed for 6 weeks. Control animals did not gain significantly more mass after 6 weeks of feeding (Table 6).

These findings were also reflected in the body mass development displaying the week-by-week increase of body mass (Figure 9). At time point week 0, when animals were assigned randomly to the dietary groups, body mass was similar, but split up into three groups already after one week. Over 12 weeks, control animals only gained 9.67 ± 0.84 g body mass, whereas this value was almost double in HF animals (Table 6). HF-fed animals had a significantly higher body mass compared with controls as early as three weeks whereas in HF/n-3 animals this significant difference was delayed until the 7th week of feeding. While HF/n-3 animals showed reduced body mass compared with HF mice over the whole time course of the experiment, this effect reached statistical significance only after 9 weeks and 12 weeks. Of note, as body mass rose in any of the 3 dietary groups, error bars grew wider showing a higher variation of body mass in animals of the same group. Additionally, the observed effect was independent of body size, since body length was not different among groups (Table 6).

In summary, animals fed HF and HF/n-3 diets had a significantly increased body mass compared with control mice as early as 3 weeks after starting the dietary regimen, but obesity was limited in HF/n-3-fed compared with HF animals, which was statistically significant after 12 weeks.

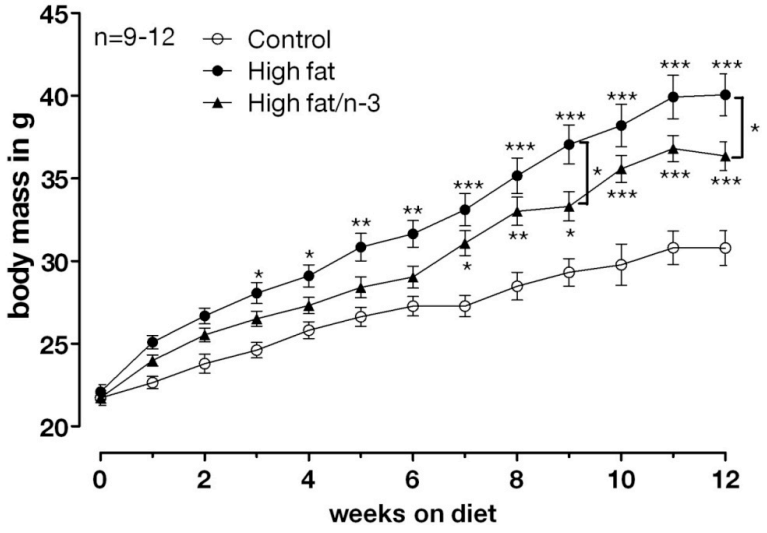

Figure 9: Body mass development in mice on different high fat diets. Male C57BL/6J mice (n=9-12) were fed on either control diet, high fat diet or high fat enriched with n-3 LC-PUFA EPA / DHA for 6 and 12 weeks. Body mass was measured weekly. All data are means ± standard error. Statistical analysis was performed using Two-way ANOVA and Bonferroni post-test. Asterisks indicate significant differences compared with control or between groups as indicated. * $p<0.05$; ** $p<0.01$; *** $p<0.001$.

4.9.2 Fat mass and lean mass

Body mass development was mirrored by fat mass determined by NMR spectroscopy (Figure 10A). After 5 weeks and 8 weeks fat mass reached significant different levels in HF and HF/n-3 mice, respectively, compared with control mice. Moreover, fat mass was significantly decreased in HF/n-3 mice compared with HF mice after 10 and 12 weeks.

Even though lean mass reached a higher level at week 3 in HF groups (Figure 10B), this effect was lost after prolonged feeding and lean mass increased only slightly in all three groups. Lean mass development only marginally contributed to body mass gain.

To prove that fat mass development was significantly modulated by n-3 LC-PUFA after 12 weeks of feeding and that this effect was independent of body mass and size, analysis of co-variance (ANCOVA) was applied. This method uses a combination of linear regression and ANOVA to eliminate body size effects from the data (Packard and Boardman, 1999). Since the pre-requisite of almost identical slopes was given here (Figure 10C, D), ANCOVA was applied. Statistical analysis thus proved the effects observed in body mass and showed a significant decrease of fat mass in HF/n-3 animals compared with HF mice after 12 weeks whereas there was no difference in lean mass between groups (Figure 10E, F).

In summary, fat mass development showed a similar pattern as body mass with an increase in HF and HF/n-3 animals compared with controls and a reductive effect of HF/n-3 diet on fat mass compared with HF diet. In contrast, lean mass did not contribute to these effects,

since it rose only slightly and at the same level in all groups. This effect was statistically significant after 12 weeks of feeding and independent of body mass.

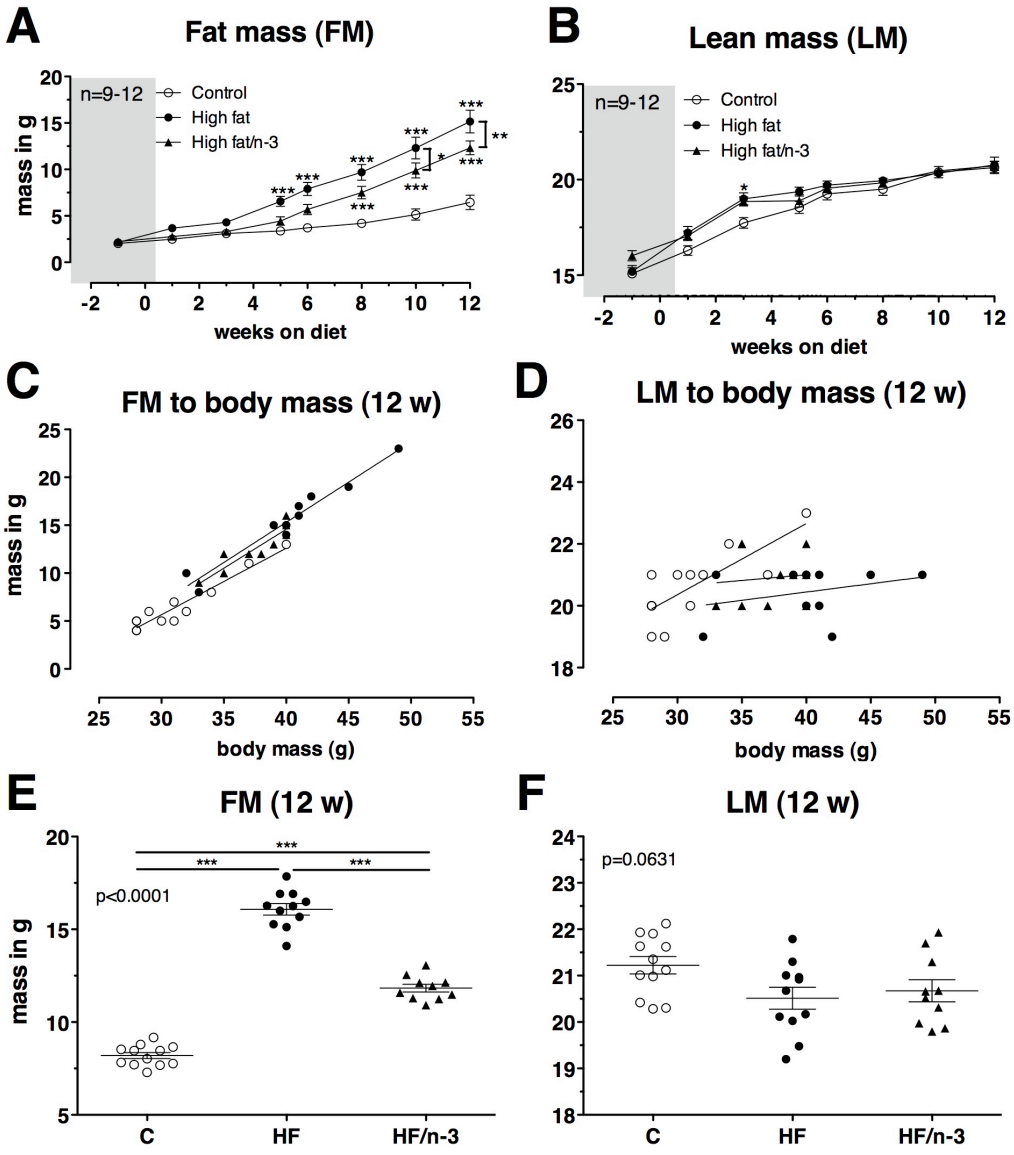

Figure 10: Fat and lean mass development in mice on different high fat diets. Male C57BL/6J mice (n=9-12) were fed on either control diet, high fat diet or high fat enriched with n-3 LC-PUFA EPA / DHA for 6 and 12 weeks. Fat (FM; **A**) and lean mass (LM; **B**) were determined by NMR spectroscopy every other week during feeding. Grey-shaded areas indicate time before switching to experimental diets (adaptation of all mice on control diet). Data are means ± standard error. Statistical analysis was performed using Two-way ANOVA and Bonferroni post-test. The dependence of FM and LM to body mass after 12 w of feeding was analyzed by ANCOVA. Linear functions were derived from linear regression in every dietary group (**C, D**) and adjusted to the median of the group. Adjusted FM and LM were then analyzed by One-way ANOVA and Tukey post-test (**E, F**). Asterisks indicate significant differences compared with control or between groups as indicated. * $p<0.05$; ** $p<0.01$; *** $p<0.001$.

Table 6: Effects of EPA / DHA on body mass and organs.
Values were calculated as mean ± standard error (n=10–12) per dietary group for 6 weeks and 12 weeks feeding. C, control diet; HF, high fat diet; HF/n-3, high fat diet enriched with n-3-LC-PUFA EPA / DHA. Letters a and b indicate a significant difference ($p<0.05$) at each time point compared to control and high fat group, respectively. Asterisks indicate a significant difference ($p<0.05$) between the same dietary group at 6 w versus 12 w feeding. Statistical analysis was performed with Two-Way ANOVA and Bonferroni post-test (for fat and lean mass: One-Way ANOVA and Tukey post-test). AT, adipose tissue; BAT; brown adipose tissue; BM, body mass; SCAT, subcutaneous adipose tissue; WAT, white adipose tissue; X, the perirenal AT comprises perirenal and retroperitoneal AT.

	6 weeks			12 weeks		
	C	HF	HF/n-3	C	HF	HF/n-3
Body mass (g)						
Initial (g)	22.21 ± 0.36	21.56 ± 0.48	21.94 ± 0.30	21.71 ± 0.45	22.10 ± 0.44	21.73 ± 0.32
Final (g)	28.68 ± 0.76	34.42 ± 0.95a*	32.52 ± 0.72a*	31.38 ± 1.10	40.83 ± 1.27a*	36.81 ± 0.89ab*
Change (g)	6.47 ± 0.49	12.86 ± 0.78a*	10.57 ± 0.65a*	9.67 ± 0.84	18.73 ± 1.21a*	15.08 ± 0.78ab*
Body length (cm)	9.00 ± 0.12	9.00 ± 0.06*	9.05 ± 0.05	9.17 ± 0.17	9.46 ± 0.13*	9.30 ± 0.08
Final fat (g)				6.45 ± 0.77	15.16 ± 1.22a	12.32 ± 0.75a
Final lean (g)				20.63 ± 0.32	20.77 ± 0.41	20.72 ± 0.25
Visceral WAT (mg)	1113.67 ± 143.19	2533.50 ± 226.15a*	2108.92 ± 134.64a*	1571.08 ± 224.95	4231.83 ± 325.96a*	3340.80 ± 255.98ab*
Mesenteric AT (mg)	244.00 ± 34.26	482.33 ± 44.70a*	388.83 ± 24.52a	277.17 ± 34.73	662.92 ± 62.68a*	510.00 ± 49.18ab
Epididymal AT (mg)	674.75 ± 80.01	1516.00 ± 142.33a*	1237.75 ± 83.37a*	965.33 ± 128.07	2567.25 ± 198.54a*	1977.10 ± 141.52ab*
Perirenal AT (mg)[X]	194.92 ± 32.96	535.17 ± 47.09a*	482.33 ± 41.22a*	328.58 ± 64.73	1001.67 ± 80.91a*	853.70 ± 72.18a*
Inguinal SCAT (mg)	210.50 ± 26.54	511.33 ± 55.01a*	379.92 ± 40.3a*	316.75 ± 47.21	898.00 ± 51.81a*	710.80 ± 52.27ab*
Interscapular BAT (mg)	145.17 ± 13.30	193.17 ± 12.00*	200.83 ± 11.48a	179.33 ± 21.23	312.00 ± 15.54a*	246.80 ± 18.23ab
Brain (mg)	467.08 ± 4.38	462.92 ± 4.45	471.50 ± 2.44	461.58 ± 3.84	465.17 ± 2.41	462.70 ± 4.09
Caecum (mg)	253.17 ± 14.78	189.50 ± 9.33a	217.75 ± 10.95a	249.50 ± 11.41	186.83 ± 8.26a	217.60 ± 9.34
Colon length (cm)	4.92 ± 0.14	4.96 ± 0.11	5.04 ± 0.10	4.83 ± 0.11	4.79 ± 0.10	4.85 ± 0.08
Heart (mg)	156.67 ± 5.01	179.83 ± 8.04a	157.00 ± 6.53b	170.33 ± 4.74	170.42 ± 4.13	164.70 ± 7.67
Kidney (mg)	383.08 ± 8.35	434.42 ± 6.81a	403.42 ± 7.18b	383.33 ± 6.11	431.50 ± 6.89a	418.10 ± 9.5a
Liver (mg)	1381.17 ± 52.13	1448.17 ± 59.83	1456.25 ± 33.52	1401.42 ± 55.32	1609.33 ± 66.59a	1493.20 ± 37.55
Lung (mg)	168.25 ± 3.81	178.17 ± 5.32	181.92 ± 7.06	185.08 ± 6.06	182.00 ± 3.27	186.70 ± 8.17
Muscle (mg)	284.75 ± 5.87	298.17 ± 8.73	275.25 ± 5.39b	291.67 ± 6.08	308.00 ± 4.26	279.40 ± 8.52a
Pancreas (mg)	184.50 ± 6.29*	226.08 ± 12.87a*	208.08 ± 8.06*	245.00 ± 11.70*	281.33 ± 18.31*	287.40 ± 12.56a*
Small intestine length (cm)	26.75 ± 0.52	27.92 ± 0.38*	29.83 ± 0.55ab	28.50 ± 0.61	30.25 ± 0.80*	31.80 ± 0.44a
Spleen (mg)	74.58 ± 2.30	88.25 ± 3.61	103.75 ± 2.62ab*	88.17 ± 4.45	87.42 ± 4.88	125.00 ± 7.79ab*
Spleen (% of BM)	0.26 ± 0.01	0.26 ± 0.01a	0.32 ± 0.01a	0.28 ± 0.02	0.22 ± 0.01a	0.34 ± 0.02ab

4.9.3 Adipose tissue depots

4.9.3.1 Masses

Analysis of different adipose tissues (AT) showed a similar pattern as for fat mass and body mass development. All white adipose organs (WAT) measured, regardless whether of subcutaneous or visceral origin, increased significantly in mass on HF diets already after 6 weeks; this was absent in interscapular brown adipose tissue (iBAT; Table 6, Figure 11). After 12 weeks this increase was about 200–300 % in WAT and 174 % in iBAT in HF compared with control mice.

Almost all adipose organs from HF/n-3 animals showed a significantly reduced mass compared with HF animals after 12 weeks except in the perirenal / retroperitoneal depot (PAT) where at least the same trend was observed (PAT, Figure 11F). This reduction was between 20 to 23 % compared with HF animals at the same time point, but only about 15 % in PAT.

A comparison of the mesenteric (MAT) and epididymal (EAT) depots showed that the effect of feeding time and HF/n-3 diet affected EAT more than MAT, as visible by lower p-values in EAT (cf. asterisks in graphs, Figure 11D, E).

Regarding the amplitudes of change, EAT resembled subcutaneous inguinal WAT (IAT). In the last 6 weeks of feeding IAT increased about 76 % in mass and EAT about 69 % by HF diet whereas this was only about 37 % in MAT. Similarly, mass of IAT increased by 87 % and of EAT by 60 % on HF/n-3 diet between weeks 6 and 12 as opposed to MAT with only 31 % increase (Table 6).

Thus, on the one hand there was increased gain of adipose tissue mass in subcutaneous AT compared with visceral AT. On the other hand, even visceral AT showed differential mass development with more gain in EAT compared with MAT. iBAT mass was decreased in mice fed HF/n-3 after 12 weeks relative to HF animals.

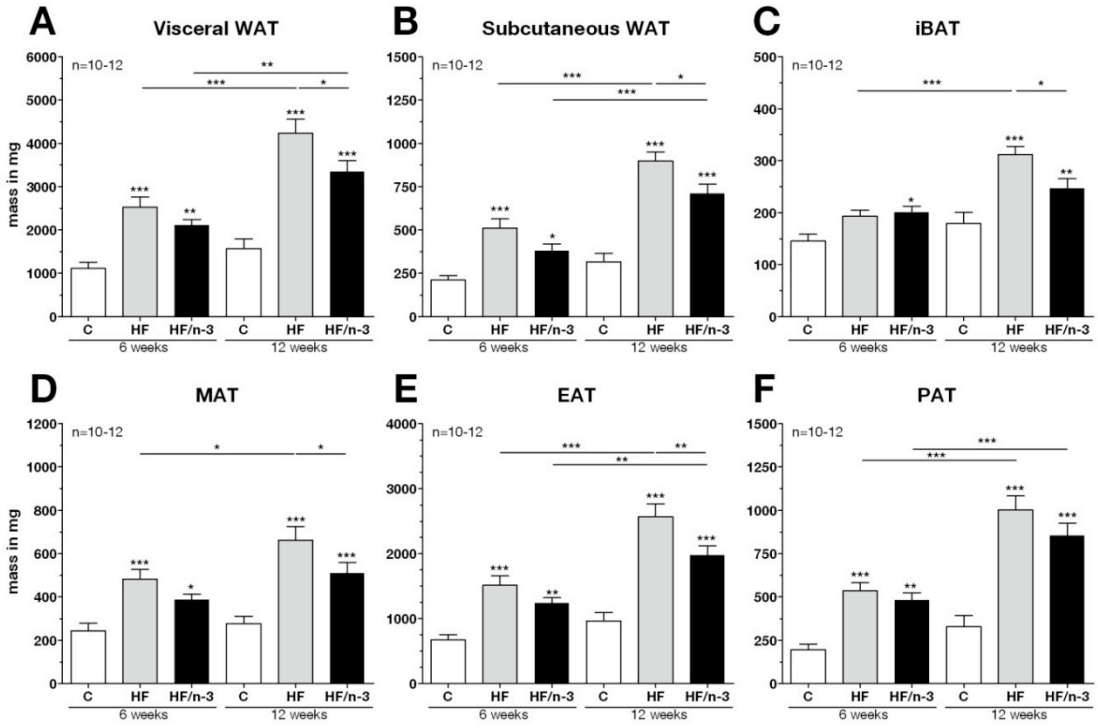

Figure 11: Adipose tissue in mice on different high fat diets. Shown are masses of white adipose tissue (WAT) and interscapular brown adipose tissue (iBAT, **C**) from mice fed C, control; HF, high fat; or HF/n-3, high fat diet enriched with n-3 LC-PUFA EPA / DHA for 6 or 12 weeks. Visceral WAT (**A**) is the sum of mesenteric (MAT, **D**), epididymal (EAT, **E)**, and perirenal/retroperitoneal (PAT, **F**) depots. Subcutaneous WAT is the mass of the inguinal depot (**B**). All data are means ± standard error. Statistical analysis was performed using Two-way ANOVA and Bonferroni post-test. Asterisks indicate significant differences compared with control at the same time point or between groups as indicated. * $p<0.05$; ** $p<0.01$; *** $p<0.001$.

4.9.3.2 Adipocyte cross-sectional area

Dietary effects on adipose tissue mass were further evaluated on a histological level by measuring adipocyte sizes, i.e. cross-sectional area of para-formaldehyde-fixed paraffin-embedded tissue sections from 12 weeks fed mice (Figure 12). In agreement with literature (Jelenik et al., 2010), it was readily apparent that subcutaneous adipocytes were only about half the size (Figure 12A) compared with visceral adipocytes (Figure 12B, C).

However, the results displayed the same findings obtained with analysis of masses: adipocytes increase in cross-sectional area on HF diet compared with control samples (2.1 to 2.3-fold). The reduction observed with HF/n-3 diet was, however, only significant in MAT (–43 %), which was roughly twice as much as in EAT (–19 %) whereas this difference was small compared with IAT (–37 %). Thus, MAT as a visceral WAT responded more like IAT compared with EAT adipocyte cross-sectional area to the HF and HF/n-3 diets.

The difference between the visceral depots MAT and EAT became even more obvious when analyzing the distribution of adipocytes according to size (Figure 13). The distribution curves

clearly showed an overlap of C and HF/n-3 adipocytes in MAT (Figure 13A) whereas in EAT (Figure 13B) distribution curves of adipocytes of HF and HF/n-3 animals overlapped.

To sum these findings up, almost all AT measured showed a similar increase of mass and adipocyte cross-sectional area with HF and HF/n-3 diets compared with control. In agreement with findings from fat mass and body mass measurements, there was a reduction of AT mass and adipocyte area under HF/n-3 compared with HF diet, which was statistically significant in most cases after 12 weeks. Only MAT adipocytes, however, were significantly reduced in size by HF/n-3. Additionally, to a reduced mass increase in MAT compared with EAT, MAT adipocytes enlarged more under HF diet, but at the same time were more responsive to the reductive effect of HF/n-3 diet than EAT adipocytes.

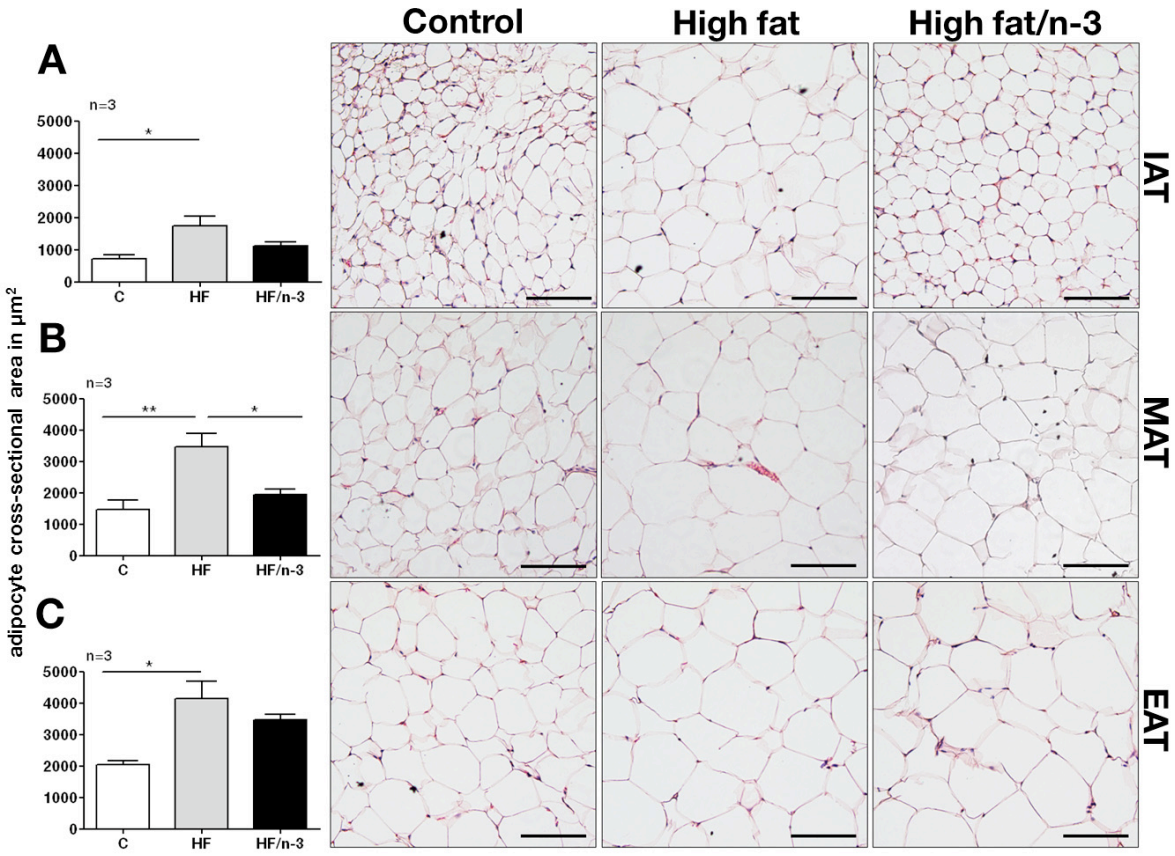

Figure 12: Adipocyte cross-sectional area. Shown are the mean adipocyte cross-sectional areas per cell ± standard error in µm² and representative H&E stained sections of subcutaneous inguinal (IAT, **A**), mesenteric (MAT, **B**) and epididymal (EAT, **C**) adipose tissue for C, control; HF, high fat; and HF/n-3, high fat diet enriched with n-3 LC-PUFA EPA / DHA. Black bars in pictures indicate scale of 100 µm. Statistical analysis was performed using One-Way ANOVA and Tukey post-test. Asterisks indicate significant differences compared with control at the same time point or between groups as indicated. * $p<0.05$; ** $p<0.01$; *** $p<0.001$.

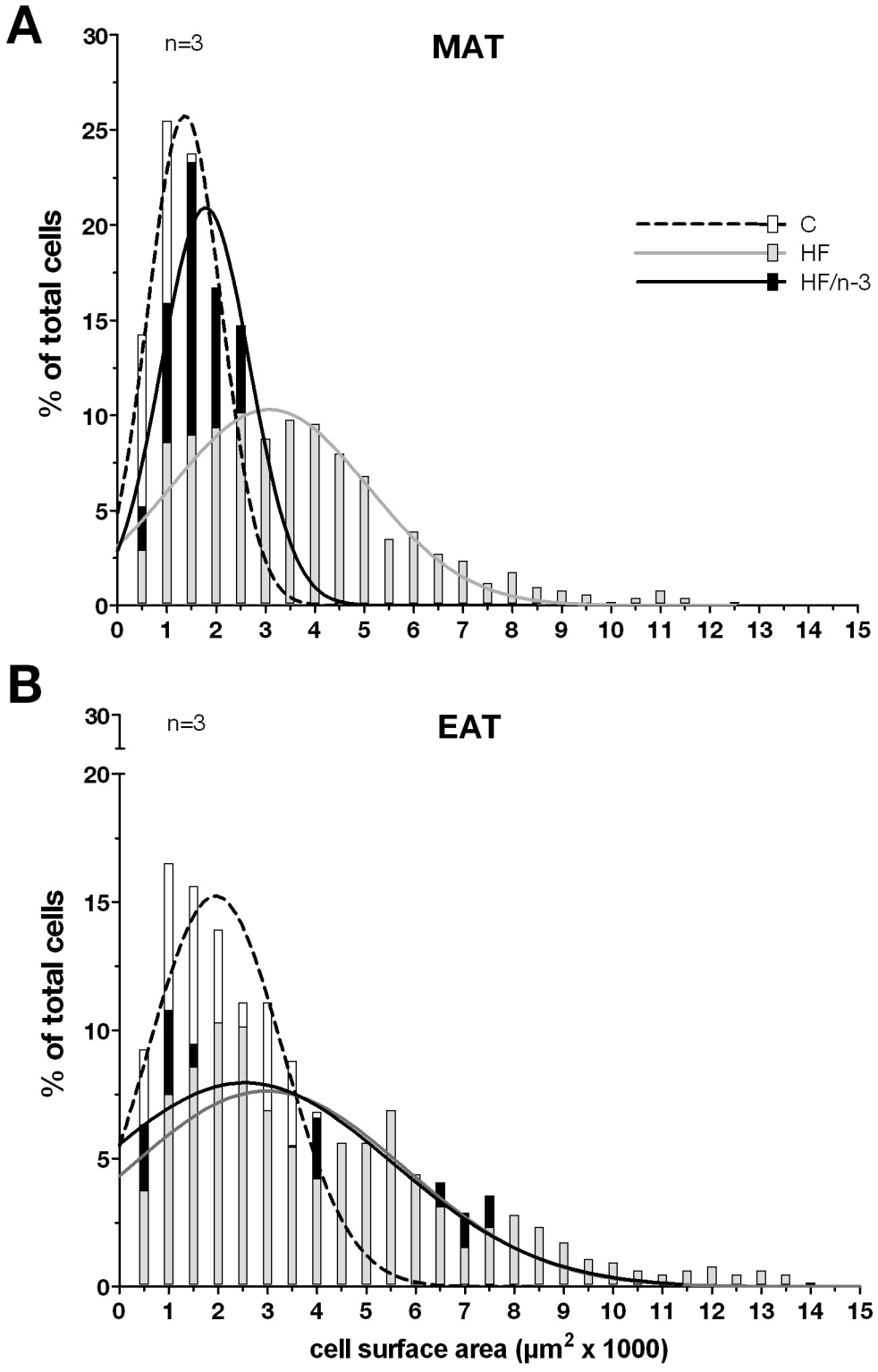

Figure 13: Distribution of adipocyte cross-sectional area in mesenteric and epididymal adipose tissue. Adipocyte cross-sectional area was plotted for MAT (**A**) and EAT (**B**) according to size as a fraction of the total number of cells and distribution curves plotted with Gaussian non-linear fit in Prism 5 (Graph Pad). C, control diet; HF, high fat diet; HF/n-3, high fat diet enriched with n-3 LC-PUFA EPA / DHA.

4.9.3.3 Gene expression

To substantiate the anti-obesity effect observed in adipose tissue mass and cross-sectional area, we investigated molecular changes on gene expression level in adipose tissue (Appendix Table 7).

Leptin is a hormone predominantly synthesized by adipocytes (Fietta, 2005) with a strong correlation of mRNA levels with adipocyte size (Guo et al., 2004) and of plasma levels with body mass index in rodents and humans (Maffei et al., 1995).

Leptin gene expression in adipose tissue correlated with fat depot mass of mice (Figure 14). This correlation was highly significant ($p<0.0001$) in both MAT (Figure 14A) and EAT (Figure 14B). Leptin gene expression was significantly increased up to 3-fold in HF and HF/n-3 mice compared with control animals. Even though a reduction of leptin mRNA levels was observed in HF/n-3 animals compared with HF mice (–20 % in MAT, –26 % in EAT), this was not significant in MAT or EAT.

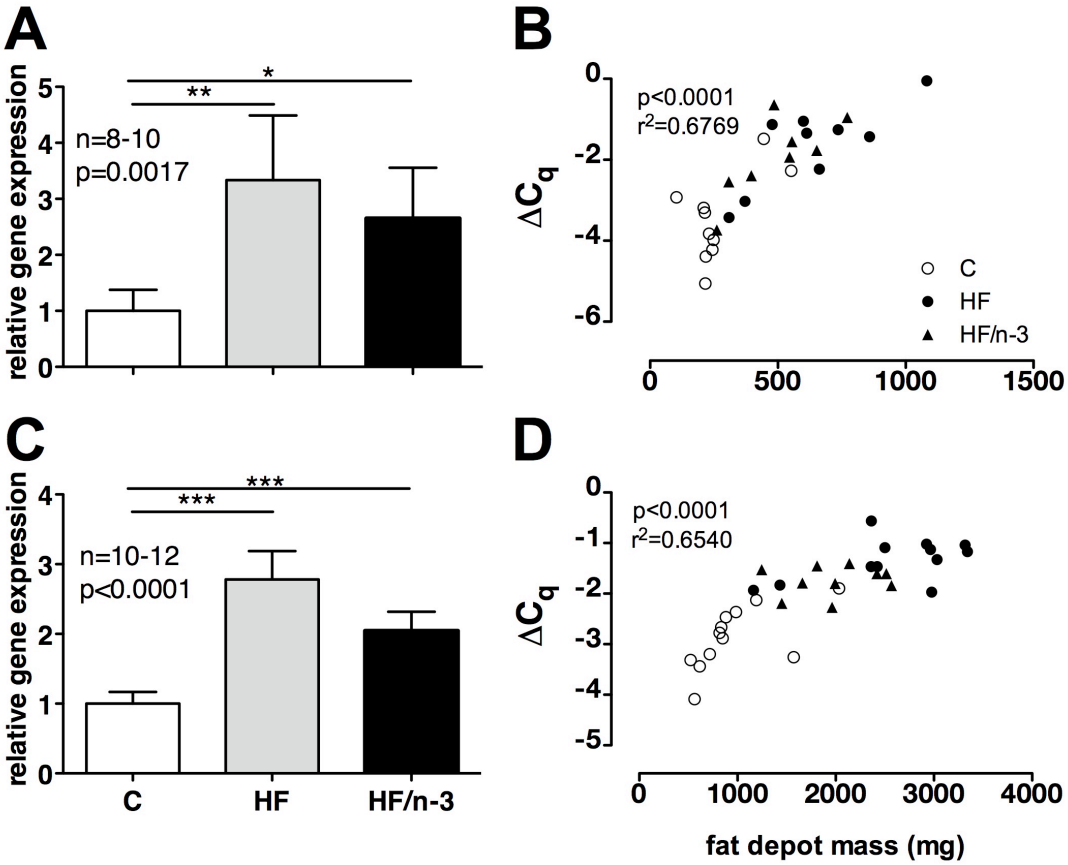

Figure 14: Leptin relative gene expression and relation to fat depot mass in murine adipose tissue. Shown are the mean gene expression levels ± standard error after RT-qPCR with 10 ng of RNA (n=8-12) for leptin in mesenteric adipose tissue (MAT; **A**) and in epididymal adipose tissue (EAT; **C**) after 12 weeks feeding on C, control diet; HF, high fat diet; or HF/n-3, high fat diet enriched with n-3 LC-PUFA EPA / DHA relative with control-fed animals and a correlation with the respective fat depot mass (MAT **B**, EAT **D**). Data were analyzed by $\Delta\Delta C_q$-method and normalized to β-actin,

glyceraldehyde-phosphate dehydrogenase and hypoxanthine guanine phosphoribosyl transferase gene expression. Statistical analysis for gene expression was performed using One-Way ANOVA and Tukey post-test. Correlation analysis was performed with Prism 5 (GraphPad) using the Pearson test. Asterisks indicate significant differences compared with control or between groups as indicated. * $p<0.05$; ** $p<0.01$; *** $p<0.001$.

To answer the question whether the observed changes in body and fat mass were due to metabolic changes, gene expression in visceral (EAT) and subcutaneous adipose tissue (IAT) was studied. N-3 LC-PUFA affect gene expression of lipogenic enzymes (Flachs et al., 2009) and biogenesis of mitochondria as the major site of fat oxidation (Flachs et al., 2005).

Acetyl-coenzyme A carboxylase α (Acacα) is an enzyme in the initiating step of fatty acid synthesis carboxylating acetyl CoA to generate malonyl CoA and has been implicated as a potential anti-obesity target (Tong, 2005). mRNA levels have been shown to be decreased in liver by fish oil treatment (Ide, 2005). Interestingly, EAT and IAT revealed significantly lower levels of Acacα mRNA on both HF and HF/n-3 with a decrease of up to 60 % compared with controls (Figure 15A, D). There was no significant difference between HF and HF/n-3; in IAT (Figure 15D) gene expression was somewhat lower on HF compared with HF/n-3 (HF; 0.52 ± 0.08; HF/n-3, 0.39 ± 0.07).

Furthermore, gene expression of diacylglycerol O-acyltransferase 2 (Dgat2), an enzyme synthesizing triacylglycerols from acyl coenzyme A and D-1,2-diacylglycerol (Cases et al., 1998) and with a known downregulation by n-3 LC-PUFA was measured (Flachs et al., 2005). A significant elevation (EAT, 1.30 ± 0.14; IAT, 2.09 ± 0.36) of Dgat2 mRNA levels was evident in both WAT depots of HF mice compared with controls (Figure 15B, E). This elevation was only marginally reduced on HF/n-3, but more in IAT compared with EAT (EAT; 1.19 ± 0.13; IAT, 1.61 ± 0.32).

Finally, the gene expression of nuclear respiratory factor 1 (Nrf1) as a marker for mitochondrial biogenesis (Kelly and Scarpulla, 2004) that shows increased gene expression on HF diet enriched with n-3 LC-PUFA (Flachs et al., 2005) was quantified but showed no significant difference between groups (Figure 15C, F). There was even a slight decrease of Nrf1 gene expression in HF/n-3 mice in EAT compared with controls (HF/n-3; 0.79 ± 0.07; $p=0.0638$).

Additionally, mRNA levels of peroxisome proliferator-activated receptor γ2 (Pparγ2), a transcription factor (Tontonoz et al., 1994) binding n-3 LC-PUFA to regulate adipogenesis and lipid metabolism gene expression (Flachs et al., 2009), did not show significant changes among groups (Appendix Table 7).

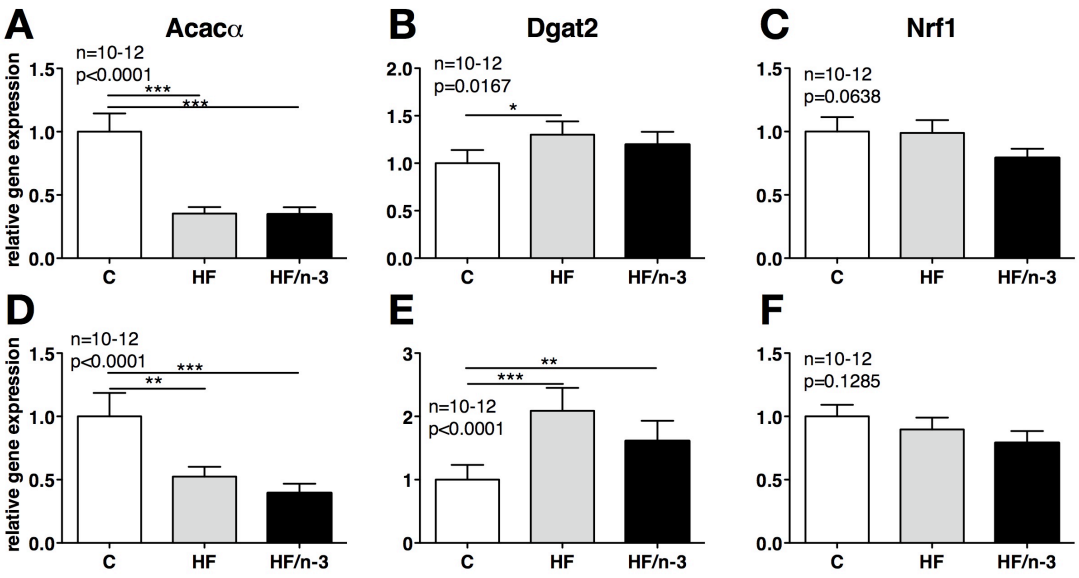

Figure 15: Relative gene expression in murine adipose tissue. Shown are the mean gene expression levels ± standard error after RT-qPCR with 10 ng of RNA (n=10–12) for acetyl coenzyme A carboxylase α (Acacα), diacylglycerol O-acyltransferase 2 (Dgat2), and nuclear respiratory factor 1 (Nrf1) in epididymal adipose tissue (EAT, **A-C**) and subcutaneous inguinal adipose tissue (IAT, **D-E**) after 12 weeks feeding on C, control diet; HF, high fat diet; or HF/n-3, high fat diet enriched with n-3 LC-PUFA EPA / DHA compared with control-fed animals. Data were analyzed by $\Delta\Delta C_q$-method and normalized to β-actin and glyceraldehyde-phosphate dehydrogenase gene expression. Statistical analysis was performed using One-Way ANOVA and Tukey post-test. Asterisks indicate significant differences compared with control or between groups as indicated. * $p<0.05$; ** $p<0.01$; *** $p<0.001$.

In spite of a lower brown adipose tissue mass observed in HF/n-3 mice (Figure 11C), it was tested if gene expression of uncoupling protein 1 (Ucp1) in adipose tissue was affected by n-3 LC-PUFA treatment (Figure 16). Ucp1 is a marker of brown adipocytes and involved in energy expenditure by non-shivering thermogenesis and commonly upregulated on high fat diets (Fromme and Klingenspor, 2010). Furthermore, it can also be induced in WAT (Guerra et al., 1998).

Gene expression of Ucp1 was increased in interscapular brown adipose tissue (iBAT; C_q-values: 17–19) with very low mRNA levels in WAT (C_q-values: 30–35). In iBAT (Figure 16A) an elevation of Ucp1 gene expression in HF/n-3 mice compared with controls was detected (1.59 ± 0.15), but no change on HF diet. Analyses in EAT (Figure 16B) and IAT (Figure 16C) did not show any significant differences among groups and high inter-individual variation.

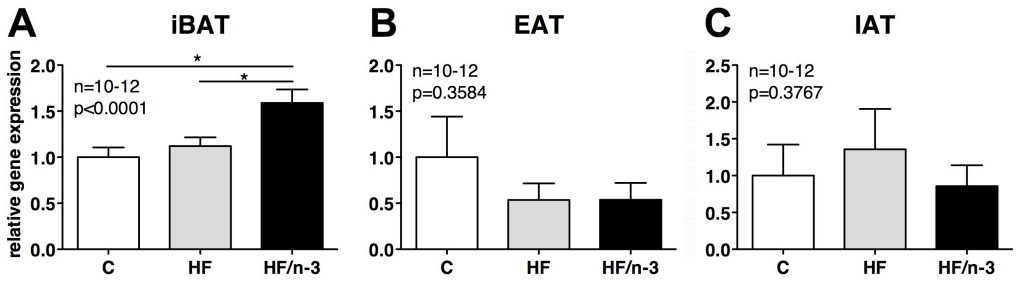

Figure 16: Ucp1 relative gene expression in murine tissues. Shown are the mean gene expression levels ± standard error after RT-qPCR with 10 ng of RNA (n=10–12) for uncoupling protein 1 (Ucp1) in interscapular brown adipose tissue (iBAT; **A**), epididymal adipose tissue (EAT; **B**) and inguinal adipose tissue (IAT; **C**) after 12 weeks feeding on C, control diet; HF, high fat diet; or HF/n-3, high fat diet enriched with n-3 LC-PUFA EPA / DHA compared with control-fed animals. Data were analyzed by $\Delta\Delta C_q$-method and normalized to β-actin and glyceraldehyde-phosphate dehydrogenase or cyclophilin B and heat shock protein 90 α (cytosolic), class B member 1 gene expression. Statistical analysis was performed using One-Way ANOVA and Tukey post-test. Asterisks indicate significant differences compared with control or between groups as indicated. * $p<0.05$; ** $p<0.01$; *** $p<0.001$.

In summary, leptin gene expression in the different dietary groups parallels the pattern observed in body and organ masses with a reduction of mRNA levels by HF/n-3 compared with HF mice. Ucp1 gene expression was elevated only in iBAT by HF/n-3 diet, but not affected in WAT by any of the diets.

Furthermore, gene expression of markers of lipogenesis in EAT and IAT was affected by HF diet (Acacα, Dgat2), but there were no n-3 LC-PUFA-specific effects. Markers for fat mitochondrial biogenesis (Nrf1) or lipid metabolism (Acacα, Dgat2) and adipogenesis (Pparγ2) modulated by n-3 LC-PUFA, did not change in gene expression in any of the dietary groups.

4.9.4 Selected organs

In addition to the effects of the HF diets on adipose tissue, also other organs involved in nutrient digestion and absorption (small intestine, Figure 17A; cecum, Figure 17B), glucose homeostasis (liver, Figure 17C; pancreas; Figure 17D) and immune function (spleen, Figure 17D, E) were affected by the treatment.

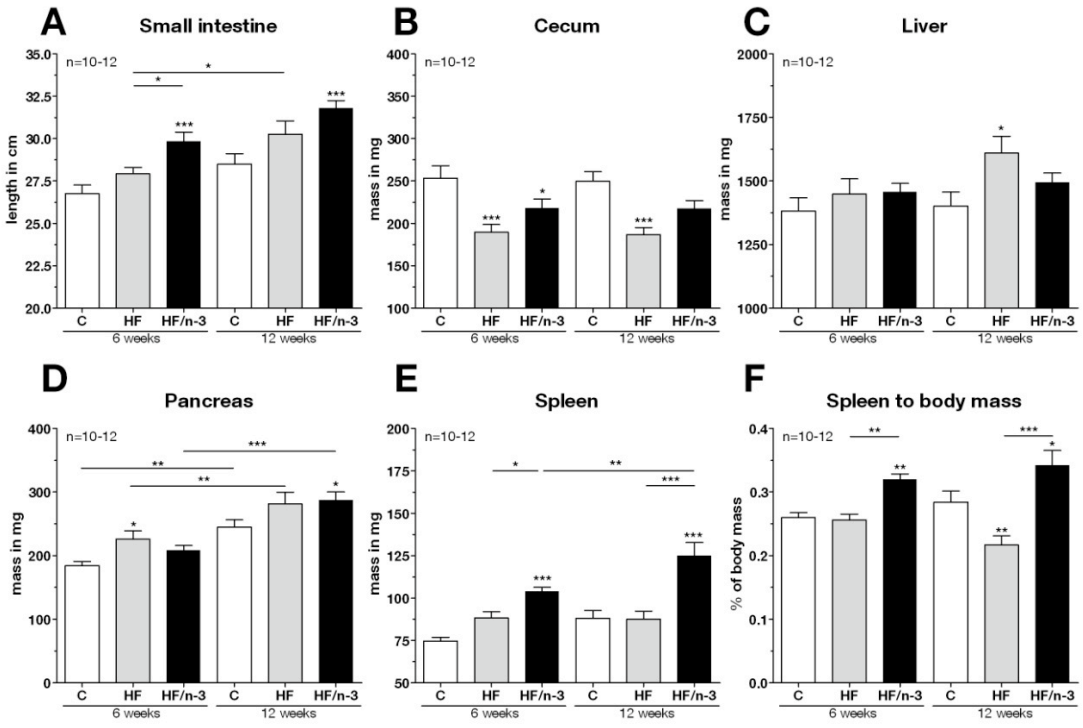

Figure 17: Selected organ lengths and masses in mice on different high fat diets. Shown are the length of the small intestine (**A**), masses of cecum (**B**), liver (**C**), pancreas (**D**), and spleen (**E**) as well as spleen mass relative to body mass (**F**) from mice fed C, control, HF, high fat; or HF/n-3, high fat diet enriched with n-3 LC-PUFA EPA / DHA for 6 or 12 weeks. All data are means ± standard error. Statistical analysis was performed using Two-way ANOVA and Bonferroni post-test. Asterisks indicate significant differences compared with control at the same time point or between groups as indicated. * $p<0.05$; ** $p<0.01$; *** $p<0.001$.

The small intestine as the site of nutrient absorption will respond to a change in dietary conditions such as an increased lipid load (de Wit et al., 2010). On a macroscopic level HF and HF/n-3 diets led to an increased length of the small intestine that was statistically significant in HF/n-3 mice compared with controls (+11–12 %, Figure 17A). Indeed, the small intestine was significantly longer in HF/n-3 compared with HF mice after 6 weeks (+7 %) with the same trend after 12 weeks (+5 %).

Diet-induced obesity and increased fat load affect the gut microbiota (Ley et al., 2005). In this study, total cecal mass was significantly decreased by 25 % in HF mice compared with control animals (Figure 17B). This decrease was dampened in HF/n-3 mice with a reduction

of only 13–14 %. Interestingly, there was no time-dependent difference, these observations were manifest already after 6 weeks and did not change thereafter.

The liver is usually one of the first organs to be affected by ectopic lipid deposition and insulin resistance under HF diet-induced obesity (Kleemann et al., 2010). The mass was significantly increased in HF fed mice compared with control mice (+15 %, Figure 17C). This effect, however, did not become significantly apparent before week 6 but was observed at week 12. In HF/n-3 mice liver mass was slightly reduced after 12 weeks respective to HF (only +7 % compared with control liver mass). This showed a similar response in mass as in adipose tissue, even though not reaching a statistically significant reduction by n-3 LC-PUFA here.

The pancreas as the insulin-producing organ is another important organ in the maintenance of glucose homeostasis counteracting hyperglycemia by increased β-cell proliferation and thus insulin secretion (Steil et al., 2001). However, the mass of the pancreas in control groups after 6 and 12 weeks showed a 33 % increase (Figure 17D).

Even though there was a trend towards a greater pancreas mass in HF and HF/n-3 animals compared with controls (+13–23 %), this was not always significantly different. After 6 weeks already HF pancreases were 23 % heavier than control ones, this effect was diminished after 12 weeks (+15 %). Moreover, pancreas mass was reduced in HF/n-3 animals compared with HF (–8 %) after 6 weeks, but not after 12 weeks (+2 %).

Interestingly, spleen mass was increased by as much as 40 % in HF/n-3 mice, but not in HF mice, regardless of the time point when compared with the control group (Figure 17E). It has been shown that spleen mass was affected by fish oil feeding (Blok et al., 1996a). This effect was also independent of body mass (Figure 17F), but could not be analyzed with ANCOVA because linear regression showed variable slopes between dietary groups (data not shown). Spleen mass was even significantly decreased in HF animals compared with controls after 12 weeks.

In summary, also other organs than adipose tissue changed in response to HF diets with variable n-3 LC-PUFA contents either directly or indirectly and contributing to overall body mass increase. Whereas HF or HF/n-3 diets led to an increase in liver mass and pancreas mass or small intestinal length and spleen mass, respectively, a reduction of cecal mass was observed on HF diet. These effects as well as the effect of HF/n-3 counteracting the HF-induced effects did not always reach statistically significant levels.

4.10 Hepatic metabolism

4.10.1 Hepatic triacylglycerols and systemic non-esterified fatty acids

The disturbance of lipid metabolism leading to a hyperlipidemic state is a hallmark of diet-induced obesity. The lipid-lowering effects of n-3 LC-PUFA in high fat diet-induced hypertriglyceridemia have been described in many intervention studies (Kajikawa et al., 2009; Jelenik et al., 2010). Therefore, the presence of ectopic triacylglycerol (TAG) deposition was assessed by histological and biochemical analysis of liver samples from mice fed for 12 weeks (Figure 18A-D). Oil Red-O (ORO) staining of liver sections showed more staining in HF mice (Figure 18B) compared with control mice (Figure 18A) whereas HF/n-3 liver sections (Figure 18C) showed similar staining like control ones. Accordingly, significantly higher TAG concentrations were detected in HF animals, whereas HF/n-3 animals had TAG levels similar to control mice (C, 137.10 ± 5.05 mg / g protein; HF, 373.50 ± 7.32 mg / g protein; HF/n-3, 160.91 ± 5.14 mg / g protein, Figure 18D).

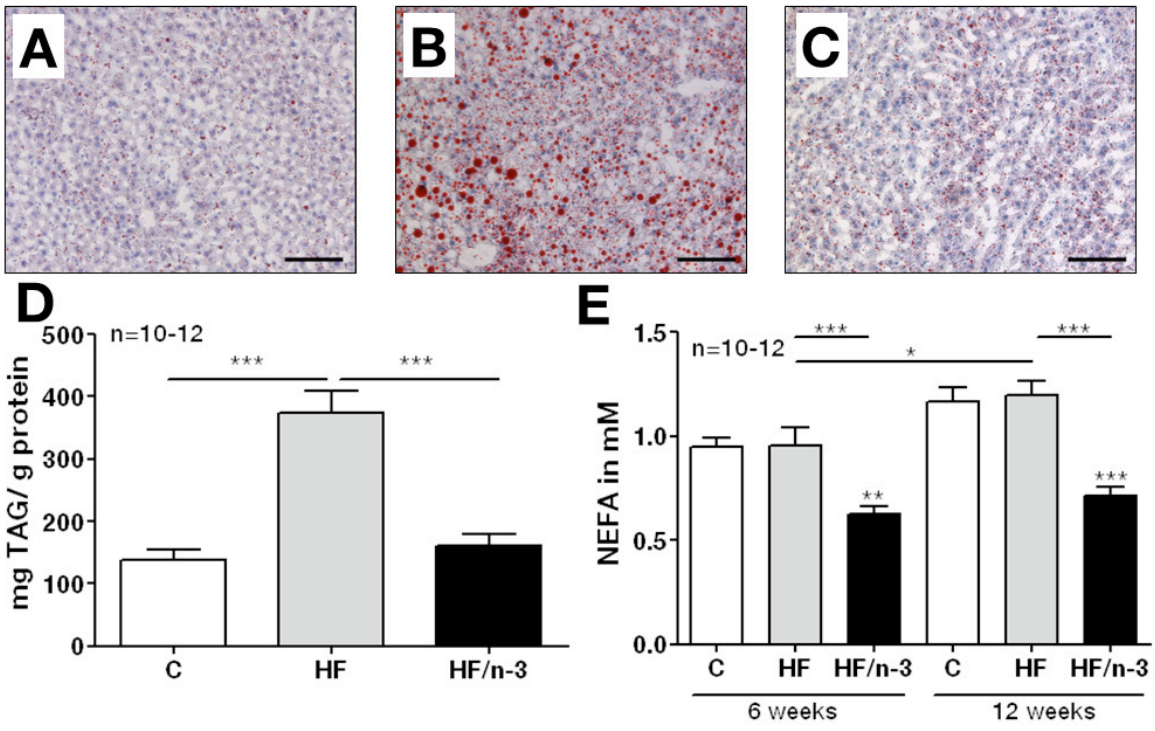

Figure 18: Detection of hepatic triacylglycerols and plasma non-esterified fatty acids. Hepatic cryosections (left lobe, 10 µm) of mice fed control diet (**A**), high fat diet (**B**), and high fat diet enriched with EPA / DHA (**C**) after 12 weeks of feeding were stained for triacylglycerols (TAG) with Oil Red O and counterstained with hematoxylin. Hepatic TAG were quantified with a colorimetric assay after 12 weeks of feeding (n=10-12) and normalized to hepatic protein content (**D**). Non-esterified fatty acids (NEFA) in plasma were quantified with a colorimetric assay after 6 weeks and 12 weeks of feeding (**E**, n=10–12). Black bars in pictures indicate scale of 100 µm. All data are means ± standard error. Statistical analysis was performed using One-Way ANOVA and Tukey post-test for TAG quantification and Two-Way ANOVA and Bonferroni post-test for NEFA measurement. Asterisks indicate significant differences compared with control at the same time point or between groups as indicated. * $p<0.05$; ** $p<0.01$; *** $p<0.001$.

In addition to hepatic TAG levels, the levels of circulating non-esterified fatty acids (NEFA) have been shown to be decreased by n-3 LC-PUFA in the postprandial state compared with other dietary treatments (Rustan et al., 1998).

Observations in this study confirmed a significant decrease of plasma NEFA by 34–38 % compared with control animals by increasing n-3 LC-PUFA in the diet (Figure 18E). In contrast to expectations, no elevation of NEFA in HF plasma was observed compared with controls.

Taken together, the results in HF/n-3 animals showed that hepatic TAG and plasma NEFA levels were similar or decreased compared with controls but always lower than in HF mice.

4.10.2 Hepatic gene and protein expression

The liver is an important metabolic organ. Therefore, effects on lipogenesis, mitochondrial and peroxisomal fatty acid oxidation and LC-PUFA synthesis were evaluated (Figure 19, Figure 20).

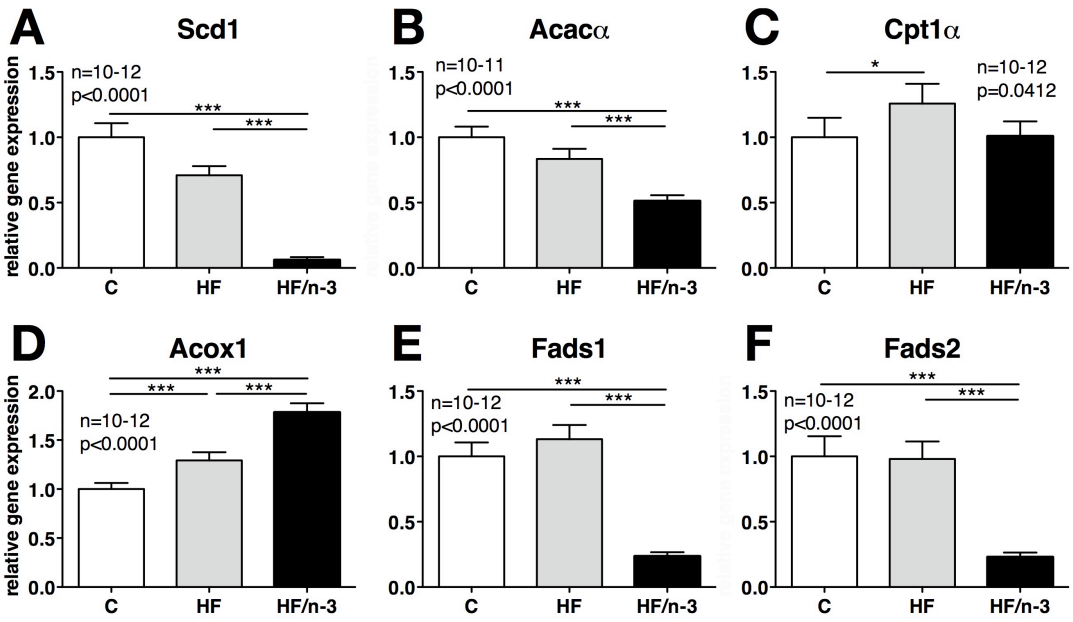

Figure 19: Relative gene expression in murine liver. Shown are the mean gene expression levels ± standard error after RT-qPCR with 10 ng of RNA (n=10–12) for stearoyl-coenzyme A desaturase 1 (Scd1; **A**), acetyl-coenzyme A carboxylase α (Acacα; **B**), carnitine O-palmitoyltransferase 1α (Cpt1α; **C**), peroxisomal acyl-coenzyme A oxidase 1 (Acox1, **D**), fatty acid desaturase 1 (Fads1, **E**) and 2 (Fads2, **F**) in liver after 12 weeks feeding on C, control diet; HF, high fat diet; or HF/n-3, high fat diet enriched with n-3 LC-PUFA EPA / DHA compared with control-fed animals. Data were analyzed by $\Delta\Delta C_q$-method and normalized to β-actin and hypoxanthine guanine phosphoribosyl transferase gene expression. Statistical analysis was performed using One-Way ANOVA and Tukey post-test. Asterisks indicate significant differences compared with control or between groups as indicated. * p<0.05; ** p<0.01; *** p<0.001.

4.10.2.1 Lipogenesis

Stearoyl-coenzyme A desaturase (Scd1) mediates the desaturation of stearoyl-CoA generating oleoyl-CoA and is the rate-limiting enzyme in monounsaturated fatty acid synthesis (Dobrzyn and Ntambi, 2004). It is downregulated by n-3 LC-PUFA (Flachs et al., 2005), which might result in increased energy expenditure (Cohen et al., 2002). Dramatically decreased mRNA levels of Scd1 were detected in liver of HF/n-3 mice compared with both control and HF animals (0.06 ± 0.02, Figure 19A).

Furthermore, the lipogenic marker Acacα showed strongly decreased gene expression compared with the other dietary groups (0.51 ± 0.05, Figure 19B). Thus, in contrast to Acacα gene expression in adipose tissue (Figure 15), there was a n-3 LC-PUFA-specific reduction of Acacα gene expression in liver.

In contrast, no change was found in Dgat2 mRNA levels and gene expression of sterol regulatory element binding protein 1c (Srebp1c), a transcription factor promoting lipogenic gene transcription (Muhlhausler et al., 2010), whose gene expression was inversely correlated to n-3 LC-PUFA intake (Appendix Table 7).

In summary, hepatic lipogenic marker gene expression was decreased by n-3 LC-PUFA treatment in some cases (Scd1, Acacα) whereas other markers (Dgat2, Srebp1c) were unaffected.

4.10.2.2 Lipid oxidation

Next, two prominent markers of fat oxidation were examined for effects on gene expression by n-3 LC-PUFA. Carnitine O-palmitoyltransferase 1α (Cpt1α) controls the rate-limiting step of mitochondrial fatty acid oxidation by transferring a fatty acid to a carnitine molecule and thus enabling its import into the mitochondrial matrix (Song et al., 2004). mRNA levels are shown to be increased by n-3 LC-PUFA treatment in liver along with Nrf1 gene expression (Flachs et al., 2005). However, neither in liver (Figure 19C) nor in adipose tissue (Appendix Table 7), the expected result could be confirmed. Cpt1α mRNA was significantly increased on HF diet (liver, 1.26 ± 0.15; EAT, 1.30 ± 0.09) whereas there was no further elevation of gene expression in HF/n-3 mice. Instead, mRNA levels were decreased and similar to controls.

Another marker of fat oxidation is the peroxisomal acyl-coenzym A oxidase 1 (Acox1) whose transcription is under PPARα-mediated control (Fan et al., 1996; Yu et al., 2003). While hepatic gene expression of Pparα was increased but without a differential effect of HF diets (HF, 1.31 ± 0.15; HF/n-3, 1.32 ± 0.16), Acox1 mRNA was increased on HF diet compared with controls (1.29 ± 0.08) but even more on HF/n-3 diet (1.78 ± 0.09; $p<0.0001$).

Thus, while the expression of a key enzyme of the entry point of mitochondrial fat oxidation (Cpt1α) was not enhanced by n-3 LC-PUFA, there was an effect on gene expression of Acox1, which is involved in peroxisomal fat oxidation.

4.10.2.3 LC-PUFA synthesis

At last, fatty acid desaturases 1 and 2 (Fads1, Fads2; Figure 19E, F) expression was examined. Both enzymes are involved in the desaturation of n-3 and n-6 LC-PUFA and regulated by their products by a feedback mechanism (Cho et al., 1999a; Cho et al., 1999b). In agreement with these observations, gene expression in HF/n-3 liver was about 4-fold lower compared with controls. No response was observed in HF mice.

4.10.2.4 AMPKα phosphorylation

To test if molecular changes in lipid metabolism elicited by n-3 LC-PUFA also affect protein expression in liver, the phosphorylation state of AMP-activated protein kinase α (AMPKα) was examined. AMPK is a key regulator of hepatic lipid metabolism by sensing cellular ATP levels and promoting PPARα-mediated gene transcription (Bronner et al., 2004). Its activity is enhanced in livers of n-3 LC-PUFA-fed rodents (Suchankova et al., 2005).

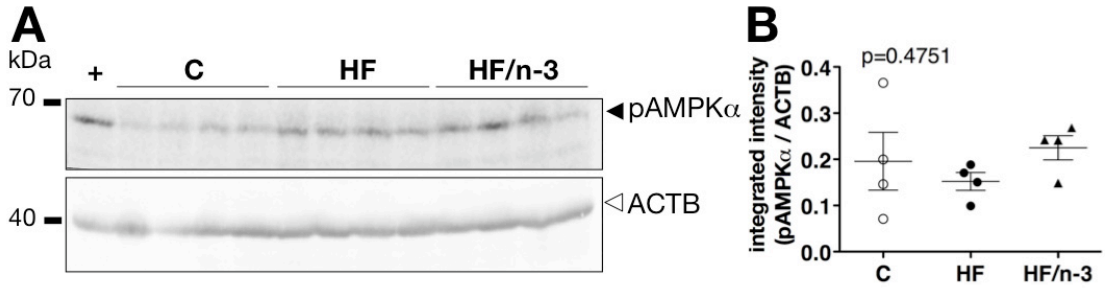

Figure 20: Murine phospho-AMPK-alpha protein expression in liver. Western blot for phospho-AMP-activated protein kinase α (pAMPKα, **A**) and densitometric analysis (**B**). 80 µg protein per lane from murine liver after 12 weeks feeding on C, control diet; HF, high fat diet; or HF/n-3, high fat diet enriched with n-3 LC-PUFA EPA / DHA were loaded on a 10 % gel. SDS-PAGE was run at 15 mA for 3 h followed by semi-dry blotting on a nitrocellulose membrane for 1 h at 200 mA. Detection was performed with monoclonal rabbit anti-mouse pAMPKα antibody (#2535, Cell Signaling, 1:500) and polyclonal rabbit anti-mouse β-actin antibody (ACTB, #4967S, Cell Signaling, 1:1000) using the Odyssey® Infrared Imaging System (LI-COR Biosciences). +, positive control (liver protein extract from C. Dahlhoff, No. HF25HFMS). Statistical analysis was performed using One-Way ANOVA and Tukey post-test. Asterisks indicate significant differences compared with control or between groups as indicated. * $p<0.05$; ** $p<0.01$; *** $p<0.001$.

Western blot analysis of phosphorylated AMPKα was tested with a phosphorylation-specific antibody (Figure 20A) and revealed elevated levels of this form in HF and HF/n-3 mice whereas control mice displayed lower levels compared with the positive control (+). Densitometric analysis (Figure 20B) showed high variation of phosphorylated AMPKα in control mice, but phosphorylated AMPKα was not different between high fat diet groups.

In summary, hepatic expression of lipid metabolism genes showed decreased mRNA levels of lipogenic enzymes (Scd1, Acacα) and an increase of PPARα-dependent peroxisomal fatty acid oxidation (Acox1) in HF/n-3 mice compared with HF animals. This finding was not reflected in protein levels of the PPARα-coactivating phosphorylated form of AMPKα. A strong inhibitory effect by n-3 LC-PUFA on gene expression was observed in LC-PUFA synthesis (Fads1, Fads2). However, some lipogenic markers (Dgat2, Srebp1c) and markers of mitochondrial fatty acid oxidation and biogenesis (Cpt1α, Nrf1) did not respond to n-3 LC-PUFA intervention.

4.11 Glucose tolerance and insulin levels

The administration of HF diets is causing an impaired glucose disposal in glucose-sensitive tissues ultimately leading to insulin resistance in mice (Buettner et al., 2006). Positive effects on glucose tolerance by n-3 LC-PUFA are not consistent in literature, but positive effects on insulin secretion have been described (Winzell et al., 2006; Neschen et al., 2007; Fedor and Kelley, 2009).

To discern the dynamics and the onset of glucose tolerance, an intraperitoneal glucose tolerance test (ipGTT) was performed after a 6 h fasting period at several time points after 4, 6, and 12 weeks of feeding (Figure 21A-C; Figure 22).

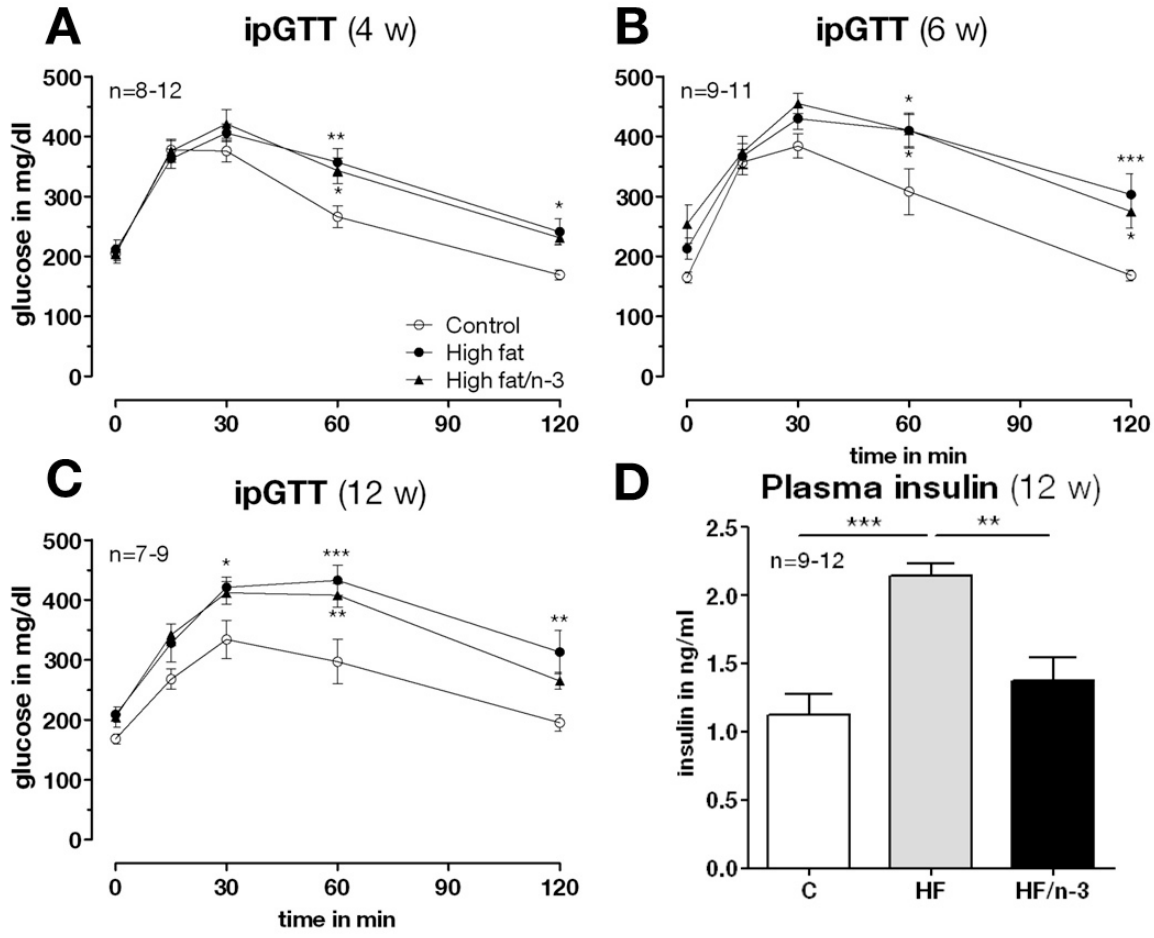

Figure 21: Intraperitoneal glucose tolerance tests (ipGTT) and fasting plasma insulin levels. After 4 (**A**), 6 (**B**), and 12 (**C**) weeks of feeding mice were deprived of food for 6 hours and then injected a sterile 20 % glucose solution (2 g / kg) intraperitoneally. Blood glucose was measured before injection (0 min) and after 15, 30, 60 and 120 min. Insulin levels were determined by ELISA (**D**) in 5 h food-deprived mice after 12 weeks of feeding (n=9-12). All data are means ± standard error. Statistical analysis for ipGTTs was performed using Two-ANOVA and Bonferroni post-test. For insulin measurement One-Way ANOVA and Tukey post-test were applied. Asterisks indicate significant differences compared with control at the same time point or between groups as indicated. * $p<0.05$; ** $p<0.01$; *** $p<0.001$.

Adverse effects of HF diets on glucose tolerance were obvious as early as after 4 weeks of feeding (Figure 21A). Even though basal glucose levels (0 min) were equal in all groups (206 ± 9 mg / dl), blood glucose was significantly higher compared with control mice in HF and HF/n-3 animals after 60 min. Furthermore, these did not reach baseline levels again like controls after 120 min. This difference between control and HF groups was also obvious when analyzing the area under the curve for the time frame 30–120 min (Figure 22C). There was no significant decrease of glucose levels by HF/n-3 compared with HF treatment.
A similar result was obtained after 6 and 12 weeks feeding (Figure 21B, C). Again, HF groups were significantly different to controls after 30–120 min. In addition, even basal blood glucose levels started to differ (6 weeks: C, 165 ± 10 mg / dl; HF, 213 ± 18 mg / dl; HF/n-3, 254 ± 33 mg / dl, p=0.0263; 12 weeks: C, 168 ± 9 mg / dl; HF, 209 ± 13 mg / dl; HF/n-3, 205 ± 17 mg / dl, p=0.0735)

Moreover, after 12 weeks (Figure 21C) blood glucose values peaked after 30 min in control and HF/n-3 mice, but not before 60 min in HF animals. Even though n-3 LC-PUFA-enriched HF diet did not lead to a statistically significant improvement of glucose clearance compared with HF diet, there was a trend for lower glucose levels in HF/n-3 mice relative to HF animals after 12 weeks (C, 195 ± 15 mg / dl; HF, 313 ± 37 mg / dl; HF/n-3, 265 ± 14 mg / dl, p=0.0043, but only C vs. HF $p<0.01$). The analysis of the area under the curve (AUC) did not yield any significant differences after 6 and 12 weeks (Figure 22D-I). However, like for the test after 4 weeks, there was at least a tendency for a positive effect of n-3 LC-PUFA on blood glucose levels at 30 to 120 min after the glucose injection after 12 weeks (C, 10565 ± 2461 AU; HF, 16400 ± 2534 AU; HF/n-3, 14056 ± 1542 AU, p=0.1986; Figure 22I).

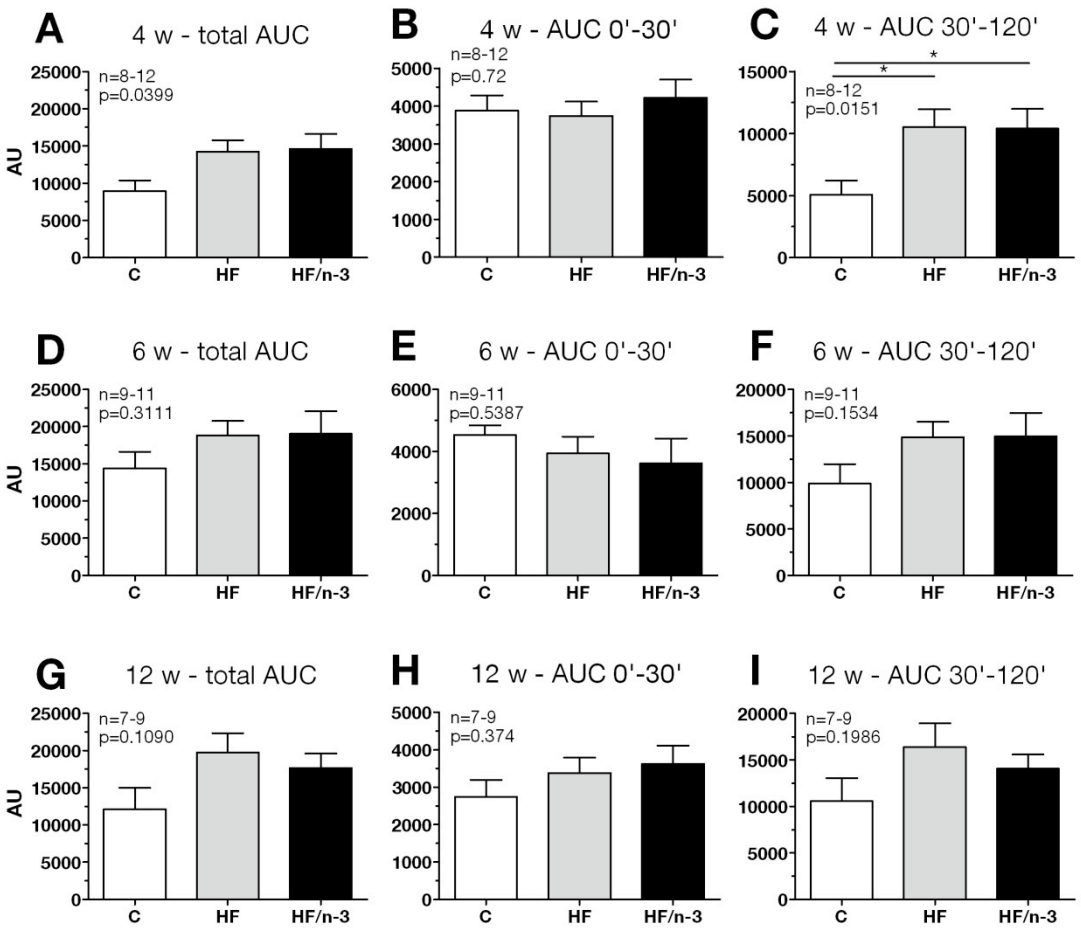

Figure 22: Area under the curve (AUC) analysis of intraperitoneal glucose tolerance tests (ipGTT). After 4 (**A-C**), 6 (**D-F**), and 12 (**G-I**) weeks of feeding mice were deprived of food for 6 hours and then injected a sterile 20 % glucose solution (2 g / kg) intraperitoneally. Blood glucose was measured before injection (0 min) and after 15, 30, 60 and 120 min. AUC was determined by correcting for base line and using total peak area in Prism 5 (GraphPad) either for the whole area (**A, D, G**) or analyzed separately for the 0 to 30 min (**B, E, H**) and the 30 to 120 min (**C, F, I**) time intervals. All data are means ± standard error. Statistical analysis was performed using One-Way ANOVA with the overall p-value given and Tukey post-test. Asterisks indicate significant differences compared with control at the same time point or between groups as indicated. * $p<0.05$; ** $p<0.01$; *** $p<0.001$; AU, arbitrary units.

In contrast to glucose tolerance, the n-3 LC-PUFA intervention compared with HF strongly affected fasting plasma insulin levels after a 5 h fasting period as measured by ELISA after 12 weeks (Figure 21D). While insulin levels in the HF group were significantly increased about 2-fold compared with controls, they were similar to insulin levels of controls in HF/n-3 animals (C, 1.12 ± 0.16 ng / ml; HF, 2.14 ± 0.09 ng / ml; HF/n-3, 1.37 ± 0.17 ng / ml). This result was reflected by the calculation of homeostatic model assessement of insulin resistance (HOMA-IR; C, 9.8 ± 1.4; HF, 22.9 ± 2.2; HF/n-3, 14.4 ± 2.0).

Adiponectin is a protein mostly derived from white adipose tissue with insulin-sensitizing roles (Ziemke and Mantzoros, 2010) and significantly lower plasma levels in obesity and

type 2 diabetes (Arita et al., 1999; Li et al., 2009). Adiponectin gene expression measured in adipose tissue was only slightly affected (Appendix Table 7). While no effect was observed in MAT (p=0.9855), HF diet led to a slight decrease in adiponectin mRNA levels on HF diet in EAT and levels similar to controls on HF/n-3 diet (HF, 0.79 ± 0.08; HF/n-3, 0.95 ± 0.08; p=0.0525).

Because blood withdrawal for insulin measurement (5 h fast) and glucose tolerance (6 h fat) was performed subsequently in the same animal, blood glucose levels were recorded at both time points to account for effects on the sensitive glucose tolerance test by prior interventions (Figure 23). Surprisingly, blood glucose levels after 5 h fasting were below 200 mg / dl ranging around 150 mg / dl whereas after another hour and just before the injection of the glucose solution for the interaperitoneal glucose tolerance test, levels were at around 200 mg / dl except for controls.

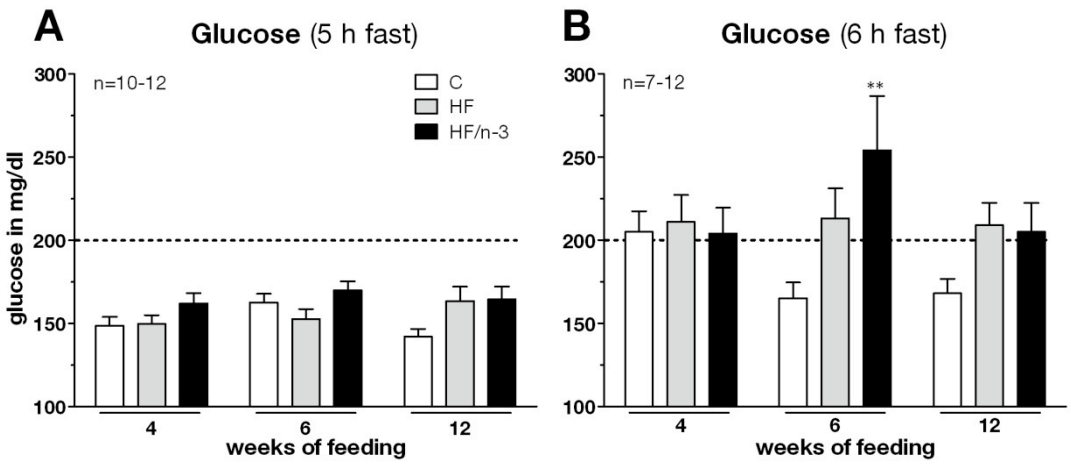

Figure 23: Fasting glucose levels in mice. Blood glucose levels were determined during blood withdrawal after a 5 h fast (**A**) and before intraperitoneal glucose injection for the glucose tolerance test after a 6 h fast (**B**) in mice fed control, high fat, and high fat diet enriched with n-3 LC-PUFA EPA / DHA after 4, 6, and 12 weeks. All data are means ± standard error. Statistical analysis was performed using Two-Way ANOVA and Bonferroni post-test. Asterisks indicate significant differences compared with control at the same time point or between groups as indicated. * $p<0.05$; ** $p<0.01$; *** $p<0.001$.

In summary, glucose tolerance was decreased in both HF and HF/n-3-treated animals compared with controls by elevated blood glucose levels already after 4 weeks. There was no significant amelioration of this phenotype by HF/n-3 diet but only trends towards the expected outcome after 12 weeks of feeding. In contrast, insulin production was decreased in HF/n-3 animals compared with HF mice and thus showed an improvement of insulin sensitivity by n-3 LC-PUFA treatment on HF diet.

4.12 Inflammation

4.12.1 Adipose tissue

Studies have shown that obesity is accompanied by immune cell filtration in adipose tissue, namely by macrophages, T cells and B cells (Weisberg et al., 2003; Kintscher et al., 2008; Winer et al., 2011). Therefore, the state of immune cell activation was characterized in an explorative targeted gene expression screening approach applying the technique of RT^2 Profiler^{TM} RT-qPCR array (SABiosciences / Qiagen) and specifically characterizing the expression of genes involved in macrophage, T and B cell activation to pools of RNA from mesenteric adipose tissue for each dietary group (Appendix Table 8).

Surprisingly, the analysis revealed a general increase of genes with a fold change (FC) of more than 1.2 on HF/n-3 diet compared with control (63 % of genes, Figure 24). 39 % more genes were upregulated in FC than in a comparison of HF with control group (24 % of genes with FC>1.2). This pointed to pro-inflammatory conditions induced by HF/n-3 more than by HF diet in this fat depot.

A direct comparison of gene expression in HF/n-3 animals relative to HF showed that more than half (51 %) of the genes were increased in expression above FC>1.2. A more detailed analysis identified that half of these genes had functions in T cell activation, proliferation, or differentiation (Figure 24B) whereas only 28 % were involved in the same processes but in B cells.

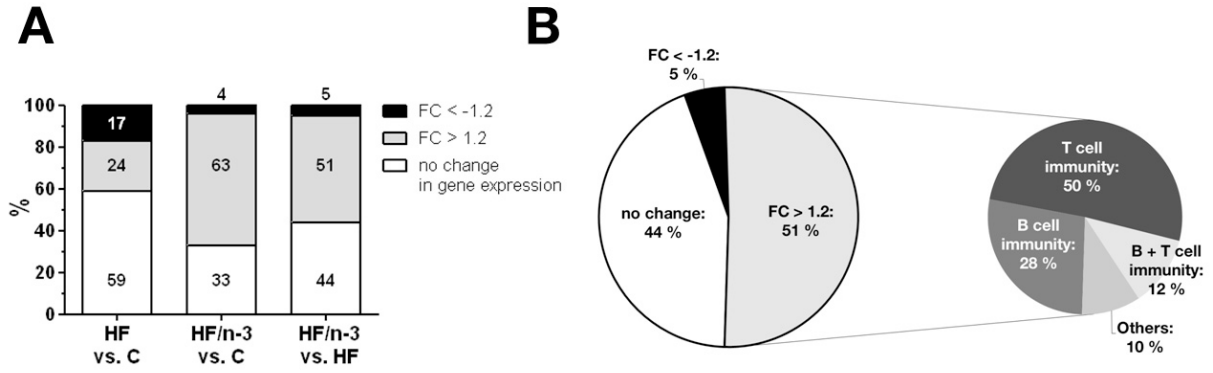

Figure 24: Gene expression regulation in RT-qPCR array of T and B cell activation in mesenteric adipose tissue. Results (Appendix Table 8) were expressed in relative fold changes (FC) for explorative gene expression analysis with "RT^2 Profiler^{TM} RT-qPCR arrays" (SABiosciences) for marker genes of T and B cell activation in mesenteric adipose tissue (MAT). FC of C, control diet; HF, high fat diet; HF/n-3, high fat diet enriched with n-3 LC-PUFA EPA / DHA were calculated relative to control group or high fat group (**A**) with a more detailed view of HF/n-3 group relative to HF group (**B**). A threshold of 1.2 FC was chosen to show upregulation (FC>1.2), downregulation (FC<-1.2) or no change (1.2>FC>-1.2) of gene expression.

As examples, direct and indirect markers of T cell differentiation Jagged2 and E3 ubiquitin protein ligase Wwp1 (Zhang et al., 2004; Van de Walle et al., 2011) were highly upregulated (Jag2, 4.59-fold; Wwp11, 5.74-fold) in HF/n-3 and to a higher extent as in HF animals

compared with control mice (Jag2, 3.11-fold; Wwp1, 3.52-fold). Some genes were even lower in expression upon HF diet and highly upregulated or not regulated on HF/n-3 compared with controls as shown for the pro-inflammatory molecule Spp1 (0.62-fold vs. 9.45-fold; Weber and Cantor, 1996; Nomiyama et al., 2007) and the T_h1-cell type differentiation promoting cytokine interferon γ (Ifng, 0.16-fold vs. 1.19-fold; Bradley et al., 1996).

In analogy to T cells, the same pattern was detected for B cell proliferation. For example, interleukin 7 operating in B cell proliferation (Milne and Paige, 2006) was upregulated 2.22-fold in HF/n-3 and 1.56-fold in HF animals. Only very few genes were downregulated upon HF/n-3 diet ("HF/n-3 vs. HF" Appendix Table 8), among them were nitric oxide synthase 2 (Nos2) and cyclin-dependent kinase inhibitor 1A (Cdkn1a), downregulated 0.80-fold and 0.68-fold, respectively.

4.12.1.1 Osteopontin

From these explorative gene expression data the highest regulated target gene (osteopontin / secreted phosphoprotein 1 [OPN / Spp1], 9.45-fold increased in HF/n-3 animals compared with control animals) was further validated. Osteopontin has been implicated in obesity (Nomiyama et al., 2007; Kiefer et al., 2010), and as chemoattractant for macrophages (Singh et al., 1990) synthesized by activated T cells (Weber and Cantor, 1996).

OPN contains multiple sites for Ser / Thr phosphorylation, N- and O-glycosylation, and sulphatation (Denhardt and Guo, 1993; Patarca et al., 1993), which explains apparent molecular weights in SDS-PAGE ranging from 20 to 75 kDa (Prince et al., 1987; Nemir et al., 1989; Denhardt and Guo, 1993; Kon et al., 2000; Sodek et al., 2000). Western blot results of this study showed a double band at approximately 55 kDa with an increased intensity of the lower double band.

The picture is further complicated by the expression of intracellular OPN (iOPN) and secreted OPN (sOPN), products of alternative translation (Shinohara et al., 2008). The Opn / Spp1 gene contains a translational 5'-AUG site and another non-AUG site as an alternative translational start site 39 nucleotides downstream. This will lead to deletion of the 16 amino acid N-terminal signal sequence and subsequently to cytoplasmatic localization of iOPN. While iOPN expression is high in DCs and macrophages, the pattern is reversed in T cells (Cantor and Shinohara, 2009).

OPN / Spp1 gene expression was verified by RT-qPCR with more biological replicates in different tissues (Figure 25). In all adipose tissue depots Spp1 mRNA expression was

increased on HF/n-3 compared with controls (MAT, 5.27 ± 1.94; Figure 25A; EAT, 8.04 ± 1.72; Figure 25D; IAT, 2.10 ± 0.56; Figure 25E). This was also confirmed with a commercially available primer (MAT, Qiagen primer, 7.41 ± 2.59; Figure 25B) and was apparent already after 6 weeks of feeding in MAT but with a lower fold change compared with 12 weeks feeding (MAT, 6 w, 2.21 ± 0.57; Figure 25C).

A similar trend was observed in isolated adipocytes and cultivated pre-adipocytes (Appendix Table 7), but the statistical power was very low (n=3–4).

No change in gene expression was observed in liver (Figure 25F). This result was also reflected by OPN plasma levels (C, 233.9 ± 8.2 ng / ml; HF, 241.1 ± 12.92 ng / ml; HF/n-3, 262.7 ± 16.92 ng / ml; p=0.2562), showing similar levels as in a previous report in mice (van Eijk et al., 2009).

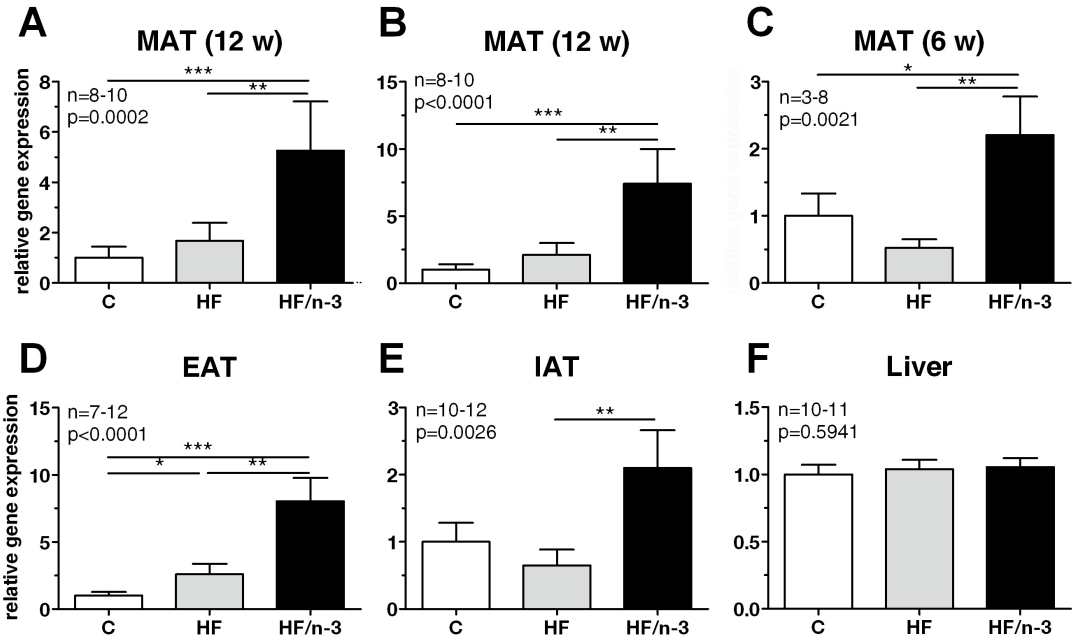

Figure 25: Spp1 relative gene expression in murine tissues. Shown are the mean gene expression levels ± standard error after RT-qPCR with 10 ng of RNA (n=3–8; 7–12) for secreted phosphoprotein 1 (Spp1 / Osteopontin) in mesenteric adipose tissue (MAT; **A-C**), epididymal adipose tissue (EAT; **D**), subcutaneous inguinal adipose tissue (IAT; **E**) and liver (**F**) after 6 and 12 weeks feeding on C, control diet; HF, high fat diet; or HF/n-3, high fat diet enriched with n-3 LC-PUFA EPA / DHA compared with control-fed animals. In **B** a commercially available primer assay was used (Qiagen). Data were analyzed by $\Delta\Delta C_q$-method and normalized to β-actin, glyceraldehyde-phosphate dehydrogenase and hypoxanthine guanine phosphoribosyl transferase gene expression. Statistical analysis was performed using One-Way ANOVA and Tukey post-test. Asterisks indicate significant differences compared with control or between groups as indicated. * p<0.05; ** p<0.01; *** p<0.001.

OPN protein expression in adipose tissue was probed with a monoclonal IgG_1 antibody that was raised in mouse against mouse recombinant OPN (Santa Cruz). Mouse OPN is a 294 amino acid protein (32459 Da) that is potentially heavily phosphorylated at its multiple serine

residues and threonine 170 in addition to N- / O-linked glycosylation sites (Protein Sequence Database Uniprot, 2012).

OPN intensities were elevated in MAT of both HF and HF/n-3 mice compared with controls (Figure 26). This effect was not statistically significant due to high inter-individual variation in protein expression (p=0.2143; n=5–6; Figure 26B). However, the lower band indicating iOPN was higher in intensity than the upper band showing sOPN (Figure 26A).

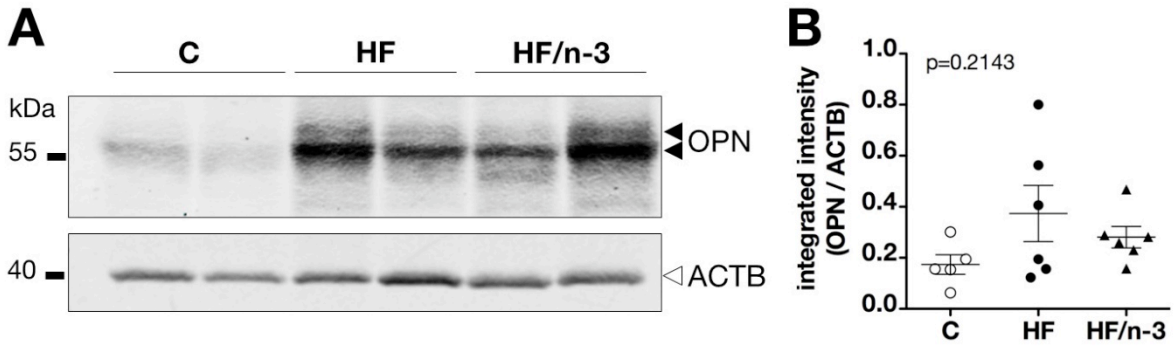

Figure 26: Murine osteopontin protein expression in mesenteric adipose tissue. Western blot for osteopontin (OPN, **A**) and densitometric analysis OPN protein expression (secreted OPN + intracellular OPN; **B**). 40 µg protein per lane from murine mesenteric adipose tissue dissected after 12 weeks feeding on C, control diet; HF, high fat diet; or HF/n-3, high fat diet enriched with n-3 LC-PUFA EPA / DHA were loaded on a 12.5 % gel. SDS-PAGE was run at 15 mA for 3 h followed by semi-dry blotting on a nitrocellulose membrane for 45 min at 400 mA. Detection was performed with monoclonal mouse anti-mouse osteopontin antibody (OPN, #SC-21742, Santa Cruz, 1:500) and polyclonal rabbit anti-mouse β-actin antibody (ACTB, #4967S, Cell Signaling, 1:1000) using the Odyssey® Infrared Imaging System (LI-COR Biosciences). Of the OPN isoforms secreted OPN is marked by the upper, intracellular OPN by the lower black arrowhead. Statistical analysis was performed using One-Way ANOVA and Tukey post-test. Asterisks indicate significant differences compared with control or between groups as indicated. * $p<0.05$; ** $p<0.01$; *** $p<0.001$.

In summary, expression of genes involved in T and B cell activation was elevated in MAT of mice fed HF/n-3 using an explorative approach with RT-qPCR array. As an example, OPN gene and protein expression was extensively validated. Similar to the array results, mRNA levels of OPN in various adipose tissues and at different time points were increased. However, this effect was absent in liver. There was no response of OPN levels in plasma depending on dietary treatment. Protein expression of OPN in MAT was similar in both HF diets, which was in contrast to gene expression. However, iOPN was more expressed than sOPN. Thus, there was a tissue-specific effect with elevated or similar levels of OPN in HF/n-3 animals compared with HF mice in adipose tissue and unchanged OPN levels in liver and plasma.

4.12.1.2 Differential expression of inflammatory genes in mesenteric and epididymal adipose tissue

As indicated by the exploratory RT-qPCR array, results pointed towards an upregulation of T and B cell activation on gene expression level by the HF/n-3 diet. This surprising finding was also confirmed with other markers involved in the modulation of inflammation as shown in the following section (Figure 27, Figure 28).

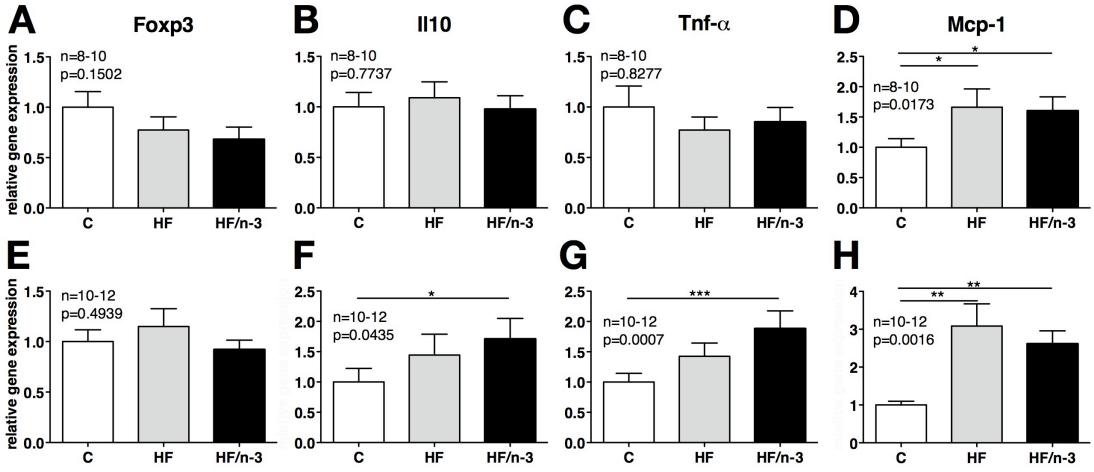

Figure 27: Relative gene expression in murine adipose tissue. Shown are the mean gene expression levels ± standard error after RT-qPCR with 10 ng of RNA (n=8–12) for forkhead box protein P 3 (Foxp3), interleukin 10 (Il10), tumor necrosis factor α (TNF-α), and macrophage chemoattractant protein 1 (Mcp-1) in mesenteric adipose tissue (MAT; **A-D**) and epididymal adipose tissue (EAT; **E-H**) after 12 weeks feeding on C, control diet; HF, high fat diet; or HF/n-3, high fat diet enriched with n-3 LC-PUFA EPA / DHA compared with control-fed animals. Data were analyzed by $\Delta\Delta C_q$-method and normalized to β-actin, glyceraldehyde-phosphate dehydrogenase and hypoxanthine guanine phosphoribosyl transferase gene expression. Statistical analysis was performed using One-Way ANOVA and Tukey post-test. Asterisks indicate significant differences compared with control or between groups as indicated. * $p<0.05$; ** $p<0.01$; *** $p<0.001$.

Regulatory T cells were decreased during adipose tissue inflammation with diminished expression of the marker molecule forkhead box protein 3 (Foxp3) in obese humans compared with lean subjects (Ilan et al., 2010; Deiuliis et al., 2011). In this study a slight decrease of Foxp3 gene expression was observed in MAT of HF/n-3 mice compared with controls (HF, 0.77 ± 0.13; HF/n-3, 0.68 ± 0.12; Figure 27A), which was not significant (p=0.1502). In EAT there was also no effect (p=0.4939; Figure 27E).

Interestingly, interleukin 10 (Il10) mRNA, a classical anti-inflammatory marker (Murray, 2005), was significantly increased in epididymal adipose tissue upon HF/n-3 (1.71 ± 0.34, p=0.0435; Figure 27F) whereas in MAT there was no obvious regulation (p=0.7737; Figure 27B).

Similarly, the pro-inflammatory cytokine tumor necrosis factor α (Tnf-α) showed significantly higher gene expression in EAT on HF/n-3 diet (1.88 ± 0.29, p=0.0007; Figure 27G). In MAT,

however, there was no significant rise in Tnf-α mRNA levels by n-3 LC-PUFA treatment (p=0.8277; Figure 27C).

Monocyte chemoattractant protein 1 (Mcp-1) mRNA, a chemokine involved in adipose tissue macrophage infiltration (Chen et al., 2005), was increased in both adipose tissue depots in a similar manner, but the regulation of gene expression was more obvious in EAT than in MAT. Gene expression was highest in HF animals (EAT, 3.08 ± 0.59, p=0.0016; Figure 27H; MAT, 1.66 ± 0.30, p=0.0173; Figure 27D) and more pronounced in EAT. The increase in Mcp-1 mRNA on HF/n-3 diet was still high compared with controls and not significantly different compared with HF mice (EAT, 2.61 ± 0.34; Figure 27E, MAT: 1.60 ± 0.23; Figure 27A).

4.12.1.3 Macrophage infiltration in adipose tissue

Obesity is associated with a chronic adipose tissue inflammatory state leading to immune cell infiltration and macrophage recruitment and differentiation of subsets (Odegaard and Chawla, 2008; Murray and Wynn, 2011). Results regarding osteopontin and Mcp-1 gene expression obtained in this study (Figure 25, Figure 27) raised the question whether also adipose tissue macrophages (ATM) were affected by the HF/n-3 diet.

Integrin α-X and mannose receptor, C type 1 genes (coding for Itgax / CD11c and Mrc1 / CD206, respectively) are markers of the pro-inflammatory M1 and anti-inflammatory M2 macrophage subsets, respectively (Fujisaka et al., 2009). Itgax, however, is also expressed on T cells (Huleatt and Lefrancois, 1995).

In both MAT and EAT an increase of Itgax mRNA was identified on HF diet in EAT, but not in MAT (EAT, 2.86 ± 0.86; Figure 28C; MAT: 1.07 ± 0.13; Figure 28A). Confirming earlier results of inflammation in HF/n-3 adipose tissue, increased expression of pro-inflammatory Itgax mRNA was detected in both MAT and EAT on HF/n-3 diet (MAT, 2.44 ± 0.33, p<0.0001; Figure 28A; EAT, 6.62 ± 1.53, p<0.0001; Figure 28C), but in EAT this elevated gene expression was about 2-fold higher than in MAT.

Expression of Mrc1 as a marker of counteracting, anti-inflammatory M2 macrophages (Odegaard and Chawla, 2008; Gordon and Martinez, 2010) was also increased on HF/n-3 in both adipose depots. Here, however, MAT showed significant changes in gene expression upon HF/n-3 diet (MAT, 1.56 ± 0.10, p<0.0001; Figure 28B; EAT, 1.17 ± 0.08, p=0.0179; Figure 28D) while with HF diet feeding there were no changes (MAT, 1.17 ± 0.07; EAT, 0.97 ± 0.06).

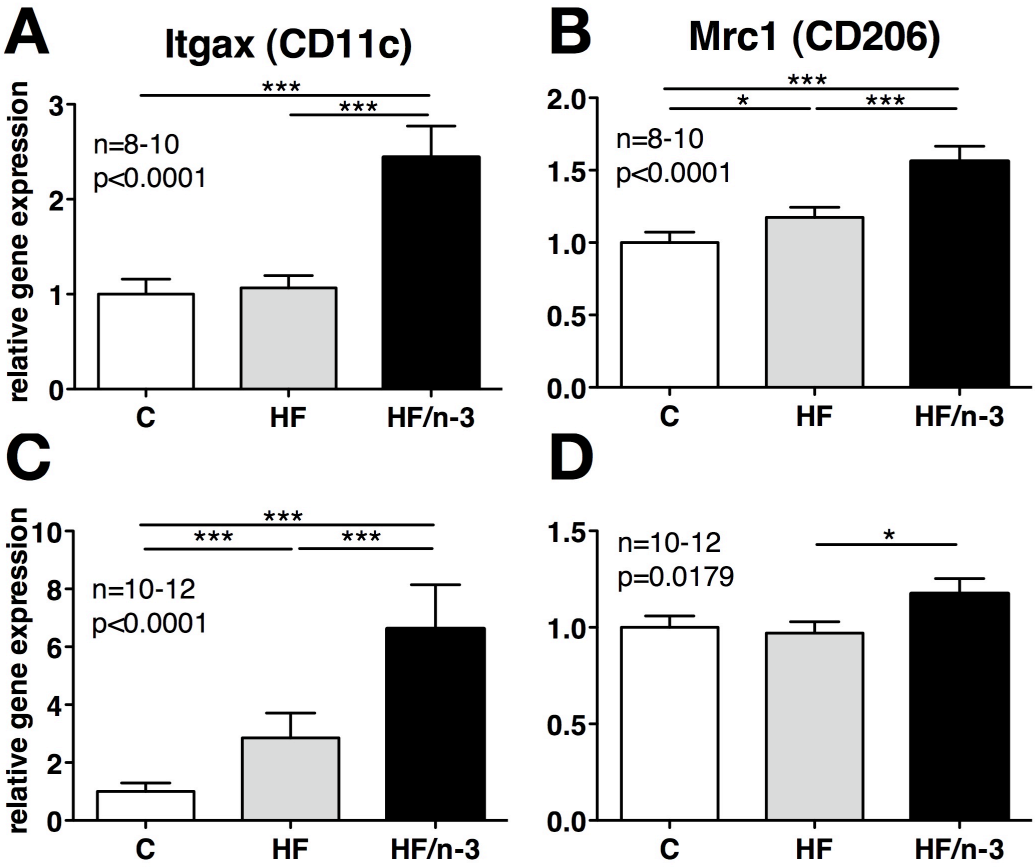

Figure 28: Relative gene expression of macrophage marker surface molecules in murine adipose tissue. Shown are the mean gene expression levels ± standard error after RT-qPCR with 10 ng of RNA (n=8–12) for integrin α-X (Itgax / CD11c) and mannose receptor, C type 1 (Mrc1 / CD206) in mesenteric adipose tissue (MAT; **A-B**) and epididymal adipose tissue (EAT; **C-D**) after 12 weeks feeding on C, control diet; HF, high fat diet; or HF/n-3, high fat diet enriched with n-3 LC-PUFA EPA / DHA compared with control-fed animals. Data were analyzed by $\Delta\Delta C_q$-method and normalized to β-actin, glyceraldehyde-phosphate dehydrogenase and hypoxanthine guanine phosphoribosyl transferase gene expression. Statistical analysis was performed using One-Way ANOVA and Tukey post-test. Asterisks indicate significant differences compared with control or between groups as indicated. * $p<0.05$; ** $p<0.01$; *** $p<0.001$.

In addition, crown-like structures were quantified (CLS; Figure 29). These are aggregates of immune cells, probably ATM, surrounding a dying adipocyte (Cinti et al., 2005). Since a clear definition of CLS is lacking (West, 2009), CLS were defined as adipocytes surrounded by more than one hematoxylin-stained nucleus (Figure 29A, B, arrowheads).

However, CLS numbers that fit this definition in MAT (Figure 29C) and EAT (Figure 29D) were low. Areas with extreme CLS aggregation were scarce and not representative (Figure 29B). Regardless of adipose depot, control mice showed 0 to 1 CLS per 10 000 adipocytes. This number was significantly increased to 5–6 CLS per 10 000 adipocytes in MAT of HF or HF/n-3 fed mice but with no difference between HF groups (C, 0.64 ± 0.39 ; HF, 6.68 ± 0.78; HF/n-3, 6.04 ± 0.78, $p<0.0001$; Figure 29B). In EAT numbers of CLS per 10 000 adipocytes were almost double compared with MAT HF mice. However, there was no significant

difference between groups but only a trend towards decreased CLS number in HF/n-3 animals (C, 0.64 ± 0.39; HF, 12.08 ± 5.17; HF/n-3, 8.27 ± 3.91, p=0.1309; Figure 29C). In EAT there was high variation among individuals.

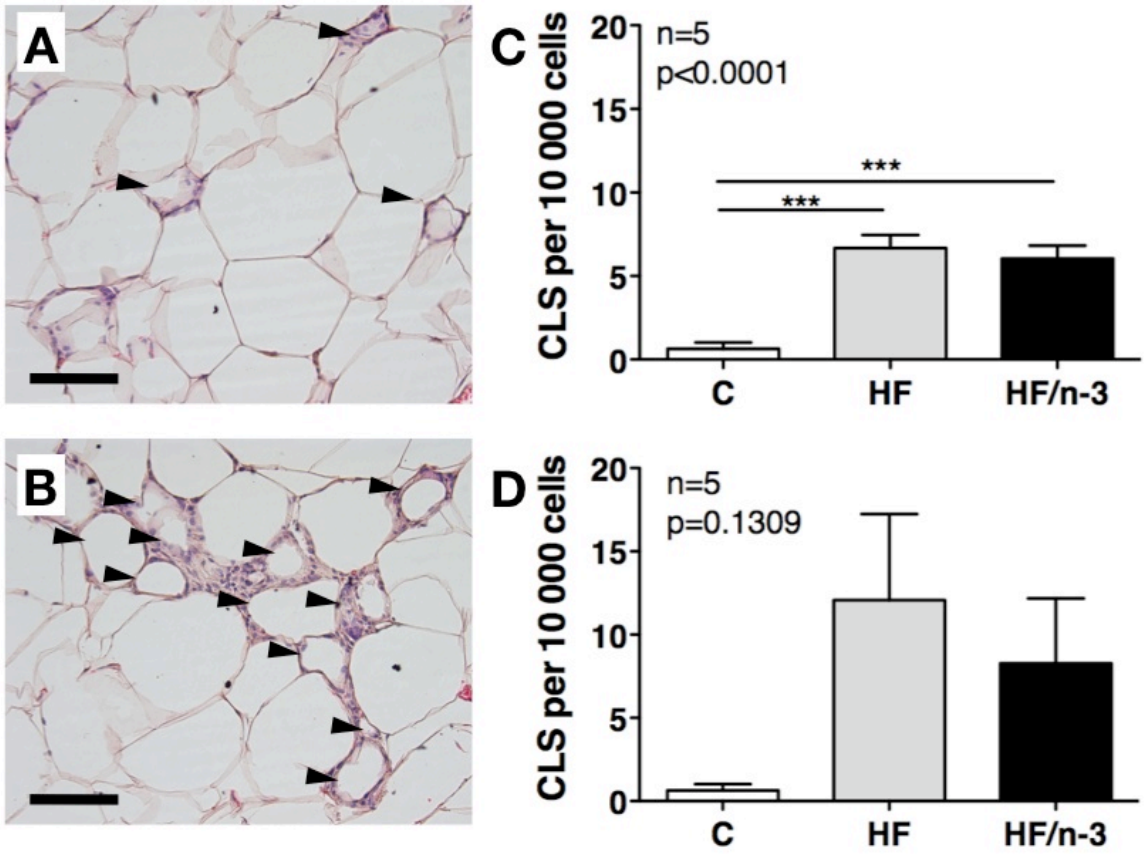

Figure 29: Crown-like structures in adipose tissue. Shown is a H&E stained section of HF EAT with crown-like structures (CLS) indicated by arrow-heads (**A, B**). CLS per 10 000 cells were calculated by counting CLS number per section and dividing by number of cells per section for MAT (**C**) and EAT (**D**) from animals fed C, control; HF, high fat; or HF/n-3, high fat diet enriched with n-3 LC-PUFA EPA / DHA. Data represent means ± standard error. Black bar in picture indicates scale of 100 µm. Statistical analysis was performed using One-Way ANOVA and Tukey post-test. Asterisks indicate significant differences compared with control at the same time point or between groups as indicated. * $p<0.05$; ** $p<0.01$; *** $p<0.001$.

In summary, in addition to genes of T and B cell activation also other molecules modulating inflammatory processes were increased in expression in adipose tissue with HF/n-3 diet. While regulatory T cell marker Foxp3 was slightly but not significantly downregulated in MAT only, more significant effects were observed in EAT compared with MAT. Only in EAT the anti-inflammatory Il10 as well as pro-inflammatory Tnf-α and Mcp-1 showed significantly elevated mRNA levels at the same time in HF/n-3 animals compared with other groups whereas there was no pronounced effect on Il10 and Tnf-α gene expression in MAT. Investigation of M1 macrophage (and T cell) marker CD11c showed an increased gene expression in both MAT and EAT but more pronounced in the latter. As with Il10 gene expression this was paralleled by an increase of anti-inflammatory mRNA, namely CD206, upregulated in both MAT and EAT of HF/n-3 animals.

Crown-like structures counted in visceral adipose tissue MAT and EAT were elevated in HF diets without a significant difference between HF and HF/n-3 animals.

4.12.2 Systemic serum amyloid A levels

Because inflammatory markers and immune cell infiltration were both increased in adipose tissue, the immuno-modulatory potential of n-3 LC-PUFA was also tested in other tissues.

First, systemic effects on inflammation were investigated by probing for levels of serum amyloid A (SAA). The SAA protein family in mice includes four isoforms that are secreted by the liver (SAA1, SAA2, SAA4) during the acute phase of the innate immune response or expressed, for example, by adipose tissue after high fat feeding (SAA3; Uhlar and Whitehead, 1999; Scheja et al., 2008). Systemically increased SAA levels have been associated with obesity-associated diseases like insulin resistance and atherosclerosis (Ridker et al., 2000; Lewis et al., 2004; Yang et al., 2006).

The determination of plasma SAA levels after 12 weeks on the experimental diets showed a significant elevation of SAA only in animals fed the HF diets (Figure 30). Compared with controls, HF animals had 1.44-fold increased SAA levels, which was even 1.67-fold compared with plasma SAA levels measured in HF/n-3 animals (C, 121.75 ± 11.73 µg / ml; HF, 175.67 ± 12.51 µg / ml; HF/n-3, 105.87 ± 8.15 µg / ml, p=0.0003).

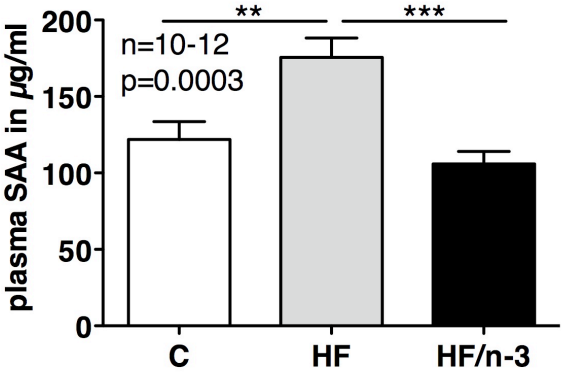

Figure 30: Serum amyloid A (SAA) plasma levels.
SAA levels in plasma were determined after 12 weeks feeding on C, control diet; HF, high fat diet; or HF/n-3, high fat diet enriched with n-3 LC-PUFA EPA / DHA compared with control-fed animals. Data are means ± standard error. Statistical analysis was performed using One-Way ANOVA and Tukey post-test. Asterisks indicate significant differences compared with control or between groups as indicated. * $p<0.05$; ** $p<0.01$; *** $p<0.001$.

4.12.3 Anti-inflammatory gene expression in small intestine

For the characterization of immunomodulatory actions of n-3 LC-PUFA in the small intestine a targeted gene expression screening approach using the RT² Profiler™ RT-qPCR array (SABiosciences / Qiagen) for genes involved in endothelial cell biology was applied (Appendix Table 9).

In contrast to earlier findings in adipose tissue regarding T and B cell activation, HF/n-3 led to decreased expression of genes involved in endothelial cell biology in the small intestine (Figure 31). A comparison of HF with control animals showed that 53 % of the genes displayed a fold change (FC) of more than 1.2 (Figure 31A). This rate is decreased by 14 % with feeding HF/n-3. In addition, HF/n-3 led to an increase of mRNA expression of genes, which were downregulated in expression compared with controls (+9 %). A direct comparison of both HF diets showed that even though almost 60 % of the genes were not regulated at all, more than one third of genes (36 %) was lower in expression by the use of n-3 LC-PUFA.

A detailed analysis of this fraction of genes revealed that the overwhelming majority of genes being decreased in expression compared with HF diet (79 %) was related to endothelial cell activation, namely the gene expression of adhesion molecules and genes involved in extracellular matrix structure and remodeling (Figure 31B; Appendix Table 9).

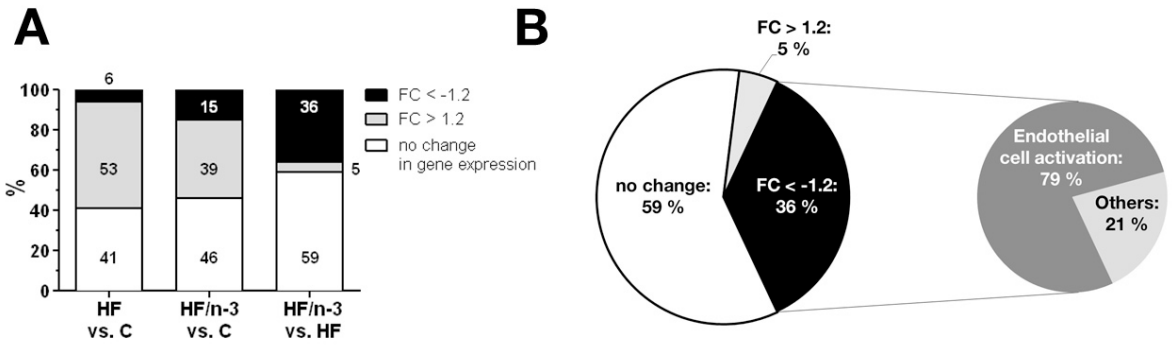

Figure 31: Gene expression regulation in RT-qPCR array of endothelial cell biology in small intestine. Results (Appendix Table 9) were expressed in relative fold changes (FC) for explorative gene expression analysis with "RT² Profiler™ RT-qPCR arrays" (SABiosciences) for marker genes of endothelial cell biology in small intestine. FC of C, control diet; HF, high fat diet; HF/n-3, high fat diet enriched with n-3 LC-PUFA EPA / DHA were calculated relative to control group or high fat group (**A**) with a more detailed view of HF/n-3 group relative to HF group (**B**). A threshold of 1.2 FC was chosen to show upregulation (FC>1.2), downregulation (FC<-1.2) or no change (1.2>FC>-1.2) of gene expression.

The gene expression of intercellular adhesion molecule 1 (Icam1), vascular cell adhesion molecule 1 (Vcam1), and endothelial-specific receptor tyrosine kinase (Tek) was confirmed in small intestine by RT-qPCR retrieving the same results. The mRNA of these molecules was, however, expressed at low levels in the intestinal tissue (C_q: 29–32).

Icam1 mediates the extravasation of leukocytes from the circulation into sites of inflammation (Steeber et al., 1999). In this situation it can be strongly induced on lymphocytes, macrophages and endothelial cells. In this study, Icam1 was significantly increased in gene expression by 1.58-fold in HF animals compared with controls (1.58 ± 0.25, p=0.0321; Figure 32A). HF/n-3 animals, however, showed mRNA levels similar to controls (1.09 ± 0.16).

Similar to the actions of Icam1, Vcam1, which is expressed mainly on activated endothelial cells, but also on macrophages and dendritic cells, mediates leukocyte rolling on and tight attachment to endothelial cells after activation (Koni et al., 2001; Ulyanova et al., 2005). Vcam1 gene expression in small intestine was elevated only in HF mice (1.76 ± 0.35, p=0.0852; Figure 32B). In HF/n-3 mice, this elevation of gene expression was less pronounced (1.27 ± 0.22).

Tek is a tyrosine kinase involved in the regulation of angiogenesis and endothelial cell growth (Sato et al., 1995). As in the array experiment, an increase of Tek gene expression was detected in HF animals (1.71 ± 0.34, p=0.0470; Figure 32C) whereas HF/n-3 animals did not show a significant change in gene expression compared with controls (1.21 ± 0.21) but slightly decreased compared with HF mice.

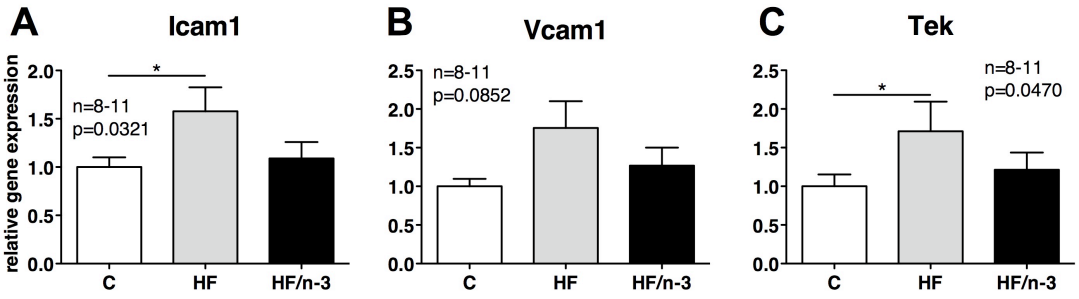

Figure 32: Relative gene expression in intestine. Shown are the mean gene expression levels ± standard error after RT-qPCR with 10 ng of RNA (n=8–11) for intercellular adhesion molecule 1 (Icam1; **A**), vascular cell adhesion molecule 1 (Vcam1; **B**), and endothelial-specific receptor tyrosine kinase (Tek; **C**) in small intestine after 12 weeks feeding on C, control diet; HF, high fat diet; or HF/n-3, high fat diet enriched with n-3 LC-PUFA EPA / DHA compared with control-fed animals. Data were analyzed by $\Delta\Delta C_q$-method and normalized to β-actin, glyceraldehyde-phosphate dehydrogenase, and hypoxanthine guanine phosphoribosyl transferase. Statistical analysis was performed using One-Way ANOVA and Tukey post-test. Asterisks indicate significant differences compared with control or between groups as indicated. * $p<0.05$; ** $p<0.01$; *** $p<0.001$.

4.12.4 Gene expression in spleen

To further investigate the analysis of n-3 LC-PUFA on inflammatory and immunomodulatory gene expression, the spleen was analyzed. In the spleen, blood is filtrated; it is a major site of lymphocyte proliferation after antigen presentation (Mebius and Kraal, 2005). As described earlier, the spleen was significantly increased in mass exclusively in HF/n-3

animals (Figure 16), which was independent of body mass. Histological observations of the spleen did not reveal obvious abnormalities (data not shown). Measuring gene expression of surface molecules identifying helper T lymphocytes (but also macrophages and dendritic cells) and cytotoxic / suppressor T lymphocytes, namely CD4 and CD8α, respectively, (Fung-Leung et al., 1991; Hanna et al., 2001), this study could not demonstrate a change in gene expression in HF animals compared with controls, but significantly lower mRNA levels of CD4 and CD8α in spleen of HF/n3 mice (Figure 33).

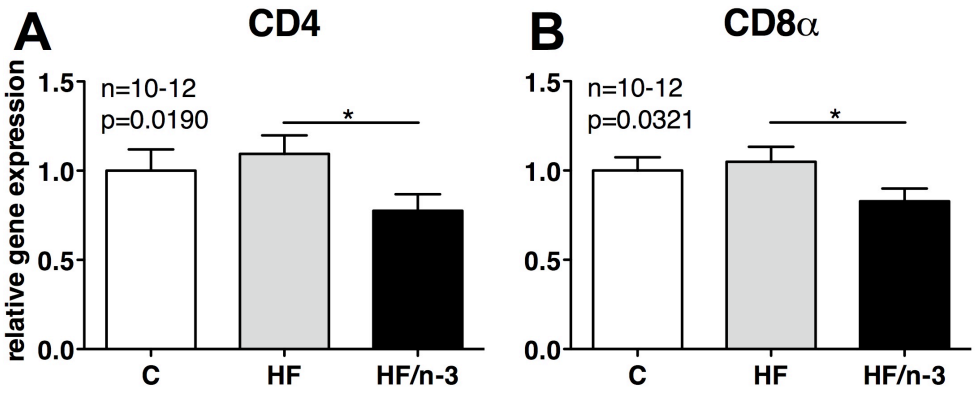

Figure 33: Relative gene expression in murine spleen. Shown are the mean gene expression levels ± standard error after RT-qPCR with 10 ng of RNA (n=10–12) for CD4 (**A**) and CD8α (**B**) in spleen after 12 weeks feeding on C, control diet; HF, high fat diet; or HF/n-3, high fat diet enriched with n-3 LC-PUFA EPA / DHA compared with control-fed animals. Data were analyzed by $\Delta\Delta C_q$-method and normalized to glyceraldehyde-phosphate dehydrogenase and hypoxanthine guanine phosphoribosyl transferase gene expression. Statistical analysis was performed using One-Way ANOVA and Tukey post-test. Asterisks indicate significant differences compared with control or between groups as indicated. * $p<0.05$; ** $p<0.01$; *** $p<0.001$.

In summary, anti-inflammatory effects exerted by HF/n-3 diet were observed in organs other than adipose tissue. In plasma, SAA levels were elevated in HF diet fed mice but not in HF/n-3 animals compared with controls. This was further substantiated by findings in the small intestine where fold changes in gene expression of HF/n-3 relative to HF animals showed a decrease in a large fraction of genes. These genes were predominantly involved in endothelial cell activation. This was verified by quantification of Icam1, Vcam1 and Tek gene expression in small intestine.

At last, despite an increased spleen size in HF/n-3 mice, decreased mRNA levels of immune cell-specific CD4 and CD8α were detected.

4.13 Metabolomics

4.13.1 Lipid molecule measurement

In the previous section, adipose tissue-related findings in inflammation were extended to other organs to receive a more holistic picture of these processes in the whole organism. Similar to that but with an omics-approach applying the Biocrates platform, the HF/n-3 diet-induced effects on nearly 200 metabolites including acyl-carnitines, phospholipids, sphingolipids, lyso-phospholipids, biogenic amines, and amino acids were investigated in liver, plasma, mesenteric and epididymal adipose tissue of mice from this study.

In summary, all the tissues analyzed demonstrated clear-cut changes of HF/n-3 diet that were not exerted by HF diet when compared with controls. Two-dimensional principal component analysis (PCA) in liver (Figure 34A) revealed that samples from animals of every dietary group were distinct in metabolite levels and regulation compared with the other dietary groups. Even more so, HF/n-3 mice were different in both, component 1 and 2, whereas control and HF animals were on the same level regarding component 1 (x-axis).

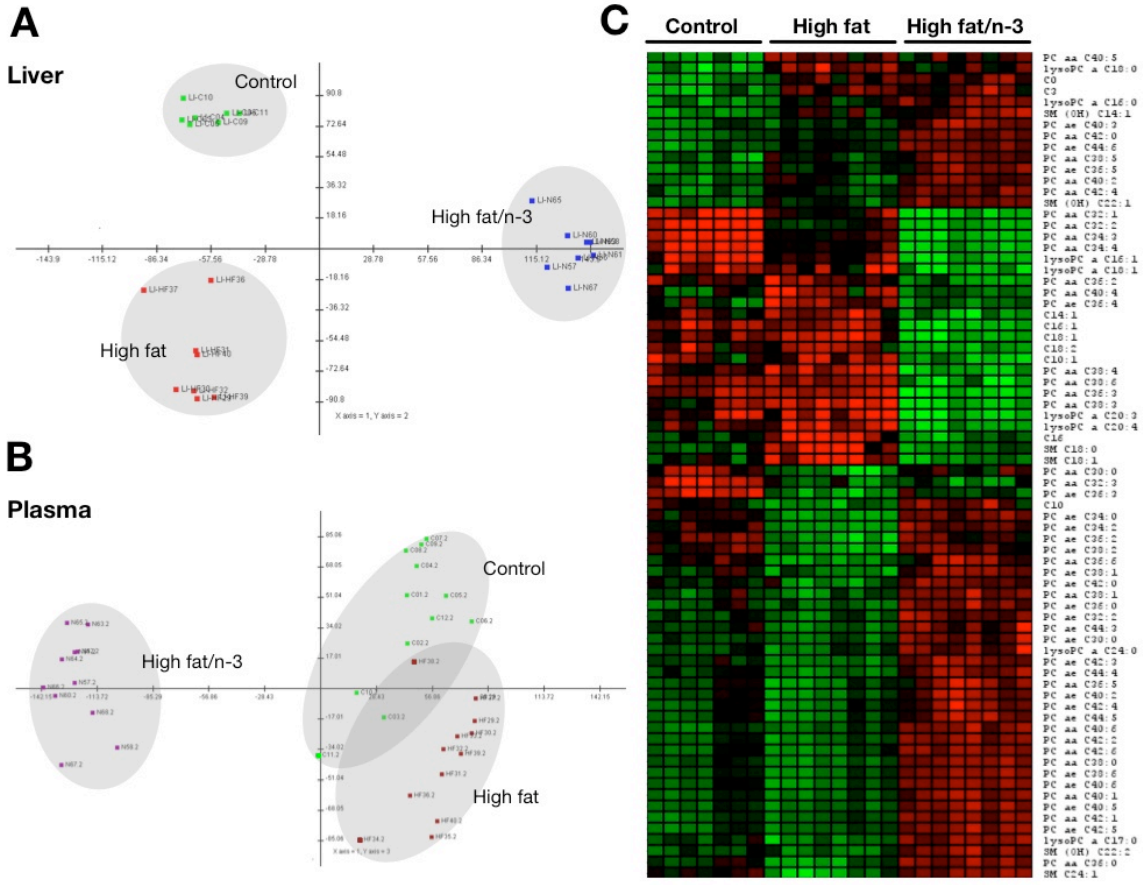

Figure 34: Overall metabolite changes in liver and plasma. Two-dimensional principal component analysis showing clusters of samples for control, high fat, and high fat/n-3 samples in liver (**A**) and plasma (**B**). Cluster analysis (**C**) shows increased (red) and decreased metabolites (green). Every column displays an animal of the control, high fat, or high fat/n-3 dietary group as indicated, every row displays a metabolite compared. Cluster and variance analysis was combined with the TIGR MeV software v4.6.0 (J. Craig Venter Institute) whereby the variance of each metabolite was separately tested via Fisher tests and Bonferroni adjustment between the three groups of samples. Clustering

was based on Euclidean distance and average linkage. Metabolite data matrices were standardized via a z-transformation and data normalized to initial tissue mass used.

In plasma, the same distinct pattern was observed (Figure 34B), but control and HF samples were more similar according to PCA. A cluster analysis of individual metabolites in liver showed that individuals group together. For most metabolites depicted here, inter-individual variation within the group was small. The red color indicates that metabolites were increased in concentration by HF and further increased by HF/n-3 (top part, Figure 34C), whereas others were not changed or decreased by controls as well as HF, but drastically upregulated in HF/n-3 (bottom part, Figure 34C).

At the level of individual metabolites the high complexity of regulation in different tissues was apparent. Considering nearly 200 metabolites, which can be analyzed, in this thesis only one example will be given.

Phospholipids are the most abundant component of the biological membrane bilayers (Lodish et al., 2008). They consist of fatty acids and are one mechanism through which fatty acids can elicit changes in biological processes.

The analysis of long chain phosphatidyl-cholines (PC) in MAT (Figure 35A) and EAT (Figure 35B) revealed a highly significant upregulation of the specific PC on HF/n-3 compared with controls or HF diet whereas HF diet PC were either decreased or on control level. Of note PC levels in MAT were almost always double compared with EAT.

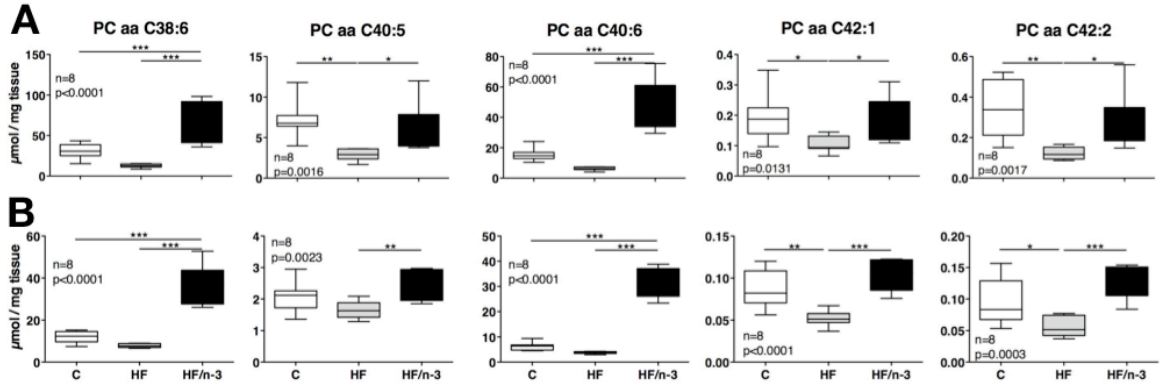

Figure 35: Long-chain phosphatidylcholines in MAT and EAT. Shown are whisker plots of the absolute levels of phosphatidiyl-cholines (PC) with fatty acids bound by ester-bonds (aa) for long-chain phosphatidylcholines in µmol / mg tissue used for analysis in MAT (**A**) and EAT (**B**). Cx:n indicates the sum of fatty acid chain lengths with x carbons containing n double bonds. Statistical analysis was performed using One-Way ANOVA and Tukey post-test. Asterisks indicate significant differences compared with control or between groups as indicated. * $p<0.05$; ** $p<0.01$; *** $p<0.001$.

4.13.2 LC-PUFA metabolites in liver

LC-PUFA can act as signaling molecules by forming eicosanoids (derived from EPA and arachidonic acid, ARA) and other oxidized adducts. In the past decade, new n-3

LC-PUFA-derived bioactive molecules, namely resolvins, protectins and maresins, with powerful anti-inflammatory and pro-resolution properties have been described (Serhan et al., 2008; Serhan et al., 2009). In collaboration with K. H. Weylandt (Charité, Berlin) and M. Rothe (Lipidomix GmbH, Berlin) the impact of a HF diet enriched with n-3 LC-PUFA EPA / DHA on metabolite levels was measured in liver (Figure 36; Appendix Table 10).

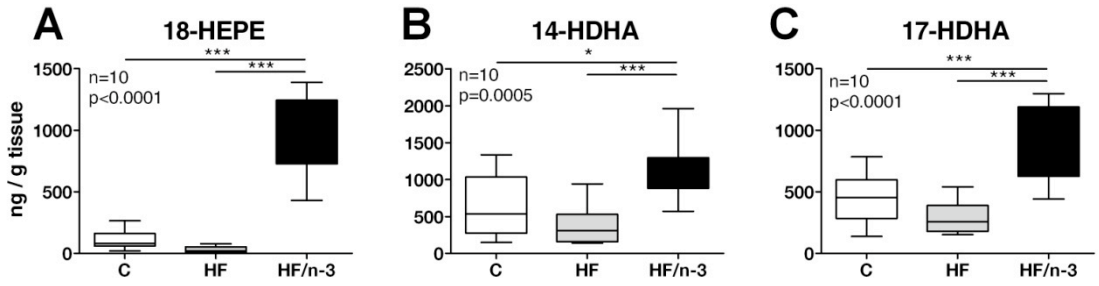

Figure 36: LC-PUFA metabolites in liver. Selected n-3 LC-PUFA metabolites derived from EPA (**A**) and DHA (**B, C**) measured in liver tissue of animals on C, control diet; HF, high fat diet; or HF/n-3, high fat diet enriched with n-3 LC-PUFA EPA / DHA. HDHA, hydroxy-docosahexaenoic acid; HEPE, hydroxy-eicosapentaenoic acid. Statistical analysis was performed using One-Way ANOVA and Tukey post-test. Asterisks indicate significant differences compared with control or between groups as indicated. * $p<0.05$; ** $p<0.01$; *** $p<0.001$.

In brief, there was a clear impact of HF/n-3 diet on the levels of ARA, EPA, and DHA-derived molecules. The HF diet did not show any changes compared with control mice. Regarding the n-6 LC-PUFA metabolites, 15-hydroxeicosatetraenoic acid (15-HETE) was the most abundant molecule. Like many others of this series hepatic levels were up to 2-fold lower in HF/n-3 animals compared with control levels.

In contrast, leukotriene B_4 (LTB_4) a pro-inflammatory eicosanoid (Crooks and Stockley, 1998), was detected only in mice on HF and HF/n-3 diets with a slight elevation on HF/n-3 (1.49-fold) compared with HF. Moreover, lipoxin A_4, a n-6 LC-PUFA-derived, but anti-inflammatory mediator (Serhan et al., 2008), was only detected in controls and HF animals, but not in those fed the n-3 LC-PUFA-rich diet.

On the other hand, EPA-derived leukotriene B_5, which is significantly less pro-inflammatory compared with LTB_4 (Terano et al., 1984), was not detected in livers of HF animals, but in animals of the other groups. DHA-derived resolvin D1 and 10,17-DiHDHA were not measurable.

All other EPA and DHA-derived molecules (HEPE, hydroxy-eicosapentaenoic acids; HDHA, hydroxy-docosahexaenoic acids) displayed a significant increase in concentration in mice on HF/n-3 diet compared with controls and HF-fed animals. Of note are three molecules that have recently been implicated with bioactive functions or as precursors of bioactive resolvins and maresins (Figure 36), namely 18-HEPE (Tjonahen et al., 2006), 14-HDHA (Serhan et al., 2009), and 17-HDHA (Bento et al., 2011).

Taken together, HF diet enriched with n-3 LC-PUFA EPA / DHA led to a decrease of n-6 and an increase of n-3 LC-PUFA-derived metabolites. This elevation was most robust for hydroxylated n-3 LC-PUFA derivatives (HEPE, HDHA).

In summary, the data presented here can only give a brief overview of the data-set retrieved through metabolite analysis in the tissues under investigation. In general, metabolites were differentially regulated by HF/n-3 compared with HF and control animals. Furthermore, there were tissue-specific changes among different tissues regarding absolute levels and regulations of metabolites. Additionally, the LC-PUFA metabolite analysis demonstrated that HF/n-3 increased n-3 LC-PUFA-derived metabolites and decreased n-6 LC-PUFA metabolites accordingly.

5 Discussion

5.1 Introduction

Obesity is a strongly increasing nutritionally caused disease (WHO, 2000) and the origin of metabolic disorders like hypertension, cardiovascular disease, type 2 diabetes and cancer (WHO, 2011). Studies have established a correlation of obesity co-mobidities with the pathological development of adipose tissue (Hauner, 2005) undergoing changes regarding secretory function, cell composition and gene and protein expression (Fried and Ross, 2004).

Emerging evidence at the beginning of this thesis indicated that especially the intra-abdominal mesenteric adipose tissue plays a vital role in the development of the observed complications during intestinal disease (Schaffler et al., 2005). In this context, the efficacy of n-3 long chain polyunsaturated fatty acids (n-3 LC-PUFA) has been proven in the amelioration of symptoms of experimental colitis in rodents (Nieto et al., 2002). Furthermore, it has been demonstrated that n-3 LC-PUFA exert an anti-obesity effect when administered in a high fat diet in rodents (Ruzickova et al., 2004) and improve adipose tissue inflammation in certain mouse models (Todoric et al., 2006; Huber et al., 2007).

The general aim of this thesis was to characterize the effects of n-3 LC-PUFA in diet-induced obesity in mice and clarify the molecular mechanisms of their anti-obesity and anti-inflammatory effects on mouse adipose tissue focusing on intra-abdominal mesenteric adipose tissue and the liver.

The results of this study show that a HF diet enriched with n-3 LC-PUFA exerted a moderate anti-obesity effect in mice with novel adipose tissue-specific effects regarding the gene expression of anti-inflammatory and pro-inflammatory molecules.

The anti-obesity effect in HF/n-3-fed mice was observed in 1) in body mass, adipose tissue mass, leptin gene expression, adipocyte size, and Ucp1 gene expression, 2) in an improvement of plasma insulin levels, and 3) by decreased plasma non-esterified fatty acids, hepatic TAG concentrations, and hepatic lipogenic gene expression along with increased enzyme mRNA levels for enzymes involved in peroxisomal but not mitochondrial β-oxidation. Surprisingly, the analysis of adipose tissue revealed 1) an increased gene expression of immune cell markers in both mesenteric and epididymal adipose tissue, 2) parallel increases of both pro- and anti-inflammatory molecule gene expression under HF/n-3 and 3) effects more pronounced in epididymal than in mesenteric adipose tissue. However, this effect was not systemic, since plasma serum amyloid A levels as well as gene expression of adhesion and angiogenesis molecules in small intestine were negatively regulated by n-3 LC-PUFA. Moreover, a suppression of immune cell activation genes was

observed in spleen. The adipose tissue-specific findings in MAT and EAT are challenging the current simplistic view that n-3 LC-PUFA act anti-inflammatory in adipose tissue. Finally, metabolite analysis in adipose tissue, plasma and liver revealed marked changes induced by HF/n-3 diet and revealed compliance effects by the dietary intervention.

5.2 Effects on obesity

5.2.1 Body mass

Because the principal intention of the study was to obtain an improvement of obesity with a reduction of body mass, and for reasons of comparability to findings already published, the dietary intervention was based on a study published by the Kopecky laboratory in 2004 (Ruzickova et al., 2004). The authors tested different n-3 LC-PUFA concentrates of marine origin in mice on high fat diet and observed a significant reduction in body mass when applying a high fat diet based on sunflower and rapeseed oil with the n-3 LC-PUFA concentrate EPAX 1050 TG in fat.

Even though several adjustments in dietary compositions were made regarding 1) quantity of fat, 2) fat source and quality, and 3) quantity of EPAX 1050 TG, animals on HF/n-3 in this study showed a moderate body mass reduction of 9 % compared with HF animals. This is in agreement with Ruzickova and co-workers who show a body mass reduction of 10–25 % depending on the amount of EPAX 1050 TG included (Ruzickova et al., 2004) and indicate that high amounts of n-3 LC-PUFA on high fat diet can reduce obesity.

Overall, the majority of studies looking for n-3 LC-PUFA effects on obesity show a reduction of body mass, but contradictory results also exist (Todoric et al., 2006; Rockett et al., 2010). In these cases, variations in experimental conditions are responsible for this including dietary composition with type of fat (plant vs. animal fat; Buettner et al., 2006) and fat quantity, animal model (rat vs. mouse; wild type vs. genetically modified; Ruzickova et al., 2004; Todoric et al., 2006), age of animal, keeping conditions (normal vs. specific pathogen-free). Table 11 in the Appendix (page 130) summarizes some of these conditions and the effects on body mass performed from a recent literature search with the keywords “n-3 body weight high-fat diet mouse”.

Total fat content applied in the high fat diets was lower in this study (25 % (w / w)) compared with Ruzickova et al. (35 % [w / w]; Ruzickova et al., 2004). While Ruzickova and co-workers did not specify the texture of their diets, diets used in this thesis were served as pellets with similar texture. The use of plant-derived oils, however, limited the content of fat that is usable for manufacturing a stable pellet. Therefore, 25 % (w / w) is the upper limit whereas higher fat contents can be achieved using fats with higher saturated fat content, e.g. coconut fat or animal fats (personal communication with A. Schumacher, Ssniff Spezialdiäten GmbH).

Similar to Ruzickova et al., in this thesis an n-3 LC-PUFA concentrate with high amounts of DHA was used. Of course, this fuels speculations about a DHA-specific effect on body mass reduction compared with EPA in this study. This has also been indicated in a recent

human study where obese children have been supplemented with high levels of DHA (300 mg) compared with EPA (42 mg) for 3 weeks (Vasickova et al., 2011). Additionally, a follow-up study to the work of Ruzickova et al. showed that mice fed the DHA-derivative α-ethyl DHA ethyl ester on high fat diet had reduced body mass increase, improved parameters of lipid metabolism and even reversed an established glucose intolerance compared with their standard high fat diet (Rossmeisl et al., 2009). However, this study did not test the effects of comparable EPA derivatives.

In this thesis a statistically significant reduction of body mass by n-3 LC-PUFA was obtained after 9 weeks and 12 weeks of feeding. A significant increase in body mass on HF diet relative to C diet was visible already after 3 weeks, but not until after 7 weeks on HF/n-3 diet. Statistically significant effects might have been masked by inter-individual variability. A study with C57BL/6J mice showed that even though these mice are inbred and should show little genetic variability, mice can be grouped into high and low gainers according to their response in body mass when put on a high fat diet with 8 weeks of age (Koza et al., 2006). Adipose tissue gene expression analysis correlated with the level of obesity observed, and it was concluded that epigenetic mechanisms might be responsible for this observation.

In fact, it is not possible to account for the keeping conditions of the mice used in this thesis before the feeding trial because they were bred commercially (Charles River Laboratories). Ideally, mice should have been bred under equal conditions in the same facility to minimize a trans-generational epigenetic effect on inter-individual variability in susceptibility to diet-induced obesity.

5.2.2 Fat mass and adipocyte size

Fat mass development reflected body mass changes and showed a significant reduction of fat mass in HF/n-3 animals compared with HF mice after 10 and 12 weeks of feeding. Fat mass development was strongly correlating with body mass (i.e. body size) as observed by the slopes of the linear function.

This analysis also revealed that lean mass did not contribute to the changes observed after 12 weeks of feeding. Ignoring body size effects and simply calculating lean mass to body mass ratios showed that lean mass was even decreasing in all groups (data not shown). This might be an effect of increasing age that is enhanced by the lack of physical activity in obese mice compromising even more muscle mass.

Taken together, these data suggest that fat mass is the major contributor to body mass changes. The results also imply that subcutaneous adipose tissue responds faster to dietary excess of fat and with greater storage capacity. This was visible when comparing masses

after 6 and 12 weeks. IAT increases more in mass upon both high fat diets compared with visceral adipose tissue. Earlier findings imply that this is due to increased hypertrophy of subcutaneous fat and decreased metabolic activity compared with visceral fat (Arner, 1995; Nielsen et al., 2004).

The comparison of MAT and EAT masses showed higher responsiveness of EAT to the anti-obesity effect of HF/n-3 diet, but this was not reflected on a cellular level as measured by adipocyte cross-sectional area. This contradiction is likely due to incomplete removal of mesenteric adipose tissue. The removal of MAT introduces inaccuracies by preventing pancreatic contamination (Caesar and Drevon, 2008).

MAT adipocyte cross-sectional area showed similar to IAT a much more pronounced decrease in cell area on HF/n-3 compared with HF than in EAT. The distribution of HF/n-3 cells in MAT was similar to cell areas observed under control diet in the same depot whereas in EAT cells from HF/n-3 and HF animals were similar in size distribution. This can be justified by the abdominal location of MAT drained by the portal vein (Matsuzawa et al., 1995). For example, in rats blood flow is elevated in mesenteric adipose tissue (West et al., 1989). Therefore, the greater response to n-3 LC-PUFA in MAT is likely due to higher metabolic activity and nutrient turnover in mesenteric fat compared with epididymal fat.

The data of this study show depot-specific differences in adipocyte size which is compatible with a study in lean C57BL/6J mice (Sackmann-Sala et al., 2012) showing that adipocytes have the biggest sizes in epididymal fat (4000–5000 μm^2) > mesenteric fat (2000–3000 μm^2) > subcutaneous adipose tissue (1000–2000 μm^2). This order reflects observations in this study, but absolute sizes differ considerably which might be caused by the fact that mice used by Sackman-Sala and colleagues were substantially older (12 months). Moreover, human data showing that subcutaneous adipocytes are larger in volume than visceral adipocytes could not be confirmed (Spalding et al., 2008).

5.2.3 Adipose tissue gene expression

On gene expression level, the above findings in mass were substantiated by a significant correlation of leptin gene expression with the respective fat depot mass in MAT and EAT, which is supported by literature showing an interdependence of leptin mRNA and plasma levels with adipocyte size and body mass index (Guo et al., 2004).

Gene expression measurements of metabolic enzymes regulating lipogenesis and lipid oxidation did not reflect the expectation of an improved lipid metabolism induced by n-3 LC-PUFA on high fat diet. Flachs et al. (Flachs et al., 2005) used a similar diet compared with Ruzickova et al. (Ruzickova et al., 2004). They observed an increased gene expression of β-oxidation markers (e.g. Cpt1α) and markers for mitochondrial biogenesis (Nrf1) with n-3

LC-PUFA in contrast to HF diet and postulated that the anti-obesity effect observed with n-3 LC-PUFA is due to increased fat oxidation in mitochondria.

In this thesis, EAT and IAT but not MAT were investigated to allow for direct comparability of gene expression with studies of Flachs et al. However, there is no evidence for an increase of Nrf1 gene expression in EAT and IAT of mice. Furthermore, Cpt1α mRNA levels in EAT were not increased by n-3 LC-PUFA treatment in comparison with HF diet. Moreover, mRNA levels of lipogenic markers were not affected differentially compared with HF diet. Even though Acacα gene expression was downregulated by HF/n-3, which is in agreement with published findings (Ide, 2005), this has also been achieved by HF treatment independently of the adipose tissue depot. This indicates effects rather induced by the fat quantity than by the fat quality. Also, Dgat2 gene expression did not indicate a significant amelioration of lipogenic enzyme activity by HF/n-3 diet.

Because adipose tissue mass and cellularity were decreased, it is likely that other mechanisms might have been responsible instead of increased fat oxidation. In fact, fat oxidation is rather small and makes up only about 0.2 % of endogenous fatty acid utilization in contrast to fatty acid export and re-esterification (Wang et al., 2003). Thus, it might be possible that adipocyte β-oxidation plays only a minor part in the reduction of adipose tissue mass.

In addition, no regulation of lipoprotein lipase gene expression was detected that would have indicated decreased lipid storage in adipocytes (Appendix Table 7). It remains speculative whether metabolic regulation might have happened on protein rather than gene expression level, but compared to Flachs et al. this is unlikely (Flachs et al., 2005).

On the other hand, non-fasting plasma NEFA levels were decreased by n-3 LC-PUFA as shown before (Rustan et al., 1998). Even though it is assumed that long chain saturated NEFA species are more involved in pancreatic β-cell toxicity than short chain or long chain polyunsaturated species (Gehrmann et al., 2010), it was not possible to discriminate between individual NEFA species because the assay shows high activity against a broad spectrum of fatty acid between C6:0 to C20:4 (WAKO, 2012), thus at least excluding the involvement of n-3 LC-PUFA.

5.2.4 Energy expenditure and Ucp1 gene expression

The lack of increased fat catabolism under HF/n-3 diet raises the question on the actual cause of the anti-obesity effect observed in adipose tissue. Food intake data did not reveal a difference between groups. Moreover, HF/n-3 animals assimilated more energy because the energy intake was increased in HF/n-3-fed mice compared with HF animals whereas

energy excretion was decreased in the same animals. This led to the highest energy efficiency in HF/n-3-fed animals.

To address this paradox, energy expenditure by locomotor activity and energy consumption were measured in a small group of animals, but data only revealed tendencies of an increased respiratory quotient and locomotor activity in HF/n-3 mice. The lack of statistical significance is probably due to a small group size. Normally, 8–12 animals are used for these measurements (personal communication with N. Rink, Molecular Nutritional Medicine, TUM). Additionally, the time-window might have been too short to display changes and introduced significant variability because as observed with the indirect calorimetry measurements, animals were probably stressed by the new small cage environment and needed at least 48 hours of adaptation which is in accordance with recommendations for C57BL/6J mice (Tschop et al., 2012) before a stable pattern was reached and food intake was stable (data not shown). Animals were measured when already fed for 8 weeks on the diets, this might have also dampened effects. Additionally, previous studies indicated that the respiratory quotient is decreased by HF feeding (Satoh et al., 2006), but this effect is likely to be lost by the lack of a control group as a reference, which could not be included in the measurement.

Literature is indicating that n-3 LC-PUFA increase energy consumption displayed by respiratory quotient (RQ). A study in rats showed elevated levels of RQ after 3-5 weeks of dietary intervention with n-3 LC-PUFA (Rustan et al., 1993). A study by Satoh et al. in 2010 showed that high fat / high sucrose (HF / HS) diet supplemented with 5 % EPA increased RQ compared with only HF / HS after 6 weeks of feeding (Sato et al., 2010). However, the time frame for measurement was very short.

Locomotor activity in mice fed the HF diet was significantly reduced relative to controls, but there was no improvement by HF/n-3. Reduced locomotor activity by Western diet has been reported (Bjursell et al., 2008), but this study did not find significant effects after HF/n-3 feeding. Since mice are nocturnally active animals, activity levels of mice in this thesis were high during the dark phase with evidence for differences between high fat groups. Probably not the time point (measured after 12 weeks of feeding) has affected the result, but rather the small number of animals studied reflected by the large variations during times indicating differences between high fat groups.

Even though from these data significant effects were not observed, one can assume that HF/n-3 fed mice increase energy expenditure by elevated energy consumption and activity. Unfortunately, it was not possible to measure body temperature in mice, since this could have indicated energy dissipation in the form of heat. However, there is evidence on gene expression level that Ucp1 might lead to extended energy expenditure at least in brown

adipose tissue. mRNA levels were upregulated 1.5-fold by n-3 LC-PUFA whereas HF diet alone did not lead to changes. These results are in line with a finding by Sadurskis et al. who showed that a diet enriched in n-3 LC-PUFA increased Ucp1 gene expression in mice by about 1.5-fold (Sadurskis et al., 1995). Thus, these data suggest a mechanism burning excessive energy stores by non-shivering thermogenesis, which could represent a pathway of increased energy expenditure by n-3 LC-PUFA. The upregulation of Ucp1 mRNA has been shown in many HF studies (Fromme and Klingenspor, 2010) even though a detailed mechanism remains elusive. In this context, a "browning" of white adipose was proposed in obesity, but this concept is counteracted by the majority of results demonstrating that Ucp1 mRNA is actually decreased in white fat during obesity (reviewed by Fromme and Klingenspor, 2010). This might be due to increased numbers of adipocytes in times of energy excess. It could be argued that the effects observed in this thesis might have been caused by mild cold stress the mice have been exposed to because they were kept at a temperature below thermoneutrality. However, differential effects observed between the dietary treatments speak against this argument.

5.2.5 Effects on liver lipid deposition and gene expression

In this thesis, HF/n-3 mice showed decreased ectopic lipid deposition in the liver compared with HF animals. Livers were significantly heavier in HF mice compared with control animals after 12 weeks and this might be due to increased hepatic lipid deposition as shown by hepatic TAG concentrations and Oil Red O-staining. In contrast, TAG levels and Oil Red O-staining were reduced in HF/n-3-fed mice. Hypotriglyceridemic efficacy of n-3 LC-PUFA has been described in animal studies (Kajikawa et al., 2009; Jelenik et al., 2010) and humans (McKenney and Sica, 2007). This is supported also by a literature search for "PUFA hepatic steatosis mouse high fat diet" (Appendix Table 12, page 131).

In contrast to adipose tissue, hepatic gene expression showed the expected downregulation of lipogenic gene expression (Scd-1, Acacα) upon HF/n-3 feeding as shown in other studies (Flachs et al., 2005; Ide, 2005). Also Fads1 and Fads2, markers of LC-PUFA lipogenesis (Sprecher, 1981), were drastically downregulated by the n-3 LC-PUFA intervention and show compliance of animals to the study which might be a feedback mechanism as indicated by early studies on these genes (Cho et al., 1999a; Cho et al., 1999b).

In contrast, Acox1, which is a target gene of PPARα-mediated activation and initiates peroxisomal β-oxidation of LC-PUFA (Fan et al., 1996), was significantly upregulated on HF/n-3. This is supported by a study showing the upregulation of peroxisomal β-oxidation

by n-3 LC-PUFA in rats (Rustan et al., 1992). However, there was no specific effect on Cpt1α, a marker of mitochondrial β-oxidation (Song et al., 2004), by HF/n-3 diet. This is in contrast to earlier findings showing an increased mitochondrial biogenesis and β-oxidation in white adipose tissue of n-3 LC-PUFA-fed mice (Flachs et al., 2005) but in agreement with the adipose tissue gene expression data of this study.

When Jelenik and co-workers from the Kopecky laboratory measured AMPKα1 or AMPKα2 activity in liver extracts of mice fed chow, HF or n-3 LC-PUFA-enriched diets, they observed significantly increased activity of AMPKα2 in livers of HF/n-3-fed mice (Jelenik et al., 2010). Furthermore, by using AMPKα2 knock-out mice, they demonstrated that HF/n-3 could similarly prevent body mass gain, hyperlipidemia and hepatic lipid deposition as in wild-type animals but these mice were not able to preserve insulin sensitivity. They proposed an AMPKα2-dependent mechanism of action of n-3 LC-PUFA to preserve insulin sensitivity by increasing hepatic lipid oxidation and decreasing lipogenesis in diet-induced obese mice.

Due to limited access to a specific AMPKα2 antibody, in this thesis the characterization of the AMPKα activation state in the liver was performed only indirectly with an antibody targeted against the phosphorylated AMPKα protein but was not found to be elevated in Western blot. Therefore, it is possible that n-3 LC-PUFA in this study did not affect AMPKα phosphorylation and might thus not be a target of n-3 LC-PUFA-mediated metabolic regulation or the detection system employing a total AMPKα antibody was not sensitive enough to show an effect. Additionally, data can only be interpreted with caution due to lack of a total AMPK control.

5.2.6 Glucose tolerance and insulin resistance

Because pAMPKα protein expression did not reveal any changes by HF/n-3, this did not allow any assumption on the improvement of insulin resistance in the liver. Actually, some studies in mice show an improvement of glucose tolerance and insulin sensitivity by n-3 LC-PUFA, but effects are not as consistent as with lipid parameters as a literature search showed (Appendix, Table 13, page 133). Indeed, while many animal studies indicate an improvement of insulin levels under an n-3 LC-PUFA regimen, a recent meta-analysis of 23 clinical trials in type-2 diabetic subjects showed that n-3 LC-PUFA neither had adverse effects on blood glucose levels nor led to any improvement (Hartweg et al., 2008).

Results from this study support the view that HF diet delays glucose clearance compared with controls (Buettner et al., 2006). However, there was no significant improvement of this impairment by HF/n-3 diet, even though blood glucose levels peaked earlier, reached lower levels after 120 min and showed a trend of improvement in area-under-the-curve analysis in HF/n-3 animals. In contrast, insulin levels in plasma were significantly improved compared

with HF animals. HF/n-3 animals were more insulin sensitive compared with HF animals despite delayed glucose tolerance.

The observation that no significant changes in glucose tolerance were detectable in this thesis can be due to high variability between animals similarly as observed with body mass and high and low responders (Burcelin et al., 2002; Koza et al., 2006). Another aspect that is frequently discussed is if the determination of the glucose dose to be injected based on body mass is appropriate in mice. In this way glucose-responsive tissues, first and foremost muscle, in obese mice are confronted with much higher doses of glucose compared with lean mice indicating that a dose calculation based on lean mass might be more suitable (Ayala et al., 2010). In contrast, human studies apply the same amount of glucose regardless of body mass or other parameters. Even though this study followed current guidelines of optimal glucose tolerance testing (Andrikopoulos et al., 2008), a significant difference was not reached. However, as the literature mentioned above indicates (Appendix, Table 13, page 133) it might as well be that in this study there was no effect (Fedor and Kelley, 2009). Additional data that indirectly support these findings are an increased pancreas mass observed in HF and HF/n-3 animals compared with control mice which is characteristic of increased α-cell and β-cell proliferation to compensate elevated glucose levels under high fat diet (Bonner-Weir, 2000; Ellingsgaard et al., 2008). Furthermore, adiponectin mRNA levels in adipose tissue were only slightly decreased in EAT without any changes in MAT. This decrease of adiponectin in EAT under HF diet indirectly indicates reduced insulin sensitivity, which might be improved by HF/n-3 (Flachs et al., 2006), but does not reach statistical significance.

At last, the experimental setup of blood withdrawal after 5 h fasting with the subsequent ipGTT after 6 h in the same mouse can have influenced the dynamics of glucose clearance in blood. In all groups and at all time points, basal glucose levels were elevated after 6 h compared to the 5 h time point. In a proposed scenario, blood withdrawal, which included removal from the home cage, fixation of the animal in a restrainer and warming of the tail vein with red light induced stress in the animal. Restraint-induced stress has been associated with hyperglycemia in mice via an elevation of glucocorticoid levels (Kainuma et al., 2009). Elevated blood glucose levels in turn might have affected the outcome of the glucose tolerance test and masked differential effects of the glucose challenge between dietary groups.

An aspect not investigated in this thesis but probably contributing to the observed anti-obesity effect is the involvement of muscle in n-3 LC-PUFA-mediated increase of energy expenditure and fatty acid oxidation. However, a study in rats investigating the effects of an

EPA-ethyl-ester on β-oxidation enzyme mRNA expression could not find significant changes after treatment in muscle, adipose tissue and liver (Perez-Echarri et al., 2009). It is not known if HF/n-3 in this thesis has induced any metabolic changes in muscle.

5.2.7 Summary

In summary, the results indicate that n-3 LC-PUFA induced a moderate anti-obesity effect in obese mice with a significant decrease in body mass upon HF diet due to decreased fat mass development and adipocyte sizes in visceral and subcutaneous adipose tissue. Because adipose tissue gene expression was not differentially regulated, it is unlikely that n-3 LC-PUFA exert relevant metabolic effects here even though plasma NEFA were significantly decreased. However, the significantly improved hepatic TAG levels, improved gene expression of hepatic lipid oxidation in peroxisomes, but not in mitochondria, and decreased hepatic lipogenesis point to the liver as the organ actively involved in the anti-obesity actions of n-3 LC-PUFA. Surprisingly, in spite of reduced obesity, HF/n-3-fed mice showed the same elevated energy intake as HF animals, decreased energy excretion via feces compared with HF animals and thus a higher assimilation efficiency. Thus, excess energy in HF/n-3-fed animals must have been expended elsewhere. While energy consumption and locomotor activity were not significantly increased, energy might have been consumed by non-shivering thermogenesis via increased Ucp1 gene expression in brown adipose tissue, which is not functionally proved. Furthermore, n-3 LC-PUFA improved insulin sensitivity but a significant effect on glucose tolerance was not discerned but could have been masked, for example, due to experimental conditions.

5.3 Effects on inflammation

A multitude of studies in humans and rodents is indicating that n-3 LC-PUFA have immunosuppressive functions and beneficially influence inflammatory diseases including cardiovascular disease (Tziomalos et al., 2007; Siddiqui et al., 2009) and rheumatoid arthritis (Calder, 2006) but with inconsistent results, for example, when investigating *ex vivo* immune function (reviewed by Fritsche, 2006).

The results of this study present evidence that at least in adipose tissue HF/n-3 can also provoke pro-inflammatory effects. This finding was initially established by the explorative analysis with the RT-qPCR array detecting increased expression of genes involved in T and B cell activation, proliferation and differentiation by HF/n-3 diet in mesenteric fat. Half of these genes were solely related to activation, proliferation and differentiation of T cells. This group of genes is even likely to be underestimated because many genes are involved in both T and B cell activation as shown by an additional group, which constituted 12 % of genes. Due to this redundancy and the complex interactions of surface molecule expression and cytokine release by different subpopulations of lymphocytes, gene expression analysis cannot clearly differentiate between markers of activation, differentiation and proliferation and cell-type specific interactions.

5.3.1 Inflammatory molecule expression in adipose tissue (Osteopontin)

Since the limitation of this array was also that only pools of RNA were applied without any biological and technical replication, the unexpected finding was confirmed with a larger set of biological replicates by RT-qPCR for osteopontin gene expression. Osteopontin gene expression showed the largest fold change on HF/n-3 diet, which fits with the notion that it is one of the most abundantly synthesized molecules by activated T lymphocytes (Weber and Cantor, 1996).

Osteopontin was originally discovered in the context of cancer (Senger et al., 1979) and bone homeostasis (Franzen and Heinegard, 1985). Its role in wound healing (Liaw et al., 1998) also implicates a function in immunobiology. In the context of high fat diet-induced obesity, osteopontin has been shown as critical for macrophage infiltration into epididymal adipose tissue and development of insulin resistance (Nomiyama et al., 2007). A study with high fat diet-induced obese and genetically obese mice showed a 40-fold and 80-fold increase of osteopontin mRNA expression in epididymal adipose tissue, respectively (Kiefer et al., 2008) which is much higher than observed in this study (up to 8-fold in EAT). However, Kiefer and co-workers also showed that osteopontin expression is highest in adipose tissue macrophages, and only 10 % of that level can be attributed to adipocytes

directly (Kiefer et al., 2008). Thus, it can be assumed that T cells and macrophages contribute most to the observed increase in gene expression.

OPN gene expression was confirmed in MAT and EAT and also with an additional set of primers. Similar to adipocyte size, a differential regulation of gene expression was detected between fat depots. OPN mRNA levels in EAT of HF/n-3 animals were higher than in MAT compared with controls. In contrast to HF/n-3 mice, osteopontin gene expression was only mildly elevated under HF diet.

On protein level, OPN appeared to be equally expressed in mesenteric adipose tissue under HF/n-3 and HF diet. However, the data of this thesis point to a differential regulation of intracellular and secreted OPN as shown by Western blot experiments revealing a more intensive iOPN band. A recent publication showed that also isoforms of osteopontin in epididymal adipose tissue of mice might be changed in response to high fat diet, but in this analysis it was not differentiated between iOPN and sOPN (Chapman et al., 2010). The difference in apparent molecular mass of about 15 kDa shown in this publication (40 kDa vs. 55 kDa) points into that direction, but this is debatable, since the original publication shows only a 5 kDa difference between isoforms (Shinohara et al., 2008) and might be explained by the use of antibodies with divergent epitopes. In macrophages, iOPN mRNA is significantly upregulated upon stimulation with toll-like receptor agonists (e.g., LPS) and negatively influences IFNβ expression in murine macrophages (Zhao et al., 2010). For macrophages, it is suggested that iOPN is only expressed upon LPS-mediated TLR stimulation via the AP-1 transcription factor while sOPN is expressed consitutively in these cells. Transferred to data obtained in this thesis, this would mean an increased activation of macrophages in mesenteric adipose tissue.

In a study published in 2010 by Wang et al., it is shown that translocation of antigen from the intestine into mesenteric adipose tissue under high fat diet leads to increasing OPN and IFNγ levels, both T_h1 cytokines. They also observed that OPN expression was not really increased in subcutaneous adipose tissue after high fat feeding, but the visceral fat was more inflamed and regulatory T cell-mediated mechanisms were upregulated to suppress the inflammation (Wang et al., 2010). Even though it has been described that numbers of Foxp3-positive regulatory T cells are associated with obesity-induced changes in visceral adipose tissue inflammation (Deiuliis et al., 2011) and that induction of these can ameliorate this process (Ilan et al., 2010), gene expression analysis did not show any differences due to dietary treatment in this thesis. This might have been due also to generally low mRNA levels (C_q=28–33). However, in the context of the cited literature the OPN gene expression data also suggest a stimulation of T_h1 type immunity in this study.

In agreement with data collected in this study, neither plasma nor liver expression data from literature convincingly show an elevation of OPN during diet-induced obesity (Kiefer et al., 2008). The protein is upregulated in patients with severe steatosis and insulin resistance with higher OPN mRNA expression in hepatocytes (Bertola et al., 2009). While some studies show an increase of OPN plasma levels up to three times of the control level (Gomez-Ambrosi et al., 2007; Nomiyama et al., 2007), others do not find systemic alterations of OPN (Kiefer et al., 2008).

Additionally, absolute levels of plasma OPN vary drastically. While Nomiyama et al. (Nomiyama et al., 2007) observe only OPN levels of 5–15 pg / ml in C57BL/6 mice, up to 250 ng / ml were detected in this study. This is more similar to the studies of van Eijk et al. observing 100–300 ng / ml with the same assay (van Eijk et al., 2009). In another study applying the same ELISA, researchers have observed even 10-fold higher levels (Kiefer et al., 2011). However, these animals had been fed for 6 months. It seems that not only the assay system but also other parameters such as feeding time play a role.

Additionally, elevated plasma levels might be misleading. For example, OPN has been shown to be elevated in morbidly obese patients after bariatric surgery. This is in contrast to other pro-inflammatory cytokines but might relate to elevated bone metabolism in times of caloric restriction (Fleischer et al., 2008; Riedl et al., 2008; West, 2009).

Furthermore, although mostly implicated in a pathological context, e.g. in atherosclerosis (Liaw et al., 1994) and autoimmunity (Lampe et al., 1991), OPN has been considered in protective mechanisms. In 2009 Heilmann and coworkers showed a dual role for OPN in experimental colitis. They observed that OPN activates innate immunity, limits tissue damage and initiates tissue repair during acute colitis, but increases a T_h1-cell dependent immune response and inflammation in chronic colitis (Heilmann et al., 2009). Thus, the data in the study presented indicate osteopontin upregulation might be of local, tissue-dependent but not so much of systemic importance and probably an adipose tissue-specific event.

5.3.2 Inflammation and macrophages

The results on OPN expression were substantiated by measuring gene expression of classical and markers of adipose tissue inflammation, namely pro-inflammatory Tnf-α, Mcp-1 and anti-inflammatory Il10. However, this analysis revealed marked changes between both MAT and EAT. In EAT there was significant upregulation of Il10 mRNA but at the same time also increased gene expression of Tnf-α and Mcp-1. While an mRNA upregulation of these markers was obvious and statistically significant under HF/n-3 and in part under HF compared with C in EAT, only Mcp-1 mRNA was significantly upregulated

also in MAT. This reflects earlier findings showing an increased OPN gene expression in EAT compared with MAT.
On the one hand, this confirms the observation of increased inflammatory gene activation under HF/n-3, but it also shows that at the same time anti-inflammatory mechanisms were switched on (Il10). Increased Mcp-1 gene expression additionally supports the specific recruitment of macrophages to adipose tissue as shown by others (Chen et al., 2005).

The experiments were also extended to macrophage surface marker gene expression. Again the amplitude of regulation compared with control-fed animals was larger in EAT than in MAT. Itgax / CD11c as a marker for M1 macrophages is, however, also expressed in T cells and dendritic cells (Huleatt and Lefrancois, 1995; Wu et al., 2010) and was highly upregulated on mRNA level upon HF/n-3 diet, which reflects the previous findings.
On the contrary, Mrc1 / CD206 is a marker for anti-inflammatory M2 macrophages (Odegaard and Chawla, 2008; Gordon and Martinez, 2010). A study in humans, however, showed that resident M2 ATM are also capable of producing inflammatory cytokines contributing to the obesity-induced complications (Zeyda et al., 2007). Mrc1 gene expression was upregulated under HF/n-3, which supports the notion that n-3 LC-PUFA might exert anti-inflammatory actions as with Il10 gene expression. At least in mice, alternatively activated M2 macrophages are probably resident in adipose tissue whereas M1 macrophages are recruited during diet-induced obesity (Lumeng et al., 2008). This might explain the larger amplitude of regulation of Itgax compared with Mrc1 in the high fat groups relative with controls.
The overlapping expression of Itgax in different cell types shows the limitations of these results regarding assumptions about cell-specific effects. Fujisaka et al. have used CD11c and CD206 to discriminate M1 and M2 macrophages in fluorescence-assisted cell sorting (FACS) analysis (Fujisaka et al., 2009) and have additionally used the specific, but total macrophage marker F4/80 (Austyn and Gordon, 1981). They used Tnf-α and Mcp-1 gene expression as further markers of M1 macrophage activation and Il10, Cd163, Cd209a gene expression for M2 macrophages. The study of Fujisaka et al. (Fujisaka et al., 2009) showed that IL-10 expression increases similarly to findings in this thesis and might be a regulatory mechanism recruiting potentially protective M2 macrophages.
Applying other markers, a publication by Oh and co-workers (Oh et al., 2010) with C57BL/6 and GPR120 knock-out animals showed that n-3 LC-PUFA supplementation led to a decrease of CD11b-positive and CD11c-positive adipose tissue macrophages with a concurrent increase of M2-associated staining of MGL1 / CD301-positive cells and

respective changes in gene expression of pro-inflammatory M1 and anti-inflammatory M2 genes.

Crown-like structures (CLS) as clusters of ATM surrounding dead adipocytes were counted in visceral adipose tissue because it is postulated that they might function in adipose tissue remodeling (Strissel et al., 2007) or macrophage phenotype switching (Lumeng et al., 2007). The low number of CLS observed indicates that immune cell infiltration might actually be rather low implying also a low level of inflammation in adipose tissue. Strissel et al. showed that HF feeding (60 en% fat) in C57BL/6 induced adipocyte death. They counted up to 20 % of dead adipocytes after 12 weeks of feeding in epididymal fat (Strissel et al., 2007). This is about 200-fold more than quantified in this thesis (10 / 10 000 cells). In a recent report Altintas and co-workers fed C57BL/6 mice a 60 en% HF diet and compared CLS numbers in various adipose tissue depots (Altintas et al., 2011). They found a significant increase of CLS by HF diet compared with controls, which was most pronounced in EAT (138-fold) and less in MAT (49-fold). This is in agreement with the findings of this study and supports the view of decreased inflammation in mesenteric fat compared with other visceral fat depots.

5.3.3 Mesenteric versus epididymal adipose tissue

The depot-specific differences between MAT and EAT have become clear during this study. Relative to control animals gene expression was not as highly regulated or not regulated at all under HF and HF/n-3 compared with EAT. Unlike many other adipose tissue depots, MAT is an adipose tissue with a more heterogenous mixture of cells than other depots (Pond, 2005). This has to be taken into account when interpreting results. MAT is located at the interface between intestinal nutrient uptake and portal circulation. It has twice the protein content compared with other adipose tissue depots (Sackmann-Sala et al., 2012). This might be due to the presence of mesenteric lymph nodes (MLN) that are absent in the epididymal compartment in mice (Pond, 2005). A higher trafficking of immune cells might discriminate MAT from EAT in structure and behavior. Although not proven, the presence of MLN might dampen inflammatory effects as observed in differences in size of adipocytes, OPN, Il10 and Tnf-α gene expression, and CLS frequency compared with EAT.

Caroline Pond's research indicates that adipose tissue surrounding lymph nodes (perinodal adipose tissue) has a special role. The perinodal adipocytes are always smaller than adipocytes remote from the lymph node (Pond, 1998). Perinodal adipocytes increase in number under chronic inflammation (Mattacks et al., 2003), which is probably mediated by elevated surface expression of cytokine receptors (MacQueen and Pond, 1998) preceding elevated lipolysis (Pond and Mattacks, 2002). A study of the same group proposes that this is probably mediated by dendritic cells resident in adipose tissue, and their number and

activity are dependent on the supply of dietary fatty acids (Mattacks et al., 2004a). Furthermore, they demonstrated that dietary sunflower oil (high in n-6 : n-3 LC-PUFA ratio) increased the number of dendritic cells in perinodal adipose tissue by 17 % whereas fish oil decreased this number by 5 % after chronic stimulation with lipopolysaccharide. This relationship was absent in remote adipose tissue. Perinodal adipose tissue *per se* contains increased levels of n-6 and n-3 LC-PUFA that decrease with distance from the lymph node (Mattacks and Pond, 1997). Moreover, the ratio of n-6 : n-3 LC-PUFA is actively adjusted and converged after immune stimulation leading to increased lipid mediator production (Mattacks et al., 2004b) and suggesting that lymphocytes are supplied by perinodal adipocytes with essential fatty acids (Pond and Mattacks, 2003) that stimulate (n-6 LC-PUFA) or attenuate (n-3 LC-PUFA) their activation and lipolysis in adipose tissue (Mattacks et al., 2002).

Taken together, these studies postulate that immune cells and adipocytes mutually control each other with the one controlling lipolysis and the other regulating activation by the supply of dietary lipids. Interestingly, perinodal adipose tissue as identified by site-specific fatty acid analysis is absent in patients of Crohn's Disease and may be defective and thus a prerequisite for abnormal immune responses observed in the disease (Westcott et al., 2005). This study also observed an increase of saturated fatty acids in lymphoid and adipose tissue, especially palmitic acid, which can also promote toll-like receptor-induced activation of dendritic cells (Lee et al., 2001).

Extrapolating these data to the results of this thesis, it is likely that MAT by the presence of MLN and perinodal adipose tissue *per se* contains elevated levels of n-3 LC-PUFA that negatively regulate immune cell activation. Myeloid dendritic cells are of the same lineage as macrophages derived from monocytic precursors (Geissmann et al., 2010), so it might be possible that Pond's hypothesis also applies to macrophage adipose tissue infiltration, but it does not allow assumptions on T and B cell activation, which was investigated in this thesis.

5.3.4 Anti-inflammatory effects

Even though the adipose tissue data indicate a pro-inflammatory effect, this thesis provides also evidence that HF/n-3 diet exerted anti-inflammatory effects relative to HF animals.

To exclude a systemic pro-inflammatory effect, serum amyloid A (SAA) levels in plasma were determined and found to be increased on HF diet whereas HF/n-3 SAA concentrations were similar to control levels. Since the ELISA kit applied used a polyclonal antibody, which detects all isoforms of serum amyloid A (cf. 4.12.2 for isoforms) expressed (personal communication with the manufacturer, Immunology Consultants Laboratory), the exact origin of SAA cannot be specified – possibly liver and white adipose tissue.

Serum SAA levels mainly originating from liver during the acute phase response can increase thousand-fold (Olsson et al., 2011). The fold change observed in this thesis was rather small (1.44-fold to 1.67-fold). On the other hand, SAA levels in HF mice were about 5-fold higher compared with a study of diet-induced obesity in C57BL/6 mice with 16 week feeding of a 59 en% HF diet detecting about 30 µg / ml of acute-phase SAA (Scheja et al., 2008).

This indicates rather mild effects of the HF diet on the one hand, but might imply an increased basal level of SAA present already in the controls. It is possible that this is the constitutively expressed isoform (Uhlar and Whitehead, 1999). It is also likely that the SAA came from other sources. The study design has imposed a chronic stimulus and this might reflect the findings of previous reports that have shown that during the non-acute phase adipocytes might be the major producers of SAA (Poitou et al., 2005; Sjoholm et al., 2005).

The effects observed in gene expression of endothelial cell activation and angiogenesis support the view that n-3 LC-PUFA are involved in improvement of vascular complications (Deban et al., 2008). Additionally, the splenic downregulation of T cell surface marker mRNA levels on HF/n-3 further reinforces the notion that the pro-inflammatory effects observed were adipose tissue-specific.

5.3.5 Origin of pro-inflammatory effects in adipose tissue

For the surprising finding of the pro-inflammatory and immunomodulatory effects observed under HF/n-3 diet, several reasons are possible.

5.3.5.1 Vitamin E deficiency

It was highlighted in this study that the spleen was increased in mass independently of body mass. Numerous studies showed that high dose fish oil feeding increased spleen size (Burns et al., 1999; Hempenius et al., 2000; Merritt et al., 2003; Lina et al., 2006) but did not find evidence for pathological changes. Instead, since effects of LC-PUFA on spleen morphology were absent, these studies interpreted it as a physiological adaptation to highly unsaturated fatty acids.

Oarada et al. (Oarada et al., 2000) showed that number of splenic cells increased but only slightly affected splenic macrophage numbers in spleen after fish oil feeding. This indirectly supports the data on decreased T cell surface marker gene expression by HF/n-3 in this thesis. Furthermore, Oarada's study links the peroxidation state of erythrocytes associated with excessive fish oil intake with increased spleen size. The spleen is the site of erythrocyte turnover and immune homeostasis (Mebius and Kraal, 2005). It is postulated that the increased spleen mass observed is not a finding primarily attributed to the observed

adipose tissue inflammation, but might be a secondary effect related to vitamin E content. Vitamin E is an antioxidant by acting as a scavenger for hydroperoxyl radicals (Traber and Stevens, 2011) and protects erythrocyte membranes. A relative lack of vitamin E induced by excess n-3 LC-PUFA could lead to elevated oxidative stress in erythrocytes, leading to physiological adaptations in the spleen.

Vitamin E levels in the mouse could therefore be an explanation for the observed contradictory effects of n-3 LC-PUFA in adipose tissue. Some studies indicated that an increased intake of fish oil diminished plasma and tissue vitamin E levels more than other oils (Meydani et al., 1987; Rabbani et al., 1999). The German Federal Institute for Risk Assessment states that vitamin E levels in mg should be 0.4-fold the amount of LC-PUFA in g. However, another approach recommends to base vitamin E levels on the number of double bonds in the fatty acids (German Federal Institue for Risk Assessment / BfR, 2004). These recommendations are, however, limited to human application only. In this study 180 mg / kg tocopherol acetate were applied (and 2.8–4.5 mg / g mixed tocopherols in EPAX 1050 TG) which is almost half compared with Ruzickova et al. (300 mg / kg; Ruzickova et al., 2004). Thus, one could speculate that an increased demand of vitamin E in HF/n-3 mice was not met leading to higher lipid peroxidation and thus inflammatory signs in adipose tissue.

5.3.5.2 Saturated Fatty Acids

Instead of sunflower, rapeseed or corn oil fed by Ruzickova et al. (Ruzickova et al., 2004) palm oil was the major fat component in the high fat diets and soybean oil the basic fat component in all diets. Palm oil was chosen as the main fat component because it is a major ingredient in human diets (Sarmidi et al., 2009; Service USDoAFA, 2012) with proven adverse health effects (Vega-Lopez et al., 2006). Palm oil has also been used in previous animal studies of diet-induced obesity (de Vogel-van den Bosch et al., 2008b; de Wit et al., 2010).

With the exception of coconut fat, palm oil contains the highest fraction of saturated fatty acids according to the United States Department of Agriculture nutrient database (USDA, 2012). The effects of different fat types are caused by the fatty acid composition. It has long been recognized that fatty acids are involved in immune modulation (Meade and Mertin, 1978) or the development of insulin resistance (Kahn et al., 2006).

The use of soybean oil and palm oil introduced major changes in fatty acid composition in the diets compared with the diets used by Ruzickova et al. Analyses of relative amounts of fatty acids showed that high fat diets used in this thesis contained high levels of saturated fatty acids, especially palmitate, and monounsaturated fatty acids, mostly oleate. Saturated

fatty acids like palmitate exert pro-inflammatory actions by acting as ligands for toll-like receptors (Lee et al., 2001; Shi et al., 2006) or inducing inflammasome-mediated insulin resistance (Wen et al., 2011). Oleate, in contrast, showed no significant effect in these studies.

These relative data, however, do neither reflect absolute amounts provided (cf. differences in total fat content) nor the absolute amount taken in by the animal (cf. differences in food intake). In this thesis, absolute fatty acid intakes by mice used in this thesis were therefore compared with Ruzickova et al. and showed that mice in this thesis had a two-fold increased palmitate intake compared with the reference study. Similarly, oleate intake was much higher in Ruzickova's cHF diet. In the light of the detrimental effects of palmitate observed in the studies above, the high fat diets in this thesis might have a higher inflammatory potential. Regarding HF/n-3, the high palmitate intake can counteract the beneficial effects of EPA and DHA. Moreover, the much higher DHA intake in Ruzickova's mice in addition to lower palmitate levels can probably unfold more anti-inflammatory effects than in the diets used in this study.

5.3.5.3 n-3 LC-PUFA per se

The notion that n-3 LC-PUFA solely act anti-inflammatory might be a simplified view supported by publications that indicate also pro-inflammatory actions of n-3 LC-PUFA. In agreement with the lipolytic and anti-lipogenic actions of n-3 LC-PUFA, dietary supplementation with EPA and DHA increased TNF-α and IL-6 production in peritoneal macrophages (Tappia et al., 1995; Petursdottir et al., 2002) and other cell types through downregulation of PGE_2 (Tai and Ding, 2010). Similar to n-3 LC-PUFA these cytokines increase lipolysis and suppress preadipocyte differentiation (Petruschke and Hauner, 1993; Zhang et al., 2002). However, also contrary effects are observed underlining the anti-inflammatory effects of n-3 LC-PUFA via NF-κB- and PPARγ-dependent mechanisms (Baeuerle and Henkel, 1994; Li et al., 2005). The effect of n-3 LC-PUFA might be dependent on the activation states of cells (Wallace et al., 2000), on the cell type studied (Blok et al., 1996b), and on polymorphisms in the genes coding for the cytokines (Markovic et al., 2004). Thus, pro- and anti-inflammatory effects of n-3 LC-PUFA can appear at the same time (Tai and Ding, 2010), which is also in agreement with the observed increased Tnf-α, Mcp-1 and Il10 gene expression in this study.

An increased immune cell activation and, for example, Tnf-α gene expression, might be a protective event resulting in decreased lipogenesis and increased lipolysis observed in this study. However, even though adipose tissue gene expression analysis in this study does not support this view, it is possible that Tnf-α levels affect other organs, for example, the liver

where lipid metabolism gene expression was regulated. TNF-α was, however, not determined in plasma.

The ratio of n-6 : n-3 LC-PUFA was 0.84 : 1 in HF/n-3 compared with 13.50 : 1 in the HF diet. Thus, n-6 and n-3 LC-PUFA were nearly balanced which complies with the ratio during human evolution whereas the HF diet ratio reflects more of a moderate Western diet ratio (Simopoulos, 2011) and thus corresponds more with the nutritional reality than some studies applying extreme ratios of up to 201 : 1, for example (Huber et al., 2007). Even though levels of n-6 and n-3 LC-PUFA relative to each other may be of relevance when considering contrasting eicosanoid effects, some researchers argue that rather absolute amounts of n-6 and n-3 LC-PUFA may play a more important role, especially when given in high quantities like in HF diet studies (Deckelbaum, 2010; Harris, 2010). However, it can only be speculated about the importance of ratio versus absolute levels of LC-PUFA in this thesis because only one diet with elevated n-3 LC-PUFA EPA / DHA was tested.
In contrast to animal studies, human intervention studies usually employ absolute expressions of n-3 LC-PUFA or relative energy of n-3 LC-PUFA intake. Calculated on the basis of fat content and food intake, n-3 LC-PUFA intake was elevated about 3-fold in this thesis (10.3 en%) and clearly exceeds the AMDR in humans and doses applied in human studies, which usually do not exceed 2–3 en% (Fritsche, 2007). Even correcting for metabolic differences by allometric scaling still yielded a 2-fold over-estimation. Thus, n-3 LC-PUFA levels applied in animal studies are much higher than in human studies but also vary significantly among studies in the same model organism. This might also account for differences observed.

An aspect that might influence the amplitude and nature of inflammatory effects is the discrimination between EPA and DHA-specific effects that is neglected in most studies. Also in this study a mixture with a DHA to EPA ratio of 3.7 : 1 (cf. Ruzickova et al. 8.8 : 1) was applied. Therefore, it can only be speculated about specific n-3 LC-PUFA effects.
Differences between EPA and DHA function already derive from their structural properties affecting membrane composition and behavior due to differences length and number of double bonds in the acyl chain. In comparison, DHA leads to the highest membrane disorganization (Onuki et al., 2006) and most pronounced effects on permeability (Ehringer et al., 1990).
Interpretation of studies investigating effects of EPA and DHA can only be done with caution. First, some studies use pre-treatment with LPS stimulation. In this case DHA may be more effective than EPA (Weldon et al., 2007). Second, in contrast to DHA, EPA and ARA

both use the same enzymes, cyclooxygenases and lipoxygenases, for the generation of eicosanoids. This might imply a greater effect of EPA on cytokine reduction than with DHA. Furthermore, EPA-derived eicosanoids may not necessarily be anti-inflammatory but also pro-inflammatory, just less bioactive compared with ARA-derived eicosanoids (Weber et al., 1986).

EPA can be synthesized from dietary essential alpha-linolenic acid and itself is a precursor for docosahexaenoic acid, but conversion is only about 2–5 % from ALA and about 8–10 % from DHA via retroconversion (Singer, 2008). DHA is the most abundant n-3 LC-PUFA in some tissues, e.g. reaching up 40 % in cell membranes of the brain (Kurlak and Stephenson, 1999). This might also explain differential effects observed between EPA and DHA in *in vitro* studies with B cells (Verlengia et al., 2004a) and T cells (Verlengia et al., 2004b).

The dose is affecting study outcome. This was shown in a study by Gorjão and co-workers in 2006 (Gorjao et al., 2006) where young males (25–45 y) supplemented with 3 g of a DHA-rich fish oil (1.62 g DHA per day, 0.78 g EPA per day) showed an increased phagocytic response in neutrophils and monocytes, augmented neutrophil chemotactic response and production of reactive oxygen species, and enhanced lymphocyte proliferation by 40 % by [2-^{14}C] thymidine incorporation.

Contrasting results where achieved in a study by Kew et al. (Kew et al., 2004). Here males (23–65 y) received 4.91 g DHA per day and showed a suppression of T lymphocyte activation as measured by CD69 expression. Administration of high-dose EPA did not have an effect.

A recent review by Gorjão et al. also indicated that DHA is highly toxic because it produces DNA fragmentation in insulin secreting RIN-m5F cells already at 0.1 mM whereas EPA showed a much lower toxicity (Gorjao et al., 2009). All these data show the ambiguity of effects exerted by specific n-3 LC-PUFA in different study settings.

As an example specifically addressing the above mentioned variations and adipose tissue inflammation, Todoric et al. in 2006 showed a reduction of adipose tissue inflammatory gene expression and macrophage infiltration in mice upon a high fat diet enriched with a n-3 LC-PUFA concentrate (Todoric et al., 2006). However, the fish oil contained slightly elevated levels of EPA (EPAX 6000 TG; EPA : DHA of 1.5 : 1). Furthermore, genetically obese db / db mice were fed either a high fat diet rich in saturated fat (HF/S, 30 en% fat from lard), in n-6 LC-PUFA (HF/6, 30 en% from safflower oil), or enriched with n-3 LC-PUFA (HF/3, 30 en% from safflower oil [60 % (w / w)] and from EPAX 6000 TG [40 % (w / w)]) for only 6 weeks. Since they did not observe an alteration of macrophage marker gene expression in spleen

and lung, they argued for adipose tissue-specific effects on inflammatory modulation in this mouse model. Notably, body mass in the HF/3 group was significantly increased compared to the other groups (+11.3–18.3 g).

Here, the use of another EPA : DHA ratio, fat source in the reference diets, the mouse model and the feeding period are important differences to parameters used in this thesis and exemplify sensitive interrelationships of study parameters.

5.3.6 Summary

In summary, the results addressing the inflammatory status of the animals showed that HF/n-3 leads to an expected downregulation of high fat diet-induced systemic levels of serum amyloid A and gene expression of endothelial cell activation in small intestine. Surprisingly, there was an adipose tissue-specific increase of inflammatory gene expression in mesenteric as well as in epididymal adipose tissue.

While pro-inflammatory effects of n-3 LC-PUFA have been observed in other studies, they have not been shown in a study setting like in this thesis before. As stated above, absolute intakes of fatty acids (palmitate vs. DHA) may have caused this unexpected effect. This might be specific to adipose tissue because of the enrichment of dietary fats in triacylglycerols and membranes. Furthermore, effects in MAT might have been dampened through the different cellular composition in comparison with EAT. Adipose tissue surrounding mesenteric lymph nodes has been shown to be involved in the modulation of immune responses that might have led to decreased effects in MAT compared with EAT. At last, the vitamin E status of the animal might be involved in the observed effects. An increased spleen size points to increased erythrocyte turnover, which might be due to increased lipid peroxidation. This is possible because the high demand of anti-oxidative vitamin E by high fish oil diets leads to decreased overall vitamin E levels. However, the vitamin E status in mice was not examined. This scarcity of vitamin E might be just one explanation of the surprising finding obtained in this study.

5.4 Metabolite analysis

Overall effects on metabolites by n-3 LC-PUFA-enriched high fat diet were striking. In contrast to the findings regarding adipose-specific inflammation under HF/n-3, the analysis using the Biocrates platform showed that metabolites were differentially regulated by n-3 LC-PUFA compared with the other diets and overall regardless of the tissue investigated. Changes were affecting all the metabolites investigated, but mostly phospholipids.

This opens the possibility of using also other tissues than blood / erythrocytes to retrieve biomarkers for the assessment of DHA and EPA status (Kuratko and Salem, 2009) and could possibly give indirect insight into the modulation of metabolic processes like fat oxidation (Kus et al., 2011) or inflammatory processes (Lankinen et al., 2009) observed in plasma so far. In this study, it is also proved that animals and food intake were compliant and that the observed changes might, in fact, directly be due to n-3 LC-PUFA intake. More clearly, LC-PUFA-induced changes were apparent in liver. The low ratio of n-6 : n-3 LC-PUFA was reflected in the decreased levels of hepatic n-6 LC-PUFA-derived metabolites whereas the n-3 LC-PUFA-derived molecules were elevated. Furthermore, molecules derived from n-3 LC-PUFA and directly or indirectly involved in the resolution of inflammation were strongly upregulated also indication an immuno-modulatory role of n-3 LC-PUFA here.

5.5 Conclusion and perspectives

This study confirms that n-3 LC-PUFA enriched in HF diet act moderately anti-obesogenic and exert anti-inflammatory effects. However, regarding adipose tissue inflammation this thesis presents novel evidence for enhanced immune cell activation under n-3 LC-PUFA on gene expression level. This is challenging the general view of n-3 LC-PUFA suppressing chronic inflammation and immune cell infiltration associated with obesity. Additionally, the findings highlight that, contrary to expectations, mesenteric adipose tissue does not show an increased inflammatory response compared with other visceral fat depots. It is thus tempting to speculate that it might even dampen the inflammatory effects observed and acts more immuno-modulatory.

The observations presented in this study are mostly based on gene expression data of cytokines and cell markers. This reflects just one layer of regulation. Even though osteopontin protein expression supports the OPN mRNA expression, other cytokines might be regulated differently on protein level, for example by differential phosphorylation and thus activation state. Thus, only assumptions can be made about their paracrine and endocrine effects in the tissue. On the other hand, gene expression data of cytokines like Tnf-α are commonly used to characterize the inflammatory state in tissues. However, whole tissue gene expression cannot provide detailed information about the cellular origin of the molecules expressed. For example, CD11c (Itgax) is a surface molecule expressed not only on macrophages, but also on dendritic cells and T lymphocytes (Huleatt and Lefrancois, 1995; Wu et al., 2010). This allows to make general assumptions about the immune cell infiltration into adipose tissue, but does not specify the cellular composition of the tissue investigated. To specifically address one population of immune cells, it would therefore be more suitable to employ fluorescence assisted cell sorting (FACS analysis) or to use histological sections for a localization of cell types or cytokines expression. For example, for the characterization of the infiltration of macrophages double stainings with F4/80 for macrophages and CD11c or CD206 targeting M1 and M2 subtypes, respectively, could be performed instead as shown by Fujisaka et al. (Fujisaka et al., 2009). Especially, mesenteric adipose tissue is very heterogenous in cell composition, since it is rich in lymph nodes. It is likely that adipocyte-specific effects are “diluted” by other cell types or that adipose tissue-specific immune cell infiltration is masked by systemic immune cell trafficking through mesenteric lymph nodes. The data in this study can just represent the median of gene expression by all the cells in one tissue.

Therefore, these data are only a hint and warrant further research in the specific effects of n-3 LC-PUFA on high fat diet. Several areas can be further explored. On the one hand, it should be investigated what the molecular reasons for the adipose tissue-specific effects

are. Is it solely caused by the fat content and composition, do vitamin E levels play a more important role? If it is fat content, it could be interesting to compare this finding with a low fat diet enriched with n-3 LC-PUFA. Furthermore, peroxide levels measured in tissues and plasma might contribute to answering this question.

Regarding mesenteric adipose tissue, it would be interesting to segregate lymph node-specific from adipocyte-specific effects. Is lymph node atrophy observed by HF feeding (Kim et al., 2008) differentially affected by n-3 LC-PUFA? Are there intra-depot specific differences between adipocytes, as pointed out by Pond's group, which affect the overall inflammatory state of the depot? Addressing this question is certainly limited given the scarce amount of mesenteric adipose tissue available in the mouse after the exclusion of pancreatic contamination and mesenteric lymph nodes. Also here, FACS analysis will probably be a solution to distinguish between cells, but will first require a thorough characterization of perinodal and non-nodal adipocyte surface molecule expression patterns.

Furthermore, the initial study design with the samples collected after 6 and 12 weeks open up the possibility for a study of the temporal dependence of n-3 LC-PUFA-induced effects. Even though osteopontin mRNA levels are already elevated after 6 weeks of feeding, other effects observed after 12 weeks might not have been fully established yet. A large set of organ samples also allows investigation of other tissues to get a more holistic picture of n-3 LC-PUFA effects in the body.

In the end, however, every outcome is most affected and limited by variations in the dietary composition. The comparison with other studies is always limited by variation in diets or lack about detailed information. Even though a standard high fat diet for studies of diet-induced obesity does not seem feasible because it depends too much on the objective of the experiment, it would at least be worthwhile to set guidelines for information about diets and experimental conditions applied in scientific publications.

6 Appendix

Table 7: RT-qPCR data in fold changes compared with control group. Shown are gene expression levels ± standard error relative to control group by RT-qPCR using 10 ng of RNA after 12 weeks feeding with C_q-range and PCR efficiency for each gene measured in the tissue measured. Data were analyzed by $\Delta\Delta C_q$-method and normalized to β-Actin, cyclophilin B, glyceraldehyde-phosphate dehydrogenase, heat shock protein 90 α (cytosolic), class B member 1, hypoxanthine guanine phosphoribosyl transferase gene expression. Asterisks indicate genes used for reference. Letters a and b indicate a significant difference ($p<0.05$) compared with control and high fat group, respectively. Statistical analysis was performed using One-Way ANOVA and Tukey post-test. X, Primer pair from Qiagen.

Tissue	Gene	Diet			p-value (ANOVA)	C_q _ C_q	PCR Efficiency	
		C	HF	HF/n-3		min max	per gene	mean (%)
adipocytes	Actb*					18-18	1.864	82.7 ± 3.1
	Gapdh*					19-20	1.851	
	Spp1 (OPN)	1.00 ± 0.42	25.04 ± 12.65a	35.03 ± 20.85a	0.0045	24-31	1.765	
iBAT	Cph*					26-27	1.82	83.3 ± 2.2
	Hsp90*					20-22	1.80	
	Ucp1	1.00 ± 0.10	1.12 ± 0.10	1.59 ± 0.15ab	<0.0001	17-19	1.88	
EAT	Acacα	1.00 ± 0.14	0.35 ± 0.05a	0.35 ± 0.06a	<0.0001	22-26	1.87	84.6 ± 0.9
	Actb*					18-19	1.88	
	Adipoq	1.00 ± 0.09	0.79 ± 0.08	0.95 ± 0.08	0.0525	18-23	1.83	
	Cpt1α	1.00 ± 0.08	1.30 ± 0.09a	1.17 ± 0.09	0.0016	24-25	1.85	
	Dgat2	1.00 ± 0.14	1.30 ± 0.14a	1.19 ± 0.13	0.0167	19-21	1.90	
	Foxp3	1.00 ± 0.12	1.15 ± 0.18	0.92 ± 0.09	0.4939	31-33	1.84	
	Gapdh*					19-20	1.86	
	Il10	1.00 ± 0.22	1.45 ± 0.34	1.71 ± 0.34a	0.0435	31-34	1.83	
	Itgax (CD11c)	1.00 ± 0.29	2.85 ± 0.86a	6.62 ± 1.53ab	<0.0001	25-29	1.85	
	Lep	1.00 ± 0.17	2.78 ± 0.41a	2.05 ± 0.27a	<0.0001	20-23	1.87	
	Lpl	1.00 ± 0.09	0.98 ± 0.09	0.93 ± 0.09	0.7163	18-20	1.90	
	Mcp-1	1.00 ± 0.10	3.08 ± 0.59a	2.61 ± 0.34a	0.0016	24-29	1.85	
	Mrc1 (CD206)	1.00 ± 0.06	0.97 ± 0.06	1.17 ± 0.08b	0.0179	23-29	1.81	
	Nrf1	1.00 ± 0.11	0.99 ± 0.10	0.79 ± 0.07	0.0638	27-29	1.90	
	Pparγ2	1.00 ± 0.10	0.88 ± 0.09	1.01 ± 0.11	0.3685	27-29	1.88	
	Spp1 (OPN)	1.00 ± 0.26	2.60 ± 0.79a	8.04 ± 1.72ab	<0.0001	25-31	1.72	
	Tnf-α	1.00 ± 0.14	1.43 ± 0.22	1.88 ± 0.29a	0.0007	29-32	1.84	
	Ucp1	1.00 ± 0.44	0.54 ± 0.18	0.54 ± 0.18	0.3584	30-35	1.83	
IAT	Acacα	1.00 ± 0.19	0.52 ± 0.08a	0.39 ± 0.07a	<0.0001	23-26	1.87	85.0 ± 1.5
	Actb*					18-19	1.87	
	Dgat2	1.00 ± 0.23	2.09 ± 0.36a	1.61 ± 0.32a	<0.0001	19-22	1.87	
	Gapdh*					19-20	1.86	
	Nrf1	1.00 ± 0.09	0.90 ± 0.09	0.79 ± 0.09	0.1285	27-29	1.87	
	Spp1 (OPN)	1.00 ± 0.29	0.65 ± 0.24	2.10 ± 0.56b	0.0026	25-31	1.76	
	Ucp1	1.00 ± 0.42	1.36 ± 0.55	0.86 ± 0.28	0.3767	31-35	1.84	
Liver	Acacα	1.00 ± 0.08	0.83 ± 0.08	0.51 ± 0.05ab	<0.0001	24-27	1.83	84.5 ± 0.9
	Acox1	1.00 ± 0.06	1.29 ± 0.08a	1.78 ± 0.09ab	<0.0001	19-21	1.85	
	Actb*					19-19	1.87	
	Cpt1α	1.00 ± 0.15	1.26 ± 0.15a	1.01 ± 0.11	0.0412	21-23	1.87	
	Dgat2	1.00 ± 0.03	0.98 ± 0.06	1.04 ± 0.04	0.5013	21-22	1.87	
	Fads1	1.00 ± 0.11	1.13 ± 0.11	0.24 ± 0.03ab	<0.0001	23-27	1.88	
	Fads2	1.00 ± 0.16	0.98 ± 0.13	0.23 ± 0.04ab	<0.0001	20-25	1.83	
	Hprt1*					25-26	1.84	

Tissue	Gene	Diet			p-value (ANOVA)	C_q - C_q min max	PCR Efficiency	
		C	HF	HF/n-3			per gene	mean (%)
Liver	Nrf1	1.00 ± 0.06	0.99 ± 0.06	1.03 ± 0.07	0.8586	28-29	1.90	84.5 ± 0.9
	Pparα	1.00 ± 0.14	1.31 ± 0.15a	1.32 ± 0.16a	0.0208	22-24	1.89	
	Scd-1	1.00 ± 0.11	0.71 ± 0.07	0.06 ± 0.02ab	<0.0001	20-28	1.79	
	Spp1 (OPN)	1.00 ± 0.07	1.04 ± 0.07	1.06 ± 0.07	0.5941	25-26	1.76	
	Srebp1c	1.00 ± 0.22	1.18 ± 0.25	0.90 ± 0.23	0.4632	23-28	1.84	
LSI	Cph*					24-27	1.81	85.0 ± 0.9
	Hsp90*					20-23	1.83	
	Icam1	1.00 ± 0.18	0.97 ± 0.14	1.01 ± 0.16	0.9599	30-33	1.84	
	Tek	1.00 ± 0.16	1.17 ± 0.19	0.98 ± 0.17	0.4179	29-33	1.85	
	Vcam1	1.00 ± 0.14	1.22 ± 0.14	1.07 ± 0.19	0.2955	29-32	1.86	
MAT	Actb*					17-19	1.85	85.4 ± 0.8
	Adipoq	1.00 ± 0.22	0.93 ± 0.16	1.00 ± 0.20	0.9855	18-20	1.87	
	Foxp3	1.00 ± 0.16	0.77 ± 0.13	0.68 ± 0.12	0.1502	28-31	1.83	
	Hprt1*					24-25	1.84	
	Il10	1.00 ± 0.14	1.09 ± 0.16	0.98 ± 0.13	0.7737	31-34	1.86	
	Itgax (CD11c)	1.00 ± 0.16	1.07 ± 0.13	2.44 ± 0.33ab	<0.0001	25-30	1.92	
	Lep	1.00 ± 0.38	3.33 ± 1.16a	2.65 ± 0.90a	0.0017	21-26	1.90	
	Lpl	1.00 ± 0.22	1.05 ± 0.19	0.99 ± 0.19	0.7681	19-22	1.86	
	Mcp-1	1.00 ± 0.14	1.66 ± 0.30a	1.60 ± 0.23a	0.0173	26-29	1.85	
	Mrc1 (CD206)	1.00 ± 0.07	1.17 ± 0.07a	1.56 ± 0.10ab	<0.0001	23-26	1.85	
	Pparγ2	1.00 ± 0.23	0.81 ± 0.15	0.82 ± 0.17	0.5833	27-30	1.86	
	Spp1 (OPN)	1.00 ± 0.45	1.68 ± 0.71	5.27 ± 1.94ab	0.0002	26-31	1.78	
	Spp1 (OPN^X)	1.00 ± 0.42	2.11 ± 0.88	7.41 ± 2.59ab	<0.0001	26-32	1.85	
	Tnf-α	1.00 ± 0.21	0.77 ± 0.13	0.85 ± 0.14	0.8277	28-32	1.86	
MAT (6 w)	Actb*					17-22	1.87	83.8 ± 4.3
	Hprt1*					24-28	1.90	
	Spp1 (OPN)	1.00 ± 0.33	0.52 ± 0.13	2.21 ± 0.57ab	0.0021	27-30	1.75	
Pre-adipocytes	Gapdh*					18-19	1.901	85.8 ± 2.7
	Hprt1*					23-25	1.867	
	Spp1 (OPN)	1.00 ± 0.40	1.11 ± 0.37	1.75 ± 0.62	0.2583	20-23	1.807	
Spleen	CD4	1.00 ± 0.12	1.09 ± 0.10	0.78 ± 0.09b	0.019	24-26	1.85	86.0 ± 0.3
	CD8a	1.00 ± 0.07	1.05 ± 0.08	0.83 ± 0.07b	0.0321	25-27	1.86	
	Gapdh*					20-21	1.87	
	Hprt1*					24-25	1.86	
USI	Actb*					17-19	1.86	85.0 ± 0.5
	Gapdh*					18-19	1.83	
	Hprt1*					25-27	1.86	
	Icam1	1.00 ± 0.10	1.58 ± 0.25a	1.09 ± 0.16	0.0321	30-32	1.87	
	Spp1 (OPN)	1.00 ± 0.50	0.89 ± 0.33	1.25 ± 0.58	0.6728	30 33	1.859	
	Tek	1.00 ± 0.15	1.71 ± 0.34a	1.21 ± 0.21	0.047	29-31	1.86	
	Vcam1	1.00 ± 0.10	1.76 ± 0.35	1.27 ± 0.22	0.0852	29-31	1.84	

Table 8: Effects of different high fat diets on mRNA expression of marker genes for immune cell activation in mesenteric adipose tissue. Shown are the results in relative fold changes for explorative gene expression analysis with "RT² Profiler™ RT-qPCR arrays" (SABiosciences) for marker genes of T and B cell activation in mesenteric adipose tissue. An equal amount of RNA from 4 animals per dietary group was pooled, and 1 µg of pooled RNA was reverse transcribed and amplified according to the manufacturer's instructions. Data were normalized and analyzed with $\Delta\Delta C_q$-method, and fold changes were calculated relative to C or HF group. Targets with C_q-values of 35 and above were excluded.

Gene		Fold regulation			Gene		Fold regulation		
		HF vs. C	HF/n-3 vs. C	HF/n-3 vs. HF			HF vs. C	HF/n-3 vs. C	HF/n-3 vs. HF
Ap3b1	Adaptor-related protein complex 3, beta 1 subunit	1.01	1.22	1.21	Il12b	Interleukin 12B	-1.90	-1.04	1.83
Bad	BCL2-associated agonist of cell death	1.14	1.16	1.01	Il15	Interleukin 15	-1.17	-1.11	1.05
Blr1	Chemochine (C-X-C motif) receptor 5	-1.11	1.13	1.24	Il18	Interleukin 18	-1.62	-1.45	1.11
Cblb	Casitas B-lineage lymphoma b	1.10	1.79	1.63	Il27	Interleukin 27	1.18	1.27	1.08
Ccnd3	Cyclin D3	1.37	1.33	-1.03	Il2ra	Interleukin 2 receptor, alpha chain	1.28	2.46	1.93
Cd1d1	CD1d1 antigen	1.55	1.33	-1.17	Il7	Interleukin 7	1.56	2.22	1.42
Cd2	CD2 antigen	-1.13	-1.13	1.00	Impdh1	Inosine 5'-phosphate dehydrogenase 1	-1.14	-1.04	1.10
Cd28	CD28 antigen	-1.24	1.28	1.59	Impdh2	Inosine 5'-phosphate dehydrogenase 2	-1.22	-1.09	1.11
Cd3d	CD3 antigen, delta polypeptide	-1.18	-1.49	-1.27	Inha	Inhibin alpha	1.04	-1.06	-1.10
Cd3e	CD3 antigen, epsilon polypeptide	-1.32	1.02	1.35	Irf4	Interferon regulatory factor 4	-1.04	1.45	1.51
Cd3g	CD3 antigen, gamma polypeptide	1.00	-1.06	-1.06	Jag2	Jagged 2	3.11	4.59	1.48
Cd4	CD4 antigen	-1.04	1.05	1.09	Ms4a1	Membrane-spanning 4-domains, subfamily A, member 1	-1.30	1.30	1.69
Cd40	CD40 antigen	1.38	1.57	1.14	Nkx2-3	NK2 transcription factor related, locus 3 (Drosophila)	-1.20	-1.16	1.03
Cd40lg	CD40 ligand	-1.07	1.14	1.22	Nos2	Nitric oxide synthase 2, inducible	2.94	2.35	-1.25
Cd74	CD74 antigen (invariant polypeptide of major histocompatibility complex, class II antigen-associated)	1.22	1.36	1.11	Pawr	PRKC, apoptosis, WT1, regulator	-1.03	-1.05	-1.02
Cd81	CD81 antigen	1.17	1.34	1.14	Pdcd1lg2	Programmed cell death 1 ligand 2	1.02	1.08	1.05
Cd8a	CD8 antigen, alpha chain	-1.27	-1.03	1.24	Pik3cd	Phosphatidylinositol 3-kinase catalytic delta polypeptide	-1.15	-1.01	1.14
Cd8b1	CD8 antigen, beta chain 1	-1.07	1.23	1.31	PiK3r1	Phosphatidylinositol 3-kinase, regulatory subunit, polypeptide 1 (p85 alpha)	-1.10	-1.10	-1.00
Cd93	CD93 antigen	1.38	1.58	1.14	Prkcd	Protein kinase C, delta	1.25	1.62	1.30
Cdkn1a	Cyclin-dep. kinase inhibitor 1A (P21)	2.51	1.71	-1.47	Prkcq	Protein kinase C, theta	-1.11	1.08	1.19
Clcf1	Cardiotrophin-like cytokine factor 1	-1.15	1.22	1.41	Prlr	Prolactin receptor	-1.50	-1.64	-1.09

Gene		Fold regulation			Gene		Fold regulation		
		HF vs. C	HF/n-3 vs. C	HF/n-3 vs. HF			HF vs. C	HF/n-3 vs. C	HF/n-3 vs. HF
Cr2	Complement receptor 2	-1.06	1.53	1.62	Ptprc	Protein tyrosine phosphatase, receptor type, C	-1.16	1.26	1.46
Csf2	Colony stimulating factor 2 (granulocyte-macrophage)	-2.29	1.09	2.51	Relb	Avian reticuloendotheliosis viral (v-rel) oncogene related B	1.11	1.06	-1.05
Cxcl12	Chemokine (C-X-C motif) ligand 12	1.04	1.72	1.65	Rgs1	Regulator of G-protein signaling 1	1.26	1.55	1.23
Cxcr4	Chemokine (C-X-C motif) receptor 4	1.59	1.79	1.13	Sit1	Suppression inducing transmembrane adaptor 1	-1.02	1.29	1.32
Dock2	Dedicator of cyto-kinesis 2	-1.14	1.29	1.47	Sla2	Src-like-adaptor 2	1.16	1.13	-1.02
Egr1	Early growth response 1	-1.05	1.33	1.40	Socs5	Suppressor of cytokine signaling 5	1.11	1.26	1.13
Flt3	FMS-like tyrosine kinase 3	1.46	1.57	1.08	Spp1	Secreted phosphoprotein 1	-1.61	9.45	15.19
Gadd45g	Growth arrest and DNA-damage-inducible 45 gamma	1.57	1.09	-1.45	Tlr1	Toll-like receptor 1	-1.08	1.58	1.71
Glmn	Glomulin, FKBP associated protein	1.08	1.55	1.43	Tlr4	Toll-like receptor 4	1.04	1.88	1.81
H2-Aa	Histocompatibility 2, class II antigen A, alpha	1.02	1.21	1.18	Tlr6	Toll-like receptor 6	-1.16	1.71	1.98
Hdac5	Histone deacetylase 5	1.11	-1.04	-1.15	Tnfrsf13b	Tumor necrosis factor receptor superfamily, member 13b	-1.22	1.21	1.48
Hdac7a	Histone deacetylase 7	1.19	1.43	1.20	Tnfrsf13c	Tumor necrosis factor receptor superfamily, member 13c	2.70	3.05	1.13
Hells	Helicase, lymphoid specific	-1.04	1.60	1.66	Tnfsf13b	Tumor necrosis factor (ligand) superfamily, member 13b	1.42	1.88	1.32
Hsp90aa1	Heat shock protein 90, alpha (cytosolic), class A member 1	1.62	1.71	1.05	Tnfsf14	Tumor necrosis factor (ligand) superfamily, member 14	1.12	1.65	1.47
Icosl	Icos ligand	1.15	1.39	1.21	Traf6	Tnf receptor-associated factor 6	1.05	1.20	1.14
Ifng	Interferon gamma	-6.30	1.19	7.49	Vav1	Vav 1 oncogene	1.02	1.41	1.38
Igbp1	Immunoglobulin (CD79A) binding protein 1	1.11	1.01	-1.10	Was	Wiskott-Aldrich syndrome homolog (human)	-1.11	1.20	1.33
Il10	Interleukin 10	-1.08	1.37	1.48	Wwp11	WW containing ubiquitin protein ligase 1	3.52	5.74	1.63

Table 9: Effects of different high fat diets on mRNA expression of marker genes for endothelial cell biology in small intestine. Shown are the results in relative fold changes for explorative gene expression analysis with "RT² Profiler™ RT-qPCR arrays" (SABiosciences) for marker genes of endothelial cell biology in small intestine. An equal amount of RNA from 4 animals per dietary group was pooled, and 1 µg of pooled RNA was reverse transcribed and amplified according to the manufacturer's instructions. Data were normalized and analyzed with $\Delta\Delta C_q$-method, and fold changes were calculated relative to C or HF group. Targets with C_q-values of 35 and above were excluded.

Gene		Fold regulation			Gene		Fold regulation		
		HF vs. C	HF/n-3 vs. C	HF/n-3 vs. HF			HF vs. C	HF/n-3 vs. C	HF/n-3 vs. HF
Ace	Angiotensin I converting enzyme (peptidyl-dipeptidase A) 1	1.18	1.16	-1.02	Il3	Interleukin 3	-1.44	-1.47	-1.02
Adam17	A disintegrin and metallopeptidase domain 17	-1.00	-1.16	-1.16	Il7	Interleukin 7	2.05	-1.21	-2.48
Agt	Angiotensinogen (serpin peptidase inhibitor, clade A, member 8)	1.73	1.25	-1.38	Itga5	Integrin alpha 5 (fibronectin receptor alpha)	1.88	1.48	-1.27
Agtr1a	Angiotensin II receptor, type 1a	3.45	1.57	-2.19	Itgav	Integrin alpha V	1.02	1.05	1.03
Angpt1	Angiopoietin 1	3.40	1.35	-2.52	Itgb1	Integrin beta 1 (fibronectin receptor beta)	1.08	1.00	-1.08
Anxa5	Annexin A5	1.34	1.18	-1.13	Itgb3	Integrin beta 3	1.15	1.09	-1.06
Bax	Bcl2-associated X protein	1.06	1.17	1.10	Kdr	Kinase insert domain protein receptor	1.26	1.51	1.20
Bcl2	B-cell leukemia/lymphoma 2	1.07	1.17	1.09	Kit	Kit oncogene	1.06	-1.12	-1.18
Bcl2l1	Bcl2-like 1	1.13	1.18	1.04	Mmp2	Matrix metallopeptidase 2	1.36	1.41	1.03
Birc1a	NLR family, apoptosis inhibitory protein 1	-1.11	-1.48	-1.33	Mmp9	Matrix metallopeptidase 9	3.67	2.94	-1.25
Birc2	Baculoviral IAP repeat-containing 2	1.15	1.05	-1.09	Nos2	Nitric oxide synthase 2, inducible	-1.17	-2.18	-1.86
Blr1	Chemochine (C-X-C motif) receptor 5	1.07	1.14	1.07	Nos3	Nitric oxide synthase 3, endothelial cell	3.48	3.42	-1.02
Casp1	Caspase 1	1.08	-1.18	-1.27	Npr1	Natriuretic peptide receptor 1	1.10	-1.11	-1.22
Casp3	Caspase 3	1.05	-1.05	-1.10	Ocln	Occludin	-1.07	-1.02	1.05
Casp6	Caspase 6	1.08	-1.02	-1.10	Pdgfra	Platelet derived growth factor receptor, alpha polypeptide	1.44	1.22	-1.18
Ccl2	Chemokine (C-C motif) ligand 2	1.70	-1.02	-1.73	Pecam 1	Platelet/endothelial cell adhesion molecule 1	1.33	1.53	1.15
Ccl5	Chemokine (C-C motif) ligand 5	-1.09	-1.05	1.04	Pgf	Placental growth factor	2.04	2.01	-1.02
Cdh5	Cadherin 5	1.33	1.10	-1.21	Plat	Plasminogen activator, tissue	1.49	1.14	-1.30
Cflar	CASP8 and FADD-like apoptosis regulator	1.26	1.04	-1.22	Plau	Plasminogen activator, urokinase	1.60	1.27	-1.26
Col18a1	Collagen, type XVIII, alpha 1	2.11	1.81	-1.17	Plg	Plasminogen	2.94	3.24	1.10
Cpb2	Carboxypeptidase B2 (plasma)	1.01	1.07	1.06	Ptgis	Prostaglandin I2 (prostacyclin) synthase	1.88	1.19	-1.58
Cradd	CASP2 & RIPK1 adaptor w/ death domain	-1.13	-1.25	-1.11	Rhob	Ras homolog gene family, member B	1.18	1.05	-1.13

Gene		Fold regulation			Gene		Fold regulation		
		HF vs. C	HF/n-3 vs. C	HF/n-3 vs. HF			HF vs. C	HF/n-3 vs. C	HF/n-3 vs. HF
Csf2	Colony stimulating factor 2 (granulocyte-macrophage)	-1.30	-1.34	-1.03	Ripk1	Receptor (TNFRSF)-interacting serine-threonine kinase 1	1.29	1.11	-1.16
Cx3cl1	Chemokine (C-X3-C motif) ligand 1	1.16	-1.09	-1.27	Sell	Selectin, lymphocyte	-1.23	-1.27	-1.03
Cxcl1	Chemokine (C-X-C motif) ligand 1	-1.26	-1.40	-1.11	Selp	Selectin, platelet	-1.13	1.08	1.22
Cxcl2	Chemokine (C-X-C motif) ligand 2	3.01	2.40	-1.25	Selplg	Selectin, platelet (p-selectin) ligand	1.08	1.27	1.17
Cxcl4	Platelet factor 4	2.14	2.18	1.02	Serpine 1	Serine (or cysteine) peptidase inhibitor, clade E, member 1	1.98	1.43	-1.39
Ecgf1	Thymidine phosphorylase	1.14	1.22	1.07	Sod1	Superoxide dismutase 1, soluble	1.35	2.17	1.60
Edn1	Endothelin 1	1.36	1.08	-1.26	Tek	Endothelial-specific receptor tyrosine kinase	2.14	1.36	-1.57
Edn2	Endothelin 2	1.23	-1.39	-1.71	Tfpi	Tissue factor pathway inhibitor	1.60	1.13	-1.42
Ednra	Endothelin receptor type A	1.98	1.66	-1.19	Tgfb1	Transforming growth factor, beta 1	-1.01	1.08	1.08
Fas	Fas (TNF receptor superfamily member 6)	-1.02	1.17	1.19	Thbd	Thrombomodulin	2.17	1.64	-1.32
Fasl	Fas ligand (TNF superfamily, member 6)	1.70	1.31	-1.29	Thbs1	Thrombospondin 1	1.49	1.49	-1.00
Fgf1	Fibroblast growth factor 1	1.06	-1.24	-1.30	Tnf	Tumor necrosis factor	1.13	1.06	-1.07
Flt1	FMS-like tyrosine kinase 1	1.20	-1.08	-1.29	Tnfaip3	Tumor necrosis factor, alpha-induced protein 3	-1.28	-1.27	1.01
Fn1	Fibronectin 1	1.96	1.85	-1.06	Tnfsf10	Tumor necrosis factor (ligand) superfamily, member 10	-1.02	-1.31	-1.28
Icam1	Intercellular adhesion molecule 1	1.50	1.48	-1.02	Vcam1	Vascular cell adhesion molecule 1	2.00	1.74	-1.15
Il11	Interleukin 11	1.57	1.99	1.27	Vegfa	Vascular endothelial growth factor A	1.05	1.02	-1.03
Il1b	Interleukin 1 beta	1.20	1.05	-1.14	Vwf	Von Willebrand factor homolog	1.26	1.41	1.12

Table 10: Lipid metabolites after feeding low fat control (C), high fat (HF) and high fat diet enriched with n-3 LC-PUFA EPA / DHA (N3) for 12 weeks in murine liver tissue. Concentrations are expressed in ng / g tissue. Low fat / Control diet (C) and high fat diets (HF, N3), diets in which 10 % and 48 % energy is provided by fat, respectively; ARA, arachidonic acid; DHA, docosahexaenoic acid; EPA, eicosapentaenoic acid; HDHA, hydroxy-docosahexaenoic acid; HEPE, hydroxy-eicosapentaenoic acid; HETE, hydroxy-eicosatetraenoic acid; FC, fold change; SD, standard deviation; LoD, limit of detection as given in Gomolka et al., 2010. Statistical analysis was performed with One-Way ANOVA and Tukey's post-test (n=10). Index letters a, b, and c indicate a significant difference between groups with $p<0.05$, $p<0.01$, and $p<0.001$, respectively.

	Compound	Control diet	High fat diet	High fat/n-3 diet	FC	FC	FC	P value	LoD (ng)
		Mean ± SD	Mean ± SD	Mean ± SD	(HF vs. C)	(N3 vs. C)	(N3 vs. HF)		
ARA-derived	Leukotriene B_4	0.0 ± 0.0	1.0 ± 3.2	1.5 ± 3.1	-	-	1.49	0.4215	0.02
	Lipoxin A_4	4.7 ± 6.4	5.7 ± 5.4	0.0 ± 0.0	1.20	0.00	0.00	0.0297	0.2
	15-HETE	1443.2 ± 720.9	1235.7 ± 724.9	610.0 ± 122.6	0.86	0.42^a	0.49	0.0112	0.04
	12-HETE	660.3 ± 565.0	575.5 ± 465.9	127.7 ± 38.9	0.87	0.19^a	0.22	0.0196	0.03
	11-HETE	104.8 ± 65.8	148.0 ± 103.4	39.7 ± 20.9	1.41	0.38^c	0.27^c	<0.0001	0.21
	9-HETE	327.8 ± 227.5	357.0 ± 254.2	142.5 ± 57.3	1.09	0.43	0.40	0.0485	0.16
	8-HETE	251.4 ± 115.8	313.4 ± 206.3	92.6 ± 25.0	1.25	0.37^a	0.30^b	0.0039	0.04
	5-HETE	671.2 ± 289.9	821.1 ± 609.9	290.1 ± 117.1	1.22	0.43	0.35^a	0.0166	0.03
EPA-derived	Leukotriene B_5	0.3 ± 0.5	0.0 ± 0.0	0.9 ± 0.5	0.00	3.12^b	$-^c$	0.0003	0.02
	18-HEPE	108.7 ± 76.7	29.7 ± 25.8	972.7 ± 298.5	0.27	8.95^c	32.72^c	<0.0001	0.1
	15-HEPE	39.1 ± 26.9	14.1 ± 11.2	249.3 ± 127.0	0.36	6.38^c	17.65^c	<0.0001	0.01
	12-HEPE	217.9 ± 262.1	63.4 ± 54.8	481.9 ± 214.6	0.29	2.21^a	7.60^c	0.0003	0.03
	9-HEPE	58.1 ± 38.3	25.1 ± 12.7	405.4 ± 194.5	0.43	6.97^c	16.13^c	<0.0001	0.1
	8-HEPE	22.1 ± 12.9	7.5 ± 6.2	189.5 ± 44.6	0.34	8.56^c	25.10^c	<0.0001	0.1
	5-HEPE	37.7 ± 15.0	29.9 ± 23.5	372.8 ± 164.5	0.79	9.89^c	12.46^c	<0.0001	0.04
DHA-derived	Resolvin D1	0.0 ± 0.0	0.0 ± 0.0	0.0 ± 0.0	-	-	-	N/A	0.05
	10,17-DiHDHA	0.0 ± 0.0	0.0 ± 0.0	0.0 ± 0.0	-	-	-	N/A	0.02
	20-HDHA	699.2 ± 298.2	462.4 ± 264.1	1819.2 ± 657.4	0.66	2.60^c	3.93^c	<0.0001	0.06
	17-HDHA	448.3 ± 201.9	297.1 ± 136.9	888.8 ± 297.7	0.66	1.98^c	2.99^c	<0.0001	0.09
	16-HDHA	283.3 ± 120.2	193.3 ± 127.6	696.8 ± 222.5	0.68	2.46^c	3.60^c	<0.0001	0.02
	14-HDHA	637.1 ± 423.6	368.5 ± 253.6	1115.7 ± 417.0	0.58	1.75^a	3.03^c	0.0005	0.07
	13-HDHA	403.1 ± 577.0	157.5 ± 112.0	498.6 ± 150.6	0.39	1.24^c	3.17^c	<0.0001	0.02
	11-HDHA	110.1 ± 43.1	98.0 ± 72.5	295.2 ± 80.1	0.89	2.68^c	3.01^c	<0.0001	0.04
	10-HDHA	119.0 ± 78.6	122.8 ± 86.9	479.6 ± 113.3	1.03	4.03^c	3.91^c	<0.0001	0.04
	8-HDHA	139.9 ± 77.0	134.0 ± 106.2	310.5 ± 154.8	0.96	2.22^b	2.32^b	0.0029	0.12
	7-HDHA	194.1 ± 106.1	155.7 ± 99.1	430.5 ± 151.2	0.80	2.22^c	2.76^c	<0.0001	0.09
	4-HDHA	158.5 ± 61.9	205.4 ± 208.3	460.2 ± 199.6	1.30	2.90^b	2.24^b	0.001	0.05

Table 11: Effects on body mass in n-3 LC-PUFA intervention studies in mice. Studies are sorted by year and were retrieved using PubMed database with the search term "*n-3 body weight high-fat diet mouse*" (access: December 28, 2011). Up / down / "-" indicate an increased / decreased / unchanged body mass to the control / HF diet, respectively. ARA, arachidonic acid; BM, body mass; DHA, docosahexaenoic acid; EPA, eicosapentaenoic acid; FO, fish oil; HF, high fat diet; MUFA, monounsaturated fatty acid; LC-PUFA, long chain polyunsaturated fatty acid; SFA, saturated fatty acid; TG or TAG, triacylglycerol. N / D, not determined; en%, energy%.

effect on BM	reference	mouse strain, age (w)	feeding period (w)	diet composition
up	(Gabrielsson et al., 2012)	Ldlr$^{-/-}$ mice, 8	8 / 16	HF diet (22 % fat (w / w) butter fat) with - beef (0.13 % ARA, N / D) or **- minced herring (8.2 % LC-PUFA, 0.09 % ARA, 2.0 % EPA, 2.9 % DHA)**
down	(Hensler et al., 2011)	aP2-Cre-ER^{T2}-PPARγ$^{L2/L2}$ mice, 12	1. 8 2. 2 or 6	1. HF diet (35 % fat (w / w) corn oil); 2. HF diet or **- HF diet + fish oil (15 % of lipids EPAX 1050 TG, 46 % EPA, 14 % DHA)**
-	(Jung et al., 2011)	C57BL/6 mice, 23	4	- chow (5 % fat (w / w)) or - HF diet + saturated FA (21 % fat: 71 % coconut, 19 % olive, 9 % safflower / corn oil) or **- HF diet + n-3 LC-PUFA (21 % fat: 95 % menhaden oil, 5 % corn oil; 6 % LC-PUFA)**
down	(Ma et al., 2011)	C57BL/6JBom Tac mice, 8	8-10	- low fat (7 % fat (w / w)) or (HF diets with either high sucrose or high casein) - HF diet + corn oil (25 % fat, 18 % from corn oil, 12 % n-6, 3 % n-3 LC-PUFA) or **- HF diet + fish oil (25 % fat, 18 % from fish oil, 4 % n-6 LC-PUFA, 6 % n-3 LC-PUFA)**
up	(Rockett et al., 2010)	C57BL/6 mice, 4-8	14	- normal diet (13 en% fat) or - HF diet (41 en% fat - 30 % SFA, 8 % MUFA, 3 % LC-PUFA) or **- HF diet + LC-PUFA (41 en% fat - 8 % SFA, 9 % MUFA, 24 % LC-PUFA with 2 % from DHA, 3 % from EPA)**
down	(Ji et al., 2009)	C57BL/6Tac aP2-fat-1 mice, 4-5	11-13	**- highly unsaturated diet (62 en% from safflower oil) or** - high carbohydrate diet (13 en% from safflower oil, 64 en% from starch / fructose 50 / 50)
down	(Kuda et al., 2009)	C57BL/6N mice, 12	20	1. HF diet (35 % fat (w / w) corn oil); **2. HF or HF + FO (15 % of lipids EPAX 1050 TG, 46 % EPA, 14 % DHA) or** - HF diet + rosiglitazone or **- HF diet + FO + rosiglitazone**
down	(Flachs et al., 2005; van Schothorst et al., 2009)	C57BL/6N mice, 16	4 or 6	<u>4 weeks</u>: - HF1 diet (20 % (w / w) fat from flaxseed oil) or - **HF1 diet + FO (20 % fat from flaxseed oil, but 44 % replaced with EPAX 1050 TG with 51 % DHA, 6 % EPA);** <u>6 weeks</u>: - **HF2 diet + FO1 (35 % (w / w) fat from corn oil, but 15 % replaced with EPAX 1050 TG) or** **- HF2 diet + FO2 (35 % (w / w) fat from corn oil, but 44 % replaced with EPAX 1050 TG)**

effect on BM	reference	mouse strain, age (w)	feeding period (w)	diet composition
-	(Huber et al., 2007)	C57BL/KsJ-lepr^{db}/lepr^{db} diabetic (db/db) mice, 7	6	- low fat diet (3 en% fat) or - HF/S diet (30 en% fat from lard) or - HF/6 diet (30 en% fat from safflower oil) or **- HF/3 diet (30 en% fat from safflower oil (60 %) + EPAX 6000 TG (40 %), 2.5 % (w / w) n-3 LC-PUFA, EPA : DHA 2:1))**
down	(Mori et al., 2007)	C57BL/6J mice, 7	20	- low fat diet (5 % (w / w) fat from TAG oil = safflower, rapeseed, perilla oils) or - HF diet (30 % TAG oil) or **- HF diet + FO (28 / 26 / 22 % TAG oil + 2 / 4 / 8 % FO = 45 % DHA, 6 % EPA)**
up	(Todoric et al., 2006)	C57BL/KsJ-lepr^{db}/lepr^{db} diabetic (db/db) mice, 7	6	- low fat diet (3 en% fat) or - HF/S diet (30 en% fat from lard) or - HF/6 diet (30 en% fat from safflower oil) or **- HF/3 diet (30 en% fat from safflower oil (60 %) + EPAX 6000 TG (40 %), 2.5 % (w / w) n-3 LC-PUFA, EPA : DHA 2:1))**
down	(Wang et al., 1999; Xin et al., 2000; Huang et al., 2004)	C57BL/6 mice, 4	13 + 6	13 weeks: - HF diet (59 en% fat from safflower oil and beef tallow) 6 weeks: - HF diet or **- HF diet + FO (59 % fat with 32 % from LC-PUFA (contains 18 % (w / w) EPA and 12 % DHA))**
down	(Ruzickova et al., 2004)	C57BL/6N mice, 16	2+5	- HF diet (35 % (w / w) fat from rapeseed + sunflower oil) or **- HF diet + FO1 (35 % fat like HF but 15 % lipids subst. by EPAX 1050 TG, 1 % EPA,11 % DHA in fat) or** **- HF diet + FO2: (35 % fat like HF but 44 % lipids subst. by EPAX 1050 TG, 3 % EPA, 29 % DHA in fat)**
down	(Ikemoto et al., 1996)	C57BL/6J (NIDDM) mice, -	19	7 HF diets (60 en% from fat with palm oil, lard, rapeseed, soybean, safflower, perilla, or **tuna fish oil (7 % EPA, 23 % DHA)**

Table 12: Effects on hepatic triacylglycerol levels in n-3 LC-PUFA intervention studies in mice. Studies are sorted by year and were retrieved using PubMed database with the search term "PUFA hepatic steatosis mouse high fat diet" (access: December 28, 2011). DHA, docosahexaenoic acid; EPA, eicosapentaenoic acid; FO, fish oil; HF, high fat diet; LC-PUFA, long chain polyunsaturated fatty acid; SFA, saturated fatty acid; TG, triacylglycerol; en%, energy%.

effect on hepatic steatosis	reference	mouse strain, age (w)	feeding period (w)	diet composition
aggra-vation	(Kus et al., 2011)	C57BL/6N mice, 12	8	- cHF diet (35 % (w / w) fat from corn oil) or **- cHF diet + FO (35 % (w / w), 15 % of lipids replaced by EPAX 1050 TG with 46 % DHA, 14 % EPA) or** - cHF diet + rosiglitazone or **- cHF diet + FO + rosiglitazone or** - cHF diet + pioglitazone or **- cHF diet + FO + pioglitazone**

effect on hepatic steatosis	reference	mouse strain, age (w)	feeding period (w)	diet composition
improve-ment	(Jelenik et al., 2010)	AMPK$\alpha 2^{-/-}$ mice, 16	9	- chow (3.4 % (w / w) fat) or - cHF diet (35 % (w / w) fat from corn oil) or **- cHF diet + FO (35 % (w / w), 15 % of lipids replaced by EPAX 1050 TG with 46 % DHA, 14 % EPA)**
improve-ment	(Koolman et al., 2010)	C57BL/6J mice, 8	6	- LF diet (6 % w / w) or - HF / SFA diet (36 % (w / w) fat from beef) or **- HF / LC-PUFA diet (36 % fat with 58 % beef and 42 % fish oil),** after 3 weeks on diets: ribonamant treatment in half of each dietary group = 6 groups
improve-ment	(Yu et al., 2010)	Tg aP2-Pparδ FVB/NJ mice, 7–8	16	- standard diet (14 en% fat) or - standard diet + Pparδ–ligand L165041 (14 en% fat) or **- high FO diet (36 en% fat from tuna) or** - high beef tallow diet (36 en% fat from beef tallow)
improve-ment	(Kajikawa et al., 2009)	mice	2	diets + daily gavage: - high fat / high sucrose diet + **EPA ethyl-ester gavage**
improve-ment	(Magdeldin et al., 2009)	C57BL/6J	4	- normal diet or - n-3 LC-PUFA diet or - n-6 LC-PUFA diet
improve-ment	(Oosterveer et al., 2009)	C57BL/6J mice, 12	6	- chow or - HF diet (beef tallow) or **- HF / LC-PUFA diet (42 % (w / w) replaced by menhaden oil** *cf. Koolman et al.*
improve-ment	(Sealls et al., 2008)	C57BL/6 mice, 4	8	- lard diet (6 % (w / w) fat from lard) or - canola diet (6 % (w / w) fat from canola oil) or **- fish / fungal oil diet (3.27 % fat from arasco oil and 2.73 % fat from menhadin oil, 5 mol% EPA, 6.7 mol% DHA)**
aggra-vation	(Agellon et al., 2007)	Fabp2$^{-/-}$ mice, 30-40	2	- SFA diet (20 % (w / w) fat from beef tallow) or **- LC-PUFA diet (20 % fat from safflower oil)**
improve-ment	(Huber et al., 2007)	C57BL/KsJ-lepr^{db}/lepr^{db} diabetic (db/db) mice, 7	6	- low fat diet (3 en% fat) or - HF/S diet (30 en% fat from lard) or - HF/6 diet (30 en% fat from safflower oil) or **- HF/3 diet (30 en% fat from safflower oil (60 %) + EPAX 6000 TG (40 %), 2.5 % (w / w) n-3 LC-PUFA, EPA : DHA 2:1))**
improve-ment	(Mori et al., 2007)	C57BL/6J mice, 7	20	- low fat diet (5 % (w / w) fat from TAG oil = safflower, rapeseed, perilla oils) or - HF diet (30 % TAG oil) or **- HF diet + FO (28 / 26 / 22 % TAG oil + 2 / 4 / 8 % FO = 45 % DHA, 6 % EPA)**

Table 13: Effects on glucose tolerance and /or insulin resistance in n-3 LC-PUFA studies.
Studies are sorted by year and were among others retrieved using PubMed database with the search term "n-3 glucose tolerance high-fat diet mouse" (access: December 28, 2011). AF, animal fat; ALA, α-linolenic acid; ARA, arachidonic acid; C, control; DHA, docosahexaenoic acid; EPA, eicosapentaenoic acid; F / FO, fish oil; FA, fatty acid; HF, high fat diet; LC-PUFA, long chain polyunsaturated fatty acid; MO, menhaden oil; MUFA, monounsaturated fatty acid; ND, normal diet; S / SFA, saturated fatty acid; TFA, trans-fatty acid; TG / TAG, triacylglycerol. N / D, not determined.

n-3 LC-PUFA effect	reference	organism, age (w)	feeding period (w)	diet composition
improve-ment	(Flachs et al., 2011)	C57BL/6J mice, 10	5 or 15	- chow, - *ad libitum* cHF diet ((35 % (w / w) fat from corn oil) or **- *ad libitum* cHF diet + FO (35 % (w / w), 15 % of lipids replaced by EPAX 1050 TG with 46 % DHA, 14 % EPA) or** - restricted 10 % w / w cHF diet or **- restricted 10 % w / w cHF diet + FO**
improve-ment	(Jeyakumar et al., 2011)	weanling female Fischer rats, -	54	- TFA (10 % (w / w) hydrogenated vegetable oil (21 % trans-fat)) or - MUFA (10 % palmolein) or **- LC-PUFA / n-6 (10 % sunflower) or** **- LC-PUFA / n-3 (10 % sunflower + fish oil with 1.7 % EPA, 1.2 % DHA)**
improve-ment	(Kasbi Chadli et al., 2011)	hamster, -	20	- control diet or - HF diet or **- HF/n-3 diet**
improve-ment	(Kus et al., 2011)	C57BL/6N mice, 12	8	- cHF diet (35 % (w / w) fat from corn oil) or **- cHF diet + FO (35 % (w / w), 15 % of lipids replaced by EPAX 1050 TG with 46 % DHA, 14 % EPA) or** - cHF diet + rosiglitazone or **- cHF diet + FO + rosiglitazone or** - cHF diet + pioglitazone or **- cHF diet + FO + pioglitazone**
improve-ment	(Lankinen et al., 2009)	men and women with imparied glucose metabolism, 40-70 years	12	**- whole grain, berries, fatty fish or** - whole grain or - refined wheat breads (control)
no change	(Tierney et al., 2011)	human MetS subjects, mean 54 years	12	- HF / SFA diet (38 en% with 6 % PUFA) or - HF / MUFA diet (38 en% with 6 % PUFA) or - LF diet (28 en% with 6 % PUFA + 1 g / day oleic sunflower oil) **- LF diet + FO (28 en% with 6 % LC-PUFA + 1 g n-3 LC-PUFA, 2 % EPA, 1.5 % DHA)**
N / C	(Vargas et al., 2011)	women (polycystic ovary syndrome), 20-45 years	6	<u>3.5 g n-3 LC-PUFA:</u> - from either flaxseed oil (545 mg ALA) or **- from fish oil (358 mg EPA, 252 mg DHA) or** - soybean oil as placebo
N / C	(Castellano et al., 2010)	healthy Duroc boars, 204 d	28	- animal fat diet (20 % (w / w) fat + 62 g animal fat with hydrogenated SFA) or **- menhaden oil diet (20 % fat + 60 g menhaden oil with 9 g EPA and 11 g DHA) or** **- tuna oil diet (20 % fat + 60 g tuna oil with 4 g EPA and 20 g DHA)**

n-3 LC-PUFA effect	reference	organism, age (w)	feeding period (w)	diet composition
improve-ment	(Jelenik et al., 2010)	AMPK$\alpha 2^{-/-}$ mice, 16	9	- chow (3.4 % (w / w) fat) or - cHF diet (35 % (w / w) fat from corn oil) or **- cHF diet + FO (35 % (w / w), 15 % of lipids replaced by EPAX 1050 TG with 46 % DHA, 14 % EPA)**
improve-ment	(Machado et al., 2010)	weaning Ldlr$^{-/-}$ mice, -	16	- HF diet + TFA (40 en% fat from hydrogenated soybean oil) or - HF diet + SFA (40 en% fat from olive, soybean, palm oil) or **- HF diet + LC-PUFA (40 en% fat from sunflower and canola, 51 % LC-PUFA)**
improve-ment	(Oh et al., 2010)	C57BL/6 or GPR120$^{-/-}$ mice, 8	15-20	15 weeks: - chow (13.5 en% fat) or - HF diet (60 en% fat) 5 weeks: **- HF diet mice switched to HF diet + MO (27 % (w / w) fat replaced by menhaden fish oil with 16 % EPA and 9 % DHA 50 and 100 mg of DHA and EPA per mouse per day, respectively)**
improve-ment	(Smith et al., 2010)	fat-1 mice, -	acute	- glucose challenge test
improve-ment	(White et al., 2010)	fat-1 mouse, 6	8	- chow diet or - HF diet (55 en% fat)
improve-ment	(Wei et al., 2010)	fat-1 mice, -		
improve-ment	(Gonzalez-Periz et al., 2009)	ob/ob mice,	5	- C diet (8.4 % (w / w) fat) or **- LC-PUFA diet (8.4 % fat with 6 % of lipids from n-3 LC-PUFA)**
improve-ment	(Ramel et al., 2008)	overweight humans, 20-40 years	8	energy-restricted diets (30 en%) with different n-3 LC-PUFA: - control (no seafood) or **- lean fish (cod) or** **- fatty fish (salmon) or** **- fish oil (EPA / DHA capsules, no other fish)**
improve-ment	(Robbez Masson et al., 2008)	Wistar rat, 8	10	- Cn-6 diet (8 % (w / w) fat from cocoa butter and sunflower oil, n-6 LC-PUFA, cornstarch, sucrose), - Fn-6 diet (8 % fat from cocoa butter and sunflower oil + 66 % fructose + n-6 LC-PUFA), - F-ALA diet (8 % fat from cocoa butter and sunflower, linseed oil) + 66 % fructose + n-3 ALA), **- Fn-3 diet (8 % fat from cocoa butter and sunflower, linseed oil, LC-PUFA oil + 66 % fructose + n-3 LC-PUFA, 8.4 % EPA, 6.9 % DHA)**
N / C	(Giacco et al., 2007)	healthy humans	12	with **fish oil (3.6 g / day)** or placebo: - MUFA diet or - SFA diet
improve-ment	(Buettner et al., 2006)	Wistar rat, 6	12	- chow (11 en% fat) or - HFL diet (42 en% fat from lard) or - HFO (42 en% fat from olive oil) or - HFC (42 en% fat from coconut) or **- HFF (42 en% fat from fish oil)**

n-3 LC-PUFA effect	reference	organism, age (w)	feeding period (w)	diet composition
improve-ment	(Mustad et al., 2006)	ob/ob mice, 4-5	4	- C-MUFA diet (45 en% fat from safflower, canola oil, lecithin) or - ALA diet (45 en% fat from safflower, flaxseed, corn oil, lecithin) or **- EPA diet (45 en% fat from sardine oil, safflower oil; 21 % EPA, 9 % DHA) or** **- DHA diet (45 en% fat from tuna, safflower, sardine oil, lecithin; 9 % EPA, 21 % DHA)**
N / C	(Winzell et al., 2006)	C57BL/6J mice, -	12	each **1 % CLA + 1 % LC-PUFA** or 2 % vegetable oil: - normal diet (11 en% fat from lard) or - HF diet (58 en% fat from lard)
improve-ment	(Taouis et al., 2002)	Wistar rats, 5	4	- control diet (12 en% fat from peanut, canola oil) or - HF/n-6 diet (58 en% fat from safflower oil) **- HF/n-3 diet (39 en% fat from safflower oil, 19 en% fat from fish oil with 5.3 % EPA and 3.6 % DHA)**
N / C	(Brynes et al., 2000)	humans, overweight and T2DM, -	3	liquid meals: - high MUFA diet (olive oil high in oleic acid) or **- high LC-PUFA diet (corn oil high in LA)**
N / C	(Fasching et al., 1996)	healthy men, mean 26 years	1	daily standard diet (35 en% fat, 33 % from SFA / MUFA / LC-PUFA): + daily carbohydrates or + SFA fat or + n-6 LC-PUFA fat or + MUFA fat
N / C	(Eritsland et al., 1994)	humans, non-diabetic, coronory artery bypass graft, -	48	- control diet or **- LC-PUFA diet (3.4 g EPA + DHA)**
improve-ment	(Budohoski et al., 1993)	rats after weaning, -	4	- control diet or **- PUFA diet (60 / 30 en% fat from sunflower oil) or** - SFA diet (60 / 30 en% butter fat, lard)

7 References

Abate N, Garg A, Peshock RM, Stray-Gundersen J, Grundy SM. 1995. Relationships of generalized and regional adiposity to insulin sensitivity in men. J Clin Invest 96:88-98.

Agellon LB, Drozdowski L, Li L, Iordache C, Luong L, Clandinin MT, Uwiera RR, Toth MJ, Thomson AB. 2007. Loss of intestinal fatty acid binding protein increases the susceptibility of male mice to high fat diet-induced fatty liver. Biochim Biophys Acta 1771:1283-1288.

Ailhaud G, Guesnet P, Cunnane SC. 2008. An emerging risk factor for obesity: does disequilibrium of polyunsaturated fatty acid metabolism contribute to excessive adipose tissue development? Br J Nutr 100:461-470.

Alexenko AP, Mao J, Ellersieck MR, Davis AM, Whyte JJ, Rosenfeld CS, Roberts RM. 2007. The contrasting effects of ad libitum and restricted feeding of a diet very high in saturated fats on sex ratio and metabolic hormones in mice. Biol Reprod 77:599-604.

Altintas MM, Azad A, Nayer B, Contreras G, Zaias J, Faul C, Reiser J, Nayer A. 2011. Mast cells, macrophages, and crown-like structures distinguish subcutaneous from visceral fat in mice. J Lipid Res 52:480-488.

Andrikopoulos S, Blair AR, Deluca N, Fam BC, Proietto J. 2008. Evaluating the glucose tolerance test in mice. Am J Physiol Endocrinol Metab 295:E1323-1332.

Arita Y, Kihara S, Ouchi N, Takahashi M, Maeda K, Miyagawa J, Hotta K, Shimomura I, Nakamura T, Miyaoka K, Kuriyama H, Nishida M, Yamashita S, Okubo K, Matsubara K, Muraguchi M, Ohmoto Y, Funahashi T, Matsuzawa Y. 1999. Paradoxical decrease of an adipose-specific protein, adiponectin, in obesity. Biochem Biophys Res Commun 257:79-83.

Arner P. 1995. Differences in lipolysis between human subcutaneous and omental adipose tissues. Ann Med 27:435-438.

Arnold C, Markovic M, Blossey K, Wallukat G, Fischer R, Dechend R, Konkel A, von Schacky C, Luft FC, Muller DN, Rothe M, Schunck WH. 2010. Arachidonic acid-metabolizing cytochrome P450 enzymes are targets of {omega}-3 fatty acids. J Biol Chem 285:32720-32733.

Austyn JM, Gordon S. 1981. F4/80, a monoclonal antibody directed specifically against the mouse macrophage. Eur J Immunol 11:805-815.

Ayala JE, Samuel VT, Morton GJ, Obici S, Croniger CM, Shulman GI, Wasserman DH, McGuinness OP. 2010. Standard operating procedures for describing and performing metabolic tests of glucose homeostasis in mice. Dis Model Mech 3:525-534.

Baeuerle PA, Henkel T. 1994. Function and activation of NF-kappa B in the immune system. Annu Rev Immunol 12:141-179.

Batra A, Okur B, Glauben R, Erben U, Ihbe J, Stroh T, Fedke I, Chang HD, Zeitz M, Siegmund B. 2010. Leptin: a critical regulator of CD4+ T-cell polarization in vitro and in vivo. Endocrinology 151:56-62.

Bento AF, Claudino RF, Dutra RC, Marcon R, Calixto JB. 2011. Omega-3 fatty acid-derived mediators 17(R)-hydroxy docosahexaenoic acid, aspirin-triggered resolvin D1 and resolvin D2 prevent experimental colitis in mice. J Immunol 187:1957-1969.

Bertola A, Deveaux V, Bonnafous S, Rousseau D, Anty R, Wakkach A, Dahman M, Tordjman J, Clement K, McQuaid SE, Frayn KN, Huet PM, Gugenheim J, Lotersztajn S, Le Marchand-Brustel Y, Tran A, Gual P. 2009. Elevated expression of osteopontin may be related to adipose tissue macrophage accumulation and liver steatosis in morbid obesity. Diabetes 58:125-133.

BfR. 2004. Verwendung von Vitaminen in Lebensmitteln - Toxikologische und ernährungsphysiologische Aspekte. p 91.

Bjursell M, Gerdin AK, Lelliott CJ, Egecioglu E, Elmgren A, Tornell J, Oscarsson J, Bohlooly YM. 2008. Acutely reduced locomotor activity is a major contributor to Western diet-induced obesity in mice. Am J Physiol Endocrinol Metab 294:E251-260.

Bligh EG, Dyer WJ. 1959. A rapid method of total lipid extraction and purification. Can J Biochem Physiol 37:911-917.

Blok WL, de Bruijn MF, Leenen PJ, Eling WM, van Rooijen N, Stanley ER, Buurman WA, van der Meer JW. 1996a. Dietary n-3 fatty acids increase spleen size and postendotoxin circulating TNF in mice; role of macrophages, macrophage precursors, and colony-stimulating factor-1. J Immunol 157:5569-5573.

Blok WL, Katan MB, van der Meer JW. 1996b. Modulation of inflammation and cytokine production by dietary (n-3) fatty acids. J Nutr 126:1515-1533.

Bonner-Weir S. 2000. Perspective: Postnatal pancreatic beta cell growth. Endocrinology 141:1926-1929.

Bradford MM. 1976. A rapid and sensitive method for the quantitation of microgram quantities of protein utilizing the principle of protein-dye binding. Anal Biochem 72:248-254.

Bradley LM, Dalton DK, Croft M. 1996. A direct role for IFN-gamma in regulation of Th1 cell development. J Immunol 157:1350-1358.

Bradley RL, Jeon JY, Liu FF, Maratos-Flier E. 2008. Voluntary exercise improves insulin sensitivity and adipose tissue inflammation in diet-induced obese mice. Am J Physiol Endocrinol Metab 295:E586-594.

Bronner M, Hertz R, Bar-Tana J. 2004. Kinase-independent transcriptional co-activation of peroxisome proliferator-activated receptor alpha by AMP-activated protein kinase. Biochem J 384:295-305.

Brynes AE, Edwards CM, Jadhav A, Ghatei MA, Bloom SR, Frost GS. 2000. Diet-induced change in fatty acid composition of plasma triacylglycerols is not associated with change in glucagon-like peptide 1 or insulin sensitivity in people with type 2 diabetes. Am J Clin Nutr 72:1111-1118.

Buckley JD, Howe PR. 2009. Anti-obesity effects of long-chain omega-3 polyunsaturated fatty acids. Obes Rev 10:648-659.

Budohoski L, Panczenko-Kresowska B, Langfort J, Zernicka E, Dubaniewicz A, Ziemlanski S, Challiss RA, Newsholme EA. 1993. Effects of saturated and polyunsaturated fat enriched diet on the skeletal muscle insulin sensitivity in young rats. J Physiol Pharmacol 44:391-398.

Buettner R, Parhofer KG, Woenckhaus M, Wrede CE, Kunz-Schughart LA, Scholmerich J, Bollheimer LC. 2006. Defining high-fat-diet rat models: metabolic and molecular effects of different fat types. J Mol Endocrinol 36:485-501.

Buettner R, Scholmerich J, Bollheimer LC. 2007. High-fat diets: modeling the metabolic disorders of human obesity in rodents. Obesity (Silver Spring) 15:798-808.

Burcelin R, Crivelli V, Dacosta A, Roy-Tirelli A, Thorens B. 2002. Heterogeneous metabolic adaptation of C57BL/6J mice to high-fat diet. Am J Physiol Endocrinol Metab 282:E834-842.

Burdge G. 2004. Alpha-linolenic acid metabolism in men and women: nutritional and biological implications. Curr Opin Clin Nutr Metab Care 7:137-144.

Burns RA, Wibert GJ, Diersen-Schade DA, Kelly CM. 1999. Evaluation of single-cell sources of docosahexaenoic acid and arachidonic acid: 3-month rat oral safety study with an in utero phase. Food Chem Toxicol 37:23-36.

Caesar R, Drevon CA. 2008. Pancreatic contamination of mesenteric adipose tissue samples can be avoided by adjusted dissection procedures. J Lipid Res 49:1588-1594.

Calder PC. 2004. n-3 Fatty acids and cardiovascular disease: evidence explained and mechanisms explored. Clin Sci (Lond) 107:1-11.

Calder PC. 2006. n-3 polyunsaturated fatty acids, inflammation, and inflammatory diseases. Am J Clin Nutr 83:1505S-1519S.

Calder PC. 2008. Polyunsaturated fatty acids, inflammatory processes and inflammatory bowel diseases. Mol Nutr Food Res 52:885-897.

Calle EE, Rodriguez C, Walker-Thurmond K, Thun MJ. 2003. Overweight, obesity, and mortality from cancer in a prospectively studied cohort of U.S. adults. N Engl J Med 348:1625-1638.

Calon F, Cole G. 2007. Neuroprotective action of omega-3 polyunsaturated fatty acids against neurodegenerative diseases: evidence from animal studies. Prostaglandins Leukot Essent Fatty Acids 77:287-293.

Calpe-Berdiel L, Escola-Gil JC, Blanco-Vaca F. 2009. New insights into the molecular actions of plant sterols and stanols in cholesterol metabolism. Atherosclerosis 203:18-31.

Cantor H, Shinohara ML. 2009. Regulation of T-helper-cell lineage development by osteopontin: the inside story. Nat Rev Immunol 9:137-141.

Carlow DA, Gold MR, Ziltener HJ. 2009. Lymphocytes in the peritoneum home to the omentum and are activated by resident dendritic cells. J Immunol 183:1155-1165.

Cases S, Smith SJ, Zheng YW, Myers HM, Lear SR, Sande E, Novak S, Collins C, Welch CB, Lusis AJ, Erickson SK, Farese RV, Jr. 1998. Identification of a gene encoding an acyl CoA:diacylglycerol acyltransferase, a key enzyme in triacylglycerol synthesis. Proc Natl Acad Sci U S A 95:13018-13023.

Castellano CA, Audet I, Laforest JP, Chouinard Y, Matte JJ. 2010. Fish oil diets do not improve insulin sensitivity and secretion in healthy adult male pigs. Br J Nutr 103:189-196.

Catalano KJ, Stefanovski D, Bergman RN. 2010. Critical role of the mesenteric depot versus other intra-abdominal adipose depots in the development of insulin resistance in young rats. Diabetes 59:1416-1423.

Chapman J, Miles PD, Ofrecio JM, Neels JG, Yu JG, Resnik JL, Wilkes J, Talukdar S, Thapar D, Johnson K, Sears DD. 2010. Osteopontin is required for the early onset of high fat diet-induced insulin resistance in mice. PLoS One 5:e13959.

Chawla A, Nguyen KD, Goh YP. 2011. Macrophage-mediated inflammation in metabolic disease. Nat Rev Immunol 11:738-749.

Chen A, Mumick S, Zhang C, Lamb J, Dai H, Weingarth D, Mudgett J, Chen H, MacNeil DJ, Reitman ML, Qian S. 2005. Diet induction of monocyte chemoattractant protein-1 and its impact on obesity. Obes Res 13:1311-1320.

Chen D, Wang MW. 2005. Development and application of rodent models for type 2 diabetes. Diabetes Obes Metab 7:307-317.

Cho HP, Nakamura M, Clarke SD. 1999a. Cloning, expression, and fatty acid regulation of the human delta-5 desaturase. J Biol Chem 274:37335-37339.

Cho HP, Nakamura MT, Clarke SD. 1999b. Cloning, expression, and nutritional regulation of the mammalian Delta-6 desaturase. J Biol Chem 274:471-477.

Choe E, Min DB. 2006. Mechanisms and Factors for Edible Oil Oxidation. Comprehensive Reviews in Food Science and Food Safety 5:169-186.

Cinti S. 2005. The adipose organ. Prostaglandins Leukot Essent Fatty Acids 73:9-15.

Cinti S, Mitchell G, Barbatelli G, Murano I, Ceresi E, Faloia E, Wang S, Fortier M, Greenberg AS, Obin MS. 2005. Adipocyte death defines macrophage localization and function in adipose tissue of obese mice and humans. J Lipid Res 46:2347-2355.

Clegg DJ, Benoit SC, Reed JA, Woods SC, Dunn-Meynell A, Levin BE. 2005. Reduced anorexic effects of insulin in obesity-prone rats fed a moderate-fat diet. Am J Physiol Regul Integr Comp Physiol 288:R981-986.

Cohen P, Miyazaki M, Socci ND, Hagge-Greenberg A, Liedtke W, Soukas AA, Sharma R, Hudgins LC, Ntambi JM, Friedman JM. 2002. Role for stearoyl-CoA desaturase-1 in leptin-mediated weight loss. Science 297:240-243.

Cook KS, Min HY, Johnson D, Chaplinsky RJ, Flier JS, Hunt CR, Spiegelman BM. 1987. Adipsin: a circulating serine protease homolog secreted by adipose tissue and sciatic nerve. Science 237:402-405.

Crooks SW, Stockley RA. 1998. Leukotriene B4. Int J Biochem Cell Biol 30:173-178.

Damude HG, Kinney AJ. 2008. Enhancing plant seed oils for human nutrition. Plant Physiol 147:962-968.

de Oliveira CC, Acedo SC, Pedrazzoli J, Jr., Saad MJ, Gambero A. 2009. Depot-specific alterations to insulin signaling in mesenteric adipose tissue during intestinal inflammatory response. Int Immunopharmacol 9:396-402.

de Urquiza AM, Liu S, Sjoberg M, Zetterstrom RH, Griffiths W, Sjovall J, Perlmann T. 2000. Docosahexaenoic acid, a ligand for the retinoid X receptor in mouse brain. Science 290:2140-2144.

de Vogel-van den Bosch HM, Bunger M, de Groot PJ, Bosch-Vermeulen H, Hooiveld GJ, Muller M. 2008a. PPARalpha-mediated effects of dietary lipids on intestinal barrier gene expression. BMC Genomics 9:231.

de Vogel-van den Bosch HM, de Wit NJ, Hooiveld GJ, Vermeulen H, van der Veen JN, Houten SM, Kuipers F, Muller M, van der Meer R. 2008b. A cholesterol-free, high-fat diet suppresses gene expression of cholesterol transporters in murine small intestine. Am J Physiol Gastrointest Liver Physiol 294:G1171-1180.

de Wit NJ, Boekschoten MV, Bachmair EM, Hooiveld GJ, de Groot PJ, Rubio-Aliaga I, Daniel H, Muller M. 2010. Dose-dependent effects of dietary fat on development of obesity in relation to intestinal differential gene expression in C57BL/6J mice. PLoS One 6:e19145.

Deban L, Correale C, Vetrano S, Malesci A, Danese S. 2008. Multiple pathogenic roles of microvasculature in inflammatory bowel disease: a Jack of all trades. Am J Pathol 172:1457-1466.

Deckelbaum RJ. 2010. n-6 and n-3 Fatty acids and atherosclerosis: ratios or amounts? Arterioscler Thromb Vasc Biol 30:2325-2326.

Deiuliis J, Shah Z, Shah N, Needleman B, Mikami D, Narula V, Perry K, Hazey J, Kampfrath T, Kollengode M, Sun Q, Satoskar AR, Lumeng C, Moffatt-Bruce S, Rajagopalan S. 2011. Visceral adipose inflammation in obesity is associated with critical alterations in tregulatory cell numbers. PLoS One 6:e16376.

Denhardt DT, Guo X. 1993. Osteopontin: a protein with diverse functions. FASEB J 7:1475-1482.

Despres JP, Nadeau A, Tremblay A, Ferland M, Moorjani S, Lupien PJ, Theriault G, Pinault S, Bouchard C. 1989. Role of deep abdominal fat in the association between regional adipose tissue distribution and glucose tolerance in obese women. Diabetes 38:304-309.

DGE. 2006. Evidenzbasierte Leitlinie. Fettkonsum und Prävention ausgewählter ernährungsmitbedingter Krankheiten. Internet: www.dge.de/pdf/ws/II-fett/DGE-Leitlinie-Fett-11-2006.pdf. Access: February 18, 2012.

Dobrzyn A, Ntambi JM. 2004. The role of stearoyl-CoA desaturase in body weight regulation. Trends Cardiovasc Med 14:77-81.

Donath MY, Shoelson SE. 2011. Type 2 diabetes as an inflammatory disease. Nat Rev Immunol 11:98-107.

Ehringer W, Belcher D, Wassall SR, Stillwell W. 1990. A comparison of the effects of linolenic (18:3 omega 3) and docosahexaenoic (22:6 omega 3) acids on phospholipid bilayers. Chem Phys Lipids 54:79-88.

Ellingsgaard H, Ehses JA, Hammar EB, Van Lommel L, Quintens R, Martens G, Kerr-Conte J, Pattou F, Berney T, Pipeleers D, Halban PA, Schuit FC, Donath MY. 2008. Interleukin-6 regulates pancreatic alpha-cell mass expansion. Proc Natl Acad Sci U S A 105:13163-13168.

Else PL, Hulbert AJ. 2003. Membranes as metabolic pacemakers. Clin Exp Pharmacol Physiol 30:559-564.

Engeset D, Andersen V, Hjartaker A, Lund E. 2007. Consumption of fish and risk of colon cancer in the Norwegian Women and Cancer (NOWAC) study. Br J Nutr 98:576-582.

EPAX. 2012. Composition of EPAX 1050 TG. Internet: http://www.epax.com/Products/EPAX_1050_TG. Access: January, 27, 2012.

Eritsland J, Seljeflot I, Abdelnoor M, Arnesen H, Torjesen PA. 1994. Long-term effects of n-3 fatty acids on serum lipids and glycaemic control. Scand J Clin Lab Invest 54:273-280.

Ernst E. 1989. Effects of n-3 fatty acids on blood rheology. J Intern Med Suppl 731:129-132.

Fan CY, Pan J, Chu R, Lee D, Kluckman KD, Usuda N, Singh I, Yeldandi AV, Rao MS, Maeda N, Reddy JK. 1996. Hepatocellular and hepatic peroxisomal alterations in mice with a disrupted peroxisomal fatty acyl-coenzyme A oxidase gene. J Biol Chem 271:24698-24710.

FAO. 2002. Food energy - methods of analysis and conversion factors. Internet: http://www.fao.org/docrep/006/Y5022E/y5022e04.htm#fn9. Access: January 17, 2012.

Fasching P, Ratheiser K, Schneeweiss B, Rohac M, Nowotny P, Waldhausl W. 1996. No effect of short-term dietary supplementation of saturated and poly- and monounsaturated fatty acids on insulin secretion and sensitivity in healthy men. Ann Nutr Metab 40:116-122.

Faust IM, Johnson PR, Stern JS, Hirsch J. 1978. Diet-induced adipocyte number increase in adult rats: a new model of obesity. Am J Physiol 235:E279-286.

Fedor D, Kelley DS. 2009. Prevention of insulin resistance by n-3 polyunsaturated fatty acids. Curr Opin Clin Nutr Metab Care 12:138-146.

Feuerer M, Herrero L, Cipolletta D, Naaz A, Wong J, Nayer A, Lee J, Goldfine AB, Benoist C, Shoelson S, Mathis D. 2009. Lean, but not obese, fat is enriched for a unique population of regulatory T cells that affect metabolic parameters. Nat Med 15:930-939.

Fietta P. 2005. Focus on leptin, a pleiotropic hormone. Minerva Med 96:65-75.

Finucane MM, Stevens GA, Cowan MJ, Danaei G, Lin JK, Paciorek CJ, Singh GM, Gutierrez HR, Lu Y, Bahalim AN, Farzadfar F, Riley LM, Ezzati M. 2011. National, regional, and global trends in body-mass index since 1980: systematic analysis of health examination surveys and epidemiological studies with 960 country-years and 9.1 million participants. Lancet 377:557-567.

Flachs P, Horakova O, Brauner P, Rossmeisl M, Pecina P, Franssen-van Hal N, Ruzickova J, Sponarova J, Drahota Z, Vlcek C, Keijer J, Houstek J, Kopecky J. 2005. Polyunsaturated fatty acids of marine origin upregulate mitochondrial biogenesis and induce beta-oxidation in white fat. Diabetologia 48:2365-2375.

Flachs P, Mohamed-Ali V, Horakova O, Rossmeisl M, Hosseinzadeh-Attar MJ, Hensler M, Ruzickova J, Kopecky J. 2006. Polyunsaturated fatty acids of marine origin induce adiponectin in mice fed a high-fat diet. Diabetologia 49:394-397.

Flachs P, Rossmeisl M, Bryhn M, Kopecky J. 2009. Cellular and molecular effects of n-3 polyunsaturated fatty acids on adipose tissue biology and metabolism. Clin Sci (Lond) 116:1-16.

Flachs P, Ruhl R, Hensler M, Janovska P, Zouhar P, Kus V, Macek Jilkova Z, Papp E, Kuda O, Svobodova M, Rossmeisl M, Tsenov G, Mohamed-Ali V, Kopecky J. 2011. Synergistic induction of lipid catabolism and anti-inflammatory lipids in white fat of dietary obese mice in response to calorie restriction and n-3 fatty acids. Diabetologia 54:2626-2638.

Fleischer J, Stein EM, Bessler M, Della Badia M, Restuccia N, Olivero-Rivera L, McMahon DJ, Silverberg SJ. 2008. The decline in hip bone density after gastric bypass surgery is associated with extent of weight loss. J Clin Endocrinol Metab 93:3735-3740.

Forman BM, Chen J, Evans RM. 1997. Hypolipidemic drugs, polyunsaturated fatty acids, and eicosanoids are ligands for peroxisome proliferator-activated receptors alpha and delta. Proc Natl Acad Sci U S A 94:4312-4317.

Franzen A, Heinegard D. 1985. Isolation and characterization of two sialoproteins present only in bone calcified matrix. Biochem J 232:715-724.

Frayn KN. 2010. Metabolic Regulation. A Human Perspective, 3 ed: Wiley-Blackwell.

Frayn KN, Karpe F, Fielding BA, Macdonald IA, Coppack SW. 2003. Integrative physiology of human adipose tissue. Int J Obes Relat Metab Disord 27:875-888.

Fried SK, Ross RR. 2004. Biology of visceral adipose tissue. Handbook of obesity, 2 ed. New York, Basel: Marcel Dekker, Inc.

Fritsche K. 2006. Fatty acids as modulators of the immune response. Annu Rev Nutr 26:45-73.

Fritsche K. 2007. Important differences exist in the dose-response relationship between diet and immune cell fatty acids in humans and rodents. Lipids 42:961-979.

Fromme T, Klingenspor M. 2010. Uncoupling protein 1 expression and high-fat diets. Am J Physiol Regul Integr Comp Physiol 300:R1-8.

Fujioka S, Matsuzawa Y, Tokunaga K, Tarui S. 1987. Contribution of intra-abdominal fat accumulation to the impairment of glucose and lipid metabolism in human obesity. Metabolism 36:54-59.

Fujisaka S, Usui I, Bukhari A, Ikutani M, Oya T, Kanatani Y, Tsuneyama K, Nagai Y, Takatsu K, Urakaze M, Kobayashi M, Tobe K. 2009. Regulatory mechanisms for adipose tissue M1 and M2 macrophages in diet-induced obese mice. Diabetes 58:2574-2582.

Fung-Leung WP, Schilham MW, Rahemtulla A, Kundig TM, Vollenweider M, Potter J, van Ewijk W, Mak TW. 1991. CD8 is needed for development of cytotoxic T cells but not helper T cells. Cell 65:443-449.

Gabrielsson BG, Wikstrom J, Jakubowicz R, Marmon SK, Carlsson NG, Jansson N, Gan LM, Undeland I, Lonn M, Holmang A, Sandberg AS. 2012. Dietary herring improves plasma lipid profiles and reduces atherosclerosis in obese low-density lipoprotein receptor-deficient mice. Int J Mol Med 29:331-337.

Gallou-Kabani C, Vige A, Gross MS, Rabes JP, Boileau C, Larue-Achagiotis C, Tome D, Jais JP, Junien C. 2007. C57BL/6J and A/J mice fed a high-fat diet delineate components of metabolic syndrome. Obesity (Silver Spring) 15:1996-2005.

Gardner HW. 1989. Oxygen radical chemistry of polyunsaturated fatty acids. Free Radic Biol Med 7:65-86.

Gehrmann W, Elsner M, Lenzen S. 2010. Role of metabolically generated reactive oxygen species for lipotoxicity in pancreatic beta-cells. Diabetes Obes Metab 12 Suppl 2:149-158.

Geissmann F, Manz MG, Jung S, Sieweke MH, Merad M, Ley K. 2010. Development of monocytes, macrophages, and dendritic cells. Science 327:656-661.

Gerster H. 1998. Can adults adequately convert alpha-linolenic acid (18:3n-3) to eicosapentaenoic acid (20:5n-3) and docosahexaenoic acid (22:6n-3)? Int J Vitam Nutr Res 68:159-173.

Ghosh S, Karin M. 2002. Missing pieces in the NF-kappaB puzzle. Cell 109 Suppl:S81-96.

Giacco R, Cuomo V, Vessby B, Uusitupa M, Hermansen K, Meyer BJ, Riccardi G, Rivellese AA. 2007. Fish oil, insulin sensitivity, insulin secretion and glucose tolerance in healthy people: is there any effect of fish oil supplementation in relation to the type of background diet and habitual dietary intake of n-6 and n-3 fatty acids? Nutr Metab Cardiovasc Dis 17:572-580.

GISSI-Investigators. 1999. Dietary supplementation with n-3 polyunsaturated fatty acids and vitamin E after myocardial infarction: results of the GISSI-Prevenzione trial. Gruppo Italiano per lo Studio della Sopravvivenza nell'Infarto miocardico. Lancet 354:447-455.

Goldberg RJ, Katz J. 2007. A meta-analysis of the analgesic effects of omega-3 polyunsaturated fatty acid supplementation for inflammatory joint pain. Pain 129:210-223.

Gomez-Ambrosi J, Catalan V, Ramirez B, Rodriguez A, Colina I, Silva C, Rotellar F, Mugueta C, Gil MJ, Cienfuegos JA, Salvador J, Fruhbeck G. 2007. Plasma osteopontin levels and expression in adipose tissue are increased in obesity. J Clin Endocrinol Metab 92:3719-3727.

Gomolka B, Siegert E, Blossey K, Schunck WH, Rothe M, Weylandt KH. 2010. Analysis of omega-3 and omega-6 fatty acid-derived lipid metabolite formation in human and mouse blood samples. Prostaglandins Other Lipid Mediat 94:81-87.

Gonzalez-Periz A, Horrillo R, Ferre N, Gronert K, Dong B, Moran-Salvador E, Titos E, Martinez-Clemente M, Lopez-Parra M, Arroyo V, Claria J. 2009. Obesity-induced insulin resistance and hepatic steatosis are alleviated by omega-3 fatty acids: a role for resolvins and protectins. FASEB J 23:1946-1957.

Gordon S, Martinez FO. 2010. Alternative activation of macrophages: mechanism and functions. Immunity 32:593-604.

Gorjao R, Azevedo-Martins AK, Rodrigues HG, Abdulkader F, Arcisio-Miranda M, Procopio J, Curi R. 2009. Comparative effects of DHA and EPA on cell function. Pharmacol Ther 122:56-64.

Gorjao R, Verlengia R, Lima TM, Soriano FG, Boaventura MF, Kanunfre CC, Peres CM, Sampaio SC, Otton R, Folador A, Martins EF, Curi TC, Portiolli EP, Newsholme P, Curi R. 2006. Effect of docosahexaenoic acid-rich fish oil supplementation on human leukocyte function. Clin Nutr 25:923-938.

Groeger AL, Cipollina C, Cole MP, Woodcock SR, Bonacci G, Rudolph TK, Rudolph V, Freeman BA, Schopfer FJ. 2010. Cyclooxygenase-2 generates anti-inflammatory mediators from omega-3 fatty acids. Nat Chem Biol 6:433-441.

Guerra C, Koza RA, Yamashita H, Walsh K, Kozak LP. 1998. Emergence of brown adipocytes in white fat in mice is under genetic control. Effects on body weight and adiposity. J Clin Invest 102:412-420.

Guilherme A, Virbasius JV, Puri V, Czech MP. 2008. Adipocyte dysfunctions linking obesity to insulin resistance and type 2 diabetes. Nat Rev Mol Cell Biol 9:367-377.

Guo KY, Halo P, Leibel RL, Zhang Y. 2004. Effects of obesity on the relationship of leptin mRNA expression and adipocyte size in anatomically distinct fat depots in mice. Am J Physiol Regul Integr Comp Physiol 287:R112-119.

Hall MN, Chavarro JE, Lee IM, Willett WC, Ma J. 2008. A 22-year prospective study of fish, n-3 fatty acid intake, and colorectal cancer risk in men. Cancer Epidemiol Biomarkers Prev 17:1136-1143.

Hallermayer R. 1976. TMSH-method, DGF-Einheitsmethoden C-VI. Deutsche Lebensmittelrundscha 10:356-359.

Hanna Z, Rebai N, Poudrier J, Jolicoeur P. 2001. Distinct regulatory elements are required for faithful expression of human CD4 in T cells, macrophages, and dendritic cells of transgenic mice. Blood 98:2275-2278.

Harris W. 2010. Omega-6 and omega-3 fatty acids: partners in prevention. Curr Opin Clin Nutr Metab Care 13:125-129.

Hartweg J, Perera R, Montori V, Dinneen S, Neil HA, Farmer A. 2008. Omega-3 polyunsaturated fatty acids (PUFA) for type 2 diabetes mellitus. Cochrane Database Syst Rev:CD003205.

Hauner H. 2005. Secretory factors from human adipose tissue and their functional role. Proc Nutr Soc 64:163-169.

Heilmann K, Hoffmann U, Witte E, Loddenkemper C, Sina C, Schreiber S, Hayford C, Holzlohner P, Wolk K, Tchatchou E, Moos V, Zeitz M, Sabat R, Gunthert U, Wittig BM. 2009. Osteopontin as two-sided mediator of intestinal inflammation. J Cell Mol Med 13:1162-1174.

Heldmaier G. 1975. Metabolic and thermoregulatory responses to heat and cold in the Djungarian hamster, Phodopus sungorus. Journal of Comparative Physiology B: Biochemical, Systemic, and Environmental Physiology 102:115-122.

Hempenius RA, Lina BA, Haggitt RC. 2000. Evaluation of a subchronic (13-week) oral toxicity study, preceded by an in utero exposure phase, with arachidonic acid oil derived from Mortierella alpina in rats. Food Chem Toxicol 38:127-139.

Hensler M, Bardova K, Jilkova ZM, Wahli W, Meztger D, Chambon P, Kopecky J, Flachs P. 2011. The inhibition of fat cell proliferation by n-3 fatty acids in dietary obese mice. Lipids Health Dis 10:128.

Hoffstedt J, Arner E, Wahrenberg H, Andersson DP, Qvisth V, Lofgren P, Ryden M, Thorne A, Wiren M, Palmer M, Thorell A, Toft E, Arner P. 2010. Regional impact of adipose tissue morphology on the metabolic profile in morbid obesity. Diabetologia 53:2496-2503.

Hooper L, Thompson RL, Harrison RA, Summerbell CD, Moore H, Worthington HV, Durrington PN, Ness AR, Capps NE, Davey Smith G, Riemersma RA, Ebrahim SB. 2004. Omega 3 fatty acids for prevention and treatment of cardiovascular disease. Cochrane Database Syst Rev:CD003177.

Horie T, Nakamaru M, Masubuchi Y. 1998. Docosahexaenoic acid exhibits a potent protection of small intestine from methotrexate-induced damage in mice. Life Sci 62:1333-1338.

Hotamisligil GS. 2006. Inflammation and metabolic disorders. Nature 444:860-867.

Hotamisligil GS, Shargill NS, Spiegelman BM. 1993. Adipose expression of tumor necrosis factor-alpha: direct role in obesity-linked insulin resistance. Science 259:87-91.

Huang XF, Xin X, McLennan P, Storlien L. 2004. Role of fat amount and type in ameliorating diet-induced obesity: insights at the level of hypothalamic arcuate nucleus leptin receptor, neuropeptide Y and pro-opiomelanocortin mRNA expression. Diabetes Obes Metab 6:35-44.

Huber J, Loffler M, Bilban M, Reimers M, Kadl A, Todoric J, Zeyda M, Geyeregger R, Schreiner M, Weichhart T, Leitinger N, Waldhausl W, Stulnig TM. 2007. Prevention of high-fat diet-induced adipose tissue remodeling in obese diabetic mice by n-3 polyunsaturated fatty acids. Int J Obes (Lond) 31:1004-1013.

Huleatt JW, Lefrancois L. 1995. Antigen-driven induction of CD11c on intestinal intraepithelial lymphocytes and CD8+ T cells in vivo. J Immunol 154:5684-5693.

Ibrahim MM. 2009. Subcutaneous and visceral adipose tissue: structural and functional differences. Obes Rev 11:11-18.

Ide T. 2005. Interaction of fish oil and conjugated linoleic acid in affecting hepatic activity of lipogenic enzymes and gene expression in liver and adipose tissue. Diabetes 54:412-423.

Ikemoto S, Takahashi M, Tsunoda N, Maruyama K, Itakura H, Ezaki O. 1996. High-fat diet-induced hyperglycemia and obesity in mice: differential effects of dietary oils. Metabolism 45:1539-1546.

Ilan Y, Maron R, Tukpah AM, Maioli TU, Murugaiyan G, Yang K, Wu HY, Weiner HL. 2010. Induction of regulatory T cells decreases adipose inflammation and alleviates insulin resistance in ob/ob mice. Proc Natl Acad Sci U S A 107:9765-9770.

Iozzo P. 2009. Viewpoints on the way to the consensus session: where does insulin resistance start? The adipose tissue. Diabetes Care 32 Suppl 2:S168-173.

ISSFAL ISftSoFAaL. 2004. Recommendations for intake of polyunsaturated fatty acids in healthy adults (Statement 3 PUFA in Adults). Internet: www.issfal.org. Access: February 18, 2012.

Jelenik T, Rossmeisl M, Kuda O, Jilkova ZM, Medrikova D, Kus V, Hensler M, Janovska P, Miksik I, Baranowski M, Gorski J, Hebrard S, Jensen TE, Flachs P, Hawley S, Viollet B, Kopecky J. 2010. AMP-activated protein kinase alpha2 subunit is required for the preservation of hepatic insulin sensitivity by n-3 polyunsaturated fatty acids. Diabetes 59:2737-2746.

Jeyakumar SM, Prashant A, Rani KS, Laxmi R, Vani A, Kumar PU, Vajreswari A. 2011. Chronic consumption of trans-fat-rich diet increases hepatic cholesterol levels and

impairs muscle insulin sensitivity without leading to hepatic steatosis and hypertriglyceridemia in female Fischer rats. Ann Nutr Metab 58:272-280.

Ji S, Hardy RW, Wood PA. 2009. Transgenic expression of n-3 fatty acid desaturase (fat-1) in C57/BL6 mice: Effects on glucose homeostasis and body weight. J Cell Biochem 107:809-817.

Jiang WG, Bryce RP, Horrobin DF, Mansel RE. 1998. Regulation of tight junction permeability and occludin expression by polyunsaturated fatty acids. Biochem Biophys Res Commun 244:414-420.

Jo J, Gavrilova O, Pack S, Jou W, Mullen S, Sumner AE, Cushman SW, Periwal V. 2009. Hypertrophy and/or Hyperplasia: Dynamics of Adipose Tissue Growth. PLoS Comput Biol 5:e1000324.

Jump DB. 2002. Dietary polyunsaturated fatty acids and regulation of gene transcription. Curr Opin Lipidol 13:155-164.

Jung UJ, Millman PN, Tall AR, Deckelbaum RJ. 2011. n-3 fatty acids ameliorate hepatic steatosis and dysfunction after LXR agonist ingestion in mice. Biochim Biophys Acta 1811:491-497.

Kahn SE, Hull RL, Utzschneider KM. 2006. Mechanisms linking obesity to insulin resistance and type 2 diabetes. Nature 444:840-846.

Kainuma E, Watanabe M, Tomiyama-Miyaji C, Inoue M, Kuwano Y, Ren H, Abo T. 2009. Association of glucocorticoid with stress-induced modulation of body temperature, blood glucose and innate immunity. Psychoneuroendocrinology 34:1459-1468.

Kajikawa S, Harada T, Kawashima A, Imada K, Mizuguchi K. 2009. Highly purified eicosapentaenoic acid prevents the progression of hepatic steatosis by repressing monounsaturated fatty acid synthesis in high-fat/high-sucrose diet-fed mice. Prostaglandins Leukot Essent Fatty Acids 80:229-238.

Karpe F, Dickmann JR, Frayn KN. 2011. Fatty acids, obesity, and insulin resistance: time for a reevaluation. Diabetes 60:2441-2449.

Kasbi Chadli F, Andre A, Prieur X, Loirand G, Meynier A, Krempf M, Nguyen P, Ouguerram K. 2011. n-3 PUFA prevent metabolic disturbances associated with obesity and improve endothelial function in golden Syrian hamsters fed with a high-fat diet. Br J Nutr:1-11.

Kelly DP, Scarpulla RC. 2004. Transcriptional regulatory circuits controlling mitochondrial biogenesis and function. Genes Dev 18:357-368.

Kew S, Mesa MD, Tricon S, Buckley R, Minihane AM, Yaqoob P. 2004. Effects of oils rich in eicosapentaenoic and docosahexaenoic acids on immune cell composition and function in healthy humans. Am J Clin Nutr 79:674-681.

Khalfoun B, Thibault G, Bardos P, Lebranchu Y. 1996. Docosahexaenoic and eicosapentaenoic acids inhibit in vitro human lymphocyte-endothelial cell adhesion. Transplantation 62:1649-1657.

Kiefer FW, Neschen S, Pfau B, Legerer B, Neuhofer A, Kahle M, Hrabe de Angelis M, Schlederer M, Mair M, Kenner L, Plutzky J, Zeyda M, Stulnig TM. 2011. Osteopontin deficiency protects against obesity-induced hepatic steatosis and attenuates glucose production in mice. Diabetologia 54:2132-2142.

Kiefer FW, Zeyda M, Gollinger K, Pfau B, Neuhofer A, Weichhart T, Saemann MD, Geyeregger R, Schlederer M, Kenner L, Stulnig TM. 2010. Neutralization of osteopontin inhibits obesity-induced inflammation and insulin resistance. Diabetes 59:935-946.

Kiefer FW, Zeyda M, Todoric J, Huber J, Geyeregger R, Weichhart T, Aszmann O, Ludvik B, Silberhumer GR, Prager G, Stulnig TM. 2008. Osteopontin expression in human and murine obesity: extensive local up-regulation in adipose tissue but minimal systemic alterations. Endocrinology 149:1350-1357.

Kim CS, Lee SC, Kim YM, Kim BS, Choi HS, Kawada T, Kwon BS, Yu R. 2008. Visceral fat accumulation induced by a high-fat diet causes the atrophy of mesenteric lymph nodes in obese mice. Obesity (Silver Spring) 16:1261-1269.

Kim SP, Ellmerer M, Van Citters GW, Bergman RN. 2003. Primacy of hepatic insulin resistance in the development of the metabolic syndrome induced by an isocaloric moderate-fat diet in the dog. Diabetes 52:2453-2460.

Kinney NE, Antill RW. 1996. Role of olfaction in the formation of preference for high-fat foods in mice. Physiol Behav 59:475-478.

Kintscher U, Hartge M, Hess K, Foryst-Ludwig A, Clemenz M, Wabitsch M, Fischer-Posovszky P, Barth TF, Dragun D, Skurk T, Hauner H, Bluher M, Unger T, Wolf AM, Knippschild U, Hombach V, Marx N. 2008. T-lymphocyte infiltration in visceral adipose tissue: a primary event in adipose tissue inflammation and the development of obesity-mediated insulin resistance. Arterioscler Thromb Vasc Biol 28:1304-1310.

Kleemann R, van Erk M, Verschuren L, van den Hoek AM, Koek M, Wielinga PY, Jie A, Pellis L, Bobeldijk-Pastorova I, Kelder T, Toet K, Wopereis S, Cnubben N, Evelo C, van Ommen B, Kooistra T. 2010. Time-resolved and tissue-specific systems analysis of the pathogenesis of insulin resistance. PLoS One 5:e8817.

Kleiber M. 1932. Body size and metabolism. HIlgardia 6:315-353.

Kleiber M. 1961. The Fire of Life. New York: Wiley.

Kliewer SA, Sundseth SS, Jones SA, Brown PJ, Wisely GB, Koble CS, Devchand P, Wahli W, Willson TM, Lenhard JM, Lehmann JM. 1997. Fatty acids and eicosanoids regulate gene expression through direct interactions with peroxisome proliferator-activated receptors alpha and gamma. Proc Natl Acad Sci U S A 94:4318-4323.

Knight SC. 2008. Specialized perinodal fat fuels and fashions immunity. Immunity 28:135-138.

Koehler C, Ott P, Benke I, Hanefeld M. 2007. Comparison of the prevalence of the metabolic syndrome by WHO, AHA/NHLBI, and IDF definitions in a German population with type 2 diabetes: the Diabetes in Germany (DIG) Study. Horm Metab Res 39:632-635.

Kon S, Maeda M, Segawa T, Hagiwara Y, Horikoshi Y, Chikuma S, Tanaka K, Rashid MM, Inobe M, Chambers AF, Uede T. 2000. Antibodies to different peptides in osteopontin reveal complexities in the various secreted forms. J Cell Biochem 77:487-498.

Koni PA, Joshi SK, Temann UA, Olson D, Burkly L, Flavell RA. 2001. Conditional vascular cell adhesion molecule 1 deletion in mice: impaired lymphocyte migration to bone marrow. J Exp Med 193:741-754.

Koolman AH, Bloks VW, Oosterveer MH, Jonas I, Kuipers F, Sauer PJ, van Dijk G. 2010. Metabolic responses to long-term pharmacological inhibition of CB1-receptor activity in mice in relation to dietary fat composition. Int J Obes (Lond) 34:374-384.

Koves TR, Ussher JR, Noland RC, Slentz D, Mosedale M, Ilkayeva O, Bain J, Stevens R, Dyck JR, Newgard CB, Lopaschuk GD, Muoio DM. 2008. Mitochondrial overload and incomplete fatty acid oxidation contribute to skeletal muscle insulin resistance. Cell Metab 7:45-56.

Koza RA, Nikonova L, Hogan J, Rim JS, Mendoza T, Faulk C, Skaf J, Kozak LP. 2006. Changes in gene expression foreshadow diet-induced obesity in genetically identical mice. PLoS Genet 2:e81.

Kuda O, Jelenik T, Jilkova Z, Flachs P, Rossmeisl M, Hensler M, Kazdova L, Ogston N, Baranowski M, Gorski J, Janovska P, Kus V, Polak J, Mohamed-Ali V, Burcelin R, Cinti S, Bryhn M, Kopecky J. 2009. n-3 fatty acids and rosiglitazone improve insulin sensitivity through additive stimulatory effects on muscle glycogen synthesis in mice fed a high-fat diet. Diabetologia 52:941-951.

Kumashiro N, Erion DM, Zhang D, Kahn M, Beddow SA, Chu X, Still CD, Gerhard GS, Han X, Dziura J, Petersen KF, Samuel VT, Shulman GI. 2011. Cellular mechanism of insulin resistance in nonalcoholic fatty liver disease. Proc Natl Acad Sci U S A 108:16381-16385.

Kuratko CN, Salem N, Jr. 2009. Biomarkers of DHA status. Prostaglandins Leukot Essent Fatty Acids 81:111-118.

Kurlak LO, Stephenson TJ. 1999. Plausible explanations for effects of long chain polyunsaturated fatty acids (LCPUFA) on neonates. Arch Dis Child Fetal Neonatal Ed 80:F148-154.

Kus V, Flachs P, Kuda O, Bardova K, Janovska P, Svobodova M, Jilkova ZM, Rossmeisl M, Wang-Sattler R, Yu Z, Illig T, Kopecky J. 2011. Unmasking differential effects of rosiglitazone and pioglitazone in the combination treatment with n-3 fatty acids in mice fed a high-fat diet. PLoS One 6:e27126.

Lampe MA, Patarca R, Iregui MV, Cantor H. 1991. Polyclonal B cell activation by the Eta-1 cytokine and the development of systemic autoimmune disease. J Immunol 147:2902-2906.

Lancet. 2011. Editorial: Two days in New York: reflections on the UN NCD summit. Lancet Oncol 12:981.

Lankinen M, Schwab U, Erkkila A, Seppanen-Laakso T, Hannila ML, Mussalo H, Lehto S, Uusitupa M, Gylling H, Oresic M. 2009. Fatty fish intake decreases lipids related to inflammation and insulin signaling--a lipidomics approach. PLoS One 4:e5258.

Lee JY, Plakidas A, Lee WH, Heikkinen A, Chanmugam P, Bray G, Hwang DH. 2003. Differential modulation of Toll-like receptors by fatty acids: preferential inhibition by n-3 polyunsaturated fatty acids. J Lipid Res 44:479-486.

Lee JY, Sohn KH, Rhee SH, Hwang D. 2001. Saturated fatty acids, but not unsaturated fatty acids, induce the expression of cyclooxygenase-2 mediated through Toll-like receptor 4. J Biol Chem 276:16683-16689.

Lemonnier D. 1972. Effect of age, sex, and sites on the cellularity of the adipose tissue in mice and rats rendered obese by a high-fat diet. J Clin Invest 51:2907-2915.

Lengqvist J, Mata De Urquiza A, Bergman AC, Willson TM, Sjovall J, Perlmann T, Griffiths WJ. 2004. Polyunsaturated fatty acids including docosahexaenoic and arachidonic acid bind to the retinoid X receptor alpha ligand-binding domain. Mol Cell Proteomics 3:692-703.

Lewis KE, Kirk EA, McDonald TO, Wang S, Wight TN, O'Brien KD, Chait A. 2004. Increase in serum amyloid a evoked by dietary cholesterol is associated with increased atherosclerosis in mice. Circulation 110:540-545.

Ley RE, Backhed F, Turnbaugh P, Lozupone CA, Knight RD, Gordon JI. 2005. Obesity alters gut microbial ecology. Proc Natl Acad Sci U S A 102:11070-11075.

Li H, Lelliott C, Hakansson P, Ploj K, Tuneld A, Verolin-Johansson M, Benthem L, Carlsson B, Storlien L, Michaelsson E. 2008. Intestinal, adipose, and liver inflammation in diet-induced obese mice. Metabolism 57:1704-1710.

Li H, Ruan XZ, Powis SH, Fernando R, Mon WY, Wheeler DC, Moorhead JF, Varghese Z. 2005. EPA and DHA reduce LPS-induced inflammation responses in HK-2 cells: evidence for a PPAR-gamma-dependent mechanism. Kidney Int 67:867-874.

Li S, Shin HJ, Ding EL, van Dam RM. 2009. Adiponectin levels and risk of type 2 diabetes: a systematic review and meta-analysis. JAMA 302:179-188.

Liaw L, Almeida M, Hart CE, Schwartz SM, Giachelli CM. 1994. Osteopontin promotes vascular cell adhesion and spreading and is chemotactic for smooth muscle cells in vitro. Circ Res 74:214-224.

Liaw L, Birk DE, Ballas CB, Whitsitt JS, Davidson JM, Hogan BL. 1998. Altered wound healing in mice lacking a functional osteopontin gene (spp1). J Clin Invest 101:1468-1478.

Lichtman AH, Clinton SK, Iiyama K, Connelly PW, Libby P, Cybulsky MI. 1999. Hyperlipidemia and atherosclerotic lesion development in LDL receptor-deficient mice fed defined semipurified diets with and without cholate. Arterioscler Thromb Vasc Biol 19:1938-1944.

Lina BA, Wolterbeek AP, Suwa Y, Fujikawa S, Ishikura Y, Tsuda S, Dohnalek M. 2006. Subchronic (13-week) oral toxicity study, preceded by an in utero exposure phase, with arachidonate-enriched triglyceride oil (SUNTGA40S) in rats. Food Chem Toxicol 44:326-335.

Livak KJ, Schmittgen TD. 2001. Analysis of relative gene expression data using real-time quantitative PCR and the 2(-Delta Delta C(T)) Method. Methods 25:402-408.

Lobstein T, Baur L, Uauy R. 2004. Obesity in children and young people: a crisis in public health. Obes Rev 5 Suppl 1:4-104.

Lodish H, Berk, Krieger, Kaiser, Scott, Bretsher, Ploegh, Matsuaira. 2008. Molecular Cell Biology: W.H. Freeman and Company.

Lolmede K, Duffaut C, Zakaroff-Girard A, Bouloumie A. 2011. Immune cells in adipose tissue: key players in metabolic disorders. Diabetes Metab 37:283-290.

Lord GM, Matarese G, Howard JK, Baker RJ, Bloom SR, Lechler RI. 1998. Leptin modulates the T-cell immune response and reverses starvation-induced immunosuppression. Nature 394:897-901.

Lumeng CN, Bodzin JL, Saltiel AR. 2007. Obesity induces a phenotypic switch in adipose tissue macrophage polarization. J Clin Invest 117:175-184.

Lumeng CN, DelProposto JB, Westcott DJ, Saltiel AR. 2008. Phenotypic switching of adipose tissue macrophages with obesity is generated by spatiotemporal differences in macrophage subtypes. Diabetes 57:3239-3246.

Ma T, Liaset B, Hao Q, Petersen RK, Fjaere E, Ngo HT, Lillefosse HH, Ringholm S, Sonne SB, Treebak JT, Pilegaard H, Froyland L, Kristiansen K, Madsen L. 2011. Sucrose counteracts the anti-inflammatory effect of fish oil in adipose tissue and increases obesity development in mice. PLoS One 6:e21647.

Machado RM, Stefano JT, Oliveira CP, Mello ES, Ferreira FD, Nunes VS, de Lima VM, Quintao EC, Catanozi S, Nakandakare ER, Lottenberg AM. 2010. Intake of trans fatty acids causes nonalcoholic steatohepatitis and reduces adipose tissue fat content. J Nutr 140:1127-1132.

MacQueen HA, Pond CM. 1998. Immunofluorescent localisation of tumour necrosis factor-alpha receptors on the popliteal lymph node and the surrounding adipose tissue following a simulated immune challenge. J Anat 192 (Pt 2):223-231.

Madsen L, Petersen RK, Kristiansen K. 2005. Regulation of adipocyte differentiation and function by polyunsaturated fatty acids. Biochim Biophys Acta 1740:266-286.

Maffei M, Halaas J, Ravussin E, Pratley RE, Lee GH, Zhang Y, Fei H, Kim S, Lallone R, Ranganathan S, et al. 1995. Leptin levels in human and rodent: measurement of plasma leptin and ob RNA in obese and weight-reduced subjects. Nat Med 1:1155-1161.

Magdeldin S, Elewa Y, Ikeda T, Ikei J, Zhang Y, Xu B, Nameta M, Fujinaka H, Yoshida Y, Yaoita E, Yamamoto T. 2009. Dietary supplementation with arachidonic acid but not eicosapentaenoic or docosahexaenoic acids alter lipids metabolism in C57BL/6J mice. Gen Physiol Biophys 28:266-275.

Markovic O, O'Reilly G, Fussell HM, Turner SJ, Calder PC, Howell WM, Grimble RF. 2004. Role of single nucleotide polymorphisms of pro-inflammatory cytokine genes in the relationship between serum lipids and inflammatory parameters, and the lipid-lowering effect of fish oil in healthy males. Clin Nutr 23:1084-1095.

Martin APSRRKRE. 1986. United States Department of Agriculture Provisional table on the content of omega-3 fatty acids and other fat componnents in selected food. In: Health Effects of Polyunsaturated Fatty Acids in Sea Foods: Academic Press.

Martin de Santa Olalla L, Sanchez Muniz FJ, Vaquero MP. 2009. N-3 fatty acids in glucose metabolism and insulin sensitivity. Nutr Hosp 24:113-127.

Mathes WF, Kelly SA, Pomp D. 2011. Advances in comparative genetics: influence of genetics on obesity. Br J Nutr 106 Suppl 1:S1-10.

Matsuzawa Y, Shimomura I, Nakamura T, Keno Y, Tokunaga K. 1995. Pathophysiology and pathogenesis of visceral fat obesity. Ann N Y Acad Sci 748:399-406.

Mattacks CA, Pond CM. 1997. The effects of feeding suet-enriched chow on site-specific differences in the composition of triacylglycerol fatty acids in adipose tissue and its interactions in vitro with lymphoid cells. Br J Nutr 77:621-643.

Mattacks CA, Sadler D, Pond CM. 2002. The effects of dietary lipids on adrenergically-stimulated lipolysis in perinodal adipose tissue following prolonged activation of a single lymph node. Br J Nutr 87:375-382.

Mattacks CA, Sadler D, Pond CM. 2003. The cellular structure and lipid/protein composition of adipose tissue surrounding chronically stimulated lymph nodes in rats. J Anat 202:551-561.

Mattacks CA, Sadler D, Pond CM. 2004a. Site-specific differences in fatty acid composition of dendritic cells and associated adipose tissue in popliteal depot, mesentery, and omentum and their modulation by chronic inflammation and dietary lipids. Lymphat Res Biol 2:107-129.

Mattacks CA, Sadler D, Pond CM. 2004b. The effects of dietary lipids on dendritic cells in perinodal adipose tissue during chronic mild inflammation. Br J Nutr 91:883-892.

Matthews DR, Hosker JP, Rudenski AS, Naylor BA, Treacher DF, Turner RC. 1985. Homeostasis model assessment: insulin resistance and beta-cell function from fasting plasma glucose and insulin concentrations in man. Diabetologia 28:412-419.

Maxwell KN, Soccio RE, Duncan EM, Sehayek E, Breslow JL. 2003. Novel putative SREBP and LXR target genes identified by microarray analysis in liver of cholesterol-fed mice. J Lipid Res 44:2109-2119.

McKenney JM, Sica D. 2007. Role of prescription omega-3 fatty acids in the treatment of hypertriglyceridemia. Pharmacotherapy 27:715-728.

Meade CJ, Mertin J. 1978. Fatty acids and immunity. Adv Lipid Res 16:127-165.

Mebius RE, Kraal G. 2005. Structure and function of the spleen. Nat Rev Immunol 5:606-616.

Merritt RJ, Auestad N, Kruger C, Buchanan S. 2003. Safety evaluation of sources of docosahexaenoic acid and arachidonic acid for use in infant formulas in newborn piglets. Food Chem Toxicol 41:897-904.

Meydani SN, Shapiro AC, Meydani M, Macauley JB, Blumberg JB. 1987. Effect of age and dietary fat (fish, corn and coconut oils) on tocopherol status of C57BL/6Nia mice. Lipids 22:345-350.

Mihalik SJ, Goodpaster BH, Kelley DE, Chace DH, Vockley J, Toledo FG, DeLany JP. 2010. Increased levels of plasma acylcarnitines in obesity and type 2 diabetes and identification of a marker of glucolipotoxicity. Obesity (Silver Spring) 18:1695-1700.

Milne CD, Paige CJ. 2006. IL-7: a key regulator of B lymphopoiesis. Semin Immunol 18:20-30.

Montgomery P, Richardson AJ. 2008. Omega-3 fatty acids for bipolar disorder. Cochrane Database Syst Rev:CD005169.

Mori T, Kondo H, Hase T, Tokimitsu I, Murase T. 2007. Dietary fish oil upregulates intestinal lipid metabolism and reduces body weight gain in C57BL/6J mice. J Nutr 137:2629-2634.

Muhlhausler BS, Cook-Johnson R, James M, Miljkovic D, Duthoit E, Gibson R. 2010. Opposing effects of omega-3 and omega-6 long chain polyunsaturated Fatty acids on the expression of lipogenic genes in omental and retroperitoneal adipose depots in the rat. J Nutr Metab 2010.

Murray PJ. 2005. The primary mechanism of the IL-10-regulated antiinflammatory response is to selectively inhibit transcription. Proc Natl Acad Sci U S A 102:8686-8691.

Murray PJ, Wynn TA. 2011. Protective and pathogenic functions of macrophage subsets. Nat Rev Immunol 11:723-737.

Musiek ES, Brooks JD, Joo M, Brunoldi E, Porta A, Zanoni G, Vidari G, Blackwell TS, Montine TJ, Milne GL, McLaughlin B, Morrow JD. 2008. Electrophilic cyclopentenone neuroprostanes are anti-inflammatory mediators formed from the peroxidation of the omega-3 polyunsaturated fatty acid docosahexaenoic acid. J Biol Chem 283:19927-19935.

Mustad VA, Demichele S, Huang YS, Mika A, Lubbers N, Berthiaume N, Polakowski J, Zinker B. 2006. Differential effects of n-3 polyunsaturated fatty acids on metabolic

control and vascular reactivity in the type 2 diabetic ob/ob mouse. Metabolism 55:1365-1374.

Muszbek L, Laposata M. 1993. Covalent modification of proteins by arachidonate and eicosapentaenoate in platelets. J Biol Chem 268:18243-18248.

NAS. 2005. Dietary Reference Intakes for Energy, Carbohydrate, Fiber, Fat, Fatty Acids, Cholesterol, Proteins, and Amino Acids (Macronutrients). In: Board NAoSIoMFaN, editor. p 770.

Nemir M, DeVouge MW, Mukherjee BB. 1989. Normal rat kidney cells secrete both phosphorylated and nonphosphorylated forms of osteopontin showing different physiological properties. J Biol Chem 264:18202-18208.

Nenseter MS, Drevon CA. 1996. Dietary polyunsaturates and peroxidation of low density lipoprotein. Curr Opin Lipidol 7:8-13.

Neschen S, Morino K, Dong J, Wang-Fischer Y, Cline GW, Romanelli AJ, Rossbacher JC, Moore IK, Regittnig W, Munoz DS, Kim JH, Shulman GI. 2007. n-3 Fatty acids preserve insulin sensitivity in vivo in a peroxisome proliferator-activated receptor-alpha-dependent manner. Diabetes 56:1034-1041.

Newberry EP, Kennedy SM, Xie Y, Sternard BT, Luo J, Davidson NO. 2008. Diet-induced obesity and hepatic steatosis in L-Fabp / mice is abrogated with SF, but not PUFA, feeding and attenuated after cholesterol supplementation. Am J Physiol Gastrointest Liver Physiol 294:G307-314.

Nielsen S, Guo Z, Johnson CM, Hensrud DD, Jensen MD. 2004. Splanchnic lipolysis in human obesity. J Clin Invest 113:1582-1588.

Nieto N, Torres MI, Rios A, Gil A. 2002. Dietary polyunsaturated fatty acids improve histological and biochemical alterations in rats with experimental ulcerative colitis. J Nutr 132:11-19.

Nishimura S, Manabe I, Nagasaki M, Eto K, Yamashita H, Ohsugi M, Otsu M, Hara K, Ueki K, Sugiura S, Yoshimura K, Kadowaki T, Nagai R. 2009. CD8+ effector T cells contribute to macrophage recruitment and adipose tissue inflammation in obesity. Nat Med 15:914-920.

Nishina PM, Verstuyft J, Paigen B. 1990. Synthetic low and high fat diets for the study of atherosclerosis in the mouse. J Lipid Res 31:859-869.

Nomiyama T, Perez-Tilve D, Ogawa D, Gizard F, Zhao Y, Heywood EB, Jones KL, Kawamori R, Cassis LA, Tschop MH, Bruemmer D. 2007. Osteopontin mediates obesity-induced adipose tissue macrophage infiltration and insulin resistance in mice. J Clin Invest 117:2877-2888.

Oarada M, Furukawa H, Majima T, Miyazawa T. 2000. Fish oil diet affects on oxidative senescence of red blood cells linked to degeneration of spleen cells in mice. Biochim Biophys Acta 1487:1-14.

Odegaard JI, Chawla A. 2008. Mechanisms of macrophage activation in obesity-induced insulin resistance. Nat Clin Pract Endocrinol Metab 4:619-626.

OECD. 2011. OECD Health Data 2011. In: Organization for Economic Co-operation and Development.

Oh DY, Talukdar S, Bae EJ, Imamura T, Morinaga H, Fan W, Li P, Lu WJ, Watkins SM, Olefsky JM. 2010. GPR120 is an omega-3 fatty acid receptor mediating potent anti-inflammatory and insulin-sensitizing effects. Cell 142:687-698.

Olsson M, Ahlin S, Olsson B, Svensson PA, Stahlman M, Boren J, Carlsson LM, Sjoholm K. 2011. Establishment of a transgenic mouse model specifically expressing human serum amyloid A in adipose tissue. PLoS One 6:e19609.

Onuki Y, Morishita M, Chiba Y, Tokiwa S, Takayama K. 2006. Docosahexaenoic acid and eicosapentaenoic acid induce changes in the physical properties of a lipid bilayer model membrane. Chem Pharm Bull (Tokyo) 54:68-71.

Oosterveer MH, van Dijk TH, Tietge UJ, Boer T, Havinga R, Stellaard F, Groen AK, Kuipers F, Reijngoud DJ. 2009. High fat feeding induces hepatic fatty acid elongation in mice. PLoS One 4:e6066.

Packard GC, Boardman TJ. 1999. The use of percentages and size-specific indices to normalize physiological data for variation in body size: wasted time, wasted effort? . Comparative Biochemistry and Physiology Part A Molecular Integrative Physiology 122:37-44.

Park Y, Harris WS. 2003. Omega-3 fatty acid supplementation accelerates chylomicron triglyceride clearance. J Lipid Res 44:455-463.

Patarca R, Saavedra RA, Cantor H. 1993. Molecular and cellular basis of genetic resistance to bacterial infection: the role of the early T-lymphocyte activation-1/osteopontin gene. Crit Rev Immunol 13:225-246.

Perez-Echarri N, Perez-Matute P, Marcos-Gomez B, Marti A, Martinez JA, Moreno-Aliaga MJ. 2009. Down-regulation in muscle and liver lipogenic genes: EPA ethyl ester treatment in lean and overweight (high-fat-fed) rats. J Nutr Biochem 20:705-714.

Perrini S, Laviola L, Cignarelli A, Melchiorre M, De Stefano F, Caccioppoli C, Natalicchio A, Orlando MR, Garruti G, De Fazio M, Catalano G, Memeo V, Giorgino R, Giorgino F. 2008. Fat depot-related differences in gene expression, adiponectin secretion, and insulin action and signalling in human adipocytes differentiated in vitro from precursor stromal cells. Diabetologia 51:155-164.

Petruschke T, Hauner H. 1993. Tumor necrosis factor-alpha prevents the differentiation of human adipocyte precursor cells and causes delipidation of newly developed fat cells. J Clin Endocrinol Metab 76:742-747.

Petursdottir DH, Olafsdottir I, Hardardottir I. 2002. Dietary fish oil increases tumor necrosis factor secretion but decreases interleukin-10 secretion by murine peritoneal macrophages. J Nutr 132:3740-3743.

Peyrin-Biroulet L, Chamaillard M, Gonzalez F, Beclin E, Decourcelle C, Antunes L, Gay J, Neut C, Colombel JF, Desreumaux P. 2007. Mesenteric fat in Crohn's disease: a pathogenetic hallmark or an innocent bystander? Gut 56:577-583.

Pischon T, Hankinson SE, Hotamisligil GS, Rifai N, Willett WC, Rimm EB. 2003. Habitual dietary intake of n-3 and n-6 fatty acids in relation to inflammatory markers among US men and women. Circulation 108:155-160.

Platell C, Cooper D, Papadimitriou JM, Hall JC. 2000. The omentum. World J Gastroenterol 6:169-176.

Poitou C, Viguerie N, Cancello R, De Matteis R, Cinti S, Stich V, Coussieu C, Gauthier E, Courtine M, Zucker JD, Barsh GS, Saris W, Bruneval P, Basdevant A, Langin D, Clement K. 2005. Serum amyloid A: production by human white adipocyte and regulation by obesity and nutrition. Diabetologia 48:519-528.

Pond CM. 1998. The Fats of Life. Cambridge: Cambridge University Press.

Pond CM. 2005. Adipose tissue and the immune system. Prostaglandins Leukot Essent Fatty Acids 73:17-30.

Pond CM, Mattacks CA. 2002. The activation of the adipose tissue associated with lymph nodes during the early stages of an immune response. Cytokine 17:131-139.

Pond CM, Mattacks CA. 2003. The source of fatty acids incorporated into proliferating lymphoid cells in immune-stimulated lymph nodes. Br J Nutr 89:375-383.

Prince CW, Oosawa T, Butler WT, Tomana M, Bhown AS, Bhown M, Schrohenloher RE. 1987. Isolation, characterization, and biosynthesis of a phosphorylated glycoprotein from rat bone. J Biol Chem 262:2900-2907.

Puglisi MJ, Hasty AH, Saraswathi V. 2011. The role of adipose tissue in mediating the beneficial effects of dietary fish oil. J Nutr Biochem 22:101-108.

Rabbani PI, Sheikh NM, Chirtel SJ, Jackson R, Ruffin G. 1999. Effects of long-term consumption of high doses of fish oil concentrates on clinical parameters in male and female rats. J Nutr Sci Vitaminol (Tokyo) 45:553-565.

Ramel A, Martinez A, Kiely M, Morais G, Bandarra NM, Thorsdottir I. 2008. Beneficial effects of long-chain n-3 fatty acids included in an energy-restricted diet on insulin resistance in overweight and obese European young adults. Diabetologia 51:1261-1268.

Randle PJ, Garland PB, Hales CN, Newsholme EA. 1963. The glucose fatty-acid cycle. Its role in insulin sensitivity and the metabolic disturbances of diabetes mellitus. Lancet 1:785-789.

Rausch ME, Weisberg S, Vardhana P, Tortoriello DV. 2008. Obesity in C57BL/6J mice is characterized by adipose tissue hypoxia and cytotoxic T-cell infiltration. Int J Obes (Lond) 32:451-463.

Richard D, Kefi K, Barbe U, Bausero P, Visioli F. 2008. Polyunsaturated fatty acids as antioxidants. Pharmacol Res 57:451-455.

Ridker PM, Hennekens CH, Buring JE, Rifai N. 2000. C-reactive protein and other markers of inflammation in the prediction of cardiovascular disease in women. N Engl J Med 342:836-843.

Riedl M, Vila G, Maier C, Handisurya A, Shakeri-Manesch S, Prager G, Wagner O, Kautzky-Willer A, Ludvik B, Clodi M, Luger A. 2008. Plasma osteopontin increases after bariatric surgery and correlates with markers of bone turnover but not with insulin resistance. J Clin Endocrinol Metab 93:2307-2312.

Ringseis R, Eder K. 2004. Dietary oxidized cholesterol increases expression and activity of antioxidative enzymes and reduces the concentration of glutathione in the liver of rats. Int J Vitam Nutr Res 74:86-92.

Robbez Masson V, Lucas A, Gueugneau AM, Macaire JP, Paul JL, Grynberg A, Rousseau D. 2008. Long-chain (n-3) polyunsaturated fatty acids prevent metabolic and vascular disorders in fructose-fed rats. J Nutr 138:1915-1922.

Roberts R, Hodson L, Dennis AL, Neville MJ, Humphreys SM, Harnden KE, Micklem KJ, Frayn KN. 2009. Markers of de novo lipogenesis in adipose tissue: associations with small adipocytes and insulin sensitivity in humans. Diabetologia 52:882-890.

Robinson SW, Dinulescu DM, Cone RD. 2000. Genetic models of obesity and energy balance in the mouse. Annu Rev Genet 34:687-745.

Rockett BD, Salameh M, Carraway K, Morrison K, Shaikh SR. 2010. n-3 PUFA improves fatty acid composition, prevents palmitate-induced apoptosis, and differentially modifies B cell cytokine secretion in vitro and ex vivo. J Lipid Res 51:1284-1297.

Rokling-Andersen MH, Rustan AC, Wensaas AJ, Kaalhus O, Wergedahl H, Rost TH, Jensen J, Graff BA, Caesar R, Drevon CA. 2009. Marine n-3 fatty acids promote size reduction of visceral adipose depots, without altering body weight and composition, in male Wistar rats fed a high-fat diet. Br J Nutr 102:995-1006.

Römisch-Margl W, Prehn C, Bogumil R, Röhring C, Suhre K, Adamski J. 2012. Procedure for tissue sample preparation and metabolite extraction for high-throughput targeted metabolomics. Metabolomics 8:133-142.

Rossmeisl M, Jelenik T, Jilkova Z, Slamova K, Kus V, Hensler M, Medrikova D, Povysil C, Flachs P, Mohamed-Ali V, Bryhn M, Berge K, Holmeide AK, Kopecky J. 2009. Prevention and reversal of obesity and glucose intolerance in mice by DHA derivatives. Obesity (Silver Spring) 17:1023-1031.

Rustan AC, Christiansen EN, Drevon CA. 1992. Serum lipids, hepatic glycerolipid metabolism and peroxisomal fatty acid oxidation in rats fed omega-3 and omega-6 fatty acids. Biochem J 283 (Pt 2):333-339.

Rustan AC, Hustvedt BE, Drevon CA. 1993. Dietary supplementation of very long-chain n-3 fatty acids decreases whole body lipid utilization in the rat. J Lipid Res 34:1299-1309.

Rustan AC, Hustvedt BE, Drevon CA. 1998. Postprandial decrease in plasma unesterified fatty acids during n-3 fatty acid feeding is not caused by accumulation of fatty acids in adipose tissue. Biochim Biophys Acta 1390:245-257.

Rustan AC, Nossen JO, Christiansen EN, Drevon CA. 1988a. Eicosapentaenoic acid reduces hepatic synthesis and secretion of triacylglycerol by decreasing the activity of acyl-coenzyme A:1,2-diacylglycerol acyltransferase. J Lipid Res 29:1417-1426.

Rustan AC, Nossen JO, Osmundsen H, Drevon CA. 1988b. Eicosapentaenoic acid inhibits cholesterol esterification in cultured parenchymal cells and isolated microsomes from rat liver. J Biol Chem 263:8126-8132.

Rutter H. 2011. Where next for obesity? Lancet 378:746-747.

Ruzickova J, Rossmeisl M, Prazak T, Flachs P, Sponarova J, Veck M, Tvrzicka E, Bryhn M, Kopecky J. 2004. Omega-3 PUFA of marine origin limit diet-induced obesity in mice by reducing cellularity of adipose tissue. Lipids 39:1177-1185.

Sackmann-Sala L, Berryman DE, Munn RD, Lubbers ER, Kopchick JJ. 2012. Heterogeneity among white adipose tissue depots in male C57BL/6J mice. Obesity (Silver Spring) 20:101-111.

Sadurskis A, Dicker A, Cannon B, Nedergaard J. 1995. Polyunsaturated fatty acids recruit brown adipose tissue: increased UCP content and NST capacity. Am J Physiol 269:E351-360.

Saito M, Kubo K. 2003. Relationship between tissue lipid peroxidation and peroxidizability index after alpha-linolenic, eicosapentaenoic, or docosahexaenoic acid intake in rats. Br J Nutr 89:19-28.

Sarmidi MR, El Enshasy HA, Hamid MA. 2009. Oil Palm: The Rich Mine for Pharma, Food, Feed and Fuel Industries. American-Eurasian Journal of Agricultural and Environmental Science 5:767-776.

Sato A, Kawano H, Notsu T, Ohta M, Nakakuki M, Mizuguchi K, Itoh M, Suganami T, Ogawa Y. 2010. Antiobesity effect of eicosapentaenoic acid in high-fat/high-sucrose diet-induced obesity: importance of hepatic lipogenesis. Diabetes 59:2495-2504.

Sato TN, Tozawa Y, Deutsch U, Wolburg-Buchholz K, Fujiwara Y, Gendron-Maguire M, Gridley T, Wolburg H, Risau W, Qin Y. 1995. Distinct roles of the receptor tyrosine kinases Tie-1 and Tie-2 in blood vessel formation. Nature 376:70-74.

Satoh Y, Kawai H, Kudo N, Kawashima Y, Mitsumoto A. 2006. Time-restricted feeding entrains daily rhythms of energy metabolism in mice. Am J Physiol Regul Integr Comp Physiol 290:R1276-1283.

Schaffler A, Scholmerich J, Buchler C. 2005. Mechanisms of disease: adipocytokines and visceral adipose tissue--emerging role in intestinal and mesenteric diseases. Nat Clin Pract Gastroenterol Hepatol 2:103-111.

Scheja L, Heese B, Zitzer H, Michael MD, Siesky AM, Pospisil H, Beisiegel U, Seedorf K. 2008. Acute-phase serum amyloid A as a marker of insulin resistance in mice. Exp Diabetes Res 2008:230837.

Schmitz G, Ecker J. 2008. The opposing effects of n-3 and n-6 fatty acids. Prog Lipid Res 47:147-155.

Sealls W, Gonzalez M, Brosnan MJ, Black PN, DiRusso CC. 2008. Dietary polyunsaturated fatty acids (C18:2 omega6 and C18:3 omega3) do not suppress hepatic lipogenesis. Biochim Biophys Acta 1781:406-414.

Senger DR, Wirth DF, Hynes RO. 1979. Transformed mammalian cells secrete specific proteins and phosphoproteins. Cell 16:885-893.

Serhan CN, Chiang N, Van Dyke TE. 2008. Resolving inflammation: dual anti-inflammatory and pro-resolution lipid mediators. Nat Rev Immunol 8:349-361.

Serhan CN, Yang R, Martinod K, Kasuga K, Pillai PS, Porter TF, Oh SF, Spite M. 2009. Maresins: novel macrophage mediators with potent antiinflammatory and proresolving actions. J Exp Med 206:15-23.

Service USDoAFA U. 2012. Oilseeds: World Market and Trade: USDA FAS.

Shi H, Kokoeva MV, Inouye K, Tzameli I, Yin H, Flier JS. 2006. TLR4 links innate immunity and fatty acid-induced insulin resistance. J Clin Invest 116:3015-3025.

Shinohara ML, Kim HJ, Kim JH, Garcia VA, Cantor H. 2008. Alternative translation of osteopontin generates intracellular and secreted isoforms that mediate distinct biological activities in dendritic cells. Proc Natl Acad Sci U S A 105:7235-7239.

Siddiqui RA, Harvey KA, Ruzmetov N, Miller SJ, Zaloga GP. 2009. n-3 fatty acids prevent whereas trans-fatty acids induce vascular inflammation and sudden cardiac death. Br J Nutr 102:1811-1819.

Simopoulos AP. 2011. Evolutionary aspects of diet: the omega-6/omega-3 ratio and the brain. Mol Neurobiol 44:203-215.

Singer P. 2008. Geringer Gehalt von Omega-3-Fettsäuren bei Vegetariern und Veganern. Komplement Integr Med 3:16-23.

Singer P. 2010. Praktische Aspekte bei der Zufuhr von Omega-3-Fettsäuren. Ernährung und Medizin 25:3-18.

Singh M. 2005. Essential fatty acids, DHA and human brain. Indian J Pediatr 72:239-242.

Singh RP, Patarca R, Schwartz J, Singh P, Cantor H. 1990. Definition of a specific interaction between the early T lymphocyte activation 1 (Eta-1) protein and murine macrophages in vitro and its effect upon macrophages in vivo. J Exp Med 171:1931-1942.

Sjoholm K, Palming J, Olofsson LE, Gummesson A, Svensson PA, Lystig TC, Jennische E, Brandberg J, Torgerson JS, Carlsson B, Carlsson LM. 2005. A microarray search for genes predominantly expressed in human omental adipocytes: adipose tissue as a major production site of serum amyloid A. J Clin Endocrinol Metab 90:2233-2239.

Skurk T, Alberti-Huber C, Herder C, Hauner H. 2007. Relationship between adipocyte size and adipokine expression and secretion. J Clin Endocrinol Metab 92:1023-1033.

Smith BK, Holloway GP, Reza-Lopez S, Jeram SM, Kang JX, Ma DW. 2010. A decreased n-6/n-3 ratio in the fat-1 mouse is associated with improved glucose tolerance. Appl Physiol Nutr Metab 35:699-706.

Smith PK, Krohn RI, Hermanson GT, Mallia AK, Gartner FH, Provenzano MD, Fujimoto EK, Goeke NM, Olson BJ, Klenk DC. 1985. Measurement of protein using bicinchoninic acid. Anal Biochem 150:76-85.

Smith RE, Horwitz BA. 1969. Brown fat and thermogenesis. Physiol Rev 49:330-425.

Sodek J, Ganss B, McKee MD. 2000. Osteopontin. Crit Rev Oral Biol Med 11:279-303.

Song S, Zhang Y, Ma K, Jackson-Hayes L, Lavrentyev EN, Cook GA, Elam MB, Park EA. 2004. Peroxisomal proliferator activated receptor gamma coactivator (PGC-1alpha) stimulates carnitine palmitoyltransferase I (CPT-Ialpha) through the first intron. Biochim Biophys Acta 1679:164-173.

Spalding KL, Arner E, Westermark PO, Bernard S, Buchholz BA, Bergmann O, Blomqvist L, Hoffstedt J, Naslund E, Britton T, Concha H, Hassan M, Ryden M, Frisen J, Arner P. 2008. Dynamics of fat cell turnover in humans. Nature 453:783-787.

Sprecher H. 1981. Biochemistry of essential fatty acids. Prog Lipid Res 20:13-22.

Stangl GI, Eder K, Kirchgessner M, Reichlmayr-Lais AM. 1994. Effect of dietary fish oil on serum lipids and lipoproteins of rats fed diets differing in cholesterol and fat. Arch Tierernahr 46:155-164.

Steeber DA, Tang ML, Green NE, Zhang XQ, Sloane JE, Tedder TF. 1999. Leukocyte entry into sites of inflammation requires overlapping interactions between the L-selectin and ICAM-1 pathways. J Immunol 163:2176-2186.

Steil GM, Trivedi N, Jonas JC, Hasenkamp WM, Sharma A, Bonner-Weir S, Weir GC. 2001. Adaptation of beta-cell mass to substrate oversupply: enhanced function with normal gene expression. Am J Physiol Endocrinol Metab 280:E788-796.

Storlien LH, Higgins JA, Thomas TC, Brown MA, Wang HQ, Huang XF, Else PL. 2000. Diet composition and insulin action in animal models. Br J Nutr 83 Suppl 1:S85-90.

Strawford A, Antelo F, Christiansen M, Hellerstein MK. 2004. Adipose tissue triglyceride turnover, de novo lipogenesis, and cell proliferation in humans measured with 2H2O. Am J Physiol Endocrinol Metab 286:E577-588.

Strissel KJ, Stancheva Z, Miyoshi H, Perfield JW, 2nd, DeFuria J, Jick Z, Greenberg AS, Obin MS. 2007. Adipocyte death, adipose tissue remodeling, and obesity complications. Diabetes 56:2910-2918.

Stulnig TM, Huber J, Leitinger N, Imre EM, Angelisova P, Nowotny P, Waldhausl W. 2001. Polyunsaturated eicosapentaenoic acid displaces proteins from membrane rafts by altering raft lipid composition. J Biol Chem 276:37335-37340.

Suchankova G, Tekle M, Saha AK, Ruderman NB, Clarke SD, Gettys TW. 2005. Dietary polyunsaturated fatty acids enhance hepatic AMP-activated protein kinase activity in rats. Biochem Biophys Res Commun 326:851-858.

Svenson KL, Von Smith R, Magnani PA, Suetin HR, Paigen B, Naggert JK, Li R, Churchill GA, Peters LL. 2007. Multiple trait measurements in 43 inbred mouse strains capture the phenotypic diversity characteristic of human populations. J Appl Physiol 102:2369-2378.

Tai CC, Ding ST. 2010. N-3 polyunsaturated fatty acids regulate lipid metabolism through several inflammation mediators: mechanisms and implications for obesity prevention. J Nutr Biochem 21:357-363.

Taouis M, Dagou C, Ster C, Durand G, Pinault M, Delarue J. 2002. N-3 polyunsaturated fatty acids prevent the defect of insulin receptor signaling in muscle. Am J Physiol Endocrinol Metab 282:E664-671.

Tappia PS, Man WJ, Grimble RF. 1995. Influence of unsaturated fatty acids on the production of tumour necrosis factor and interleukin-6 by rat peritoneal macrophages. Mol Cell Biochem 143:89-98.

Terano T, Salmon JA, Moncada S. 1984. Biosynthesis and biological activity of leukotriene B5. Prostaglandins 27:217-232.

Tian DR, Li XD, Shi YS, Wan Y, Wang XM, Chang JK, Yang J, Han JS. 2004. Changes of hypothalamic alpha-MSH and CART peptide expression in diet-induced obese rats. Peptides 25:2147-2153.

Tierney AC, McMonagle J, Shaw DI, Gulseth HL, Helal O, Saris WH, Paniagua JA, Golabek-Leszczynska I, Defoort C, Williams CM, Karsltrom B, Vessby B, Dembinska-Kiec A, Lopez-Miranda J, Blaak EE, Drevon CA, Gibney MJ, Lovegrove JA, Roche HM. 2011. Effects of dietary fat modification on insulin sensitivity and on other risk factors of the metabolic syndrome--LIPGENE: a European randomized dietary intervention study. Int J Obes (Lond) 35:800-809.

Tilg H, Moschen AR. 2006. Adipocytokines: mediators linking adipose tissue, inflammation and immunity. Nat Rev Immunol 6:772-783.

Tjonahen E, Oh SF, Siegelman J, Elangovan S, Percarpio KB, Hong S, Arita M, Serhan CN. 2006. Resolvin E2: identification and anti-inflammatory actions: pivotal role of human 5-lipoxygenase in resolvin E series biosynthesis. Chem Biol 13:1193-1202.

Todoric J, Loffler M, Huber J, Bilban M, Reimers M, Kadl A, Zeyda M, Waldhausl W, Stulnig TM. 2006. Adipose tissue inflammation induced by high-fat diet in obese diabetic mice is prevented by n-3 polyunsaturated fatty acids. Diabetologia 49:2109-2119.

Tong L. 2005. Acetyl-coenzyme A carboxylase: crucial metabolic enzyme and attractive target for drug discovery. Cell Mol Life Sci 62:1784-1803.

Tontonoz P, Hu E, Spiegelman BM. 1994. Stimulation of adipogenesis in fibroblasts by PPAR gamma 2, a lipid-activated transcription factor. Cell 79:1147-1156.

Traber MG, Stevens JF. 2011. Vitamins C and E: beneficial effects from a mechanistic perspective. Free Radic Biol Med 51:1000-1013.

Trayhurn P, Wang B, Wood IS. 2008. Hypoxia in adipose tissue: a basis for the dysregulation of tissue function in obesity? Br J Nutr 100:227-235.

Tschop MH, Speakman JR, Arch JR, Auwerx J, Bruning JC, Chan L, Eckel RH, Farese RV, Jr., Galgani JE, Hambly C, Herman MA, Horvath TL, Kahn BB, Kozma SC, Maratos-Flier E, Muller TD, Munzberg H, Pfluger PT, Plum L, Reitman ML, Rahmouni K, Shulman GI, Thomas G, Kahn CR, Ravussin E. 2012. A guide to analysis of mouse energy metabolism. Nat Methods 9:57-63.

Tziomalos K, Athyros VG, Mikhailidis DP. 2007. Fish oils and vascular disease prevention: an update. Curr Med Chem 14:2622-2628.

Uhlar CM, Whitehead AS. 1999. Serum amyloid A, the major vertebrate acute-phase reactant. Eur J Biochem 265:501-523.

Ulyanova T, Scott LM, Priestley GV, Jiang Y, Nakamoto B, Koni PA, Papayannopoulou T. 2005. VCAM-1 expression in adult hematopoietic and nonhematopoietic cells is controlled by tissue-inductive signals and reflects their developmental origin. Blood 106:86-94.

Uniprot. 2012. Protein Sequence Database. Internet: http://www.uniprot.org/uniprot/P10923. Access: February 8, 2012.

USDA. 2012. Nutrient database, Release 24". In: United States Department of Agriculture. Internet: http://ndb.nal.usda.gov/. Access: February 28, editor.

Vague J. 1947. La différenciation sexuelle, facteur déterminant des formes de l'obésité. Presse Méd 55:339-340.

Van de Walle I, De Smet G, Gartner M, De Smedt M, Waegemans E, Vandekerckhove B, Leclercq G, Plum J, Aster JC, Bernstein ID, Guidos CJ, Kyewski B, Taghon T. 2011. Jagged2 acts as a Delta-like Notch ligand during early hematopoietic cell fate decisions. Blood 117:4449-4459.

van Eijk M, Aten J, Bijl N, Ottenhoff R, van Roomen CP, Dubbelhuis PF, Seeman I, Ghauharali-van der Vlugt K, Overkleeft HS, Arbeeny C, Groen AK, Aerts JM. 2009. Reducing glycosphingolipid content in adipose tissue of obese mice restores insulin sensitivity, adipogenesis and reduces inflammation. PLoS One 4:e4723.

van Schothorst EM, Flachs P, Franssen-van Hal NL, Kuda O, Bunschoten A, Molthoff J, Vink C, Hooiveld GJ, Kopecky J, Keijer J. 2009. Induction of lipid oxidation by polyunsaturated fatty acids of marine origin in small intestine of mice fed a high-fat diet. BMC Genomics 10:110.

Varga O, Harangi M, Olsson IA, Hansen AK. 2009. Contribution of animal models to the understanding of the metabolic syndrome: a systematic overview. Obes Rev 11:792-807.

Vargas ML, Almario RU, Buchan W, Kim K, Karakas SE. 2011. Metabolic and endocrine effects of long-chain versus essential omega-3 polyunsaturated fatty acids in polycystic ovary syndrome. Metabolism 60:1711-1718.

Vasickova L, Stavek P, Suchanek P. 2011. Possible effect of DHA intake on body weight reduction and lipid metabolism in obese children. Neuro Endocrinol Lett 32:64-67.

Vega-Lopez S, Ausman LM, Jalbert SM, Erkkila AT, Lichtenstein AH. 2006. Palm and partially hydrogenated soybean oils adversely alter lipoprotein profiles compared with soybean and canola oils in moderately hyperlipidemic subjects. Am J Clin Nutr 84:54-62.

Verlengia R, Gorjao R, Kanunfre CC, Bordin S, de Lima TM, Martins EF, Newsholme P, Curi R. 2004a. Effects of EPA and DHA on proliferation, cytokine production, and gene expression in Raji cells. Lipids 39:857-864.

Verlengia R, Gorjao R, Kanunfre CC, Bordin S, Martins De Lima T, Martins EF, Curi R. 2004b. Comparative effects of eicosapentaenoic acid and docosahexaenoic acid on proliferation, cytokine production, and pleiotropic gene expression in Jurkat cells. J Nutr Biochem 15:657-665.

von Bergmann K, Sudhop T, Lutjohann D. 2005. Cholesterol and plant sterol absorption: recent insights. Am J Cardiol 96:10D-14D.

Wajchenberg BL. 2000. Subcutaneous and visceral adipose tissue: their relation to the metabolic syndrome. Endocr Rev 21:697-738.

WAKO. 2012. Internet: http://www.wakodiagnostics.com/r_nefa.html. Access: February, 28, 2012.

Wallace FA, Miles EA, Calder PC. 2000. Activation state alters the effect of dietary fatty acids on pro-inflammatory mediator production by murine macrophages. Cytokine 12:1374-1379.

Wallis JG, Watts JL, Browse J. 2002. Polyunsaturated fatty acid synthesis: what will they think of next? Trends Biochem Sci 27:467.

Wang CY, Liao JK. 2012. A mouse model of diet-induced obesity and insulin resistance. Methods Mol Biol 821:421-433.

Wang H, Storlien LH, Huang XF. 1999. Influence of dietary fats on c-Fos-like immunoreactivity in mouse hypothalamus. Brain Res 843:184-192.

Wang T, Zang Y, Ling W, Corkey BE, Guo W. 2003. Metabolic partitioning of endogenous fatty acid in adipocytes. Obes Res 11:880-887.

Wang Y, Li J, Tang L, Charnigo R, de Villiers W, Eckhardt E. 2010. T-lymphocyte responses to intestinally absorbed antigens can contribute to adipose tissue inflammation and glucose intolerance during high fat feeding. PLoS One 5:e13951.

Weber GF, Cantor H. 1996. The immunology of Eta-1/osteopontin. Cytokine Growth Factor Rev 7:241-248.

Weber PC, Fischer S, von Schacky C, Lorenz R, Strasser T. 1986. The conversion of dietary eicosapentaenoic acid to prostanoids and leukotrienes in man. Prog Lipid Res 25:273-276.

Wei D, Li J, Shen M, Jia W, Chen N, Chen T, Su D, Tian H, Zheng S, Dai Y, Zhao A. 2010. Cellular production of n-3 PUFAs and reduction of n-6-to-n-3 ratios in the pancreatic beta-cells and islets enhance insulin secretion and confer protection against cytokine-induced cell death. Diabetes 59:471-478.

Weisberg SP, McCann D, Desai M, Rosenbaum M, Leibel RL, Ferrante AW, Jr. 2003. Obesity is associated with macrophage accumulation in adipose tissue. J Clin Invest 112:1796-1808.

Weldon SM, Mullen AC, Loscher CE, Hurley LA, Roche HM. 2007. Docosahexaenoic acid induces an anti-inflammatory profile in lipopolysaccharide-stimulated human THP-1 macrophages more effectively than eicosapentaenoic acid. J Nutr Biochem 18:250-258.

Wen H, Gris D, Lei Y, Jha S, Zhang L, Huang MT, Brickey WJ, Ting JP. 2011. Fatty acid-induced NLRP3-ASC inflammasome activation interferes with insulin signaling. Nat Immunol 12:408-415.

West DB, Prinz WA, Greenwood MR. 1989. Regional changes in adipose tissue blood flow and metabolism in rats after a meal. Am J Physiol 257:R711-716.

West DB, York B. 1998. Dietary fat, genetic predisposition, and obesity: lessons from animal models. Am J Clin Nutr 67:505S-512S.

West M. 2009. Dead adipocytes and metabolic dysfunction: recent progress. Curr Opin Endocrinol Diabetes Obes 16:178-182.

Westcott E, Windsor A, Mattacks C, Pond C, Knight S. 2005. Fatty acid compositions of lipids in mesenteric adipose tissue and lymphoid cells in patients with and without Crohn's disease and their therapeutic implications. Inflamm Bowel Dis 11:820-827.

White PJ, Arita M, Taguchi R, Kang JX, Marette A. 2010. Transgenic restoration of long-chain n-3 fatty acids in insulin target tissues improves resolution capacity and alleviates obesity-linked inflammation and insulin resistance in high-fat-fed mice. Diabetes 59:3066-3073.

WHO. 2000. Obesity: preventing and managing the global epidemic. Report of a WHO consultation. World Health Organ Tech Rep Ser 894:1-253.

WHO. 2011. World Health Statistics Report. WHO Press:19.

Wilkosz S, Ireland G, Khwaja N, Walker M, Butt R, de Giorgio-Miller A, Herrick SE. 2005. A comparative study of the structure of human and murine greater omentum. Anat Embryol (Berl) 209:251-261.

Winer DA, Winer S, Shen L, Wadia PP, Yantha J, Paltser G, Tsui H, Wu P, Davidson MG, Alonso MN, Leong HX, Glassford A, Caimol M, Kenkel JA, Tedder TF, McLaughlin T, Miklos DB, Dosch HM, Engleman EG. 2011. B cells promote insulin resistance through modulation of T cells and production of pathogenic IgG antibodies. Nat Med 17:610-617.

Winzell MS, Pacini G, Ahren B. 2006. Insulin secretion after dietary supplementation with conjugated linoleic acids and n-3 polyunsaturated fatty acids in normal and insulin-resistant mice. Am J Physiol Endocrinol Metab 290:E347-354.

Woodworth HL, McCaskey SJ, Duriancik DM, Clinthorne JF, Langohr IM, Gardner EM, Fenton JI. 2010. Dietary fish oil alters T lymphocyte cell populations and exacerbates disease in a mouse model of inflammatory colitis. Cancer Res 70:7960-7969.

Wu H, Perrard XD, Wang Q, Perrard JL, Polsani VR, Jones PH, Smith CW, Ballantyne CM. 2010. CD11c expression in adipose tissue and blood and its role in diet-induced obesity. Arterioscler Thromb Vasc Biol 30:186-192.

Xin X, Storlien LH, Huang XF. 2000. Hypothalamic c-fos-like immunoreactivity in high-fat diet-induced obese and resistant mice. Brain Res Bull 52:235-242.

Yang RZ, Lee MJ, Hu H, Pollin TI, Ryan AS, Nicklas BJ, Snitker S, Horenstein RB, Hull K, Goldberg NH, Goldberg AP, Shuldiner AR, Fried SK, Gong DW. 2006. Acute-phase serum amyloid A: an inflammatory adipokine and potential link between obesity and its metabolic complications. PLoS Med 3:e287.

Yaqoob P. 2010. Mechanisms underlying the immunomodulatory effects of n-3 PUFA. Proc Nutr Soc 69:311-315.

Yki-Jarvinen H. 2002. Ectopic fat accumulation: an important cause of insulin resistance in humans. J R Soc Med 95 Suppl 42:39-45.

Yoshioka M, Bolduc C, Raymond V, St-Amand J. 2008. High-fat meal-induced changes in the duodenum mucosa transcriptome. Obesity (Silver Spring) 16:2302-2307.

Yu R, Kim CS, Kwon BS, Kawada T. 2006. Mesenteric adipose tissue-derived monocyte chemoattractant protein-1 plays a crucial role in adipose tissue macrophage migration and activation in obese mice. Obesity (Silver Spring) 14:1353-1362.

Yu S, Rao S, Reddy JK. 2003. Peroxisome proliferator-activated receptors, fatty acid oxidation, steatohepatitis and hepatocarcinogenesis. Curr Mol Med 3:561-572.

Yu YH, Wang PH, Cheng WT, Mersmann HJ, Wu SC, Ding ST. 2010. Porcine peroxisome proliferator-activated receptor delta mediates the lipolytic effects of dietary fish oil to reduce body fat deposition. J Anim Sci 88:2009-2018.

Zeyda M, Farmer D, Todoric J, Aszmann O, Speiser M, Gyori G, Zlabinger GJ, Stulnig TM. 2007. Human adipose tissue macrophages are of an anti-inflammatory phenotype but capable of excessive pro-inflammatory mediator production. Int J Obes (Lond) 31:1420-1428.

Zhang HH, Halbleib M, Ahmad F, Manganiello VC, Greenberg AS. 2002. Tumor necrosis factor-alpha stimulates lipolysis in differentiated human adipocytes through activation of extracellular signal-related kinase and elevation of intracellular cAMP. Diabetes 51:2929-2935.

Zhang X, Srinivasan SV, Lingrel JB. 2004. WWP1-dependent ubiquitination and degradation of the lung Kruppel-like factor, KLF2. Biochem Biophys Res Commun 316:139-148.

Zhang Y, Proenca R, Maffei M, Barone M, Leopold L, Friedman JM. 1994. Positional cloning of the mouse obese gene and its human homologue. Nature 372:425-432.

Zhao W, Wang L, Zhang L, Yuan C, Kuo PC, Gao C. 2010. Differential expression of intracellular and secreted osteopontin isoforms by murine macrophages in response to toll-like receptor agonists. J Biol Chem 285:20452-20461.

Zhao Y, Joshi-Barve S, Barve S, Chen LH. 2004. Eicosapentaenoic acid prevents LPS-induced TNF-alpha expression by preventing NF-kappaB activation. J Am Coll Nutr 23:71-78.

Ziemke F, Mantzoros CS. 2010. Adiponectin in insulin resistance: lessons from translational research. Am J Clin Nutr 91:258S-261S.

8 Abbreviations

aa	indicates ester bond in phosphatidyl-choline (in contrast to ether bond)
Acacα	acetyl-coenzyme A carboxylase a
Acox1	peroxisomal acyl-coenzyme A oxidase 1
ACTB	β-actin
ALA	α-linoleic acid
AMDR	acceptable macronutrient distribution range
AMP	adenosine monophosphate
ANCOVA	analysis of co-variance, statistical test
ANOVA	analysis of variance, statistical test
AP-1	activator protein 1 (transcription factor)
ARA	arachidonic acid
AT	adipose tissue
AT-COX2	aspirin-triggered cyclooxygenase 2
ATM	adipose tissue macrophage
ATP	adenosine 5'-triphosphate
AU	arbitrary unit
AUC	area under the curve
BAT	brown adipose tissue
BCA	bicinchoninic acid (protein quantification assay)
BfR	Federal Institute for Risk Assessment (Bundesinstitut für Riskoforschung)
BHT	butylhydroxytoluene (anti-oxidant)
BLAST	basic local alignment search tool
C	control (low fat) diet
C57BL/6J	inbred wild type mouse strain used in this study
CCR2	chemokine (C-C motif) receptor 2
CD11b	cluster of differentiation antigen 11b
CD11c	cluster of differentiation antigen 11c (=Itgax)
CD163	cluster of differentiation antigen 163
CD206	cluster of differentiation antigen 206 (=Mrc1)
CD209a	cluster of differentiation antigen 209a
CD301	cluster of differentiation antigen 301 (=MGL1)
CD69	cluster of differentiation antigen 69
Cdkn1a	cyclin-dependent kinase inhibitor 1a
cDNA	complementary deoxyribonucleic acid
CLS	crown-like structure
Cpt1α	carnitine O-palmitoyltransferase 1a
C_q-value	threshold cycle value in RT-qPCR
CYP450	cytochrome P450
d	day (unit)
Da	dalton (unit)
$\Delta\Delta C_q$	method to quantify gene expression after RT-qPCR
DEE	daily energy expenditure
Dgat2	diacylglycerol O-acyltransferase 2
DGE	German Nutrition Society (Deutsche Gesellschaft für Ernährung)
DHA	docosahexaenoic acid
DiHDHA	di-hydroxy-DHA
DIO	diet-induced obesity
DTT	dithiotreitol
EAT	epididymal adipose tissue
EDTA	ethylene diamine tetra-acetic acid
EFOX	electrophilic oxo-derivative
ELISA	enzyme-linked immunosorbent assay
ELOVL	elongation of very long chain fatty acids protein (elongase)
en%	energy%
EPA	eicosapentaenoic acid
EPAX	brand name of fish oil concentrate used in this study

EPAX 1050 TG	n-3 LC-PUFA concentrate used in this study
F4/80	macrophage surface molecule
FA	fatty acid
FACS	fluorescence-activated cell sorting
Fads1	fatty acid desaturase 1
Fads2	fatty acid desaturase 2
FAO	UN Food and Agriculture Organization
FC	fold change
FM	fat mass
Foxp3	forkhead box protein P 3
g	gram
GC-FID / GC-MS	gas chromatography coupled with flame ionization detector or mass spectrometer
GI	GeneInfo Identifier
GPR120	g protein-coupled receptor 120
GV-SOLAS	German Society for Animal Experimentation (Gesellschaft für Versuchstierkunde)
h	hour (unit)
H&E	hematoxylin & eosin stain
HDHA	hydroxy-DHA
HEPE	hydroxy-eicospentaenoic acid
HETE	hydroxy-eicosatetraenoic acid
HF	high fat diet
HF/n-3	high fat diet enriched with n-3 LC-PUFA EPA / DHA
HOMA-IR	homeostatic model assessment of insulin resistance
HS	high sugar / sucrose diet
IAT	inguinal adipose tissue
iBAT	interscapular brown adipose tissue
Icam1	Intercellular adhesion molecule 1
IFNβ / γ	interferon β / γ
IL-6	interleukin 6
Il10 (IL10)	interleukin 10 gene (protein)
Il7 (IL7)	interleukin 7 gene (protein)
iOPN	intracellular OPN
ipGTT	intraperitoneal glucose tolerance test
ISSFAL	International Society for the Study of Fatty Acids
Itgax	integrin α-X (=CD11c)
IVC	individually ventilated cages
Jag2	jagged 2
kcal	kilocalorie (energy unit)
kGy	kilogray (SI unit of absorbed radiation)
kJ	kilojoule (SI unit of energy)
KOH	potassium hydroxide
LA	linoleic acid
LC-PUFA	long chain polyunsaturated fatty acid
LM	lean mass
LoD	limit of detection
LOX	lipoxygenase
LPS	lipopolysaccharide
LSI	lower small intestine
LTB_4	leukotriene B4
M1	type 1 macrophage
M2	type 2 macrophage
MAT	mesenteric adipose tissue
Mcp-1	macrophage chemoattractant protein 1
MGL1	macrophage galactose-type C-type lectin 1 (=CD301)
MLN	mesenteric lymph node
Mrc1	mannose receptor, C type 1 (=CD206)
mRNA	messenger RNA

MS	mass spectrometry
MUFA	monounsaturated fatty acid
n-3 LC-PUFA	omega-3 long chain polyunsaturated fatty acid
n-6 LC-PUFA	omega-6 long chain polyunsaturated fatty acid
NAS	U.S. National Academy of Sciences
NCBI	U.S. National Center for Biotechnology Information
NEFA	non-esterified fatty acid
NF-κB	nuclear factor kappa-light-chain-enhancer of activated B cells
NMR	nuclear magnetic resonance (applied in NMR spectroscopy)
Nos2	nitric oxide synthase 2, inducible
NP-40	Nonidet P-40®
Nrf1	nuclear respiratory factor 1
OECD	Organisation for Economic Co-operation and Development
OPN	osteopontin (=secreted phosphoprotein 1)
ORO	Oil Red O
pAMPKα1 / 2	phosphorylated AMP-activated protein kinase α 1 / 2 subunit
PAT	perirenal / retroperitoneal adipose tissue
PBS	phosphate-buffered saline
PC	phosphatidyl-choline
PCA	principal component analysis
PPARα / δ / γ	peroxisome proliferator-activated receptor α / δ / γ
PUFA	polyunsaturated fatty acid
RIN-m5F	rat insulinoma cell line
RIPA	radio-immunoprecipitation assay buffer
RNA	ribonucleic acid
RQ	respiratory quotient
RT	reverse transcription; room temperature
RT-qPCR	reverse transcription quantitative polymerase chain reaction
RvD	resolvin D
RvE	resolvin E
SAA	serum amyloid A
Scd1	stearoyl-coenzyme A desaturase 1
SFA	saturated fatty acid
SI	small intestine
sOPN	secreted OPN
scWAT	subcutaneous white adipose tissue (=SCAT)
SDS-PAGE	sodium dodecyl-sulphate polyacrylamide gel electrophoresis
SPF	specific pathogen-free
Spp1	secreted phosphoprotein 1
Spp1	secreted phosphoprotein 1 (=OPN)
Srebp1c	sterol regulatory element binding protein 1c
TAE	tris / acetate / EDTA buffer (gel electrophoresis)
TAG	triacylglycerol
TBE	tris / borate / EDTA buffer (gel electrophoresis)
TBS	tris-buffered saline
TBS-T	tris-buffered saline + Tween-20®
Tek	endothelial tyrosine kinase
TEMED	tetramethylethylenediamine
TG	triacylglycerol
T_h1	type of helper T cell
TMS	trimethylsilyl
TMSH	tri-methylsulfoniumhydroxide
Tnf-α	tumor necrosis factor α
Tris	tris hydroxymethyl aminomethane
TSE	TSE Systems, company
TUM	Technische Universität München
Ucp1	uncoupling protein 1
UN	United Nations
U.S.	United States of America

USDA	U.S. Department of Agriculture
USI	upper small intestine
Vcam	Vascular adhesion molecule
VCO_2	volume of carbon dioxide output per time
VO_2	volume of oxygen output per time
v / v	volume in volume
vWAT	visceral white adipose tissue
w / v	weight in volume
w / w	weight in weight
WAT	white adipose tissue
WHO	World Health Organization
Wwp1	E3 ubiquitin-protein ligase

9 Materials

9.1 Primers

target gene		primer sequence (5' - 3')	size (bp)
acyl-Coenzyme A oxidase 1, palmitoyl (Acox1)	forward	5'-GAG ATG GAT AAT GGC TAC CTG AAG-3'	172
	reverse	5'-AAA CCA TGG TCC CAT ATG TCA GC-3'	
adiponectin (Adipoq)	forward	5'-AGA TGC AGG TCT TCT TGG TCC T-3'	135
	reverse	5'-GCT GAG CGA TAC ACA TAA GCG-3'	
β-actin (Actb)	forward	5'-CCA CTG CCG CAT CCT CTT CC-3'	137
	reverse	5'-GCC ACA GGA TTC CAT ACC CAA GA-3'	
carnitine palmitoyltransferase 1α, liver (Cpt1α)	forward	5'-GTC CCA GCT GTC AAA GAT ACC G-3'	244
	reverse	5'-ATG GCG TAG TAG TTG CTG TTA ACC-3'	
CD4	forward	5'-TAG AGG AGG TTC GCC TTC GC-3'	146
	reverse	5'-CCT CCT CTT TCC TGT TCT CCA GC-3'	
CD8, α chain	forward	AGA AAG TGA ACT CTG CTG CTA CCA A	93
	reverse	AAT CTT CTG GTC TCT GGG GCT G	
cyclophilin B (Cph, Ppib)	forward	5'-TCG TCT TTG GAC TCT TTG GAA-3'	118
	reverse	5'-TCC TTG ATG ACA CGA TGG AA-3'	
endothelial-specific receptor tyrosine kinase (Tek)	forward	5'-GAT GTG ACC AGA GAA TGG GCG AA-3'	145
	reverse	5'-AGG AAG GAT GCT TGT TGA CGC AT-3'	
fatty acid desaturase 1 (Fads1, D5D)	forward	5'-ACC CAC CAA GAA TAA AGC GCT AA-3'	134
	reverse	5'-CAG CCA CAT CCA GCA GCA G-3'	
fatty acid desaturase 2 (Fads2, D6D)	forward	5'-ACC GTG GCA AAA GCT CTC AG-3'	151
	reverse	5'-GAG AGG ATG AAC CAG GCA AGG C-3'	
glyceraldehyde-3-phosphate dehydrogenase (Gapdh)	forward	5'-CCT GGA GAA ACC TGC CAA GTA TG-3'	132
	reverse	5'-GAG TGG GAG TTG CTG TTG AAG TC-3'	
heat shock protein 90 α (cytosolic) B 1 (Hsp90αb1)	forward	5'-AGG AGG GTC AAG GAA GTG GT-3'	215
	reverse	5'-TTT TTC TTG TCT TTG CCG CT-3'	
hypoxanthine guanine phosphoribosyl transferase (Hprt1)	forward	5'-GTC GTG ATT AGC GAT GAT GAA CC-3'	124
	reverse	5'-GTC TTT CAG TCC TGT CCA TAA TCA G-3'	
intercellular adhesion molecule 1 (Icam1 / CD54)	forward	5'-GTC TAC AAC TTT TCT GCT CCG GT-3'	114
	reverse	5'-GCT CAC AAG AAC CAC CTT CGA C-3'	
integrin alpha X (Itgax / CD11c)	forward	5'-GCA GGA GTG TCC AAA GCA AGA C-3'	121
	reverse	5'-CTG AAG CTG GCT CAT CAC AGC-3'	
interleukin-10 (Il10)	forward	5'-GCT GTC ATC GAT TTC TCC CCT G-3'	90
	reverse	5'-AGA CAC CTT GGT CTT GGA GCT T-3'	
leptin	forward	5'-ACA TTT CAC ACA CGC AGT CGG-3'	140
	reverse	5'-AGG CAG GCT GGT GAG GAC CT-3'	
mannose receptor, C type 1 (Mrc1 / CD206)	forward	5'-GCC AGG ACG AAA GGC GGG AT-3'	147
	reverse	5'-GGA GTT GTT GTG GGC TCT GGT G-3'	
monocyte chemoattractant protein-1 (Mcp-1)	forward	5'-GCT CAG CCA GAT GCA GTT AAC G-3'	142
	reverse	5'-GCT TGG TGA CAA AGA CTA CAG CTT-3'	
peroxisome proliferator activated receptor α (Pparα)	forward	5'-CCA GTA CTT AGG AAG CTG TCC G-3'	150
	reverse	5'-TAT TCG ACA CTC GAT GTT CAG GG-3'	
peroxisome proliferator activated receptor γ 2 (Pparγ2)	forward	5'-ACT CTG GGA GAT TCT CCT GTT GTC-3'	84
	reverse	5'-CAT GGT GGT TTC TTG TGA AGT GCT-3'	
secreted phosphoprotein 1 (Spp1, Opn)	forward	5'-CCA GAT CCT ATA GCC ACA TGG CT-3'	72
	reverse	5'-AGC ATT CTG TGG CGC AAG GA-3'	
stearoyl-Coenzyme A desaturase 1 (Scd1)	forward	5'-GGC TGT CAA AGA GAA GGG C-3'	152
	reverse	5'-AAG TCT CGC CCC AGC AGT A-3'	
sterol regulatory element binding transcription factor 1c (Srebp1c)	forward	5'-ATG GAT TGC ACA TTT GAA GAC ATG-3'	168
	reverse	5'-AGA GGA GGC CAG AGA AGC AG-3'	

target gene		primer sequence (5' - 3')	size (bp)
tumor necrosis factor α (Tnf-α)	forward	5'-CCA CGT CGT AGC AAA CCA CCA A-3'	151
	reverse	5'-GAA GAG AAC CTG GGA GTA GAC AAG G-3'	
uncoupling protein 1 (Ucp1)	forward	5'-CTG GGA GAG AAA CAC CTG CCT C-3'	92
	reverse	5'-CTC TGT AGG CTG CCC AAT GAA CA-3'	
vascular cell adhesion molecule 1 (Vcam1)	forward	5'-CGT GGA CAT CTA CTC TTT CCC CA-3'	98
	reverse	5'-TGT CTG GAG CCA AAC ACT TGA CC-3'	
acetyl-Coenzyme A carboxylase α (Acacα)	Qiagen order no. QT01554441		76
diacylglycerol O-acyltransferase 2 (Dgat2)	Qiagen order no. QT00134477		128
forkhead box protein P 3 (Foxp3)	Qiagen order no. QT00138369		93
lipoprotein lipase (Lpl)	Qiagen order no. QT01750469		108
nuclear respiratory factor 1 (Nrf1)	Qiagen order no. QT01051820		148
secreted phosphoprotein 1 (Spp1, Opn)	Qiagen order no. QT00157724		92

9.2 Antibodies

Item (order no.)	Company	City	Country
Rabbit anti-mouse p-AMPKα (2535S)	Cell Signaling / New England Biolabs GmbH	Frankfurt am Main	Germany
Rabbit anti-mouse β-Actin (4967S)	Cell Signaling / New England Biolabs GmbH	Frankfurt am Main	Germany
Mouse anti-mouse osteopontin (SC-21742)	Santa Cruz Biotechnology, Inc.	Heidelberg	Germany
IRDye680CW goat anti-rabbit (302)	LI-COR Biosciences GmbH	Bad Homburg	Germany
IRDye680CW goat anti-mouse (303)	LI-COR Biosciences GmbH	Bad Homburg	Germany

9.3 Consumables

Item	Company	City	Country
48-well, 24-well, 12-well, 6-well cell culture cluster	Corning® Inc., Sigma-Aldrich Chemie GmbH	München	Germany
96-well plate	Nunc / Thermo-Fisher Scientific	Langenselbold	Germany
Aluminum foil	Sylvana, Penny-Markt GmbH	Köln	Germany
Bedding and nesting material	Abedd® LAB & VET Service GmbH	Wien	Austria
Biosphere® filter tips (10, 100, 1000 µl)	Sarstedt AG & Co. KG	Nümbrecht	Germany
Bone scissors	Fine Science Tools GmbH	Heidelberg	Germany
Boxes for freezing	Zefa-Laborservice GmbH	Harthausen	Germany
Buckets for homogenization	Retsch GmbH	Haan	Germany
Cage, type I (200 cm^2)	Ehret GmbH & Co. KG	Emmendingen	Germany
Cage, type III (825 cm^2)	Ehret GmbH & Co. KG	Emmendingen	Germany
Cell culture flask, 75 cm^2 and 175 cm^2	Falcon™, BD Biosciences	Heidelberg	Germany
Cool rack 96-wells	Eppendorf AG	Hamburg	Germany
Corning® Costar® "stripette", disposable pipettes 2; 5; 10; 25; 50 ml	Corning® Inc., Sigma-Aldrich Chemie GmbH	München	Germany
Corning® Costar® reagent reservoirs	Corning® Inc., Sigma-Aldrich Chemie GmbH	München	Germany
Cotton gloves, Softline	Zefa-Laborservice GmbH	Harthausen	Germany
Cover slips 24 x 60 mm	Menzel GmbH & Co. KG	Braunschweig	Germany
Cuvettes, polystyrene	Sarstedt AG & Co. KG	Nümbrecht	Germany
Detergent "Baktolin"	Bode-Chemie GmbH	Hamburg	Germany
Dewar flask	KGW-Isotherm	Karlsruhe	Germany
Dismozon® pur desinfectant	Bode-Chemie GmbH	Hamburg	Germany
Disposable pipettes 2; 5; 10; 25; 50 ml	Falcon™, BD Biosciences	Heidelberg	Germany

Item	Company	City	Country
Dissection scissors	Fine Science Tools GmbH	Heidelberg	Germany
Eppendorf Combitips plus	Eppendorf AG	Hamburg	Germany
Eppendorf Multipette® plus	Eppendorf AG	Hamburg	Germany
Food rack divider	Tobias Ludwig	Weihenstephan	Germany
Forceps	Fine Science Tools GmbH	Heidelberg	Germany
Gel chamber, sled, comb	UniEquip GmbH	Planegg	Germany
Glass plates, clips, rubber, chamber, combs	Biometra GmbH	Göttingen	Germany
Glassware (beakers, cylinders, funnels)	Diagonal GmbH &Co KG	Münster	Germany
Heat sealing film	Eppendorf AG	Hamburg	Germany
Histosettes	Simport Scientific	Beloeil	Canada
Hypothalamus dissection mold	AG Klingenspor	Weihenstephan	Germany
Ignition thread	Parr Instrument Co.	Moline	USA
Lab coat	CWS-boco GmbH	Dreieich	Germany
Laboratory aluminum foil	Carl Roth GmbH & Co. KG	Karlsruhe	Germany
Latex gloves, size "L"	Rösner-Mautby Meditrade GmbH	Kiefersfelden	Germany
Low Profile Blades SEC*35*™	Richard Allan Scientific/Microm/Thermo Scientific	Walldorf	Germany
Microtube boxes	Zefa Laborservice	Harthausen	Germany
Microtube PP, 1.5 ml	Paul Böttger OHG	Bodenmais	Germany
Microtube PP, 2 ml	Diagonal GmbH & Co. KG	Münster	Germany
Microtube tough-spots®	Diversified Biotech	Boston	USA
Microvette®, K-EDTA, 0.5 ml	Sarstedt AG & Co. KG	Nümbrecht	Germany
Microvette®, Li-Heparin, 0.5 ml	Sarstedt AG & Co. KG	Nümbrecht	Germany
Mini-PROTEAN® TGX™ Precast gels	Bio-Rad Laboratories GmbH	München	Germany
Minisart syringe filter, 0.22 µm	Sartorius AG	Göttingen	Germany
Mortar	Morgan Technical Ceramics - Haldenwanger	Waldkraiburg	Germany
Multi-channel pipette 30-300 µl	Brand GmbH & Co. KG	Wertheim	Germany
Myjector® U-100 insulin syringe, 0.5 ml	Terumo® Europe N.V.	Leuven	Belgium
Needle	Karl Hammacher GmbH	Solingen	Germany
Neubauer cell counting chamber (hemocytometer)	Paul Marienfeld GmbH & Co. KG	Lauda-Königshofen	Germany
OPTITRAN BA-S85 nitrocellulose membrane (0.45 µm)	Whatman GmbH	Dassel	Germany
Pap pen	Kisker Biotech GmbH & Co. KG	Steinfurt	Germany
Paper towels	Anton Schlecker	Ehingen	Germany
Parafilm®	Pechiney Plastic Packaging	Chicago	USA
Pasteur pipettes, glass	Zefa-Laborservice GmbH	Harthausen	Germany
Pencil	Faber-Castell AG	Steinfurt	Germany
Pestle	Morgan Technical Ceramics - Haldenwanger	Waldkraiburg	Germany

Item	Company	City	Country
Pipettes 10; 200, 1000 µl	Gilson Intl. B.V.	Limburg	Germany
Pipettes 2,5; 10; 100, 1000 µl	Eppendorf AG	Hamburg	Germany
Pipetting aid	Gilson Intl. B.V.	Limburg	Germany
Plastic beakers	Vitlab®	Großostheim	Germany
Plastic ware (beakers, cylinders, funnels)	Diagonal GmbH &Co KG	Münster	Germany
Pressurizer for tablets	IKA®-Werke GmbH & Co. KG	Staufen	Germany
Purple nitrile exam gloves, size "XL"	Kimberley-Clark Health Care	Zaventem	Belgium
Pursept A	Merz GmbH & Co. KGaA	Frankfurt am Main	Germany
Reaction tubes, 0.2 ml	Zefa-Laborservice GmbH	Harthausen	Germany
Reaction tubes, 0.5 ml	Brand GmbH & Co. KG	Wertheim	Germany
Reaction tubes, 2 ml (safe-lock)	Eppendorf AG	Hamburg	Germany
Restrainer	Bruker BioSpin GmbH	Rheinstetten	Germany
Safety goggles	UVEX Winter Holding	Fürth	Germany
Scalpel	B. Braun Melsungen	Melsungen	Germany
Schlundsonde (= gerade Knopfkanüle, 22 Gauge; Länge: 25 mm; Durchmesser: 1,25 mm	Fine Science Tools GmbH	Heidelberg	Germany
Spatula	Carl Roth GmbH & Co. KG	Karlsruhe	Germany
Stainless steel beads	Qiagen	Hilden	Germany
SuperFrost® Plus & Polysine® slides	Menzel GmbH & Co. KG	Braunschweig	Germany
Sylgaard dishes for fixation of tissue	AG Schemann		
TECNIPLAST® Green Line IVC Sealsafe PLUS, Typ II Käfig, Grundfläche von 540 cm^2	TECNIPLAST Deutschland GmbH	Hohenpeißenberg	Germany
Tips, blue 1000 µl	Brand GmbH & Co. KG	Wertheim	Germany
Tips, white, 10 µl	Brand GmbH & Co. KG	Wertheim	Germany
Tips, yellow, 100 µl	Brand GmbH & Co. KG	Wertheim	Germany
Tissue culture petri dish	Falcon™, BD Biosciences	Heidelberg	Germany
Tissue-Tek cryomolds, intermediate	Sakura Finetek Europe B.V.	Alphen aan den Rijn	Netherlands
Tube racks	Brand GmbH & Co. KG	Wertheim	Germany
Tubes, 15 ml	Greiner Bio-One GmbH	Frickenhausen	Germany
Tubes, 50 ml	Greiner Bio-One GmbH	Frickenhausen	Germany
Twin.tec real-time PCR plates 96	Eppendorf AG	Hamburg	Germany
Waste bags	PAA Laboratories GmbH	Pasching	Austria
Water bottle	Vitlab®	Großostheim	Germany
Weighing dish, blue	Carl Roth GmbH & Co. KG	Karlsruhe	Germany
Whatman paper	Carl Roth GmbH & Co. KG	Karlsruhe	Germany

9.4 Chemicals

Item	Company	City	Country
1 kb DNA ladder	New England Biolabs GmbH	Frankfurt am Main	Germany
2-(N-morpholino)ethanesulfonic acid (MES)	Boehringer Mannheim / Roche Diagnostics	Mannheim	Germany
3,3'-Diaminobenzidine (DAB) staining solutions	Sigma-Aldrich Chemie GmbH	Taufkirchen	Germany
Acetic acid (100 %)	Merck KGaA	Darmstadt	Germany
Acrylamide / Bisacrylamide "Roti-Gelektrophorese" Gel 30	Carl Roth GmbH & Co. KG	Karlsruhe	Germany
Agarose, peqGOLD universal	Peqlab biotechnology GmbH	Erlangen	Germany
Alpha linoleic acid	Sigma-Aldrich Chemie GmbH	Taufkirchen	Germany
Alpha linolenic acid	Sigma-Aldrich Chemie GmbH	Taufkirchen	Germany
Ammoniumpersulphate (APS)	Bio-Rad Laboratories GmbH	München	Germany
Aquatex® aqueous mounting medium	Merck KGaA	Darmstadt	Germany
BCA protein assay kit	Pierce / Thermo Fisher Scientific	Bonn	Germany
Boric acid	Merck KGaA	Darmstadt	Germany
Bovine serum albumine (A6003-25G)	Sigma-Aldrich Chemie GmbH	Taufkirchen	Germany
Bradford protein assay dye reagent	Bio-Rad Laboratories GmbH	München	Germany
Bromophenolblue	Merck KGaA	Darmstadt	Germany
Calcium chloride ($CaCl_2$)	Merck KGaA	Darmstadt	Germany
Carbogen gas (CO_2 & O_2)	Linde Gas	Unterschleißheim	Germany
Carbon dioxide (CO_2 solid; "dry ice")	TKD GmbH	Fraunberg-Tittenkofen	Germany
Chloroform	Carl Roth GmbH & Co. KG	Karlsruhe	Germany
Citric acid	CLN GmbH	Niederhummel	Germany
Collagenase	Biochrom AG	Berlin	Germany
Coomassie Brilliant Blue G 250	SERVA Electrophoresis GmbH	Heidelberg	Germany
D-MEM (Dulbecco's Modified Eagle Medium)	Invitrogen / Life Technologies GmbH	Darmstadt	Germany
D-MEM (Dulbecco's Modified Eagle Medium) F-12	Invitrogen / Life Technologies GmbH	Darmstadt	Germany
Dimethylsulphoxide (DMSO)	Sigma-Aldrich Chemie GmbH	Taufkirchen	Germany
Dithiotreitol (DTT)	AppliChem GmbH	Darmstadt	Germany
dNTP mix (200 mM)	Qiagen GmbH	Hilden	Germany
DPP IV inhibitor	Millipore GmbH	Schwalbach	Germany
ECL Advance™ blocking agent	GE Healthcare	München	Germany
Eosine	medite Medizintechnik AG	Nunningen	Switzerland
Ethanol	J.T. Baker, Mallinckrodt	Deventer	Netherlands

Item	Company	City	Country
Ethanol, denatured	CLN GmbH	Niederhummel	Germany
Ethidium bromide	Carl Roth GmbH & Co. KG	Karlsruhe	Germany
Fetal calf serum "Gold"	PAA Laboratories GmbH	Pasching	Austria
Food C	Ssniff Spezialdiäten GmbH	Soest	Germany
Food HF	Ssniff Spezialdiäten GmbH	Soest	Germany
Food HF/n-3	Ssniff Spezialdiäten GmbH	Soest	Germany
Formaldehyde, 37 %	Carl Roth GmbH & Co. KG	Karlsruhe	Germany
Gene Ruler, 50 bp ladder	Fermentas GmbH	St. Leon-Rot	Germany
Glucose monohydrate	Sigma-Aldrich Chemie GmbH	Taufkirchen	Germany
Glucose solution, 20 %	B. Braun Melsungen	Melsungen	Germany
Glycerol	Carl Roth GmbH & Co. KG	Karlsruhe	Germany
Glycine	Merck KGaA	Darmstadt	Germany
Glycine-glycine	Bachem Holding AG	Bubendorf	Switzerland
H_3PO_4 (phosphoric acid), 85 %	Merck KGaA	Darmstadt	Germany
Hämalaun (Emallume)	WALDECK GmbH & Co. KG	Münster	Germany
HBSS (Hanks' Balanced Salt Solution) + Mg^{2+}, Ca^{2+}	Invitrogen / Life Technologies GmbH	Darmstadt	Germany
Hematoxylin (Gill)	Carl Roth GmbH & Co. KG	Karlsruhe	Germany
Hydrochloric acid (HCl)	Carl Roth GmbH & Co. KG	Karlsruhe	Germany
hydrogen peroxide, 30 %	Merck KGaA	Darmstadt	Germany
Isopentane (2-Methylbutane)	Carl Roth GmbH & Co. KG	Karlsruhe	Germany
Isopropanol	J.T. Baker, Mallinckrodt	Deventer	Netherlands
Magnesium chloride ($MgCl_2$)	Merck KGaA	Darmstadt	Germany
Magnesium sulphate ($MgSO_4$)	Merck KGaA	Darmstadt	Germany
Methanol	Merck KGaA	Darmstadt	Germany
NEG-50® cryo matrix	Richard Allan Scientific / Microm / Thermo Scientific	Walldorf	Germany
Nitrogen, liquid	Linde Gas	Unterschleißheim	Germany
Nonidet P-40®	Sigma-Aldrich Chemie GmbH	Taufkirchen	Germany
Oil Red O	Sigma-Aldrich Chemie GmbH	Taufkirchen	Germany
Oligo-dT Primer	Promega Corporation	Mannheim	Germany
Oligonucleotides (PCR primer)	Metabion	Martinsried	Germany
Orange G	Sigma-Aldrich Chemie GmbH	Taufkirchen	Germany
Oxygen	Linde Gas	Unterschleißheim	Germany
P2 "last forever" transparent nail polish	dm Drogeriemarkt	Karlsruhe	Germany
PageBlue™ Protein staining solution	Fermentas GmbH	St. Leon-Rot	Germany
Pageruler, prestained	Fermentas GmbH	St. Leon-Rot	Germany
Para-Formaldehyde	Sigma-Aldrich Chemie GmbH	Taufkirchen	Germany

Item	Company	City	Country
Paraplast®	Carl Roth GmbH & Co. KG	Karlsruhe	Germany
Penicillin / Streptomycin	PAA Laboratories GmbH	Pasching	Austria
Peroxidase blocking solution	Dako Deutschland GmbH	Hamburg	Germany
Phenylisothiocyanate	Merck KGaA	Darmstadt	Germany
Phosphatase inhibitor	Sigma-Aldrich Chemie GmbH	Taufkirchen	Germany
Phosphate-buffered saline in tablets	Sigma-Aldrich Chemie GmbH	Taufkirchen	Germany
Phosphate-buffered saline, ready-made	Biochrom AG	Berlin	Germany
PhosSTOP phosphatase inhibitor cocktail	Roche Diagnostics GmbH	Mannheim	Germany
Ponceau S	Sigma-Aldrich Chemie GmbH	Taufkirchen	Germany
Potassium chloride (KCl)	Merck KGaA	Darmstadt	Germany
Potassium hydroxide (KOH)	Merck KGaA	Darmstadt	Germany
Protease inhibitor	Sigma-Aldrich Chemie GmbH	Taufkirchen	Germany
QIAzol® Lysis Reagent	Qiagen	Hilden	Germany
Rnase inhibitor RNasin®	Promega Corporation	Mannheim	Germany
Rnase-Zap®	Sigma-Aldrich Chemie GmbH	Taufkirchen	Germany
Roti®-HistoKitt	Carl Roth GmbH & Co. KG	Karlsruhe	Germany
Sodium azide (NaN_3)	Merck KGaA	Darmstadt	Germany
Sodium chloride (NaCl)	Merck KGaA	Darmstadt	Germany
Sodium dihydrogen phosphate (NaH_2PO_4)	Merck KGaA	Darmstadt	Germany
Sodium dodecyl-sulphate (SDS)	Omnilab GmbH & Co. KG	Bremen	Germany
Sodium hydrogen carbonate ($NaHCO_3$)	Merck KGaA	Darmstadt	Germany
Sodium hydroxide (NaOH)	Merck KGaA	Darmstadt	Germany
Sodium sulphate (Na_2SO_4)	Merck KGaA	Darmstadt	Germany
Sodium-deoxycholate	Sigma-Aldrich Chemie GmbH	Taufkirchen	Germany
Streptavidin / HRP	Dako Deutschland GmbH	Hamburg	Germany
Sucrose	Sigma-Aldrich Chemie GmbH	Taufkirchen	Germany
Tetramethylethylenediamine (TEMED)	Merck KGaA	Darmstadt	Germany
TissueTEK O.C.T.	Sakura Finetek Germany GmbH	Staufen	Germany
Titriplex® Ethylenediaminetetraacetic acid (EDTA)	Merck KGaA	Darmstadt	Germany
Tri-sodium-citrate-dihydrate	Carl Roth GmbH & Co. KG	Karlsruhe	Germany
Tris base	AppliChem GmbH	Darmstadt	Germany
Triton® X-100	Sigma-Aldrich Chemie GmbH	Taufkirchen	Germany
Trypan blue solution (0.4 %)	Sigma-Aldrich Chemie GmbH	Taufkirchen	Germany
Tween® 20	Sigma-Aldrich Chemie GmbH	Taufkirchen	Germany
VectaMount™ permanent mounting medium	Vector Laboratories/Biozol Diagnostica Vertrieb GmbH	Eching	Germany

Item	Company	City	Country
Water, nuclease-free	Sigma-Aldrich Chemie GmbH	Taufkirchen	Germany
Water, purified	SG Water USA, LLC	Nashua	USA
Xylol	Carl Roth GmbH & Co. KG	Karlsruhe	Germany
ε-Amino-n-caproic acid	Sigma-Aldrich Chemie GmbH	Taufkirchen	Germany

9.5 Kits

Item	Company	City	Country
Absolute IDQ™ Kit p180	Biocrates Life Sciences AG	Innsbruck	Austria
Agilent RNA 6000 Nano Kit	Agilent Technologies	Waldbronn	Germany
Cholesterol Quantitation Kit	BioVision, Inc.	Mountain View	USA
Glucagon Like Peptide-1 (Active) ELISA	Millipore GmbH	Schwalbach	Germany
HotStarTaq® PCR Kit	Qiagen GmbH	Hilden	Germany
Cholesterol, colorimetric test	Boehringer Mannheim / R-Biopharm	Darmstadt	Germany
miRNeasy® Mini Kit	Qiagen GmbH	Hilden	Germany
mRNeasy® Mini Kit	Qiagen GmbH	Hilden	Germany
Murine serum amyloid A ELISA	ICL	Portland	USA
NEFA-HR(2) qantitation kit	Wako Chemicals GmbH	Neuss	Germany
Omniscript® reverse transcription kit	Qiagen GmbH	Hilden	Germany
Quantikine® Mouse Osteopontin Immunoassay	R&D Systems GmbH	Wiesbaden	Germany
QuantiTect® SYBR® Green PCR kit	Qiagen GmbH	Hilden	Germany
RNase-free DNase set	Qiagen GmbH	Hilden	Germany
Triglyceride liquicolor^{mono} quantitation kit	Human Diagnostics	Wiesbaden	Germany
Ultra Sensitive Mouse Insulin ELISA Kit	Crystal Chem., Inc.	Downers Grove	USA

9.6 Machines

Item	Company	City	Country
Agilent 2100 Bioanalyzer	Agilent Technologies GmbH	Böblingen	Germany
Asus eeePC Notebook	ASUSTeK COMPUTER INC.	Taipei	Taiwan
Binocular Stemi 2000-CS with KL 1500 LCD	Carl Zeiss MicroImaging GmbH	Jena	Germany
CaloSys process control (994620 series ultramat / oxymat 6)	Siemens / TSE Systems	Bad Homburg	Germany
Centrifuge 5415 R	Eppendorf AG	Hamburg	Germany
Centrifuge 5424	Eppendorf AG	Hamburg	Germany
Centrifuge 5430	Eppendorf AG	Hamburg	Germany
Centrifuge 5810	Eppendorf AG	Hamburg	Germany
Climate simulation station	Feutron Klimasimulation GmbH	Langenwetzendorf	Germany
Concentrator 5301	Eppendorf AG	Hamburg	Germany
DNA / RNA UV-Cleaner UVC / T-M-AR	UniEquip GmbH	Planegg	Germany
Electrophoresis power supply CONSORT E861	Consort	Turnhout	Belgium
FreeStyle Lite glucometer	Abbott Diabetes Care	Alameda	USA
FreeStyle Lite test stripes	Abbott Diabetes Care	Alameda	USA
Freezer -20 °C Liebherr premium	Liebherr GmbH	Biberach	Germany
Freezer "ThermoForma"	Thermo Fisher Scientific	Schwerte	Germany
Freezer "ThermoScientific HeraFreeze"	Thermo Fisher Scientific	Schwerte	Germany
Fridge 4 °C Liebherr	Liebherr GmbH	Biberach	Germany
Heat sealer	Eppendorf AG	Hamburg	Germany
Heraeus Megafuge 1.0 R	Heraeus, Thermo Scientific	Waltham	USA
HeraSafe bench	Heraeus / Thermo Fisher Scientific	Waltham	USA
Homogenizer ("Dispergierwerkzeug")	Miccra (ART Labortechnik)	Mühlheim	Germany
HTS-XT microplate extension for FT-IR	Bruker BioSpin GmbH	Rheinstetten	Germany
Ice machine AF 100	Scotsman ice systems	Milan	Italy
Incubator HeraCell 150	Thermo Fisher Scientific	Schwerte	Germany
Julabo SW 22	JULABO GmbH	Seelbach	Germany
Leica ST 5020	Leica Microsystems GmbH	Wetzlar	Germany
Mass spectrometer QTRAP5500	AB SCIEX Germany GmbH	Darmstadt	Germany
Microscope Axiovert 40 C with Axio Cam ICC3	Carl Zeiss MicroImaging GmbH	Jena	Germany
Microscope DMI 4000B with Leica CTR 4000 and Leica UV source	Leica Microsystems GmbH	Wetzlar	Germany
Microtome HM 355 S	Microm / Thermo Fisher Scientific	Walldorf	Germany
Mikrom AP280-1/2/3	Microm / Thermo Fisher Scientific	Walldorf	Germany

Item	Company	City	Country
Mikrom SB 80 water bath	Microm / Thermo Fisher Scientific	Walldorf	Germany
Mikrotom-Kryostat Cryo-Star HM 560 MV	Microm / Thermo Fisher Scientific	Walldorf	Germany
Mini Centrifuge GMC-060	LMS Group	Tokyo	Japan
Mini scale EW3000-2M	Kern GmbH	Balingen	Germany
Mini scale PE360	Mettler-Toledo	Ingolstadt	Germany
"The Minispec" mq 7.5 NMR analyzer	Bruker BioSpin GmbH	Rheinstetten	Germany
ND-1000 Spectrophotometer	Peqlab biotechnology GmbH	Erlangen	Germany
Odyssey® Infrared Imaging System	LI-COR Biosciences GmbH	Bad Homburg	Germany
Oven Venticell	MMM Medcenter Einrichtungen GmbH	München	Germany
Parr® 6300 Calorimeter	Parr Instrument Co.	Moline	USA
Power pack P25 T	Biometra GmbH	Göttingen	Germany
Power Shot G5 digital camera	Canon, Inc.	Lake Success	USA
Printer	Intas Science Imaging Instruments GmbH	Göttingen	Germany
Realplex^4 Mastercycler epgradient S	Eppendorf AG	Hamburg	Germany
S20-K SevenEasy™ pH meter	Mettler-Toledo	Ingolstadt	Germany
Scale, max 820 g	Sartorius AG	Göttingen	Germany
Sonificator UW 2070	Bandelin electronic GmbH & Co. KG	Berlin	Germany
Spectrophotometer infinite M2000	Tecan Austria GmbH	Gröding	Germany
Spectrophotometer Ultrospec 3100pro	Amersham Biosciences / GE Healthcare	München	Germany
Thermocycler T3000	Biometra GmbH	Göttingen	Germany
Thermomixer comfort	Eppendorf AG	Hamburg	Germany
Timer	Oregon Scientific GmbH	Neu-Isenburg	Germany
Tissue Lyser II	Qiagen GmbH / Retsch GmbH	Hilden	Germany
Tissue Processor Leica TP1020	Leica Microsystems GmbH	Wetzlar	Germany
Titramax 100 with Inkubator 1000	Heidolph Instruments GmbH & Co. KG	Schwalbach	Germany
TSE Systems Calorimetry, Modul „CaloSys“	TSE Systems	Bad Homburg	Germany
TSE Systems Drinking & Feeding Monitor, Modul „ActiMot”	TSE Systems GmbH	Bad Homburg	Germany
UV-VIS gel electrophoresis detection system	Intas Science Imaging Instruments GmbH	Göttingen	Germany
Vacuum centrifuge (SpeedVac SPDIIIV)	Savant / Thermo Fisher Scientific	Marietta	USA
VARIOSCAN	Electron / Thermo Fisher Scientific	Marietta	USA
Vortexer "Vortex Genie 2"	Bender-Hobein	Gera	Germany
Vortexer 2x^3	Velp Scientifica	Usmate	Italy
WiseMix RK 2D digital rocker	Witeg GmbH	Wertheim	Germany

9.7 Software

Item	Company	City	Country
2100 Expert Software vB.02.06.SI418	Agilent Technologies GmbH & Co. KG	Waldbronn	Germany
Analyst software v1.5.1	AB SCIEX Germany GmbH	Darmstadt	Germany
AxioVision v4.6.3	Carl Zeiss MicroImaging GmbH	Jena	Germany
Bruker Minispec plus + OPUS v5.5	Bruker BioSpin GmbH	Rheinstetten	Germany
ChemDraw Ultra v12.0.3.1216	CambridgeSoft	Cambridge	USA
Image-Pro Plus v7.0	Media Cybernetics, Inc.	Bethesda	USA
ImageJ	Open Source (Wayne Rasband (NIH))	Bethesda	USA
Intas GDS	Intas Science Imaging Instruments GmbH	Göttingen	Germany
Leica Application Suite v3.7	Leica Mikrosysteme Vertrieb GmbH	Wetzlar	Germany
LinRegPCR v12.16	Dr. J.M. Ruijter, Academic Medical Center	Amsterdam	Netherlands
MetIQ software v1.2.2	Biocrates Life Sciences AG	Innsbruck	Austria
Microsoft Office	Microsoft Deutschland GmbH	Unterschleißheim	Germany
NanoDrop ND-1000 v3.7.1	PEQLAB Biotechnologie GmbH (Thermo Scientific)	Erlangen	Germany
Odyssey application software v3.0	LI-COR Biosciences GmbH	Bad Homburg	Germany
Photoshop CS	Adobe Systems GmbH	München	Germany
Prism v5.0	GraphPad Software, Inc.	La Jolla	USA
Realplex v2.0	Eppendorf AG	Hamburg	Germany
SkanIt v2.2.184	Thermo Electron Corporation	Marietta	USA
Software OPUS v6.5	Bruker BioSpin GmbH	Rheinstetten	Germany
Tecan i-control v1.7.1.12	Tecan Austria GmbH	Gröding	Germany
TIGR MeV software v4.6.0	J. Craig Venter Institute	Rockville	USA
TSE Labmaster v2.1.5	TSE Systems GmbH	Bad Homburg	Germany

10 List of Figures

11 List of Tables

12 Acknowledgements

First of all I want to thank Prof. Dr. Hannelore Daniel and Prof. Dr. J. J. Hauner for their trust in me, their strong support and valuable discussions. Not only have I profited in a professional way, but also on a personal level.

I am very grateful to have Dr. Bernhard Bader as my supervisor. With his outstanding scientific creativity he taught me to look at things from many different angles and not just taking things for granted. With his questions, Bernhard showed me that accuracy is the foundation of good science.

I thank Prof. Martin Klingenspor for discussion regarding data analysis, for providing me with books on metabolic topics and for taking the chair in the dissertation procedure.

Special thanks to my collaboration partner and creative mind at Charité, Dr. Karsten H. Weylandt.

Learning methods, discussing results, handling mice… — all the experiments I have performed and the (personal) challenges I have taken, it would have never been possible without the support of excellent colleagues. First and foremost, I want to thank Christoph Dahlhoff, Charles Desmarchelier, Kerstin Hartwig, Katharina Heller, Dominika Kolodziejczak, Isabelle Mack, Eva-Maria Sedlmeier, and Kirsten Uebel.
I also thank Anna Bandhari, Florian Bolze, Tobias Fromme, Nico Gebhardt, Lisa Gruber, Alexander Haag, Elisabeth Hofmair, Manuela Hubersberger, Patricia Izidoro-Ziehlke, Elmar Jocham, Hermine Kienberger, Tim Lubinus, Aline Lukacs, Mena Marth, Stephanie May, Sabine Mocek, Ramona Pais, Silvia Pitariu, Constanze Pscheidt, Tina Reichelt, Nadine Rink, Manuela Sailer, Christian Scherling, Ronny Scheundel, Katrin Seyfarth, and Johanna Welzhofer for helping me with the mice and everything that was related to it.

My thanks also goes to Dorothea Wörner, who held together the students in the GRK1482 research training group, and to Sylvia Heinrich, who always has an open ear for her PhD students.

I thank Stefanie Worsch for taking over this project, I am very confident that you will continue this project successfully!

This thesis would never have been possible with the life-long support of the dearest people I have — my family:

From my heart I thank

Tobias Henning for any kind of support one can think of — starting with breakfast and ending with pushing me through the writing phase.

my grandmother Christel Felauer, my father Mario Ludwig, my mother Birgit Ringhand and Volker Ringhand for continuous support.

Thank you!

Funding

German Research Foundation (Deutsche Forschungsgemeinschaft - DFG), Graduiertenkolleg GRK 1482 - “Interface functions of the intestine between luminal factors and host signals”